# Detection and Characterization of Coronaviruses from African bat species

By Marike Geldenhuys

Submitted in partial fulfilment of the requirements for the degree

MAGISTER SCIENTIAE (MICROBIOLOGY)

in the

Department of Microbiology and Plant Pathology
Faculty of Natural and Agricultural Sciences
University of Pretoria
Pretoria, South Africa

(09 May 2012)

Supervisor: Dr. Wanda Markotter
Co-supervisors: Dr. Jacqueline Weyer and Prof. Louis H. Nel

I, Marike Geldenhuys declare that the thesis, which I hereby submit for the degree MSc Microbiology at the University of Pretoria, is my own work and has not previously been submitted by me for a degree at this or any other tertiary institution.

SIGNATURE:……

DATE: ……

# Acknowledgements

**I would like to sincerely thank the following individuals for their guidance and academic input in this project**

Dr. Wanda Markotter (University of Pretoria), Prof. Louis H. Nel (University of Pretoria) and Dr. Jacqueline Weyer (Centre for Emerging and Zoonotic Diseases, National Institute for Communicable Diseases of the National Health Laboratory Service) for their supervision and guidance.

**A special word of thanks to**

Stewart McCulloch (University of Pretoria), Teresa Kearney (Ditsong museum of Natural Sciences) and Peter Taylor (University of Venda) for bat identification and sample collection.

The National Research foundation (NRF) and the Poliomyelitis Research Foundation (PRF) for financial support.

The friends and colleagues in Virology lab 9-11 and 9-34 at the University of Pretoria, for their advice, encouragement, and support during the project.

To my family, for their support and love.

## Summary


### Detection and Characterization of Coronaviruses from African bat species

By Marike Geldenhuys

Supervisor: Dr. W. Markotter

Co-supervisors: Dr. Jacqueline Weyer and Prof. Louis H. Nel

Department of Microbiology and Plant Pathology

Faculty of Natural and Agricultural Sciences

University of Pretoria

For the degree MSc (Microbiology)

The severe acute respiratory disease syndrome or SARS epidemic emerged in Hong Kong, China, in 2002 with a mortality rate of 15%. The etiological agent for SARS was identified to be a previously unrecognized coronavirus (SARS-CoV) which was found to be zoonotic in origin. A possible reservoir for the SARS-CoV was proposed to be the Chinese horseshoe bat species (*Rhinolophus* spp.) due to the detection of SARS-related bat coronaviruses (BtCoV) within these bat species. Since the SARS-CoV epidemic, new interest regarding the origin and pathogenicity of coronaviruses has been generated. As such, surveillance studies of BtCoV in numerous bat species have been performed in Asia, Europe, North and South America as well as 3 African countries. Recent BtCoV investigations in Kenya, Ghana and Nigeria identified BtCoV from both the *Alpha*- and *Betacoronavirus* genera and provided the first evidence for the presence of coronaviruses in African bats. Previously, the presence of antibodies against SARS-related CoV has been reported in two bat species native to South Africa. This study investigated the possible presence of BtCoV in a panel of bat specimens collected from sites in South Africa and Rwanda, and how they are related to previously detected BtCoVs from other parts of the world.

Here we report the development of two PCR assays, the PanBtCoV/9 primer nested RT-PCR and PanBat/AB/6 primer hemi-nested RT-PCR assay, which were used in coronavirus detection from alimentary specimens collected from 15 bat genera. The combined assays amplified coronavirus RNA from 5 samples of the 201 analysed samples collected in South Africa (n=113) and Rwanda (n=88).

Three alphacoronaviruses were detected in 3 different South African bat species, *Miniopterus* spp. (*Miniopterus*-Bat coronavirus/Irene/South Africa/2009), *Neoromicia capensis* (*Neoromicia*-Bat coronavirus/167/South Africa/2007), and *Mops midas* (*Mops*-Bat coronavirus/1364/South Africa/2011). From Rwanda, a single betacoronavirus, *a* SARSr-

CoV was detected within 2 *Rhinolophus* spp. individuals (*Rh*-BtCoV/441/Rwanda/08 and *Rh*-BtCoV/445/Rwanda/08). Phylogenetic analysis of these sequences was performed and showed that the South African *Miniopterus* alphacoronavirus and the Rwandan betacoronavirus cluster together with previously detected African BtCoV from the same host genera. The South African alphacoronavirus from *Mops midas* was closely related to an alphacoronavirus identified within another member of the *Molossidae* family, *Chaerephon* spp. from Kenya. Being the first BtCoV identified from the *Neoromicia* genus, no African BtCoV sequences were available for comparison and as such the virus clustered together with European BtCoV from the *Nyctalus* spp., another member of the *Vespertilioninae* subfamily.

This study has detected the first BtCoV viral RNA from the native bat species of South Africa and Rwanda, providing confirmation to the presence of bat coronaviruses circulating in these countries. From these preliminary results further investigations into the prevalence and infection cycles of bat coronaviruses in specific bat populations can be performed in the future.

The possibility of either these alpha- or betacoronaviruses spilling over and eventually adapting to and infecting other species, though unlikely, cannot be excluded since such rare events are hypothetically responsible for the establishment coronaviruses in humans, livestock, poultry and pets. Caution may still be merited when interacting with bats in roosts and caves.

# Table of Contents

# List of Abbreviations

| | |
|---|---|
| $3CL^{pro}$ | 3C-like proteinase |
| ADRP | ADP-ribose 1”-phosphatase |
| AlphaCoV | Alphacoronavirus genus |
| ACE2 | Angiotensin-converting enzyme 2 |
| BetaCoV | Betacoronavirus genus |
| BCoV | Bovine coronavirus |
| BtCoV | Bat coronavirus |
| CoV | Coronavirus |
| CCoV | Canine coronavirus |
| CL | chymotrypsin-like |
| CRCoV | Canine respiratory coronavirus |
| CEACAM1/2 | Carcinoembryonic antigen-related adhesion molecule 1 and 2 |
| DNA | Deoxyribonucleic acid |
| DuCoV | Duck coronavirus |
| EqCoV | Equine coronavirus |
| ExoN | Exonuclease |
| FCoV | Feline coronavirus |
| FIPV | Feline infectious peritonitis virus |
| GoCoV | Goose coronavirus |
| HCoV229E | Human coronavirus 229E |
| HCoVHKU1 | Human coronavirus HKU1 |
| HCoVOC43 | Human coronavirus OC43 |
| HCoVNL63 | Human coronavirus NL63 |
| HE | Hemagglutinin-esterase |
| HECV | Human enteric coronavirus |
| Hel | Helicase |
| HCoV | Human coronavirus |
| IBV | Infectious bronchitis virus |
| ICTV | International Committee for the Taxonomy of Viruses |
| Kb | Kilo-basepair |
| Mi-BatCoV 1 | Miniopterus bat coronavirus 1 |
| Mi-BatCoV HKU8 | Miniopterus bat coronavirus HKU8 |
| MHV | Murine hepatitis virus |
| mya | Million years ago |
| NendoU/XendoU | Uridylate-specific endoribonuclease |

| | |
|---|---|
| nm | Nanomole |
| nsp | Non structural protein |
| nt | nucleotide |
| O-MT | Ribose-2'-Omethyltransferase |
| ORF | Open reading frame |
| PCoV | Puffinosis virus |
| PCR | Polymerase chain reaction |
| PEDV | Porcine epidemic diarrhea virus |
| Pi-BatCoV HKU5 | *Pipistrellus* bat coronavirus HKU5 |
| PiCoV | Pigeon coronavirus |
| PhCoV | Pheasant coronavirus |
| PL | Papain-like proteinases |
| Pp1a | Polyprotein 1a |
| Pp1ab | Polyprotein 1ab |
| PHEV | porcine hemagglutinating encephalomyelitis virus |
| PRC | Rat coronavirus |
| PRCoV | Porcine respiratory coronavirus |
| RdRp | RNA dependent RNA polymerase |
| Rh-BatCoV HKU2 | Rhinolophus bat coronavirus HKU2 |
| RNA | Ribonucleic acid |
| Ro-BatCoV HKU9 | Rousettus bat coronavirus HKU9 |
| RT | Reverse transcription |
| SARS | Severe acute respiratory syndrome |
| SARS-CoV | Severe acute respiratory syndrome virus |
| SARS-HCoV | Severe acute respiratory syndrome human coronavirus |
| SARSr-CoV | Severe acute respiratory syndrome-related coronavirus |
| SARSr-Rh-BatCoV HKU3 | *Rhinolophus* SARS-related coronavirus HKU3 |
| SARSr-Rh-BatCoV RP3 | *Rhinolophus* SARS-related coronavirus Rp3 |
| Sc-BatCoV 512 | *Scotophilus* bat coronavirus 512/05 |
| Taq | *Thermus aquaticus* |
| TGEV | Porcine transmissible gastroenteritis virus |
| TM | Transmembrane domain |
| TuCoV | Turkey coronavirus |
| Ty-BatCoV HKU4 | Tylonycteris bat coronavirus HKU4 |
| ZBCoV | Zaria bat coronavirus |

## Copyright permission

The majority of the figures used in this thesis do not possess copyright protection and may be reused for academic purposes. Certain figures in the text are from copyright protected journal articles and permission for academic reuse has been granted from the publishers. The publisher permission licences are indicated at the end of the figure legends.

# Chapter 1: Literature Review

## 1.1 Introduction

Coronaviruses are positive sense RNA viruses, which belong to the *Coronaviridae* family in the *Nidovirales* Order (Masters, 2006). These enveloped viruses may cause any number of diseases ranging from acute to chronic respiratory, enteric, hepatic as well as central nervous system diseases in birds, animals, and humans (Masters, 2006; Weiss and Navas-Martin, 2005). Coronaviruses (CoV) are known to be transmitted through either the respiratory route of infection or by the faecal-oral route.

Since the identification of the first coronavirus in 1937, infectious bronchitis virus (IBV) by Beaudette and Hudson, and up to 2001 only 10 coronaviruses had been identified (Beaudette and Hudson, 1937). All known coronaviruses at that time caused relatively mild symptoms in their respective hosts. However, since 2002 more than 17 coronaviruses have been detected due to increased surveillance for new pathogens in different species.

Current interest in coronaviruses was reinitiated with the 2002 severe acute respiratory syndrome (SARS) outbreak in China. The initial outbreak spread to over 5 continents and 33 counties, causing over 8,000 infections, and resulting in more than 700 deaths. Using cell culturing techniques and electron microscopy researchers could identify the etiological agent of the outbreak as a coronavirus. Ksiazek *et al*., (2003) studied patients with respiratory symptoms including those of SARS and detected only antibodies against the virus in the serum of SARS patients. Due to the lack of antibodies against this virus in the general population, SARS would thus appear to have been due to a newly emergent disease agent.

Animal species in the wild animal markets of Hong Kong and Guangdong China, which are also sold as bush meat, were also analyzed for the presence of the SARS virus. Those that tested positive for the presence of the virus including palm civets (*Paguma larvata)* and raccoon dogs (*Nyctereutes procyonoides*) also suffered the clinical symptoms of SARS. A 'SARS-like' coronavirus was found in the Chinese horseshoe bat (*Rhinolophus* spp.). The human SARS-CoV strain Tor2 share a 92% overall sequence identity to the SARS*r-Rh*-BatCoV Rp3 detected in *Rh. sinicus* (*Rh. pearsoni* corrected to *Rh. sinicus*) (Li *et al*., 2005; Yuan *et al*., 2010). When a comparison was made of the spike proteins of the SARS-like coronavirus from horseshoe bats and the human SARS coronavirus it was discovered that within the S1 domain there was only a 64% genetic homology between the spike protein genes (Li *et al*., 2005). Since the SARS-like coronaviruses detected in bats were the most closely related to the SARS-CoV that infected humans and civets in the markets, as well as the large diversity of SARS-like bat coronaviruses detected within the *Rhinolophus* genus, it is now generally believed that bats are the original reservoir for the SARS virus and that the virus circulated in an intermediate host for several years before

infecting humans and palm civets (Vijaykrishna *et al.*, 2007). With this new discovery, bats were sampled more frequently for the presence of coronaviruses and it was found that bats harbour a huge variety of previously unknown coronaviruses.

It has been suggested by Vijaykrishna *et al.*, (2007) and Woo *et al.,* (2009) that bats are the natural reservoirs for all coronavirus lineages and that the coronaviruses that infect other animals were originally derived from a bat coronaviruses.

## 1.2 The Etiological agent

### 1.2.1 The Coronavirus Genome

Coronaviruses are large RNA viruses of approximately 80-120 nm but have been known to be as small as 50nm or as large as 200nm. These viruses also possess the largest known genome for any RNA virus, ranging between 28-32 kilo-basepairs (kb) (Figure 1.1) that is both capped and polyadenylated (Masters, 2006).

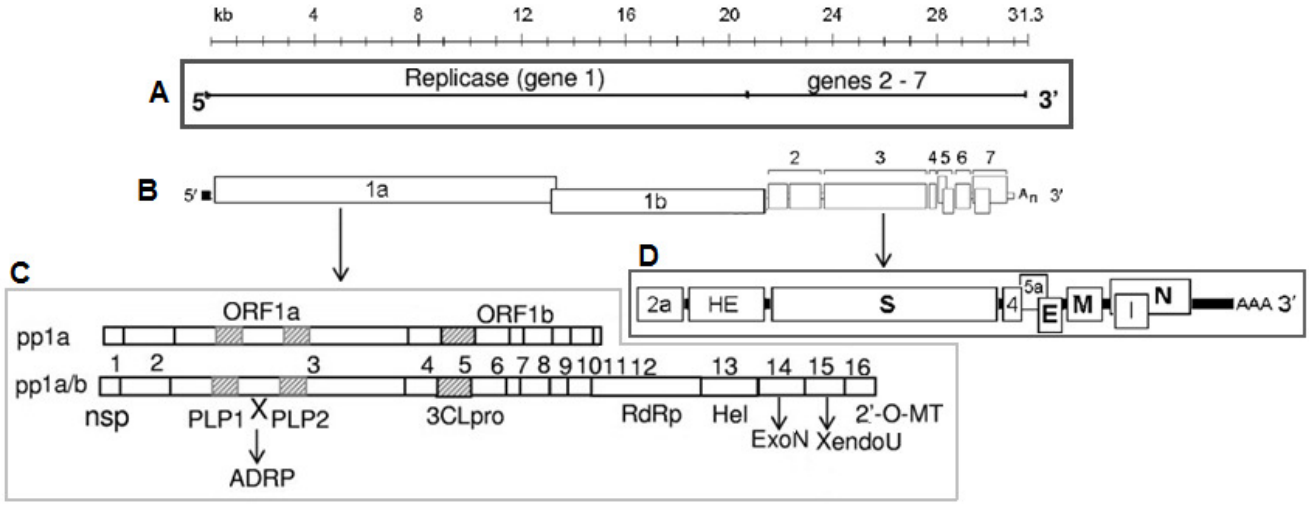


**Figure 1.1:** General structure of the coronavirus genome. **A**) Overview of the genome composition. **B**) The genome is comprised of various open reading frames (ORF) commencing with ORF1ab that comprises of all the non-structural proteins synthesized by the genome. ORF that encode for structural proteins follows along with accessory proteins that may vary between isolates. **C**) Displays several important ORF in the replicase gene that are used in coronavirus classification, including the PL regions (papain-like proteinases), ADP-ribose 1"-phosphatase (ADRP), chymotrypsin-like ($3CL^{pro}$) proteinase, the RNA dependent RNA polymerase, helicase, Exonuclease and XendoU/NendoU and methyl transferase. **D**) Displays the structural protein genes of the genome: the spike, envelope, membrane, and nucleocapsid genes as well as accessory genes such as 2a, 4 and 5a as well as the HE and I genes that are unique to Betacoronaviruses. (Parts A and B modified from Masters, 2006 (Permission to use from Elsevier Publisher, Licence no. 2901791212400); Parts C and D modified from Weiss and Navas-Martin, 2005).

## *I. Replication genes*

The genes that encode the enzymes for the replication of coronaviruses are located in the first open reading frame (ORF) of the genome. This ORF takes up two-thirds of the whole genome, and is expressed as two polyproteins (pp1a and pp1ab) that are cleaved by proteases also encoded by ORF1: papain-like proteases ($PL1^{pro}$ and $PL2^{pro}$) and 3C-like proteinase ($3CL^{pro}$) (Weiss and Navas-Martin, 2005). All nidoviruses (+ssRNA viruses) possess a highly conserved multi-domain replicase gene that is composed of various domains essential for both successful RNA synthesis as well as the production of complete progeny virions. Figure 1.2 illustrates the positions of various replicase polyprotein domains that will be discussed below including the 7 conserved domains that are used currently to discriminate between species within the 3 new genera (Gorbalenya *et al.*, 2006).

Typically coronaviruses possess a conserved heptanucleic acid sequence at the joining junction between ORF1a and 1b. This sliding sequence (UUUAAAC) followed by the sequence for a pseudoknot structure is translated by a -1 RNA- mediated ribosomal frame shift. As such, when translation occurs the sequence that should have been read as UUUAAACGGG becomes translated as UUUAAAC**C**GGG (Gorbalenya *et al.*, 2006; Woo *et al.*, 2010).

Papain-like proteinases are encoded within nsp 3, and cleave the ORF at several positions (Figure 1.2; at the orange and blue arrows). Interestingly, the $PL^{pro}$ encoded by *Avian coronavirus* IBV is not proteolytically active. For this reason, it is speculated that the PL domain may have additional functions in the replication cycle not purely proteolytic (Gorbalenya *et al.*, 2006).

The 7 domains listed below and in Table 1.1 are used to delineate species within the new coronavirus genera, meaning that if they belong to the same species they share a 90% amino acid identity in these 7 domains:

**Table 1.1: The 7 conserved domains of the replicase polyprotein (ORF1ab) that is used for the classification of coronaviruses.**

| Domain in replicase polyprotein: | Gene: |
|---|---|
| Nsp3 | ADP-ribose 1”-phosphatase (ADRP) |
| Nsp5 | 3C-like main proteinase (3CL) |
| Nsp12 | RNA dependent RNA polymerase (RdRp) |
| Nsp13 | Helicase with N-terminal Zn-binding domain (Z+Hel) |
| Nsp14 | 3’-to-5’ exoribonuclease (ExoN) |
| Nsp15 | Uridylate-specific endoribonuclease (NendoU) |
| Nsp16 | Ribose-2’-*O*methyltransferase (O-MT) |

**(Nsp=non-structural protein)**

- **ADP-ribose 1''-phosphatase**: ADRP which is referred to as X in Figure 1.2, is located at nsp3 with no known function (Gorbalenya *et al.*, 2006).
- **3C-like main proteinase**: The N-terminal part of polyprotein 1a contains the $3CL^{pro}$ gene as well as the flanking transmembrane domains (TM) (nsp 5 in Figure 1.2). The $3CL^{pro}$ processes highly conserved parts of the polyprotein, cleaving the C-terminal region of the polyprotein 1a and polyprotein 1ab at sites 8-11 (Gorbalenya *et al.*, 2006). This highly specific cleavage is conserved in all Nidoviruses.
- **RNA dependent RNA polymerase**: the RdRp gene is the largest conserved domain within the ORF and s responsible for RNA synthesis.
- **Helicase with N-terminal Zn-binding domain (ZBD and HEL1)**: The helicase domain and the ZBD are required for NTPase activity and nucleic acid duplex unwinding.
- **ExoN or 3'-to-5' exoribonuclease**: this enzyme is involved in coronavirus nucleic acid recombination, repair and proof- reading during RNA synthesis (Gorbalenya *et al.*, 2006).
- **Uridylate-specific endoribonuclease or NendoU**: this $Mn^{2+}$-dependent enzyme cleaves RNA (double stranded and less efficiently single stranded RNA) at specific uridylate-containing sequences. NendoU is important for RNA synthesis and the correct production of progeny virions.
- **Ribose-2'-*O*methyltransferase (O-MT)**: also encoded by the ORF1ab polyprotein is subsequently cleaved from the C-terminal of the polyprotein to be released as a mature enzyme (Gorbalenya *et al.*, 2006).

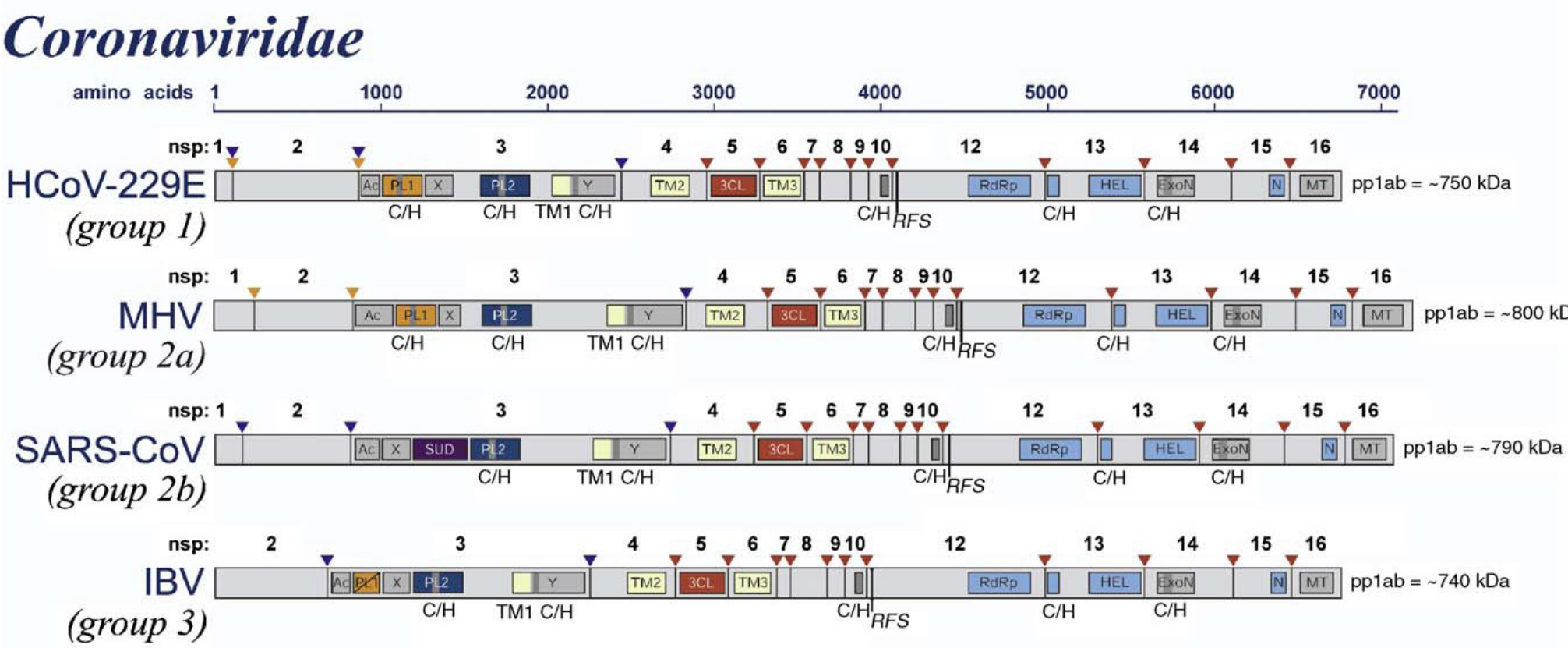


**Figure 1.2:** The domain organization for replicase pp1ab polyprotein of an alphacoronavirus, human coronavirus (HCoV) 229E, the betacoronaviruses, murine hepatitis virus (MHV) and SARS-CoV, as well as a gammacoronavirus, Infectious bronchitis virus (IBV). The arrows along the top of the genomes indicate sites that are cleaved by either papain-like proteinases (orange/blue) or chymotrypsin-like (3CLpro) proteinase in red. The proteolytic cleavage products are numbered as nsp1-16. TM: transmembrane domains; AC, X and Y: domains with conserved features; RdRp: RNA-dependent RNA synthesis; HEL: Helicase; ExoN: exonuclease; N or NendoU: Uridylate-specific endoribonuclease; MT: methyl transferase (Gorbalenya *et al.*, 2006, Permission to use from Elsevier Publisher, Licence no. 2880650826422).

## *II. Structural proteins*

There are typically 4 structural proteins encoded for by the coronavirus genome. These include the spike/peplomer (S) protein, the envelope (E) protein, the membrane (M) protein, and the nucleocapsid (N) protein that coils into a helically symmetrical nucleocapsid (Figure 1.3). The structural genes follow after ORF1, beginning with the spike protein and ending in the nucleocapsid protein gene and the genes are always sequentially present in the following order: S-E-M-N (Masters, 2006). The spike protein will be discussed in detail below since changes in the spike protein gene are responsible for the host species range and tissue tropism of different coronaviruses.

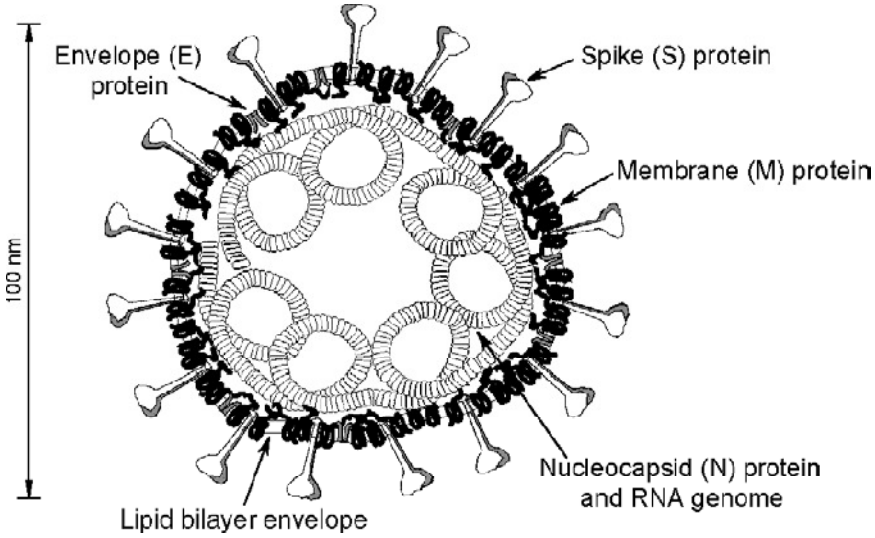


**Figure 1.3**: The coronavirus virion structure with annotations for structural proteins (Masters, 2006; Permission to use from Elsevier Publisher, Licence no. 2901791212400)

### *The spike protein*

The spike glycoprotein is responsible for receptor recognition and attachment as well as the fusion between the viral and host cell membranes. The spike protein can be divided into two sections, the S1 region or amino terminal region and the S2 region or the carboxy-terminal region. The protein forms trimers (Figure 1.4), which result in the typical coronavirus surface spikes that can be seen under electron microscopes. Only a small part of the S2 region of the spike protein is located inside the virion particle (the transmembrane and endodomain); the majority of the protein is encompassed by its ectodomain that includes the rest of the S2 region as well as the entire S1 region (Masters, 2006).

The S1 region of the spike protein is the most divergent part of the protein and may vary extensively even among strains of the same species. However, the S2 region may conversely be the most conserved region of the protein even across all coronavirus genera. The S1 region of the spike protein is the main component of the protein responsible for

receptor recognition. S1 binds to the receptor, resulting in conformational changes of the spike protein. The S2 region of the protein then causes the fusion between the viral and host cell membranes (Masters, 2006).

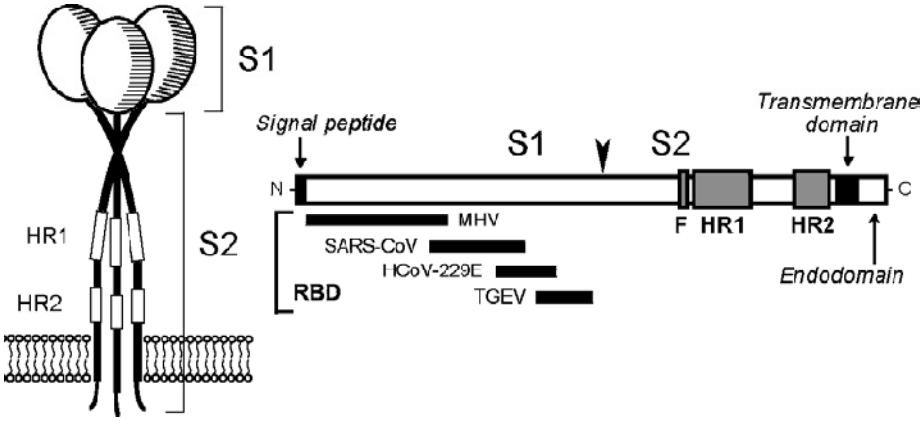


**Figure 1.4:** Structure of the spike protein showing the 2 subunits, S1 and S2. The arrow head between S1 and S2 indicates the protease cleavage position. The receptor binding domains (RBD) of 4 coronaviruses and the signal peptide region in S1 are also indicated on the linear map, as well as the heptad repeat regions (HR1 and 2), fusion peptide (F), transmembrane- and endodomains in the S2 region (Masters, 2006; Permission to use from Elsevier Publisher, Licence no. 2901791212400).

The morphology of the spike protein may change between the different coronavirus genera, and even within different species of the same genus. In the gammacoronaviruses and certain members of the betacoronaviruses the spike protein is usually cleaved into S1 and S2 by the host's trypsin-like protease in the Golgi apparatus (the arrow head in Figure 1.4). However, in some alphacoronaviruses as well as certain betacoronaviruses such as the SARS-HCoV, the spike protein remains uncleaved (Masters, 2006).

There are no universal receptors for coronaviruses. The receptors may be different within genera and even for coronaviruses specific to particular hosts. Table 1.2 indicates the receptors that are known for specific coronaviruses.

**Table 1.2: The known cellular receptors for existing coronaviruses**

| Genus | Coronavirus | Receptor | Host | Reference |
|---|---|---|---|---|
| *Alphacoronavirus* | TGEV | Porcine aminopeptidase N | Pig | Delmas *et al.*, 1992 |
| | PRCoV | Porcine aminopeptidase N | Pig | Delmas *et al.*, 1994 |
| | FIPV | Feline aminopeptidase N | Cat | Tresnan *et al.*, 1996 |
| | FCoV | Feline aminopeptidase N | Cat | Tresnan *et al.*, 1996 |
| | CCoV | Canine aminopeptidase N | Dog | Benbacer *et al.*, 1997 |
| | HCoV-229E | Human aminopeptidase N | Human | Yeager *et al.*, 1992 |
| | HCoV-NL63 | Human angiotensin-converting enzyme 2 (ACE2) | Human | Hofmann *et al.*, 2005 |
| *Betacoronavirus* | MHV | Murine CEACAM1 and 2• | Mouse | Nedellec *et al.*, 1994 |
| | BCoV | 9-*O*-acetyl sialic acid | Cattle | Schultze *et al.*, 1991 |
| | SARS-CoV | Human angiotensin-converting enzyme 2 (ACE2) | Human | Li *et al.*, 2003 |
| | HCoV-OC43 | Neu5, 9Ac2-containing moiety | Human | Weiss and Navas-Martin, 2005 |
| *Gammacoronavirus* – no receptors have been determined | | | | |

• CEACAM1/2= Carcinoembryonic antigen-related adhesion molecule 1 and 2

The majority of alphacoronaviruses (for which receptors are known) appear to utilize the aminopeptidase N enzyme (CD13) of their respective host species. The zinc-binding protease is located on the host cell surface and is associated with small peptide digestion at epithelium cells of the enteric and respiratory system. However, the receptor is also found on human neural tissue, making it susceptible to the human coronavirus HCoV-229E. Interestingly, HCoV-229E and the other human alphacoronavirus HCoVNL63 have been found not to use the same receptor (Table 1.2). Instead HCoVNL-63 uses angiotensin-converting enzyme 2 (ACE2) as its receptor, also a zinc-binding carboxypeptidase, the same receptor that the betacoronavirus SARS-HCoV uses (Masters, 2006). Table 1.2 shows the variety of receptors used by the betacoronaviruses.

### *III. Non-essential proteins*

There are several genes present in coronavirus genomes that encode proteins that are termed 'accessory'. These proteins are considered non-essential as they are not required for viral growth in cell culture (Gorbalenya *et al.*, 2006). It is believed that the accessory genes may have roles in enhancing replication as well as virulence within the natural host. Accessory genes may be specific to a group of coronaviruses in a phylogenetic cluster or specific to single species:

- SARS-HCoV contains a unique domain in its nsp 3 region that is termed SUD. The domain is apparently capable of tolerating substitutions and deletions that have negligible effects on viral replication (Snijder *et al.*, 2003).
- Some members of *Betacoronavirus* 1 such as BCoV and the *Murine coronavirus* (MHV) possess an additional structural protein, namely the hemagglutinin-esterase (HE) protein that forms a second spike protein. The gene encoding the HE protein may possibly have been obtained from a recombination event with an influenza virus, presumably Influenza C (Weiss and Navas-Martin, 2005).
- In addition some of the members of *Betacoronavirus* genus also possess the internal (I) protein. This nonessential protein of unknown function is usually encoded within the ORF of the N protein.
- Each strain of coronavirus species may possess its own set of unique accessory genes. Many of the newly discovered bat coronaviruses possess numerous additional genes for which no function is known.

## 1.2.2 Coronavirus genome plasticity

Coronaviruses, being RNA viruses, are subject to higher mutation rates than DNA viruses. The RNA dependent RNA polymerase (RdRp) of coronaviruses lack the proof reading capability that many DNA polymerases possess, thus resulting in a relatively high mutation rate in the genomes of coronaviruses, namely 1 error every replication cycle (Holmes and Rambaut, 2004). The high mutation rate in the coronaviruses will produce a large population of genetically variable viruses, some possibly more capable of crossing species barriers through rapidly adapting to new receptors and establishing productive infections. However, it is this high mutation rate experienced by RNA viruses that puts a limit to their maximum genome size and therefore sets a limit to the maximum adaptation complexity that these viruses may reach.

Coronaviruses are the largest RNA viruses and are faced with issues of rapid mutation frequencies and genome size (Holmes and Rambaut, 2004). In order to make up

for the small space available in the genome, RNA viruses such as the coronaviruses encode multiple functions in overlapping regions of the genome. Due to this very few nucleotides are 'allowed' to vary, since missense and nonsense mutations may lead to altered protein structure/activity and hence influence the fitness of the viruses.

The recombination frequencies of coronaviruses are speculative. It is presumed that coronaviruses are capable of frequent recombination (due to the discontinuous replication of the genome) with other coronaviruses as well as other viruses such as influenza, during co-infection of the same host cell. Potential recombination opportunities have been reported by Lau *et al*. (2007) with the discovery of several bat-CoV, *Rhinolophus bat coronavirus HKU2* and the SARS*r-Rh*-BatCoV, infecting the same host on multiple occasions. As discussed above, it is also believed that the hemagglutinin-esterase gene possessed by some betacoronaviruses was obtained through a recombination event with influenza C virus (Holmes and Rambaut, 2004). These combined factors has lead to a rapid evolutionary rate which is capable of generating new strains of coronaviruses that are able to adapt to new host species (Woo *et al.*, 2006a).

## 1.3 Coronavirus taxonomy

### 1.3.1 Coronavirus taxonomy based on antigenic relatedness

Coronaviruses belong to the family *Coronaviridae* in the order *Nidovirales*, which encompasses all positive sense, single stranded (ss) RNA viruses. Previously all known coronaviruses have been classified into the genus *Coronavirus* and subsequently into one of three phylogroups (Figure 1.5). Groups 1 and 2 are composed of mammalian and human coronaviruses while group 3 consists mainly of avian coronaviruses. The phylogroups were separated based originally on serological cross-reactivity and later also on genome sequence analysis and unique accessory proteins (Gorbalenya *et al.*, 2004; Weiss and Navas-Martin, 2005).

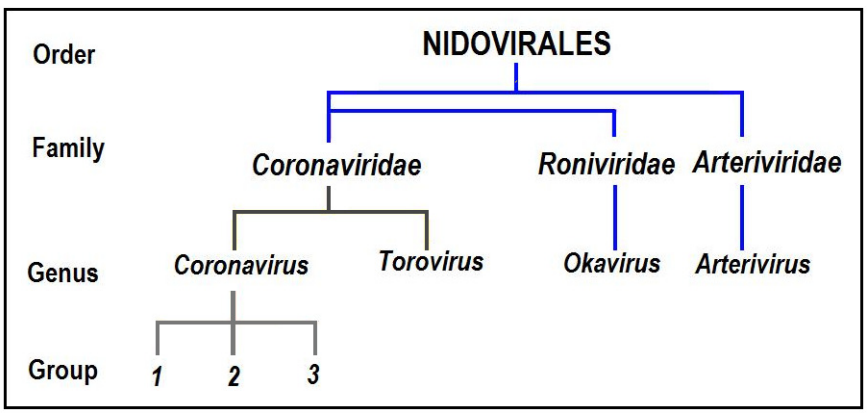

**Figure 1.5**: Nidovirus taxonomy utilised until 2009, which phylogenetically groups the *Coronavirus* genus into 3 groups based on antigenic relatedness (Modified from the ICTV Virus Taxonomy: 2009 release).

Group 1 coronaviruses contain the human coronaviruses HCoVNL63 and HCoV229E that predominantly cause mild respiratory infections. Other group 1 coronaviruses include the mammalian coronaviruses canine CoV (CCoV), feline infectious peritonitis (FIPV), and the porcine coronaviruses: porcine epidemic diarrhea virus (PEDV) and porcine transmissible gastroenteritis virus (TGEV) (Weiss and Navas-Martin, 2005).

The group 2 coronaviruses contains the human coronavirus HCoVOC43 (a common cold virus) and newly identified human coronavirus HKU1 (causes more severe respiratory tract infections). The mammalian coronaviruses in group 2 consist of bovine CoV (BCoV), porcine hemagglutinating encephalomyelitis virus (PHEV) and murine hepatitis virus (MHV). Group 3 coronaviruses are the avian coronaviruses such as avian IBV and turkey coronavirus (TCoV) (Gonzãlez *et al.*, 2003).

The first concerns with the classification system based on antigenic cross-reactivity began in the 1990s, when PEDV and HCoV229E were discovered. The new coronaviruses were difficult to classify as they had characteristics that conflicted with the classification system and did not share antigenic cross-reactivity to any members of the known coronavirus groups. However, sequence information of the new coronaviruses clustered with group 1 coronaviruses. PEDV and HCoV229E also shared a unique ORF specific to group 1 coronaviruses, though the viruses were phylogenetically very different from other group 1 coronaviruses such as TGEV (Gorbalenya *et al.*, 2004).

The International Committee on Taxonomy of Viruses (ICTV) chose to officially recognize PEDV and HCoV229E as members of group 1 coronaviruses rather than creating a new group to incorporate these viruses, thereby changing the classification criteria for coronaviruses from the antigenic cross-reactivity of groups and the properties of the viral proteins to a classification based on full length genome sequences and the genetic relationships that can be discerned from them (Gorbalenya *et al.*, 2004). This approach is scrutinized and there are no definitive guidelines developed to deal with future classification difficulties yet.

### 1.3.2 Emergence of SARS-CoV

When SARS emerged in 2003 and the full genome sequence generated, initial phylogenetic analysis showed that it did not cluster with any of the previously known groups. SARS-CoV displayed a pattern of unique ORF in the 3' end of the genome, as well as a unique internal gene organization of the replicase gene's subunit nsp3. It contains a

large domain termed SUD and possesses only one papain-like protease gene domain instead of two as is seen in other coronaviruses.

Marra *et al*. (2003) proposed that SARS-CoV should be classified into a putative group 4. However, when the individual gene segments of SARS-CoV was compared with other existing coronaviruses it consistently showed that SARS-CoV grouped as a sister group to group 2 coronaviruses. This indicated that SARS-CoV may have diverged earlier from another group 2 coronavirus and thus Snijder *et al*. (2003) proposed that it should be classified as a subgroup of group 2, subgroup 2b. SARS was thus classified as a group 2b coronavirus by the ICTV (Vijaykrishna *et al*., 2007).

When SARS and newly discovered bat SARS-related coronaviruses were phylogenetically compared to existing coronaviruses (also using pair-wise comparisons) it revealed that both coronaviruses shared a low sequence homology to group 2 and group 3 coronaviruses. The authors Tang *et al*. (2006) suggested yet again that they be classified as a new group, putative group 4 along with putative group 5 for the novel coronaviruses that so far has exclusively occurred in bats.

### 1.3.3 New Coronavirus taxonomy

However in 2008, due to the increasing diversity of coronaviruses among all phylogroups (resulting in the creation of various subgroups: 1a, 1b, 2a, 2b, 2c, 2d, 3a, 3b, 3c, 3d) the ICTV (CODE 2008.085-126V) regrouped and renamed the coronaviruses taxonomy, mainly to replace the 3 phylogroups with genera. Within the order of *Nidovirales*, the family *Coronaviridae* was split into two subfamilies, the *Coronavirinae* and *Torovirinae* (Figure 1.6). The old phylogroups within the subfamily were reorganized in genera and renamed as *Alphacoronavirus, Betacoronavirus* and *Gammacoronavirus* (ICTV Virus Taxonomy: 2009 release).

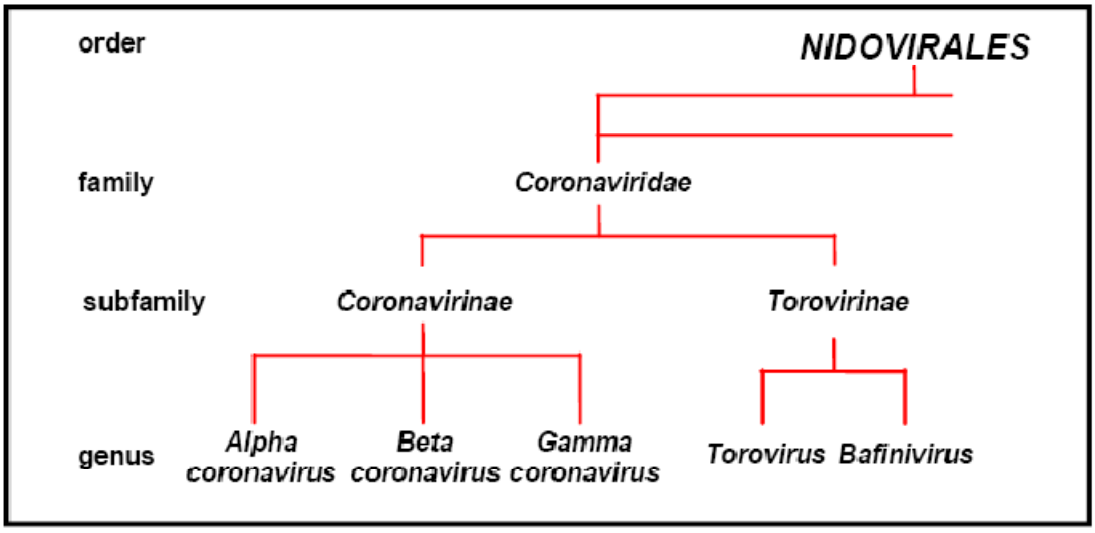

**Figure 1.6:** The current taxonomic organization of the *Nidovirales* order as proposed by the ICTV. The new taxonomy elevates the previous *Coronavirus* genus to a subfamily and the previously known phylogenetic groups within the genus are now themselves elevated to genus level.

The revision of the taxonomy was justified based both on rooted phylogeny and pair-wise comparisons performed using 7 family-wide (*Coronaviridae*-specific) conserved domains in the replicase polyprotein 1ab (Table 1.1) along with the structural protein's genes (spike, envelope, membrane and nucleocapsid protein). In these rooted trees coronaviruses tend to form 3 separate monophyletic groups. The intergroup pair-wise amino acid identity scores between the structural and nonstructural protein genes for the older, previously known coronaviruses are comparable to those in genera of various other RNA virus families. Thus, the ICTV proposed to change the phylogroups into separate genera.

The species boundary criteria set up by the ICTV is as follows:

i. New coronaviruses are assigned to a species within a genus based on both pair-wise comparisons and rooted phylogeny of the 7 conserved *Coronaviridae*-specific domains of the replicase gene (Table 1.1). Members of a genus share greater than 90% amino acid identity in these 7 conserved domains.
ii. Only complete genome sequences for newly discovered coronaviruses are considered for taxonomy, and new species are designated within a genus when the genome shares less than 90% amino acid identity within the 7 ORF 1 domains and possesses a unique set of accessory proteins.

Table 1.3 and Figure 1.7 shows the current classification of the known coronaviruses (for which full genome sequences are available) into species. As of yet, only 3 genera are recognized by the ICTV but a 4$^{th}$ genus (*Deltacoronavirus*) has been proposed by Woo *et al*., (2010), which would include the newly identified avian coronaviruses such as Bulbul CoV HKU11, Thrush CoV HKU12 and Munia CoV HKU13.

The previously referred to 'SARS-like' bat coronaviruses were named the *SARS related coronavirus* species cluster and as such all future references to these bat coronaviruses will be made according to the ICTV classification.

**Table 1.3: The current classification of coronavirus species within the three genera designated by the new classification system set up by the Coronavirus research group of the ICTV.**

| **Genus Alphacoronavirus (previously group 1)** | | |
|---|---|---|
| **Species:** | **Members of the species/abbreviation:** | **Additional Comments:** |
| *Alphacoronavirus 1* | • *Feline coronavirus* (FCoV)<br>• *Canine coronavirus* (CCoV)<br>• *Transmissible gastroenteritis virus* (TGEV) | *Alphacoronavirus 1* also called *Geselavirus* is a new species that is composed of closely related coronaviruses in domestic animals (all FCoV and CCoV, as well as TGEV). All members of this species contains either one (NS7a) or two (NS7a and NS7b) ORF downstream of the N gene. |
| *Human coronavirus 229E* | • HCoV229E | Existing coronavirus |
| *Human coronavirus NL63* | • HCoVNL63 | Existing coronavirus |
| *Porcine endemic diarrhea virus* | • PEDV | Existing coronavirus |
| *Rhinolophus bat coronavirus HKU2* | • *Rh*-BatCoV HKU2 | New species |
| *Scotophilus bat coronavirus 512/05* | • *Sc*-BatCoV 512 | New species |
| *Miniopterus bat coronavirus 1* | • *Mi*-BatCoV 1 | New species |
| *Miniopterus bat coronavirus HKU8* | • *Mi*-BatCoV HKU8 | New species |
| **Genus Betacoronavirus (previously group 2)** | | |
| **Species:** | **Members of the species/abbreviation:** | **Additional Comments:** |
| *Betacoronavirus 1* | • *Bovine coronavirus* (BCoV)<br>• *Porcine hemagglutinating encephalomyelitis virus* (PHEV)<br>• *Human enteric coronavirus* (HECV)<br>• *Human coronavirus OC43* (HCoVOC43)<br>• *Equine coronavirus* (EqCoV)<br>• *Canine respiratory coronavirus* (CRCoV) | *Betacoronavirus 1* is a new species comprised of previously established group 2 coronaviruses of humans, cattle, swine, horses and a newly recognized virus of dogs. For all members of *Betacoronavirus 1* there are full genome sequences available (except for HECV and CRCoV) and there is above 96% identity in the specified ORF 1ab domains, justifying the inclusion of the viruses into one species. |
| *Murine coronavirus* (MuCoV) | • *Murine hepatitis virus* (MHV)<br>• *Rat coronavirus* (PRC)<br>• *Puffinosis virus* (PCoV) | The new species *Murine coronavirus* accommodates the previously established Coronaviruses of mice, rats and a coronavirus allegedly from puffins (a murine coronavirus variant). There is only a complete genome sequence available for MHV, and the sequence identity within the ORF 1ab domains to other *Betacoronaviruses* is below the species demarcation threshold of 90%. |

| | | |
|---|---|---|
| *Human coronavirus HKU1* | • HCoV HKU1 | New species |
| *Rousettus bat coronavirus HKU9* | • *Ro*-BatCoV HKU9 | New species |
| *Tylonycteris bat coronavirus HKU4* | • *Ty*-BatCoV HKU4 | New species |
| *Pipistrellus bat coronavirus HKU5* | • *Pi*-BatCoV HKU5 | New species |
| *SARS-related coronavirus* (SARSr-CoV) | • SARS*r-Rh*-BatCoV HKU3<br>• SARS-HCoV<br>• SARS*r-Rh*-BatCoV RP3 | *SARS-related coronavirus* is a new species that is to replace the existing uncertainty in classification among the SARS and SARS-related coronaviruses. The SARS-CoV of humans and animals such as palm civets, raccoon dogs, Chinese ferret badgers and bats are all included within this species. The species thus also includes the distantly related SARS-BatCoV isolates such as *SARS-Rh*-BatCoV HKU3, SARS*r-Rh*-BatCoV and *SARSr-Rh*-BatCoV 273. These viruses (29 separate coronaviruses) share >97% amino acid sequence identity in the specified ORF1ab domains which is far above the species demarcation threshold of 90%. |

**Genus Gammacoronavirus (previously group 3)**

| **Species:** | **Members of the species/abbreviation:** | **Additional Comments:** |
|---|---|---|
| *Avian coronavirus* | • *Infectious bronchitis virus* (IBV)<br>• *Turkey coronavirus* (TuCoV)<br>• *Duck coronavirus* (DuCoV)<br>• *Goose coronavirus* (GoCoV)<br>• *Pheasant coronavirus* (PhCoV)<br>• *Pigeon coronavirus* (PiCoV) | *Avian coronavirus* is a new *Gammacoronavirus* species composed of new and existing avian coronaviruses such as IBV. The sequence identity between IBV and TuCoV of the ORF 1ab domains are greater than 94%, again far over the species demarcation threshold that requires only 90% amino acid identity. Only partial sequences are available for the remaining avian coronaviruses such as DuCoV, GoCoV, PhCoV, and PiCoV. These viruses were assigned to the *Avian coronavirus* species since they were previously known to be related to both IBV and TuCoV. |
| *Beluga whale coronavirus SW1* | • *Beluga whale coronavirus SW1* (BWCoV SW1) | *Beluga whale coronavirus* SW1 must be designated to a new species due to the highly divergent sequence comparisons of the conserved ORF1ab domains between it and other Gammacoronaviruses. The amino sequence identity with *Avian Coronavirus is* <67%, significantly below the required 90% species demarcation threshold. |

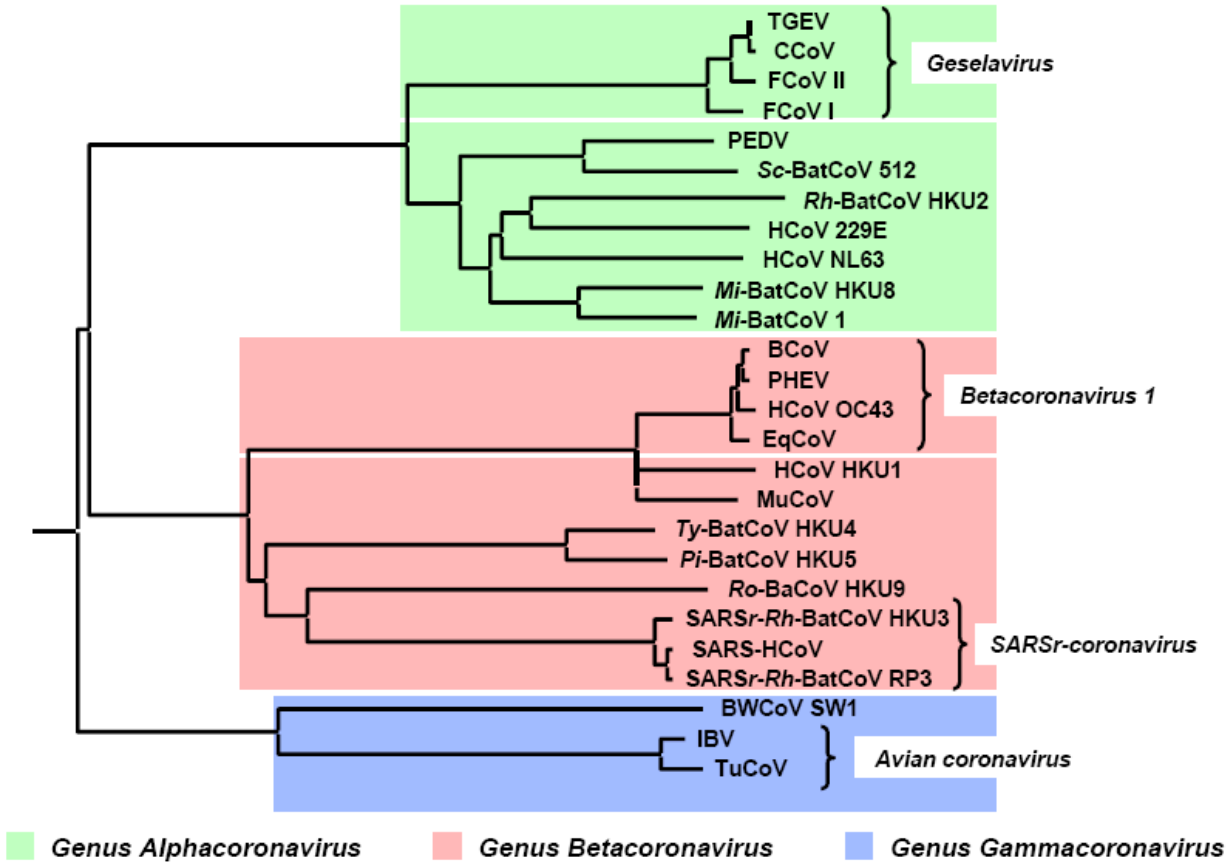


**Figure 1.7:** Neighbour-Joining phylogenetic tree of the RdRp gene multiple amino acid alignments. The tree shows the relationships between the newly proposed CoV genera as well as the relationships between the members of the new species *Alphacoronavirus 1*, *Betacoronavirus 1, Severe acute respiratory syndrome-related coronavirus* and *Avian coronavirus* (ICTV Virus Taxonomy: 2009 release).

Certain virology terminology such as strain, genotype and lineage are regularly used and often interchangeably. For clarification, in the subsequent text, the term 'lineage' is used in an evolutionary capacity. A lineage refers to a line of descent, and new species are the results of speciation from direct ancestor species i.e. it was suggested that the SARS related coronavirus species cluster spilt-off early from the *Betacoronavirus* lineage and diverged into the currently known clade (Woo *et al.*, 2010).

Genotypes of a species refer to the genetic variants that exist in that species. A strain refers to individual virus subtypes of a species that could be grouped into a genotype. The terms strain and genotype are best resolved with the example of the novel human coronavirus HKU1. Studies analysing different strains of the HCoV-HKU1 virus identified several instances of recombination events between different strains. As such the HCoV-HKU1 virus could be divided into 3 genotypes; genotype A consisting of 13 HCoV-HKU1 stains, genotype B consisting of 3 HCoV-HKU1 stains and genotype C consisting of 6 HCoV-HKU1 stains (Woo *et al.*, 2006b).

## 1.4 Coronavirus pathogenesis and immune responses

Coronaviruses (CoV) generally cause either respiratory tract or gastrointestinal infections in domestic and wild mammals and birds, and only respiratory tract infections in humans. The infections may be either acute or chronic affecting either the enteric or central nervous systems depending on the coronavirus causing the infection.

### 1.4.1 Human Coronaviruses

Prior to the identification of SARS-CoV, only 2 human coronaviruses (HCoV) were known to exist, HCoV-229E (*Alphacoronavirus*) and HCoV-OC43 (*Betacoronavirus*). Both of these HCoV were known as viruses that cause the common cold, only resulting in mild upper respiratory tract infections. However after the identification of the first CoV to cause a severe respiratory infection in humans, SARS-CoV (*Betacoronavirus*), an additional 2 HCoV was identified; HCoV-HKU1 (*Betacoronavirus*) and HCoV-NL63 (*Alphacoronavirus*). The HCoV-HKU1 was identified in China from a patient with severe pneumonia and HCoV-NL63 was identified in the Netherlands from a patient suffering from bronchiolitis and conjunctivitis. HCoV-NL63 is typically associated with children and the elderly and has also subsequently been identified in other parts of the world, in another part of Europe (Belgium), in Asia (Hong Kong and Japan), North America (Canada) and Australia. Compared to the animal coronaviruses, very little is known about the pathogenesis of human coronaviruses.

### 1.4.2 Mammalian Coronaviruses

There are several economically important CoV infecting domestic animals. One such virus is transmissible gastroenteritis virus (TGEV), which causes enteritis and foetal diarrhea in swine. In adult pigs only mild gastroenteritis is typically observed, however the virus is particularly significant in newborn piglets as it results in high mortality rates leading to large economic losses. TGEV infects the epithelia of the small intestine leading to possibly fatal gastroenteritis. Infections of the respiratory tract have also been observed resulting in respiratory complications. Porcine respiratory coronavirus (PRCoV) is a naturally occurring attenuated form of TGEV that infects the epithelia of the respiratory tract and lungs. Infections of PRCoV can result in interstitial pneumonia. The genomes of TGEV and PRCoV share 96% nucleotide identity, with large deletions present in the spike gene of PRCoV when compared to the TGEV spike gene. These deletions are capable of altering the tropism of PRCoV as well as decrease the virulence of the virus.

Porcine endemic diarrhea virus (PEDV) occurs in swine in Europe, Asia and North America and like TGEV causes gastroenteritis with increased severity in younger pigs., No

cross serological protection is conferred between PEDV and TGEV and it is more similar to the human CoV 229E (it is capable of replicating in Vero cells) than to TGEV.

Serology of cattle worldwide shows that bovine coronavirus (BCoV) is universal. BCoV is capable of causing both respiratory and gastrointestinal infections resulting in calf diarrhea and winter dysentery in adults. No vaccines are available for BCoV. Like BCoV, another well known betacoronavirus is murine hepatitis virus (MHV) and is possibly the most studied coronavirus. MHV exists as numerous strains and each strain possesses different tissue tropism and virulence. Typically, MHV causes hepatitis and encephalitis in mice and is capable of causing progressive demyelinating encephalitis, and as such is studied for its applications in the treatment of multiple sclerosis.

Canine coronavirus (CCoV) is capable of replicating within the intestinal mucosa of dogs and as such can cause either mild or severe gastrointestinal infections of dogs. Feline coronavirus exist as two variants, feline enteric coronavirus (FeCoV) and feline infectious peritonitis virus (FIPV). FeCoV replicated in feline in an asymptomatic carrier state and persistent infections may result in FIPV, a severe and fatal viral infection. FIPV not only replicates within the epithelia of the respiratory and intestinal tracts, but also invades and replicates within macrophages resulting in viremia and systemic infection that can cause both ocular and neurologic complications. There are also no successful vaccines available against FIPV.

Since the identification of SARS-CoV in 2002, additional mammalian CoV have also been identified in beluga whales (Mihindukulasuriya et al. 2008), arctic seals (Nollen et al. 2010) giraffes (Hasoksuz et al. 2007), Asian leopard cats and ferret badgers (Dong et al. 2007) etc. However beyond the initial identification no additional information is available for the pathogenesis of these viruses.

### 1.4.3 Avian Coronaviruses

Several avian coronaviruses exist that cause large scale economic losses in the poultry industry. The most important and well known virus is infectious bronchitis virus (IBV). This severe respiratory virus is spread through aerosols and as such is highly contagious and has a high fatality rate in chicks. IBV replicates in the epithelia of the upper respiratory tract as well as the bronchi. IBV infection may also result in more severe complications.

## 1.5 The SARS Coronavirus

### 1.5.1 SARS Coronavirus

The SARS coronavirus (SARS-CoV) was identified as the etiological agent of SARS. The virus was identified by isolation from infected human lung tissue and sputum and inoculated into Vero E6 cells. SARS-HCoV infects humans and is very closely related to the SARS-CoV that infects in palm civets (an intermediate host) and several other animals present in the animal markets of Hong Kong and Guangdong, China. SARS infection is accompanied with a wide scope of clinical features such as lower respiratory tract infection, fever, diarrhea, and lymphopenia. The main route of infection of the virus may be air-borne via sputum droplets, though transmission may include alternate routes such as blood or fecal-oral transmissions (Weiss and Navas-Martin, 2005).

### 1.5.2 SARS outbreaks

The SARS epidemic occurred in two separate outbreaks. The first started in November 2002, lasting from November to July, 2003. The first outbreak caused more than 8,000 infections, resulting in more than 700 deaths. Later in 2003, in the same region in China that the first outbreak occurred, sporadic outbreaks of SARS were reported that finally dissipated in early 2004 (Wang *et al.*, 2006).

Molecular epidemiological studies performed by Song et al. (2005), revealed that the SARS-HCoV from the later outbreaks was not derived from the same SARS virus as in the earlier outbreaks. The SARS-HCoV from 2002-2003 possessed a 29-bp deletion in ORF 8a/b that was not present in the SARS-HCoV from the 2003-2004 sporadic outbreaks, indicating that two independent species cross-over events may have occurred. The milder SARS-HCoV from the later outbreaks was most likely derived from the common ancestor coronavirus that also does not share this 29-bp deletion which was discovered in the more virulent strains of SARS-HCoV in 2002-2003.

This may also indicate that future SARS outbreaks can be expected (Wang *et al.*, 2006), especially with different SARS-related coronaviruses being discovered from bat populations in different regions of China. Thus, understanding the coronavirus reservoir distribution and mode of transmission to new species becomes essential in order to understand the spread and occurrence of future outbreaks.

### 1.5.3 The possible reservoir of SARS-CoV

It was suspected that the SARS epidemic may have been as a result of a zoonotic transmission from an unknown animal reservoir to humans, and several animals in the wild animal markets in China were sampled and analyzed for the presence of the SARS

virus or antibodies (Guan *et al.*, 2003; Kan *et al.*, 2005). The samples taken from the animals as well as surfaces in the markets were tested with an RT-PCR assay to detect the presence of viral nucleic acid, as well as virus isolation attempts and detecting the presence of neutralizing antibodies in the sera of the animals.

After the initial SARS outbreak several palm civets and a raccoon dog tested positive for coronavirus RNA with the RT-PCR assay that was designed to target the nucleocapsid gene (Guan *et al.*, 2003). SARS-CoV was successfully isolated in cell culture from 4 palm civet specimens (2 of which also were positive with the RT-PCR) as well as from the raccoon dog specimen. Five sera samples (from palm civets, raccoon dog and a Chinese ferret badger) tested positive for neutralizing antibodies against the SARS-CoV. When it became apparent that palm civets were somehow involved in the SARS epidemic, all market civets were culled. Re-introduction of civets into the markets was allowed after the 2002-2003 SARS epidemic was stopped.

Analysis of the animal markets during the 2003-2004 outbreaks of SARS showed that the animal markets were very highly contaminated with SARS-CoV (Kan *et al.*, 2005). Palm civets, raccoon dogs and several other animal species were swabbed and analysed for SARS-CoV as well as random swabs of animal cages, cash tables and walls in 4 blocks of the market. All palm civets (n=91) and raccoon dogs (n=15) analysed were positive for SARS-CoV and 22 of 24 environmental swabs were also shown positive for SARS-CoV. Of note is that the SARS-CoV sequences obtained from the market swabs did not possess the same 29-bp deletion present in the epidemic SARS-HCoV.

More than 10 mammalian species have experimentally been shown to be susceptible to infection by SARS, including rats, which are among the species that display asymptomatic infections. It is thus suspected that if the SARS-CoV spread to rats during any of the previous outbreaks, that they may have been responsible for aiding the spread of the virus to humans and could do so again in future with another outbreak (Wang *et al.*, 2006).

Palm civets were considered to be an intermediate host for the SARS virus. However, there are no viruses similar to SARS-CoV found in wild palm civets or in palm civets on breeding farms as would be expected if the virus originated from these animals (Lau *et al.*, 2007). A study by Kan *et al.* (2005) sampled palm civets from 25 civet farms in 12 different provinces (which supply the Hong Kong and Guangdong animal markets) for the presence of similar coronaviruses, though none were found. SARS-CoV was only detected in market civets with viral titres peaking at approximately day 7 after introduction into the market. The civets have also been shown to shed the virus periodically as well as remain persistently infected, with virus found in the spleen even at 35 days after experimental infection. It can thus be concluded that exposure from the reservoir or other

intermediate hosts, initiates in the animal markets and that certain animal species in the market are capable of maintaining the virus for long periods of time.

Serological surveys were also performed on the sera taken from wild life traders in the markets during the initial SARS outbreak. The sera were tested for antibodies by neutralization assays and indirect immunofluorescence assays. None of the traders indicated that they experienced any SARS-related coronavirus symptoms though the surveys revealed that they possessed antibodies against SARS and SARS-related viruses, indicating past exposure to the virus (Guan *et al.*, 2003).

Bats were also tested for the presence of SARS-CoV. In 2005, Li *et al.*, reported that the natural reservoirs of SARS-CoV may be *Rhinolophus* spp. commonly referred to as the Chinese horseshoe bats. Four species of bats from the *Rhinolophus* genus analysed (from two provinces) by either serological methods or by PCR assays tested positive for infection by a SARS-related coronavirus, which includes the species *Rh. pearsoni, Rh. macrotis, Rh. pussilus and Rh. ferrumequinum*. Approximately 84% of the *Rh. sinicus* tested possessed antibodies to a recombinant nucleocapsid protein of SARS. According to the authors, such a high seroprevalence and wide distribution of seropositive bats is in accordance to what would be expected from a natural reservoir host.

The bat SARS-related coronaviruses were closely related to the human and civets SARS-CoV. The human and civet SARS-CoV share a 92% overall sequence identity to SARS*r-Rh*-BatCoV Rp3 (*Rh. pearsoni* corrected to *Rh. sinicus*) (Yuan *et al.*, 2010), and an 88% overall sequence identity to SARS*r-Rh*-BatCoV HKU3 (also *Rh. sinicus*). The overall nucleotide sequence identity between SARS*r-Rh*-BatCoV Rp3 and SARS*r-Rh*-BatCoV HKU3 is 89%. There is also greater sequence diversity between the bat SARS-related CoV than between the human and civet SARS-CoV.

As would be expected, the most variable region of the genomes was in the S1 domain of the spike protein. Another highly variable region is in ORF 10 (also known as ORF 8) that lies upstream of the nucleocapsid protein (Wang *et al.*, 2006). This is the same region that contained the 29-bp deletion in the highly virulent late phase SARS-HCoV from the 2002-2003 though not present in the palm civet SARS, human SARS from the 2003-2004 outbreak and bat SARS- related viruses. This would also indicate that the SARS-CoV and bat SARS- related CoV share common ancestors (Wang *et al.*, 2006).

The natural reservoir of a virus usually displays no clinical symptoms of infection due to the co-evolution of host and virus (Wang *et al.*, 2006). Palm civets and many other animal species in the live animal market experienced clinical symptoms to natural SARS-CoV infection. The wild life traders in the wet markets were also reported to possess antibodies against the virus, possibly as a result of regular contact with the source of the virus. It is thus speculated that many animals in the markets act as intermediate amplifier

hosts for SARS-CoV and that *Rhinolophus* spp. may be a reservoir source for the virus since several SARS-related CoV species of have been detected in a number of *Rhinolophus* species, though the virus appears to be asymptomatic in the bats.

## 1.6 Coronaviruses detected in bat species

### 1.6.1 Bat Coronavirus species diversity

The search for coronaviruses in bats began after the discovery of a SARS- related coronaviruses in bat species from the genus *Rhinolophus*. Analysis of bat species started in Asia and continued with several studies in Europe, North and South America as well as Africa. A diverse range of coronavirus species were discovered in bats, more so than in any other mammalian species, though extensive surveillance for coronaviruses had thus far only been performed within bat species. Due to the newly discovered bat coronavirus (BtCoV) diversity, the previous classification of coronaviruses had to be adjusted to encompass the large diversity of new BtCoV.

Publications that identified new BtCoV submitted suggestions as to how to classify the new viruses into the previously known phylogroups (Tang *et al.*, 2006; Woo *et al.*, 2006a), mostly by creating either subgroups within the phylogroups or by creating new phylogroups. An example of this would be that Marra *et al.* (2003) proposed that the SARS-CoV and SARS-related CoV be classified into a new phylogroup, group 4, due to the fact that the viruses were sufficiently different from other existing coronaviruses. Snijder *et al.* (2003) however proposed that SARS-CoV be classified within the existing group 2 coronaviruses as subgroup 2b since the SARS-CoV cluster shared common ancestry with other group 2 coronaviruses. Many newly discovered BtCoV were similar to existing group 1 and 2 coronaviruses and as such were temporarily classified into subgroups 1b, 2c, 2d etc. The new classification criteria discussed in Section 1.3, changed phylogroups to genera and as such the coronaviruses within the ‘subgroups’ would become species within the respective genera (on the condition that the viruses in the subgroups met the specific species delineation criteria).

The newly identified BtCoV will be discussed below according to the continent it was identified on. However, there are no full sequences available for most BtCoV and as such very few have been formally classified according to the new classification criteria. Thus in the next section, each BtCoV will be referred to as reported in the original publication.

### 1.6.2 Asia

The BtCoV detected in Asian countries are listed in Table 1.4 along with their host species. A total of approximately 30 BtCoV have been identified from 18 bat species in the *Pteropodidae, Vespertilionoidea, Rhinolophidae* bat families (Poon *et al.*, 2005; Li *et al.*, 2005; Tang *et al.*, 2006; Woo *et al.*, 2006a; Woo *et al.*, 2007; Lau *et al.*, 2010a; Lau *et al.*, 2010b; Watanabe *et al.*, 2010; Yuan *et al.*, 2010; Shirato *et al.*, 2011). BtCoV surveillance studies have a general BtCoV nucleic acid prevalence percentage of between 6 and 12%.

**Table 1.4: Summary of the coronaviruses detected in various Asian bat species**

| Bat species | Bat coronavirus | Genus (group)* | Reference |
|---|---|---|---|
| *Cynopterus brachyotis* (Lesser dog-faced fruit bat) | BtCoV/1525G2/08 | *Betacoronavirus* (gp2d) | Watanabe *et al.*, 2010 |
| *Eonycteris spelaea* (Cave nectar bat) | BtCoV/1525G2/08 | *Betacoronavirus* (gp2d) | Watanabe *et al.*, 2010 |
| Hipposideros armiger (Great round leaf bat) | Ha BtCoV Ratcha | *Alphacoronavirus* (gp1) | Gouilh *et al.*, 2011 |
| *Hipposideros larvatus* (Horsfield's leaf-nosed bat) | Hl BtCoV Tata | *Betacoronavirus* (gp2d) | Gouilh *et al.*, 2011 |
| *Miniopterus fuligunosus* (Eastern bent-winged bat) | BtCoV/M.ful./Japan/01/2009<br>BtCoV M.ful./Japan/02/2010<br>BtCoV M.ful./Japan/02/2009<br>BtCoV M.ful./Japan/01/2010<br>BtCoV M.ful./Japan/03/2010 | *Alphacoronavirus* (gp1) | Shirato *et al.*, 2011 |
| *Miniopterus magnater* (Greater bent-winged bat) | Bat-CoV (*Mi*-BatCoV 1A)$^{\Delta}$ | *Alphacoronavirus* (gp1) | Chu *et al.*, 2006 |
| | BtCoVHKU7 | *Alphacoronavirus* (gp1) | Woo *et al.*, 2006a |
| *Miniopterus pusillus* (Lesser bent-winged bat) | Bat-CoV (*Mi*-BatCoV 1B)$^{\Delta}$ | *Alphacoronavirus* (gp1) | Chu *et al.*, 2006 |
| | BtCoVHKU8 (*Mi*-BatCoV HKU8)$^{\Delta}$ | *Alphacoronavirus* (gp1) | Woo *et al.*, 2006a |
| *Miniopterus schreibersi* (Schreiber's long-fingered bat) | Bat-CoV (*Mi*-BatCoV 1) $^{\Delta}$ | *Alphacoronavirus* (gp1) | Poon *et al.*, 2005 |
| | BtCoV/A773/05 | *Alphacoronavirus* (gp1) | Tang *et al.*, 2006 |
| | BtCoV/A911/05 | *Alphacoronavirus* (gp1) | Tang *et al.*, 2006 |
| *Myotis ricketti* (Rickett's big-footed bat) | BtCoV/701/05 | *Alphacoronavirus* (gp1) | Tang *et al.*, 2006 |
| | BtCoV/821/05 | *Alphacoronavirus* (gp1) | Tang *et al.*, 2006 |
| | BtCoVHKU6 | *Alphacoronavirus* (gp1) | Woo *et al.*, 2006a |
| *Pipistrellus abramus* (Japanese pipistrelle) | BtCoV/355/05 | *Betacoronavirus* (gp2c) | Tang *et al.*, 2006 |
| | BtCoVHKU5 (*Pi*-BatCoV HKU5)$^{\Delta}$ | *Betacoronavirus* (gp2c) | Woo *et al.*, 2006a |
| *Pipistrellus pipistrellus* (Common pipistrelle) | BtCoV/434/05 | *Betacoronavirus* (gp2c) | Tang *et al.*, 2006 |
| *Ptenochirus jagori* (Greater musky fruit bat) | BtCoV/1525G2/08 | *Betacoronavirus* (gp2d) | Watanabe *et al.*, 2010 |

| | | | |
|---|---|---|---|
| *Rhinolophus ferrumequinum* (Greater horseshoe bat) | Bat-SARS-CoV Rf1 | *Betacoronavirus* (gp2b) | Li *et al*., 2005 |
| | BtCoV/970/06 | *Alphacoronavirus* (gp1) | Tang *et al*., 2006 |
| | BtCoV/273/04 | *Betacoronavirus* (gp2b) | Tang *et al*., 2006 |
| | BtCoV/355/05 | *Betacoronavirus* (gp2c) | Tang *et al*., 2006 |
| *Rhinolophus macrotis* (Big-eared horseshoe bat) | BtCoV/279/04 | *Betacoronavirus* (gp2b) | Tang *et al*., 2006 |
| *Rhinolophus pearsoni* (Pearson's horseshoe bat) | BtCoV/970/06 | *Alphacoronavirus* (gp1) | Tang *et al*., 2006 |
| *Rhinolophus sinicus* (Chinese horseshoe bat) | BtCoVHKU2 (*Rh*-BatCoV HKU2)$^{\Delta}$ | *Alphacoronavirus* (gp1) | Woo *et al*., 2006a |
| | Bat-SARS-CoV HKU3 (SARS*r*-*Rh*-BatCoVHKU3)$^{\Delta}$ | *Betacoronavirus* (gp2b) | Lau *et al*., 2005b; Woo *et al*., 2006a |
| | Bat-SARS-CoV Rp3 (SARS*r*-*Rh*-BatCoV RP3)$^{\Delta}$ | *Betacoronavirus* (gp2b) | Yuan *et al*., 2010 |
| | BtCoV/A1018/06 | *Betacoronavirus* (gp2b) | Tang *et al*., 2006 |
| *Rousettus amplexicaudatus* (Geoffroy's rousette bat) | BtCoV/1525G2/08 | *Betacoronavirus* (gp2d) | Watanabe *et al*., 2010 |
| *Rousettus lechenaulti* (Leschenault's rousette bat) | BtCoVHKU10 | *Alphacoronavirus* (gp1) | Woo *et al*., 2007 |
| | BtCoVHKU9 or (*Ro*-BatCoV HKU9)$^{\Delta}$ | *Betacoronavirus* (gp2d) | Woo *et al*., 2007 |
| *Scotophilus kuhlii* (Lesser Asiatic yellow house bat) | BtCoV/512/05 (*Sc*-BatCoV 512)$^{\Delta}$ | *Alphacoronavirus* (gp1) | Tang *et al*., 2006 |
| | BtCoV/515/05 | *Alphacoronavirus* (gp1) | Tang *et al*., 2006 |
| | BtCoV/527/05 | *Alphacoronavirus* (gp1) | Tang *et al*., 2006 |
| | BtCoV/1552G1/08 | *Alphacoronavirus* (gp1) | Watanabe *et al*., 2010 |
| *Tylonycteris pachypus* (Lesser bamboo bat) | BtCoV/133/05 | *Betacoronavirus* (gp2c) | Tang *et al*., 2006 |
| | BtCoVHKU4 (*Ty*-BatCoV HKU4)$^{\Delta}$ | *Betacoronavirus* (gp2c) | Woo *et al*., 2006a |

The $^{\Delta}$ symbol indicates the formal species name of the specific BtCoV as decided by the ICTV (see table 1.3). *The grouping may not be referred to in the same manner in the table above as in the original publication. Tang *et al*. (2006) refers to BtCoV discovered to belong to groups 4 and 5 (subgroups 2b and 2c respectively). For simplicity, the table above indicates the BtCoV classification according to the new taxonomy and refers in brackets to the old subgroup classification by Woo *et al*. (2006).

Many of the formally accepted coronavirus species were detected within China, in the Hong Kong Special Administrative region and include bat coronaviruses such as *Rhinolophus bat coronavirus HKU2, Tylonycteris bat coronavirus HKU4, Pipistrellus bat coronavirus HKU5, Miniopterus bat coronavirus HKU8, Rousettus bat coronavirus HKU9* along with SARSr-*Rh*-BatCoV HKU3 (Lau *et al.* 2005b), and *Mi*-BatCoV 1 (Poon *et al.* 2005) (Table 1.4).

Poon *et al*. (2005) was the first study to identify a non-SARS-related coronavirus in bat species. The study tested several animal species (not only bat) and discovered coronaviruses in only 3 of the 12 bat species analysed. They identified a novel bat coronavirus, bat-CoV (renamed *Mi*-BatCoV 1 by the new classification system) in 3

different *Miniopterus* species, *Miniopterus pusillus, Miniopterus magnater* and *Miniopterus schreibersii*. The *Mi*-BatCoV 1 was not detected in other bat species analyzed, even *Myotis ricketti* that is commonly found roosting with *Miniopterus* bats. Further surveillance of the *Miniopterus* species in the Hong Kong SAR region could show that two distinct lineages of Bat-CoV 1 were circulating within these bat species (Chu *et al.*, 2006). The two Bat-CoV 1 lineages were also observed to displayed specific host tropism, Bat-CoV 1A was only detected within *M. magnater* and Bat-CoV 1B was only detected within *M. pusillus.*

BtCoV unique to Leschenault's rousette (*Rousettus leschenaulti)* bats were detected in the Guangdong province in China. These BtCoV, BtCoV-HKU9 and BtCoV-HKU10, showed a less than 70% and 80% overall nucleic acid sequence identity, respectively, to all previously known coronaviruses (Woo *et al.*, 2007). Further analysis of *Ro*-BtCoVHKU9 has reported co-infections of *R. leschenaulti* with 3 possible genotypes of *Ro*-BtCoVHKU9. Co-infections of the same bats with different genotypes likely lead to recombination events between genotypes and thereby resulting in new genotypes. Events such as this are possibly readily enabled due to the dense roosting behaviour common to *Rousettus* bats (Lau *et al.*, 2010b). Only a few reports have previously documented the simultaneous infections of more than one genotype. CCoV type 1 and 2 is frequently observed to naturally co-infect the same canine host with no noticeable effects on pathogenesis.

*Rhinolophus bat coronavirus HKU2 (*Woo *et al.*, 2006a) is of special interest due to the irregularities in its genome. This virus has thus far only been detected in Chinese horseshoe bats (in the Hong Kong and Guangdong provinces). Through the analysis of the genome sequence Lau et al. (2007) found that *Rh*-BtCoV HKU2 possesses the smallest genome for any coronavirus discovered to date, being only 27,164 base pairs in length. The gene phylogeny of Rh-BtCoV-HKU2 mostly grouped with the *Alphacoronavirus* genus and was found to be most similar to BtCoV/512/05 from *Scotophilus kuhlii*, the lesser Asian house bat (Tang *et al.*, 2006). The genome also revealed a unique spike protein that appeared to be phylogenetically distinct from the rest of the genome. The spike gene sequence shared deletions in its C-terminal sequence that is also seen in betacoronaviruses, along with abnormal deletions in the N-terminal region that significantly shorten the spike gene. Many of the expected conserved amino acids were not present in the sequence and the spike gene shared <27% amino acid identity with the spike genes of all other known coronaviruses. Interestingly, the spike protein contains a peptide of 15 amino acids in length that is homologous to a corresponding peptide in the receptor binding motif of the SARS-CoV and SARSr-Rh-CoV S1 domain (Lau *et al.*, 2007). This homologous peptide could suggest a common ancestry.

Another notable observation of HKU2 is the ORF that is present downstream of the nucleoprotein gene. Very few previous coronaviruses have been documented to possess an ORF at the 3' end of the nucleoprotein gene (as it is usually at the end of the coronavirus genome). Certain exceptions include FIPV and TGEV as well as the new BtCoV *Ro-BatCoV HKU9*, *Sc-BatCoV 512/05* and now *Rh-BatCoV HKU2*. ORF downstream of the nucleoprotein gene may thus be more frequent in BtCoV, though the ORF in HKU2 has yet to be assigned a function.

Extensive surveillance has been performed for SARS-related CoV in the bat species of the Hong Kong and Guangdong provinces of China. One particular study only analysed *Rhinolophus* spp. (n=1401) and detected SARSr-*Rh*-BtCoV in 15.7% and *Rh*-BatCoV HKU2 in 15.5% of the bats (Lau *et al.*, 2010a). Interestingly, during subsequent sampling analysis (recapture), 20 bats from 7 sampling locations tested positive for the presence of both SARSr-*Rh*-BtCoV and *Rh*-BatCoV HKU2 and 7 bats were found to be co-infected at the time of sampling.

The study performed by Watanabe *et al*. (2010) was the first surveillance study of coronaviruses in bats in the Philippines. Of only 52 bats sampled comprising of 6 different species, a prevalence of 55.8% (of both alpha- and betacoronaviruses) was observed. A novel alphacoronavirus, BtCoV/Phil/Dil/1552G1/08, was identified from *Scotophilus kuhlii*, and displayed a 95% nucleotide identity to BtCoV/China/A515/05 (Tang *et al.*, 2006). The insectivorous bat species *Scotophilus kuhlii* is commonly found throughout the Philippines, Taiwan, and a large part of eastern Asia. The close similarity between BtCoV/Phil/Dil/1552G1/08 and BtCoV/China/A515/05 seems to indicate that similar viruses are broadly circulating in this bat species.

The betacoronavirus identified in the study, BtCoV/Phil/Dil/1525G2/08, was detected in 4 frugivorous bat species (Table 1.4) and shared >98% nt identity to each other also shows a 83% nucleotide identity to *Ro*-BatCoV HKU9 (Woo *et al.*, 2007). The BtCoV/Phil/Dil/1525G2/08 was mostly only detected with a nested PCR suggesting that the viruses replicate to low amounts.

In Japan, a colony of *Miniopterus fulginosus* containing males and non-breeding females, in the Wakayama prefecture of Japan was investigated for the presence of BtCoV (Shirato *et al.*, 2011) and several strains of a *Miniopterus* alphacoronavirus closely related to *Mi-BtCoV HKU7-1* (95% nucleotide identity) was detected. The two spike genes identified in the Japanese *Miniopterus* alphacoronaviruses only share 64% genetic homology.

Gouilh *et al.*, (2011) remarked on the sampling bias from BtCoV studies performed to date, focusing largely on the *Rhinolophidae* family of bats, which can be expected due to

first identification of SARSr-BtCoV from this family. Also, the SARSr-BtCoV appeared to be restricted to *Rhinolophus* spp, until the identification of SARSr-BtCoV from *Hipposideros* spp. in Ghana. Gouilh *et al.*, (2011) hypothesized that a there is a much larger diversity of SARSr-BtCoV present in *Hipposideros* species than identified thus far due to the *Rhinolophus* sampling bias. Thus, surveillance of the bat species of Thailand was conducted with the aim of increasing the number of *Hipposideros* spp. analysed for BtCoV. Analysis of 25 bat species (n=552) yielded an alpha- and a betacoronavirus (Table 1.4) from 2 separate *Hipposideros* species from two independent colonies. Both viruses appeared, from the phylogenetic reconstruction of the 438bp fragment of the RdRp gene, to be novel BtCoV of <78% nucleotide identity to the closest previously known BtCoV. The study also reports viral persistence for up to 18 months in the *Hipposideros* colony from which *H. larvatus*/BtCoV/Tata (BetaCoV) was identified.

### 1.6.3 Australia

Unpublished data of both alpha- and betacoronaviruses from Australia by Smith and colleagues were submitted to NCBI's Genbank (Smith *et al.*, 2008; *Unpublished*) as well as presented to the Australian Biosecurity Cooperative Research Centre for Emerging Infectious Disease (Smith *et al.*, 2010). The study identified 4 BtCoV from Australia in 6 bat species (Table 1.5).

**Table 1.5: Summary of the coronaviruses detected in various Australian bat species**

| Bat species | Bat coronavirus | Genus (group) | Reference |
|---|---|---|---|
| *Miniopterus australis* (Little bent-wing bat) | M.aus/Aus/BtCoV/180/1996<br>M.aus/Aus/BtCoV088/2007<br>M.aus/Aus/SEQ/132/2007 | *AlphaCoV* (gp1) | Smith *et al.*, 2010 |
| *Miniopterus schreibersii* (Schreiber's long-fingered bat) | M.sch/Aus/NT/xxx/2008<br>M.sch/Aus/SEQ/146/2007 | *AlphaCoV* (gp1) | Smith *et al.*, 2010 |
| *Myotis macropus* (Southern Myotis) | M.mac/Aus/SEQ/034/2008 | *AlphaCoV* (gp1) | Smith *et al.*, 2010 |
| *Pteropus alecto* (Black flying-fox) | P.ale/Aus/SEQ/xxx/2009 | *BetaCoV* (gp2) | Smith *et al.*, 2010 |
| *Rhinolophus megaphyllus* (Smaller horseshoe bat) | R.meg/Aus/FNQ/100/200 | *AlphaCoV* (gp1) | Smith *et al.*, 2010 |
| *Rhinonicteris aurantius* (Orange leaf nosed bat) | R.aur/Aus/NT/000/2006 | *BetaCoV* (gp2) | Smith *et al.*, 2010 |

The study identified both alpha and betacoronaviruses in Australian bat species, however since the study has not yet been reported in a publication, the exact phylogenetic position, similarity between known BtCoV and host restriction of these 4 reported viruses are not yet available. Gouilh *et al.*, (2011) references the study due to the identification of a

betacoronavirus in *Rhinonicteris aurantius*, a bat species endemic to Australia and though it belongs to the *Hipposideridae* family has been suggested to be situated phylogenetically between the *Rhinolophidae* and *Hipposideridae* families. Similarly, the betacoronavirus detected from *Rhinonicteris aurantius* was also phylogenetically situated between the monophyletic clades of the *Rhinolophidae* and *Hipposideridae* SARS related betacoronaviruses.

### 1.6.4 North and South America

The BtCoV detected within countries in North and South America is listed in Table 1.6 along with their host species. A total of approximately 9 BtCoV have been identified from 5 bat species in the *Vespertilionoidea and Phyllostomidae* bat families (Dominguez *et al.*, 2007; Brandão *et al.*, 2008; Carrington *et al.*, 2008).

**Table 1.6: Summary of the coronaviruses detected in bat species from the Western hemisphere**

| Bat species | Bat coronavirus | Genus (group)* | Reference |
|---|---|---|---|
| *Eptesicus fuscus* (Big brown bat) | RM-Bat-CoV 65 | *AlphaCoV* (gp1) | Dominguez *et al.*, 2007 |
| | RM/BtCoV/453/07/EF | *AlphaCoV* (gp1) | Osborne *et al.*, 2011 |
| | RM/BtCoV/61/07/EF | *AlphaCoV* (gp1) | Osborne *et al.*, 2011 |
| *Myotis lucifugus* (Little brown bat) | RM/BtCoV/15/06/ML | *AlphaCoV* (gp1) | Osborne *et al.*, 2011 |
| *Myotis occultus* (The occult bat) | RM-Bat-CoV 3 | *AlphaCoV* (gp1) | Dominguez *et al.*, 2007 |
| | RM-Bat-CoV 6 | *AlphaCoV* (gp1) | Dominguez *et al.*, 2007 |
| | RM-Bat-CoV 11 | *AlphaCoV* (gp1) | Dominguez *et al.*, 2007 |
| | RM-Bat-CoV 27 | *AlphaCoV* (gp1) | Dominguez *et al.*, 2007 |
| | RM-Bat-CoV 48 | *AlphaCoV* (gp1) | Dominguez *et al.*, 2007 |
| *Myotis volans* (Long-legged myotis) | RM/BtCoV/433/07/MV | *AlphaCoV* (gp1) | Osborne *et al.*, 2011 |
| | RM/BtCoV/09-07/09/MV | *AlphaCoV* (gp1) | Osborne *et al.*, 2011 |
| | RM/BtCoV/429/07/MV | *AlphaCoV* (gp1) | Osborne *et al.*, 2011 |
| *Glossophaga soricina* (Pallas's long-tongued bat) | Bt-CoV/Trinidad/1CO7B | *AlphaCoV* (gp1) | Carrington *et al.*, 2008 |
| *Carollia perspicillata* (Seba's short-tailed bat) | Bt-CoV/Trinidad/1FY2B | *AlphaCoV* (gp1) | Carrington *et al.*, 2008 |
| *Desmodus rotundus* (The vampire bat) | BatCoVDR/2007 | *BetaCoV* (gp2) | Brandão *et al.*, 2008 |

*The grouping may not be referred to in the same manner in the table above as in the original publication.

#### *I. North America*

The bat species inhabiting the Rocky mountain region in North America were investigated for the presence of BtCoV (Dominguez *et al.*, 2007). Alphacoronavirus RNA was detected in 6 fecal samples (n=28) from 2 of the 7 bat species tested, *Myotis occultus*

and *Eptesicus fuscus*. The alphacoronavirus identified from *Myotis occultus* showed similarity to Asian *Myotis* BtCoV-HKU6 (Figure 1.8). The alphacoronavirus identified from the *Eptesicus fuscus* bats were most similar to BtCoVHKU2, detected from the *Rhinolophidae* bat family (which does not occur in the western hemisphere).

Subsequently, an in-depth surveillance of the bat species of the Colorado Rocky mountain region from 2007-2009 was performed that included both urban and rural bat roosts, totalling 17 species from 2 families (n=1044) (Osborne *et al.*, 2011). Four of the bat species (*Eptesicus* and 3 *Myotis* species) were positive for bat coronaviruses (cluster A represented by RM/BtCoV/453/07/EF, cluster B represented by RM/BtCoV/09-07/09/MV, cluster C represented by RM/BtCoV/429/07/MV) which were similar to the North American bat coronaviruses from Dominguez *et al.*, 2007 (Cluster A similar to RM-BtCoV65, cluster B similar to RM-BtCoV6, cluster C similar to RM-BtCoV3; Figure 1.8). Due to the length of the study it was observed that virus clearance took approximately 6 weeks in urban roosts. Of note is the high prevalence of BtCoV in urban bat roosts; when sampled, the urban roosts always tested positive for BtCoV (5/5 roosts), whereas only 2 of the 16 rural roosts sampled were positive for BtCoV.

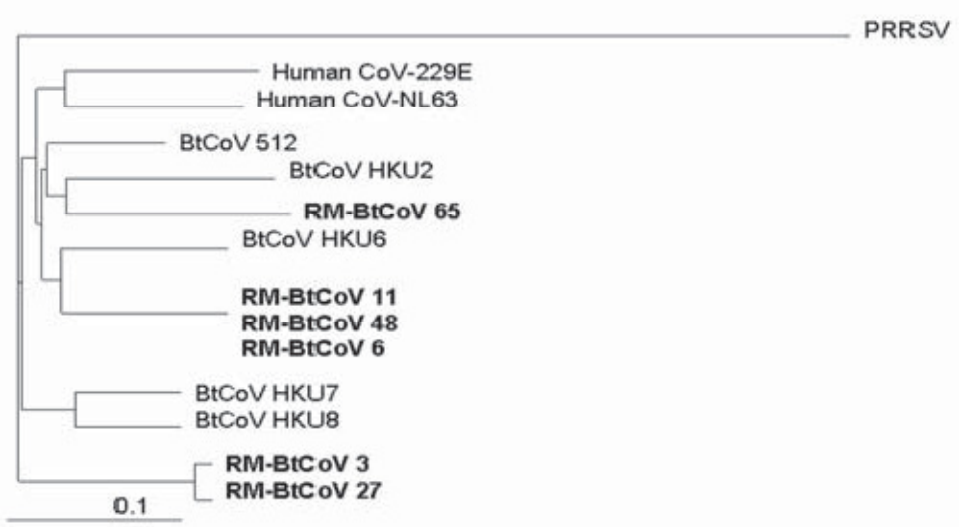


**Figure 1.8:** Phylogenetic relationship of the North American alphacoronaviruses to the Asian related alphacoronaviruses using 440 bp sequence of the RNA-dependent RNA polymerase gene (ORF 1b). The bar indicates a 0.1 nucleotide substitution per site with out-group Porcine respiratory and reproductive syndrome virus (PRRSV) (Dominguez *et al.*, 2007).

### *II. South America*

Two separate studies in South America revealed BtCoV from both the *Alphacoronavirus* and *Betacoronavirus* genera. As part of the bat rabies surveillance projects performed in Brazil, 7 *Desmodus rotundus* (vampire bats) were screened for the presence of coronaviruses (Brandão *et al.*, 2008). A betacoronavirus, BatCoV/DR/2007,

was detected in one sample and showed 93.6% nucleic acid identity in the amplified segment of ORF1b, to other betacoronaviruses such as BCoV and HCoVOC43. BtCoV/DR/2007 only showed an 82.3% nucleic acid identity to other betacoronavirus BtCoVs, and showed a higher similarity (72.5%) to gammacoronaviruses than to alphacoronaviruses (69.9%). Interestingly, BtCoV/DR/2007, only shared a 66.6% nucleic acid identity with the SARS-CoV (Brandão *et al.*, 2008).

Carrington *et al.* (2008) performed a coronavirus surveillance study in Trinidad. Alphacoronaviruses were detected in 2 *Phyllostomidae* bat species, *Glossaphaga soricina* and *Carollia perspicillata*. The alphacoronaviruses clustered closely with other human coronaviruses and diverged from each other by 27.8% nucleotide identity in 3,800 bp segment of the RdRP gene, and only 15.5% at the amino acid level.

### 1.6.5 Europe

The BtCoV detected in European countries are listed in Table 1.7 along with their host species. A total of approximately 36 BtCoV have been identified from 20 bat species in the *Vespertilionidae, Miniopteridae, and Rhinolophidae* bat families, that were related to previously identified BtCoV (Gloza-Rausch *et al.*, 2008; Drexler *et al.*, 2010; Reusken *et al.*, 2010; Rihtarič *et al.*, 2010).

**Table 1.7: Summary of the coronaviruses detected in bat species from Europe**

| Bat species | Bat coronavirus | Genus (group)* | Reference |
|---|---|---|---|
| *Eptesicus isabellinus* | Eptesicus-BtCoV/M/Iberia | *BetaCoVs* (gp2) | Falcón *et al.*, 2011 |
| *Hypsugo savii* (Savi's pipistrelle) | *Hypsugo* -BtCoV/J/Iberia<br>*Hypsugo* -BtCoV/L/Iberia | *BetaCoVs* (gp2) | Falcón *et al.*, 2011 |
| *Miniopterus schreibersi* (Schreiber's long-fingered bat) | *Mi*-BatCoV $1^{\Delta}$-related:<br>BtCoV/M. sch/BR98-55/08 | *AlphaCoV* (gp1) | Drexler *et al.* 2010 |
| | BtCoVHKU7-related:<br>BtCoV/M. sch/BR98-30/08<br>BtCoV/M. sch/BR98-31/08 | | Drexler *et al.* 2010 |
| | *Mi*-BatCoV HKU8$^{\Delta}$-related:<br>BtCoV/M. sch/BR96-37/08<br>BtCoV/M. sch/BR96-40/08<br>BtCoV/M. sch/BR98-14/08<br>BtCoV/M. sch/BR98-18/08<br>BtCoV/M. sch/BR98-52/08<br>BtCoV/M. sch/BR98-53/08 | | Drexler *et al.* 2010 |
| | Mi-BtCoV/A/Iberia | *AlphaCoV* (gp1) | Falcón *et al.*, 2011 |
| *Myotis bechsteinii* (Bechstein's bat) | Lineage 1 in figure 13:<br>BtCoV/M. bec/D6.6/07 | *AlphaCoV* (gp1) | Gloza-Rausch *et al.* 2008 |
| *Myotis blythii* (Lesser mouse-eared bat) | My-BtCoV/B/Iberia | *AlphaCoV* (gp1) | Falcón *et al.*, 2011 |

| | | | |
|---|---|---|---|
| *Myotis dasycneme* (The pond bat) | Lineage 1 in figure 13: BtCoV/M. das/D3.28/07 BtCoV/M. das/D3.33/07 BtCoV/M. das/D3.14/07 BtCoV/M. das/D3.4/07 BtCoV/M. das/D3.26/07 BtCoV/M. das/D3.2/07 BtCoV/M. das/D3.6/07 BtCoV/M. das/D3.38/07 BtCoV/M. das/D5.17/07 BtCoV/M. das/D3.9/07 BtCoV/M. das/D3.15/07 BtCoV/M. das/D2.2/07 BtCoV/M. das/D3.8/07 BtCoV/M. das/D3.3/07 BtCoV/M. das/D3.5/07 BtCoV/M. das/D3.20/07 BtCoV/M. das/D3.10/07 BtCoV/M. das/D3.13/07 | *AlphaCoV* (gp1) | Gloza-Rausch *et al.* 2008 |
| | Lineage 1 in figure 14: BtCoV/M. das/NL-VM3/10 BtCoV/M. das/NL-VM34/10 BtCoV/M. das/NL-VM62/10 BtCoV/M. das/NL-VM73/10 BtCoV/M. das/NL-VM84/10 BtCoV/M. das/NL-VM105/10 | *AlphaCoV* (gp1) | Reusken *et al.* 2010 |
| | Lineage 7 in figure 14: BtCoV/M. das/NL-VM2/10 BtCoV/M. das/NL-VM7/10 BtCoV/M. das/NL-VM284/10 | *AlphaCoV* (gp1) | Reusken *et al.* 2010 |
| *Myotis daubentonii* (Daubenton's bat) | Lineage 4 in figure 13: BtCoV/M. dau/D7.3/07 BtCoV/M. dau/D8.45/07 BtCoV/M. dau/D8.46/07 BtCoV/M. dau/D6.38/07 BtCoV/M. dau/D6.42/07 BtCoV/M. dau/D8.32/07 | *AlphaCoV* (gp1) | Gloza-Rausch *et al.* 2008 |
| | Lineage 4 in figure 14: BtCoV/M. dau/NL-VM222/10 BtCoV/M. dau/NL-VM303/10 BtCoV/M. dau/NL-VM361/10 | *AlphaCoV* (gp1) | Reusken *et al.* 2010 |
| | My-BtCoV/H/Iberia | *AlphaCoV* (gp1) | Falcón *et al.*, 2011 |
| *Myotis myotis* (Greater mouse-eared bat) | My-BtCoV/I/Iberia | *AlphaCoV* (gp1) | Falcón *et al.*, 2011 |
| | My-BtCoV/N78-5/2008 | *AlphaCoV* (gp1) | Drexler *et al.*, 2011 |
| *Nyctalus lasiopterus* (Greater noctule bat) | *Nyctalus*-BtCoV/C/Iberia *Nyctalus*-BtCoV/D/Iberia *Nyctalus*-BtCoV/E/Iberia *Nyctalus*-BtCoV/F/Iberia *Nyctalus*-BtCoV/G/Iberia | *AlphaCoV* (gp1) | Falcón *et al.*, 2011 |
| *Nyctalus leisleri* (Lesser noctule) | BtCoV/N. lei/BNM98-30/08 | *AlphaCoV* (gp1) | Drexler *et al.* 2010 |
| *Nyctalus noctula* (Common noctule) | Lineage 5 in figure 14: BtCoV/N. noc/NL-VM176/10 BtCoV/N. noc/NL-VM182/10 BtCoV/N. noc/NL-VM199/10 BtCoV/N. noc/NL-VM366/10 | *AlphaCoV* (gp1) | Reusken *et al.* 2010 |
| *Pipistrellus kuhlii* (Kuhl's Pipistrelle) | *Pipistrellus*-BtCoV/I'/Iberia | *AlphaCoV* (gp1) | Falcón *et al.*, 2011 |
| *Pipistrellus nathusii* (Nathusius's pipistrelle) | Lineage 2 in figure 13: BtCoV/P. nat/D5.16/07 BtCoV/P. nat/D5.73/07 | *AlphaCoV* (gp1) | Gloza-Rausch *et al.* 2008 |
| *Pipistrellus pipistrellus* (Common pipistrelle) | Lineage 6 in figure 14 BtCoV/P. pip/NL-VM312/10 | *AlphaCoV* (gp1) | Reusken *et al.* 2010 |
| | BtCoV/P. pip/NL-VM314/10 | *BetaCoVs* (gp2) | Reusken *et al.* 2010 |

| | | | |
|---|---|---|---|
| *Pipistrellus pygmaeus* (Soprano pipistrelle) | Lineage 3 in figure 13: BtCoV/P. pyg/D5.70/07 BtCoV/P. pyg /D5.71/07 BtCoV/P. pyg /D5.85/07 | *AlphaCoV* (gp1) | Gloza-Rausch *et al.* 2008 |
| *Pipistrellus spp.* | *Pipistrellus*-BtCoV/K/Iberia | *AlphaCoV* (gp1) | Falcón *et al.*, 2011 |
| *Rhinolophus blasii* (Blasius's horseshoe bat) | ***Rh*-BatCoV HKU2$^{\Delta}$ related:** BtCoV/Rhi. bla/BB98-41/08 | *AlphaCoV* (gp1) | Drexler *et al.* 2010 |
| | **SARS*r-Rh*-BtCoV $^{\Delta}$ related:** BtCoV/Rhi. bla/BB 98-16/08 BtCoV/Rhi. bla/BB 98-18/08 BtCoV/Rhi. bla/BM48-31/08 BtCoV/Rhi. bla/BM48-48/08 BtCoV/Rhi. bla/BM98-65/08 | *BetaCoVs* (gp2) | Drexler *et al.* 2010 |
| | **BtCoV/Rhi. bla/BM98-15/08 related:** BtCoV/Rhi. bla/BB 98-15/08 BtCoV/Rhi. bla/BM48-39/08 BtCoV/Rhi. bla/BM98-05/08 BtCoV/Rhi. bla/BR 98-12/08 | *AlphaCoV* (gp1) | Drexler *et al.* 2010 |
| *Rhinolophus euryale* (Mediterranean horseshoe bat) | ***Rh*-BatCoV HKU2$^{\Delta}$ related:** BtCoV/Rhi. eur/BR98-19/08 | *AlphaCoV* (gp1) | Drexler *et al.* 2010 |
| | **SARS*r-Rh*-BtCoV $^{\Delta}$ related:** BtCoV/Rhi. eur/BB 98-43/08 BtCoV/Rhi. eur/BM48-12/08 BtCoV/Rhi. eur/BM98-01/08 BtCoV/Rhi. eur/BM98-05/08 BtCoV/Rhi. eur/BM98-13/08 BtCoV/Rhi. eur/BR 98-19/08 | *BetaCoVs* (gp2) | Drexler *et al.* 2010 |
| | **BtCoV/Rhi. bla/BM98-15/08 related** | *AlphaCoV* (gp1) | Drexler *et al.* 2010 |
| *Rhinolophus ferrumequinum* (Greater horseshoe bat) | **SARS*r-Rh*-BtCoV $^{\Delta}$ related:** BtCoV/Rhi. fer/BM48-34/08 BtCoV/Rhi. fer/BM48-35/08 BtCoV/Rhi. fer/BNM98-29/08 | *BetaCoVs* (gp2) | Drexler *et al.* 2010 |
| | **BtCoV/Rhi. bla/BM98-15/08 related:** BtCoV/Rhi. fer/BM48-28/08 | *AlphaCoV* (gp1) | Drexler *et al.* 2010 |
| *Rhinolophus hipposideros* (Lesser horseshoe bat) | SLO1A0066 | *BetaCoVs* (gp2) | Rihtaric *et al.* 2010 |
| | SLO1A0050 | *BetaCoVs* (gp2) | Rihtaric *et al.* 2010 |
| | SLO1A0082 | *BetaCoVs* (gp2) | Rihtaric *et al.* 2010 |
| *Rhinolophus mehelyi* (Mehely's horseshoe bat) | **SARS*r-Rh*-BtCoV $^{\Delta}$ related:** BtCoV/Rhi. meh/BM48-32/08 BtCoV/Rhi. meh/BM98-07/08 | *BetaCoVs* (gp2) | Drexler *et al.* 2010 |

The $^{\Delta}$ symbol indicates the formal species name of the specific BatCoV as decided by the ICTV (see table 1.3). *The grouping may not be referred to in the same manner in the table above as in the original publication. The majority of the coronavirus names in the table are shortened abbreviations of their full taxa names as follows: identification code/typical host/strain or isolate/ collection year, instead of the longer versions used in their original publications that usually follow the pattern: identification code/strain or isolate/typical host/country/collection year.

In Northern Germany, 4 monophyletic *Alphacoronavirus* lineages were detected within 5 *Vespertilionidae* bat species, namely *Myotis bechsteinii, Myotis dasycneme, Myotis daubentonii, Pipistrellus nathusii,* and *Pipistrellus pygmaeus* (Figure 1.13) (Gloza-Rausch *et al.*, 2008). These German lineages formed a sister clade with BtCoV identified in *Myotis* species in Asia, such as BtCoV-HKU6, BtCoV/A701/05 *and* BtCoV/A821/05 (Woo *et al.*, 2006a;Tang *et al.*, 2006). The nucleic acid distances between the lineages 1, 2, and 3 were 6%-8% and to lineage 4 was 12%–13%. The distance from the German lineages to the Chinese sister clade of the *Myotis ricketti* BtCoVHKU6 was 15%–17%.

As explained in Section 1.3, genotypes of a species refer to the genetic variants that exist in that species and a lineage refers to a direct line of descent, and that new species are the results of speciation from direct ancestor species. In the context of the publication by Gloza-Rausch *et al.,* (2008), the term 'genotype' may have been better suited to replace the term 'lineage'.

Within the German region, Rhineland-Palatinate, a detailed 3 year virological study was performed on a maternity colony of *Myotis myotis* (Drexler *et al.* 2011). An alphacoronavirus, BtCoV/N78-5, which is closely related to *My-BtCoV HKU6*, was frequently detected within fecal samples collected from the colony with between 20 and 100% alphacoronavirus RNA prevalence. The detection rate of the alphacoronavirus was observed to fluctuate depending on the state of the colony and would increase after parturition.

In the Netherlands, a coronavirus RNA prevalence of 16.9% was identified from surveying 211 bats comprising of 13 European bat species (Reusken *et al*., 2010). The first European betacoronavirus was detected in the *Pipistrellus pipistrellus* (Common pipistrelle; Table 1.7) and was found to be related to the BtCoV-HKU5, also identified in Chinese *Pipistrellus* species. Also detected were alphacoronaviruses of similar lineages to those identified in German *P. pipistrellus* (Table 1.6, designated lineage 6), alphacoronaviruses in 2 Myotis spp. (Table 1.7, designated lineages 1, 4, 7) as well as a new coronavirus host species, *Nyctalus noctula* (Table 1.6, designated lineage 5).

Multiple coronaviruses have been reported from the *Pipistrellus* genus (Table 1.7). This genus of bat is also non-migratory and frequently found roosting within urban areas and thus human-bat interaction also occurs regularly. Thus surveillance of such bat species becomes essential in identifying the potential for zoonotic transmissions.

In 2010, Drexler *et al*., published a surveillance study of the *Vespertilionidae* and *Rhinolophidae* bats in Europe, focusing on Bulgaria. The study observed that SARS-related coronaviruses in Bulgaria were exclusively present in *Rhinolophidae* bats and were detected at high frequencies (26%) as well as high concentrations, reaching a maximum of $2.4 \times 10^8$ copies/gram faeces. In addition, two alphacoronavirus clades were also detected in *Rhinolophidae* bats; a clade related to *Rh*-BatCoV HKU2 as well as a novel lineage represented by BtCoV/BB98-15/Rh bla/Bulgaria/08 (Table 1.7). Double infections of the 389 *Rhinolophidae* bats analyzed, involving both SARS-related betacoronaviruses and alphacoronaviruses, occurred in 6.2% bats with triple infections being observed in 0.5% of bats.

Surveillance of European *Miniopterus* spp. detected all 3 *Miniopterus* BatCoV lineages first identified in China, namely, *Mi*-BatCoV 1, *Mi*-BatCoV HKU8 (Table 1.4) as well as *Mi*-BatCoV HKU7 (not formally recognized as a species yet). The *Miniopterus* bats

were also observed to be both doubly and triply infected as with the *Rhinolophus* bats (Drexler *et al.*, 2010; Lau *et al.*, 2010b). After the first identification of an alphacoronavirus in *Nyctalus* spp. in Reusken *et al.*, (2010), an additional alphacoronavirus clade was detected in *Nyctalus leisleri*, BtCoV/BNM98-30/Nyc lei/Bulgaria/2008 (Table 1.7).

Surveillance for BtCoV in Slovenia identified SARSr-*Rh*-CoV in *Rhinolophus hipposideros,* one of seven bat species analysed in the study (Rihtarič *et al.*, 2010). The SARSr-*Rh*-CoV from *Rhinolophus hipposideros* (prevalence of 38.8%) were closely related, sharing 99.5-100% nucleotide identity, and shared 85% nucleic acid identity to the previously identified SARSr-*Rh*-BtCoV Rp3/2004.

The Iberian Peninsula (Spain and Portugal) is an important land bridge for the migration of bat species to and from Africa and Europe. As such Falcón *et al.*, (2011) analysed 26 of the 30 Iberian bat species (n=576) for the presence of BtCoV and identified 14 BtCoV of both the *Alpha*- and *Betacoronavirus* genera from 9 bat species (Table 1.7). Six lineages were phylogenetically identified with two novel independent lineages recognised to be occurring in multiple bat species (Lineages C, D, E, F, G, I and I'). In contrast to the majority of bat surveillance studies performed to date, Falcón *et al.*, (2011) reported that different species of bats from the same location harboured the same genetic lineages (lineages A and B from *Miniopterus* spp. and *Myotis* spp. respectively, as well as lineages G and I from *Nyctalus and Myotis* respectively). Interestingly 2 of the viruses (both alphacoronaviruses) were identified from oral swabs, few previous studies have identified BtCoV from oral swabs and as such is not largely collected anymore for coronavirus surveillance (Section 1.5.7 D further discusses BtCoV tissue tropism).

### 1.6.6 Africa

The BtCoV detected in African countries are listed in Table 1.8 along with their host species. A total of approximately 14 BtCoV have been identified from 8 African bat species in the *Miniopteridae, Molossidae, Hipposideridae, Megadermatidae,* and *Pteropodidae* bat families (Tong *et al.*, 2009; Pfefferle *et al.*, 2009; Quan *et al.*, 2010).

**Table 1.8: Summary of the coronaviruses detected in bat species from Africa**

| Bat species | Bat coronavirus | Genus (group)* | Reference |
|---|---|---|---|
| *Cardioderma cor* (Heart-nosed bat) | **Not specified**#/ identified CoV referred to as: | | Tong *et al.*, 2009 |
| | BtCoVA970-like | *AlphaCoV* | |
| *Chaerephon sp.* (Free tail bat) | **Not specified**#/ identified CoV referred to as: | | Tong *et al.*, 2009 |
| | BtHKU7-like | *AlphaCoV* | |
| | HCoV229E-like | *AlphaCoV* | |
| | SARS-CoV-like | *BetaCoV* | |
| | BtKY18-like (Unique) | *BetaCoV* | |
| *Eidolon helvum* (Straw-colored fruit bat) | **Not specified**#/ identified CoV referred to as: | | Tong *et al.*, 2009 |
| | BtKY18-like | *BetaCoV* | |
| *Hipposideros commersoni* (Commerson's leaf-nosed bat) | **Not specified**#/ identified CoV referred to as: | *BetaCoV* | Tong *et al.*, 2009 |
| | BtHKU9-like | | |
| | Zaria bat coronavirus (ZBCoV) | *BetaCoV* | Quan *et al.*, 2010 |
| *Hipposideros cf. ruber* (Sundevall's roundleaf Bat) | BtCoV/Hip.sp/GhanaKwam/19/2008 | *AlphaCoV* | Pfefferle *et al.*, 2009 |
| | BtCoV/Hip.sp/GhanaBuo/344/2008 | *AlphaCoV* | Pfefferle *et al.*, 2009 |
| | BtCoV/Hip.sp/GhanaKwam/8/2008 | *AlphaCoV* | Pfefferle *et al.*, 2009 |
| | BtCoV/Hip.sp/GhanaKwam/20/2008 | *BetaCoV* | Pfefferle *et al.*, 2009 |
| | BtCoV/Hip.sp/GhanaBuo/348/2008 | *BetaCoV* | Pfefferle *et al.*, 2009 |
| *Miniopterus africanus* (African long-fingered bat) | **Not specified**#/ identified CoV referred to as: | | Tong *et al.*, 2009 |
| | BtCoV1A-like | *AlphaCoV* | |
| *Miniopterus inflatus* (Greater long-fingered Bat) | **Not specified**#/ identified CoV referred to as: | | Tong *et al.*, 2009 |
| | BtCoV1A-like | *AlphaCoV* | |
| *Miniopterus minor* (Least long-fingered bat) | **Not specified**#/ identified CoV referred to as: | | Tong *et al.*, 2009 |
| | BtCoV1A-like | *AlphaCoV* | |
| *Miniopterus natalensis* (Natal long-fingered bat) | **Not specified**#/ identified CoV referred to as: | | Tong *et al.*, 2009 |
| | BtCoV1A-like | *AlphaCoV* | |
| *Otomops martiensseni* (Large-eared free-tailed bat) | **Not specified**#/ identified CoV referred to as: | | Tong *et al.*, 2009 |
| | BtHKU7-like | *AlphaCoV* | |
| *Rousettus aegyptiacus* (Egyptian fruit bat) | **Not specified**#/ identified CoV referred to as: | | Tong *et al.*, 2009 |
| | BtCoVA970-like | *AlphaCoV* | |
| | BtKY18-like (Unique) | *BetaCoV* | |
| | BtHKU9-like | *BetaCoV* | |

*The grouping may not be referred to in the same manner in the table above as in the original publication. # symbol is used to highlight the fact that Tong *et al.* (2009) did not specify bat coronaviruses identified in the study as they correspond to specific bat species but referred to coronaviruses identified as similar to other

coronaviruses discovered in previous studies, e.g. as being BtHKU9-like. BtKY18-like are coronaviruses different to previously identified coronaviruses, so far unique to the Kenyan (KY) coronaviruses.

In 2007, Müller *et al*., used serological methods to screen African bat samples for antibodies that would target coronavirus antigens. The study used ELISA techniques to analyse 248 serum samples collected from 1986 to 1989, from 16 bat species in total, in the Mpumalanga and Limpopo provinces of South Africa. Two bat species were positive for antibodies against SARS-CoV, *Rousettus aegyptiacus* (37.9% seropositivity in 11/29 from Limpopo province) and *Mops condylurus* (15.8% (3/19) in Limpopo and 11.5% (11/96) in Mpumalanga provinces). The results suggest that certain bat species may have been exposed to betacoronaviruses from the SARSr-CoV cluster and may possibly even harbour such viruses, however, further exploration into coronaviruses in African bat species would be required.

The coronavirus diversity study by Tong *et al*., (2009) was the first in-depth surveillance study aimed at bat coronaviruses performed in Africa (based in Kenya). The aim was to determine whether the diversity of coronaviruses in bat species seen on other continents was also present in Africa. The authors believe that the extent of the diversity of the coronaviruses in African bat species may possibly be greater than the diversity discovered elsewhere (Tong *et al*., 2009). The authors identified 42 distinct coronavirus sequences (prevalence of 19% from fecal samples) from both the *Alpha*- and *Betacoronavirus* genera in the Kenyan bat species including viruses related to SARSr-CoV (Figure 1.9). The majority of the RNA sequences were most related to *Alphacoronavirus* genus and were closely related BtCoV1A, BtCoVHKU7, BtCoVHKU8, BtCoVA970 and HCoV229E (between 77-88% nucleotide identity in the amplified segment of the RdRp gene).

The novel betacoronaviruses were divided into 3 clusters. Two isolates from the *Chaerophon* spp. were found to be related to the SARS-related cluster (BtCoVKY15 in Figure 1.9). The sequences showed an 89% sequence identity to the previously characterized SARS-related CoV, BtCoVRF1, and an 80% nucleic acid sequence identity to the corresponding RdRp segment in SARS-HCoV (Urbani strain). The second cluster grouped with the newly characterized BtCoV-HKU9 (previously group 2d), showing greater than 95% nucleotide identity. The last cluster contains no previously known coronaviruses and shares less than 75% nucleotide identity to BtCoV-HKU9 (BtCoVKY18, BtCoVKY19, and BtCoVKY20, etc.). This cluster was designated the BtCoVKY18-like cluster (table 1.7) (Tong *et al*., 2009).

Figure 1.9 encounters the same bootstrap problem as Figure 1.10. The bootstrap values around certain nodes on the left of the tree are not supported well. For example, the

branch split between the gammacoronaviruses and the SARS-related cluster is only 40%. This may be as a result of the small segment in the RdRp gene used in the phylogenetic tree and may become better resolved when a larger segment is used or if more than one gene is used to infer phylogeny. The 121bp segment of the RdRp gene that is used in the Kenyan study is from a highly conserved part of the polymerase gene, but phylogenetic conclusions drawn from such a small segment should be considered with caution. The coronavirus RNA identified from Kenyan bat species thus require more detailed investigation.

In Ghana, 12 species of insectivorous bats were analysed for the presence of BtCoV RNA and a prevalence of 9.76% was identified (Pfefferle *et al*., 2009). Coronaviruses belonging to both the *Alpha-* and *Betacoronavirus* genera were identified in the fecal material of 15.4% of *Hipposideros caffer ruber* bats from 2 caves (Figure 1.10).

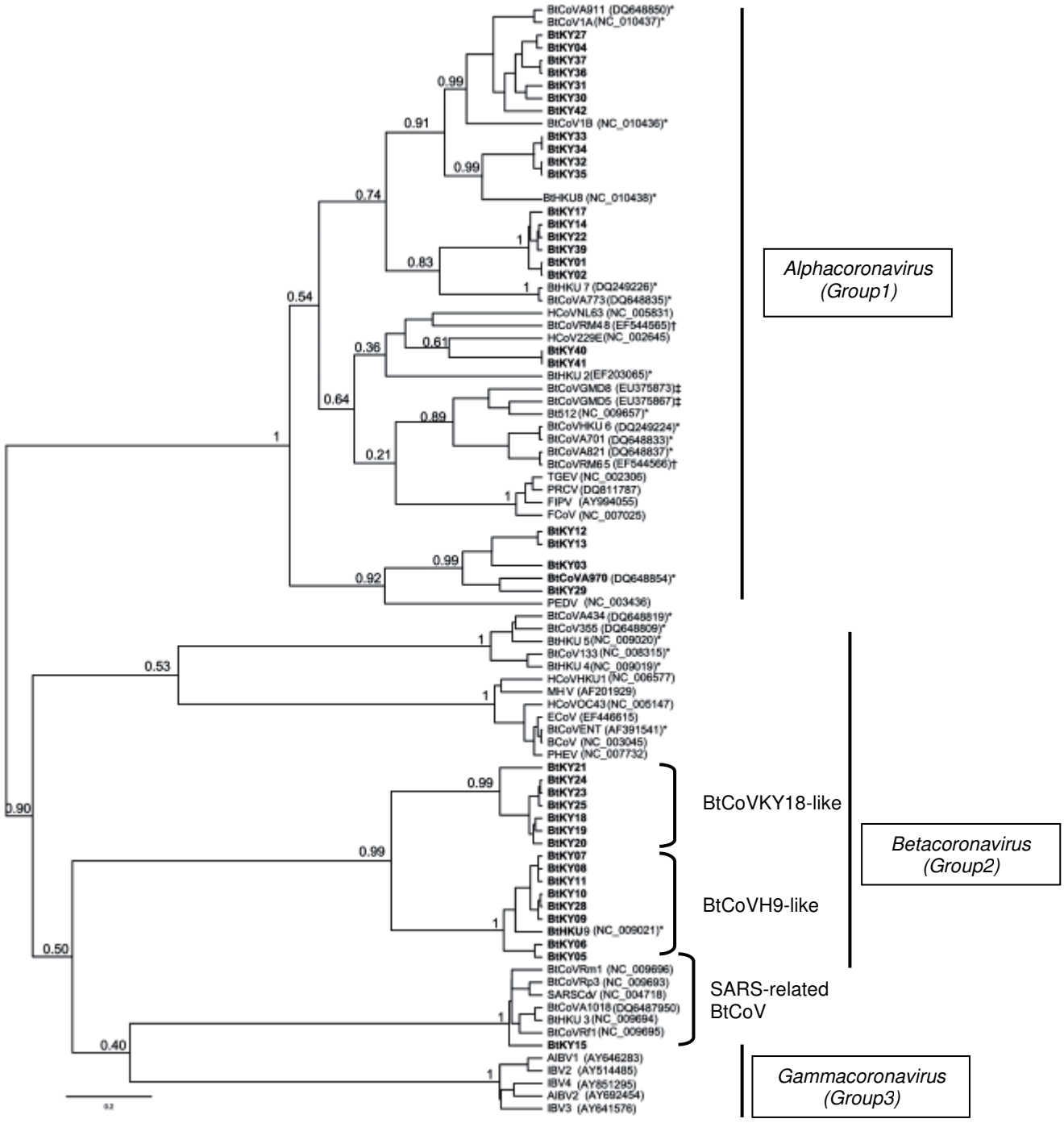


**Figure 1.9**: Phylogenetic tree of the novel Kenyan bat coronaviruses constructed from a 121nt fragment of the RdRp gene (ORF 1b) (Modified from Tong *et al.*, 2009).

The alphacoronaviruses from Ghana cluster closely to the human coronavirus HCoV229E (sharing 86.50%-91.90% nucleotide (nt) identity in the amplified 817 nt fragment) with 100% bootstrap support and a Bayesian posterior probability of 1.0. The betacoronaviruses from Ghana appear to be related to the SARSr-CoV cluster, sharing only 72.2% nucleic identity with SARS-CoV.

The latest surveillance study reported from Africa was by Quan *et al.*, (2010) where a novel betacoronavirus, Zaria bat coronavirus (ZBCoV), was identified in a gastrointestinal tract sample taken from a *Hipposideros commersoni* bat from the tourist caves in Nigeria. ZBCoV possesses a unique genome organization, sharing only 70% nucleotide identity to any other known coronaviruses and is most related to the SARSr-BtCoV subgroup but not closely related enough to be classified within this subgroup. Molecular clocking using a 659 nt conserved RdRp segment suggests that the recently identified betacoronaviruses from Ghana and ZBCoV may have possess a common ancestor approximately 1400 years ago. Mean pairwise nucleotide similarity of the partial RdRp gene region of the clade containing ZBCoV and the betacoronaviruses from Ghana compared to the SARS-related CoV clade was 73% and was postulated to be sufficiently divergent from other betacoronaviruses to be considered as a new species.

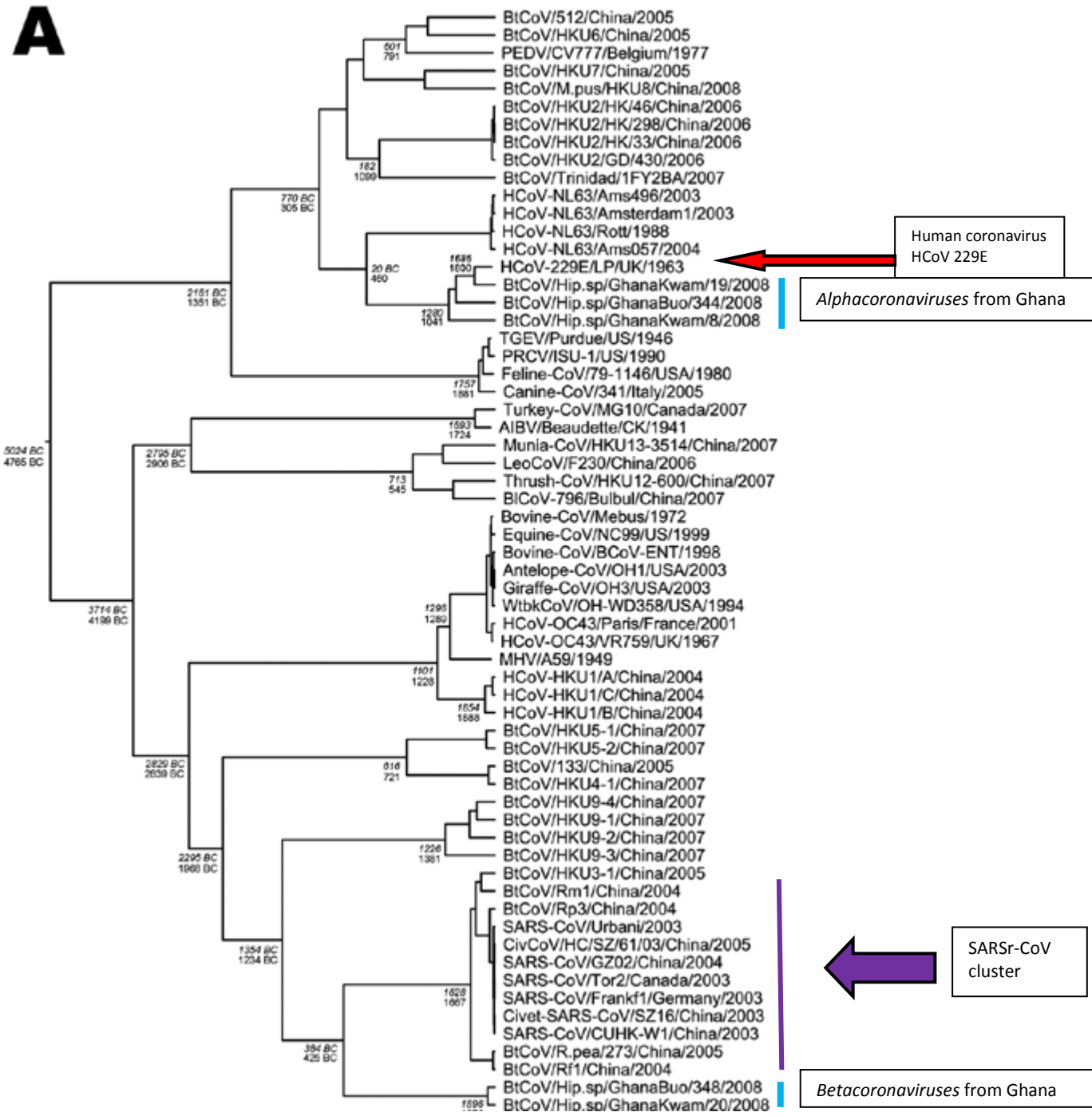


**Figure 1.10**: Phylogenetic tree of the RdRp gene (817 nt fragment) of the coronaviruses identified in Ghana. Bayesian inference was used to assemble root point dates under a relaxed lognormal molecular clock assumption with a codon-based substitution model (SRD06). Estimated dates of diversification of CoV lineages at root points are shown in italics (Modified from Pfefferle *et al.*, 2009).

### 1.6.7 Species specificity of bat coronaviruses

Several bat coronavirus detection studies in countries such as China, Bulgaria, Japan and Kenya have detected BtCoV in *Miniopterus* species, which typically form distinct clades in the *Alphacoronavirus* genus. *Mi-BtCoV1A* was the first non-SARS-related bat coronavirus identified in 3 separate species of *Miniopterus* (Table 1.4) (Poon *et al*., 2005). Figures 1.11 - 1.12 indicating phylogenetic relationships of various BtCoV detection studies highlighting the *Miniopterus* BtCoV. No *Miniopterus* species globally tested thus far have proven to be negative for BtCoV (Table 1.9).

It can be speculated that *Miniopterus* alphacoronaviruses may have been present in an ancestor species of *Miniopterus* before species divergence. And as such the alphacoronaviruses may have co-evolved with their hosts, subsequently diverging slowly from the ancestor alphacoronavirus, even as their host migrated to different continents.

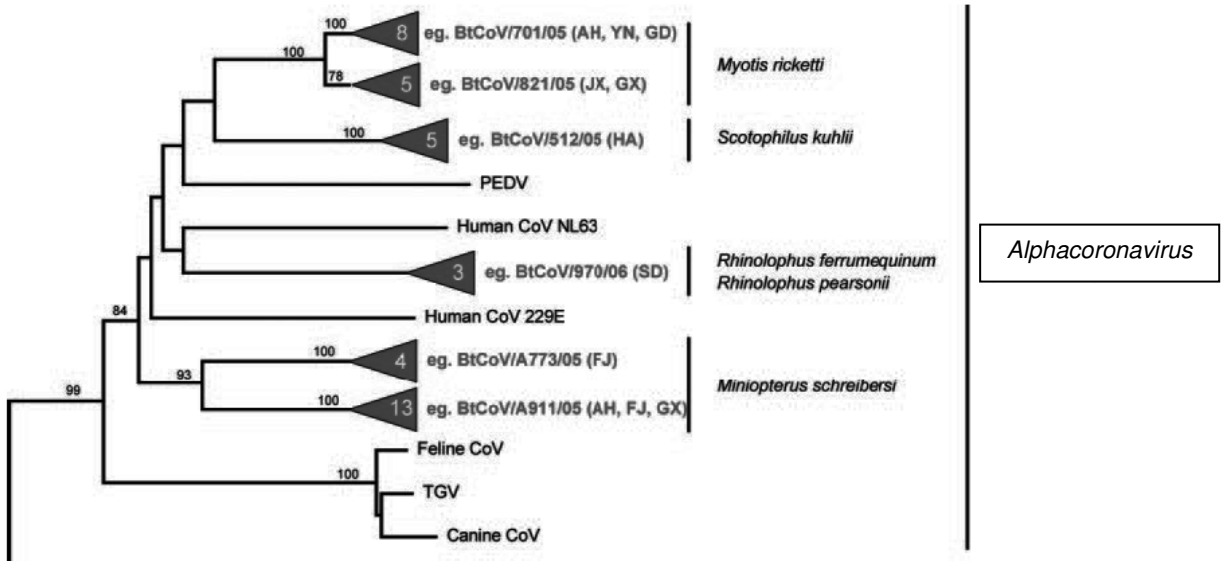


**Figure 1.11:** Partial phylogenetic analysis of the RdRp gene, showing only the *Alphacoronavirus* genus and BtCoV identified in China by Tang et al. 2006. The *Mi*-BtCoV condescend clades are shown by the *Miniopterus schreibersi* species name (Modified from Tang et al. 2006).

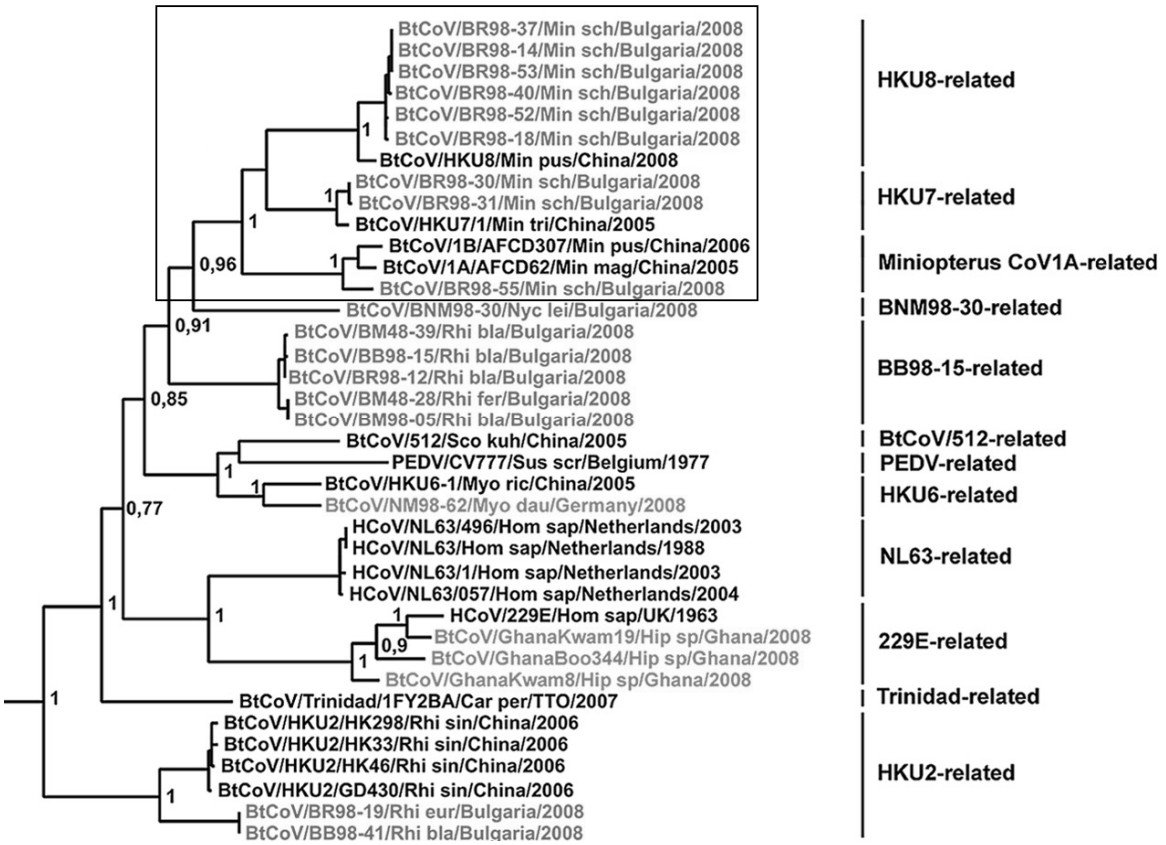


**Figure 1.12:** Phylogenetic analysis of the alphacoronaviruses identified in Bulgaria (grey), in comparison to closely related BtCoV (black), constructed with Bayesian analysis of an 816 nt segment of the RdRp gene. The *Miniopterus* BtCoVs are indicated in the block (modified from Drexler et al. 2010).

A total of 18 *Myotis* species have been analysed for the presence of BtCoV, of which 6 species have been found to possess alphacoronaviruses (Table 1.9). My-BtCoV HKU6 was first identified in *Myotis ricketti* in China (Woo *et al.,* 2006). Since then *Myotis* alphacoronaviruses related to My-BtCoVHKU6 have been detected in Europe and North America. Figure 1.13 shows the *Myotis* BtCoV lineages (genotypes) identified in the Northern part of Germany (Gloza-Raush *et al.,* 2008) and Figure 1.14 shows the *Myotis* BtCoV identified in the Netherlands, grouped according to the same lineage (genotype) derivation system (Reusken *et al.,* 2010). *Pipistrellus* spp. alphacoronaviruses also constitutes part of the European *Myotis* BtCoV genotypes.

The *Myotis* alphacoronaviruses from Germany, China and the United States have shown an interesting trend in BtCoV. Figure 1.8 shows the North American *Myotis* BtCoV identified from *Myotis occultus.* The North American *Myotis* BtCoVs were more closely related to the European and Chinese *Myotis* BtCoV from the same genus than the other North American coronaviruses from the unrelated *Eptesicus* bat spp. (located at the thick black line in Figure 1.13). Thus, as with the *Miniopterus* BtCoV, it could be speculated that an ancestor *Myotis* alphacoronavirus may have been present in ancient *Myotis* bats and diverged as the species separated and colonized different parts of the globe.

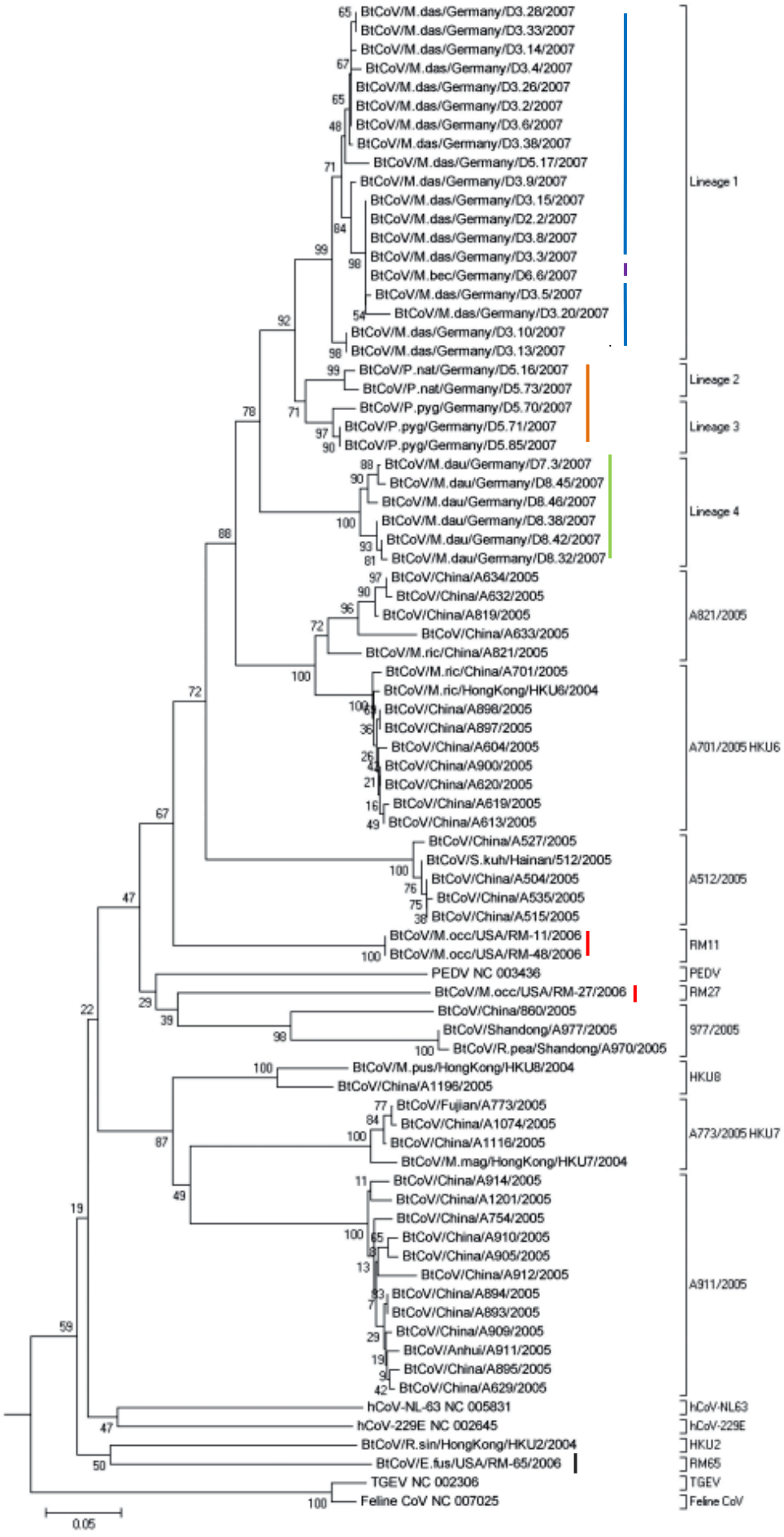

**Figure 1.13:** Phylogenetic analysis of the monophyletic alphacoronavirus clades identified in northern German bat species. The lineages (1–4) are phylogenetically compared to other alphacoronaviruses from mammals and other bat species. The names shown on the right of the tree indicate the bat CoV prototype strains or the type strains of established mammalian CoV species. The **light blue line** indicates the coronaviruses identified in *M. dasycneme* (lineage 1), the **purple line** indicates the coronaviruses identified in *M. bechsteinii* (also lineage 1), and the **green line** indicates the lineage 4coronaviruses identified in *M. daubentonii*. The **orange line** denotes the coronaviruses from the *Pipistrellus* bats genus identified in Germany (lineage 2 and 3). The **red line** denotes the position of the coronaviruses from the *Myotis* bats in North America. The **black line** shows the position of the *Eptesicus* spp. bat coronaviruses in relation to the *Myotis* spp. coronaviruses from North America and Asia. MEGA4 was used in the analyses, as well as the neighbour-joining algorithm with Kimura correction and a bootstrap test of phylogeny. The bootstrap values at the nodes are indicated as percentages of 1,000 repetitive analyses. The tree is rooted with a Leopard CoV, ALC/GX/F230/06 (Modified from Gloza-Rausch *et al.*, 2008)

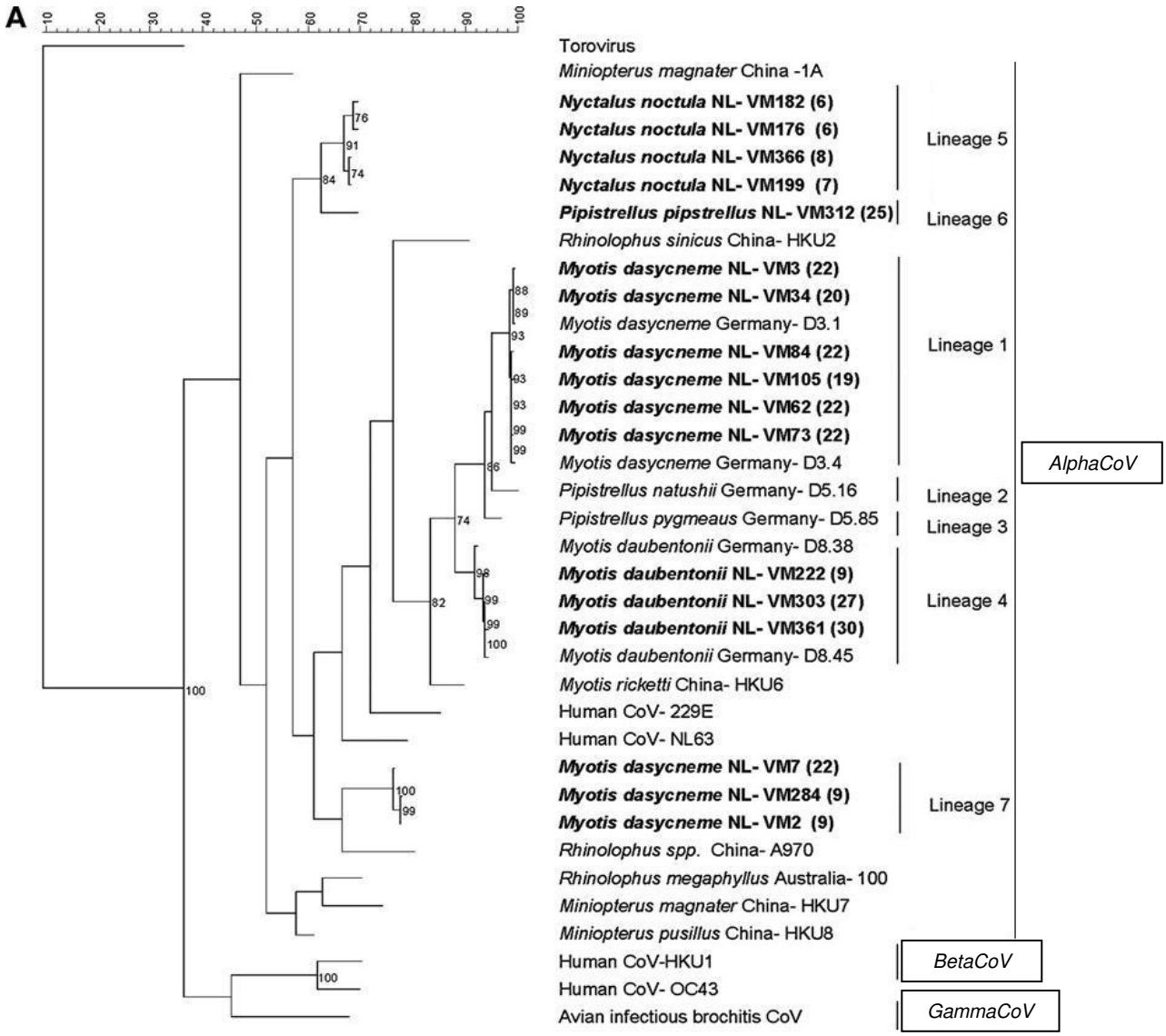


**Figure 1.14:** Phylogenetic analysis of a 334 nt fragment of the RdRp gene of the BtCoV identified in the Netherlands. Bootstraps at the nodes are indicated in percentages and only values >70 are depicted. Torovirus is used as the outgroup. (modified from Reusken *et al.*, 2010)

When the *Rhinolophus* genus was first implicated as a betacoronavirus reservoir, and possibly a reservoir for the SARS-related BtCoV, several studies have focused bat coronavirus detection on this genus (discussed in detail in Section 1.5.3). As a result, 18 species have been analysed thus far with only 8 species having been shown to be harbouring BtCoVs (Table 1.9).

Detailed *Rhinolophus* spp. investigations have been performed in the Hong Kong and Guangdong provinces in China (Lau *et al.* 2010a). A study of 1401 *Rhinolophus sinicus* (Chinese horseshoe bat) identified a prevalence of SARSr-*Rh*-CoV RNA in 15.7%. Twenty instances of co-infections were noted in *Rhinolophus sinicus* with *Rh*-BatCoV HKU2, also identified in the sampled bats in a prevalence of 15.5%. Possible recombination was also reported to have occurred between different strains of SARSr-*Rh*-CoV. Sliding window analysis of SARSr-Rh-BatCoV strains Rm1, Rf1, and Rp3 (using SARSr-CoV SZ3 as the query sequence) showed a possible breakpoint at the intergenic region between ORF1ab and the spike gene. Thus, it may be possible that civet SARSr-CoV strain SZ3 might be a potential recombinant formed from SARSr-Rh-BatCoV strain Rp3 (Guangxi province) and SARSr-Rh-BatCoV strain Rf1 (Hubei province), suggesting that civet SARSr-CoV may have evolved from a ancestor that is a recombinant between strains SARSr-Rh-BatCoV Rp3 and SARSr-Rh-BatCoV Rf1 or it might be a direct recombinant from yet undiscovered SARS-related BtCoV species which are closely related to SARSr-Rh-BatCoV Rp3 and SARSr-Rh-BatCoV Rf1. Figure 1.15 shows the phylogenetic clustering of the studied sequences by genome region. Several other possible recombination breakpoints were also observed between different strains of SARSr-*Rh*-CoV.

In the European study, the authors observed that the SARS-related CoV in Bulgaria were exclusively present in *Rhinolophidae* bats in 2 monophyletic clades (the first from *Rh. eurylae*, and the other from *Rh. ferrumequinum, Rh. mehelyi and Rh. blasii)* (Figure 1.16). The European SARSr-*Rh*-CoV, BtCoV/BM48-31/Rh bla/Bulgaria/08 (Table 1.7), showed higher similarity to SARS-HCoV, than the Chinese SARSr-*Rh*-CoV showed to SARS-HCoV in certain regions of the genome. SARS-HCoV and SARS*r-Rh*-BatCoV Rp3 (its closest SARSr-*Rh*-CoV relative) share an overall nucleotide similarity of 78% while SARS-CoV and BtCoV/BM48-31/Rhi bla/08 share an overall nucleotide similarity of 74.7%. However, the receptor binding domain (RBD) of SARS*r-Rh*-BatCoV Rp3 only shares 33% nucleotide identity with that of SARS-CoV with 2 notable deletions while BtCoV/BM48-31/Rhi bla/08 shares 68% nucleotide identity to the RBD of SARS-CoV with only 1 notable deletion. Though, by utilizing recombinant SARS-CoV spike protein bound to the BtCoV/BM48-31/Rhi bla/08 spike protein, human sera from SARS patients and polyclonal

rabbit serum, Drexler *et al.,* (2010) could show that there was no functional antigenic relatedness of the spike proteins.

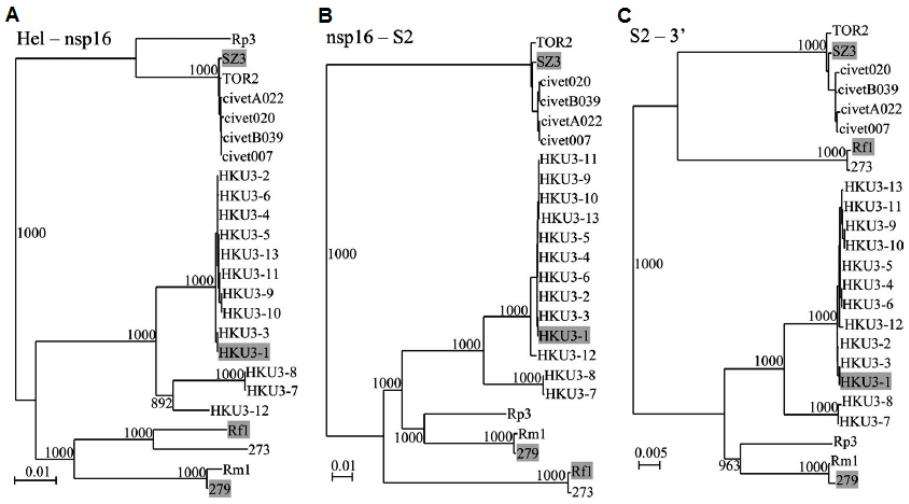


**Figure 1.15:** Neighbour-joining phylogenetic analysis constructed using Kimura's two-parameter correction method on regions corresponding to A) ORF1ab (positions 16400 to 20700 nt), B) Intergenic region (positions 20700 to 25000nt). C) Spike to 3' end (positions 25000nt to 3' end). Shaded strains, SARSr-Rh-BatCoV strain 279/04 (279), civet SARSr-CoV strain SZ3, and SARSr-Rh-BatCoV strain HKU3-1 were examined by bootscan analysis. Bootstrap values were calculated from a 1,000 repetitions (modified from Lau et al. 2010).

The studies performed in Ghana and Thailand (Pfefferle *et al.,* 2008, and Gouilh *et al.,* 2011) identified SARS-related BtCoV within *Hipposideros* hosts, even persisting within a *Hipposideros* colony for up to 18 months. Likewise Zaria BtCoV from Nigeria, a novel betacoronavirus closely related to the SARSr-CoV lineage was also detected from a host of the *Hipposideros* genus. Similar to the *Miniopterus* and *Myotis* BtCoV, the phylogeny of the SARS-related BtCoV correspond to their host species, irrespective of location of the host species. Due to the sister taxa relationship that *Rhinolopidae* and *Hipposideridae* bats share, Gouilh *et al.,* (2011) thus hypothesised that betacoronaviruses related to the SARSr-CoV lineage may have been present in the ancestor of *Rhinolophidae* and *Hipposideridae* before divergence into separate families and that these viruses subsequently co-evolved within these families diverging further into different betacoronavirus species.

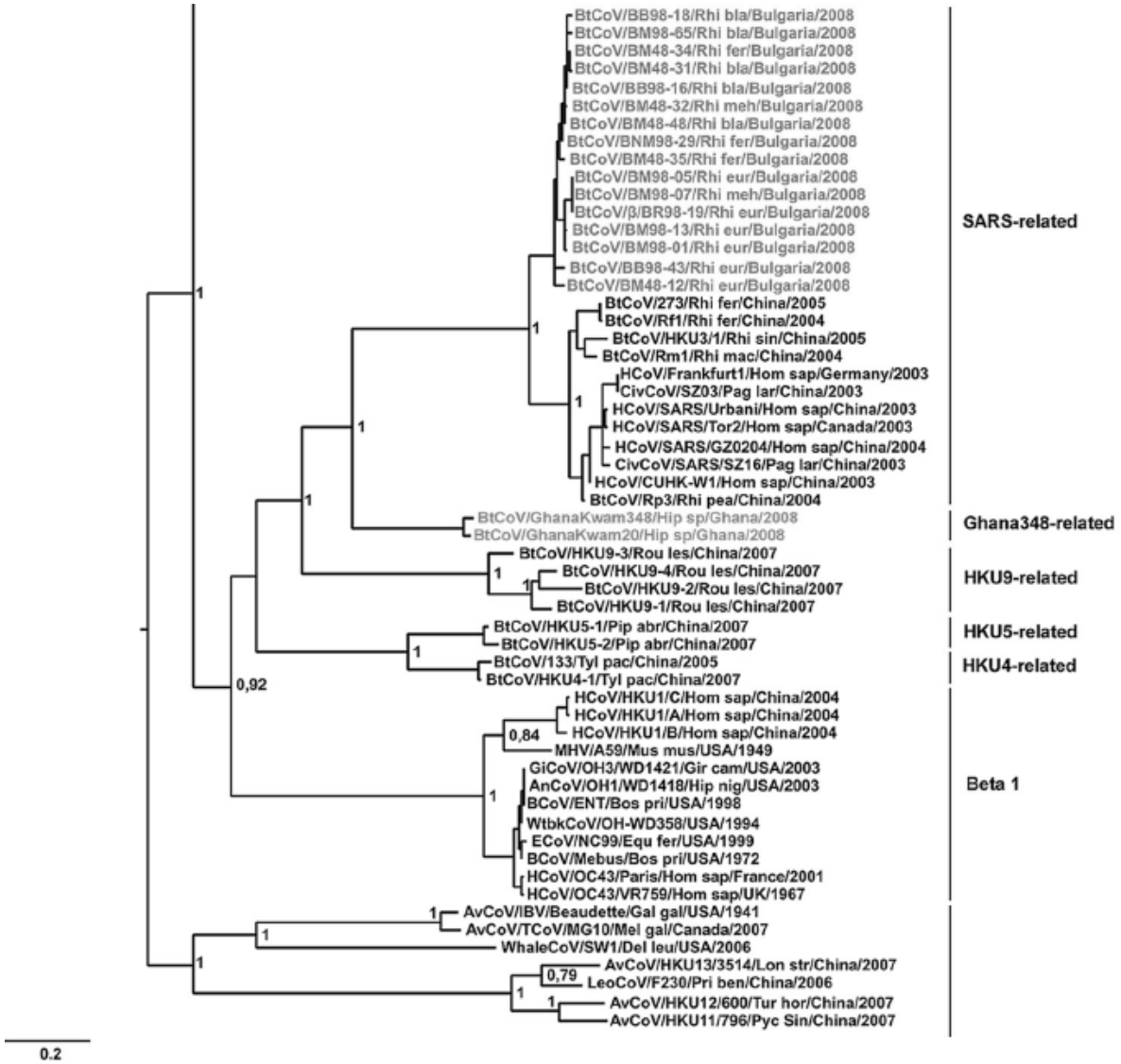


**Figure 1.16:** Phylogenetic analysis of the betacoronaviruses identified in Bulgaria (grey), in comparison to relevant closely related SARSr-BtCoV (black), constructed with Bayesian analysis of an 816 nt segment of the RdRp gene (modified from Drexler *et al.,* 2010).

Certain observations regarding BtCoV have been reported several times in the various BtCoV surveillance studies. One such observation is that BtCoV generally display strict species-specific host restriction (Tang *et al.*, 2005, Gloza-Raush *et al.*, 2008, Dominguez *et al.*, 2007, Osborne *et al.*, 2011, Gouilh *et al.*, 2011). Mostly, the coronaviruses that originated from the same bat species or genus clustered together when phylogenetically analyzed, regardless of location. For example in China, *Miniopterus spp.* and *Myotis spp.* are often found to roost together. Coronaviruses detected in *Miniopterus spp.* such as *Mi*-BatCoV 1A and BtCoV/A911/05 have only been detected in *Miniopterus* hosts, even when *Myotis spp.* from the same cave roost were also analysed. Likewise, coronaviruses detected in *Myotis spp.* such as *My*-BatCoV-HKU6 and BtCoV/821/05 has only been detected in *Myotis* hosts. These findings suggested that the genus-specific

coronaviruses have very narrow host ranges and may possibly frequently be transmitted between different species of the genera.

Similar species specificity was also observed for the BtCoV in the *Nyctalus* genus in Bulgaria and Germany. The same *Nyctalus spp.* coronaviruses identified in Bulgaria, was detected in *Nyctalus leisleri* sampled in Munster Germany, 2000km away from the initial sampling location in Bulgaria (97.7% nt identity).

Even though all the afore mentioned coronaviruses are alphacoronaviruses, the viruses from each genus grouped together in their own clade, regardless of the geographic location that the viruses and their hosts were sampled at (Poon *et al.*, 2005; Tang *et al.*, 2006). An example of this can be supplied when investigating the *Myotis spp*. BtCoV. The *Myotis*-BtCoV from Asia, Europe and North America phylogenetically group more closely together to each other than they do to any other of the local BtCoV that occur in other bat genera in their respective countries (Gloza-Rausch *et al.*, 2008; Dominguez *et al.*, 2007; Drexler *et al.*, 2011; Reusken *et al.*, 2010).

Gouilh *et al.,* (2011), hypothesized that species-specificity of certain BtCoV may be explained by typical behaviour displayed by certain species that result in species barriers to cross-transmission of viruses. In the study in Thailand, Gouilh *et al.,* (2011) observed spatial segregation between different species that inhabit the same cave roosts (e.g. *Hipposideros* spp. colonised a separate part of the cave than the *Taphozous* spp. with no intermingling). This species spatial segregation would thus limit cross-species transmissions.

In an apparent converse to the strict genus-specificity displayed by many BtCoV, it has also been observed that a single species of coronavirus may also be present in more than one bat species. This may be attributed to BtCoV spill over into other bat species. The betacoronavirus identified in the Philippines, BtCoV/1525G2/08, was reported to have been found in at least 4 *Pteropodidae* bat species. Similarly, bat species have also been found to harbour more than one type of BtCoV. From the Iberian Peninsula, lineages of similar alphacoronaviruses were detected in both *Nyctalus* and *Myotis* spp. A *Rhinolophus ferrumequinum* bat in China was found to harbour 3 separate bat coronaviruses: BtCoV/970/06 (alphacoronavirus; also present in *Rh. pearsoni*), BtCoV/273/04 (betacoronavirus (group 4)), and BtCoV/355/05 (betacoronavirus (group 5) also detected in *P. abramus*). It is unclear whether these viruses are actively replicating within these hosts or are merely being detected after spill over events.

The BtCoVs, *Ty*-BatCoV-HKU4 (*Tylonycteris pachypus*) and *Pi*-BatCoV-HKU5 (*Pipistrellus abramus*) are very similar to each other phylogenetically; however, they were detected in separate bat species and display strict species specificity. It may be possible that these viruses shared the same ancestor coronavirus from a previous spill over event

and so have diverged into separate species through their respective adaptations to new hosts.

### 1.6.8 Bat coronavirus infection

Most reported observations are that the bats from which coronaviruses have been identified appear to be healthy. In the surveillance study performed by Tang *et al.,* (2006), the study was able to detect BtCoV in samples taken during a 17 month sampling period at several locations. They thus hypothesised that the BtCoV may cause persistent or long term infections in their hosts. Gouilh *et al*., (2011) reported betacoronavirus viral persistence in a *Hipposideros* colony in Thailand for 18 months. Similarly, Osborne *et al*., (2011) reported repeated detection of the same alphacoronavirus in urban roosts of *Eptesicus fuscus* in North America within a 3 year period. However, the limit of virus clearance of individual bats was 6 weeks, indicating viral persistence in roosts but not in individuals. The study by Lau *et al.,* (2010a) found that by repeated sampling and BtCoV detection in *Rhinolophus sinicus* analysed in the study, that the bats were capable of clearing the SARSr-*Rh*-BtCoV detected in a time period of between 2 weeks to 4 months. Therefore the authors speculated that BtCoV such as the SARSr-*Rh*-BtCoV may result in acute, self-limiting infection in their hosts.

Another interesting observation noted by the authors, was that bats positive for SARSr-*Rh*-BtCoV displayed lower body weights that those negative for the virus, even though no disease symptoms were evident. The observations may suggest that SARSr-*Rh*-BtCoV infection may be associated with minor weight-loss, however further investigations will have to be performed on the pathogenesis of BtCoV. This phenomenon was not observed for *Rh*-BatCoV HKU2 also detected in the study. Gouilh *et al*., (2011) hypothesized that the weight loss of *Rhinolophidae* bats may be due to a loss of fitness as a result of the infection of the SARSr-BtCoV in the *Rhinolophidae* host. Similar symptoms have not been observed for *Hipposideros* bat species harbouring SARSr-BtCoV, and as such the authors suggest that *Hipposideros* hosts may be more resistant to SARSr-BtCoV infection or perhaps the SARSr-BtCoV in the *Rhinolophus sinicus* population may have acquired additional virulence factors also limiting the long term persistence of the virus within the bat populations.

The RNA of coronaviruses is most commonly detected from alimentary specimen taken from bats as well as fecal and rectal samples (such as swabs or fecal pellets). This might indicate that BtCoV could potentially be enteric viruses in bats, multiplying in the gastrointestinal tract and shed through the faeces (Poon *et al*., 2005). Respiratory specimens such as oral swabs were initially also taken for BtCoV detection. However, few studies have detected BtCoV from these sample types, and may possibly only be when the

viruses were present at very high titres (Poon *et al.*, 2005; Chu *et al.*, 2006). Detection in oral specimens may be when the viral infection may have reached another stage of infection for particular BtCoVs or it may simply due to a particular sampling time in the infection cycle or since the pathogenesis of BtCoV is so poorly understood it may be that virus replication could occur independently in the intestinal and respiratory tract (Falcón *et al.*, 2011). Alphacoronaviruses from *Miniopterus* and *Myotis* spp. have been detected in oral swabs (Poon *et al.*, 2005; Chu *et al.*, 2006; Falcón *et al.*, 2011). Some of the *Miniopterus* specimens from Hong Kong possessed Bat-CoV 1 in both fecal and oral specimens, however, none of the Iberian bats positive for alphacoronaviruses in the oral swabs also possessed the viruses in their fecal material (Falcón *et al.*, 2011).

The properties of coronavirus infections in bats may be due to specific behavioural features of the host organisms. Bats roost together in colonies of between thousands to millions of individuals. As such bats are almost constantly in contact with each other and social behaviour between individuals includes grooming. Therefore, a bat infected with a coronavirus could enter the colony and through social grooming may allow the spread of the viruses through contact with saliva or fecal particles present on the fur. It is purported that the viruses will replicate asymptomatically within the gastrointestinal tract and be shed through the faeces (and less commonly saliva). New individuals may then become infected and perpetuate the spread of the virus throughout the colony. BtCoV are observed to replicate within their hosts in low levels leading to short lived infections with persistent shedding.

Several studies have performed serological surveys of coronaviruses in bats (Muller et al. 2007; Li et al. 2005) and detected the presence of neutralizing antibodies against SARSr-CoV, which would also likely detect other antigentically similar members of the genus. However, the presence of these antibodies merely indicates viral exposure and not necessarily infection of the hosts. Bats that do become infected with BtCoV are able to produce a neutralizing antibody response capable of clearing the virus from the system within several weeks. Upon re-infection with the same virus from infected individuals within the same roost or from bats encountered during migration to alternative habitats, as reported in Lau *et al.* (2010a), the virus may then be cleared more rapidly.

### 1.6.9 Experimental infections

The BtCoV study from the Philippines by Watanabe *et al.*, (2010) also performed experimental oral infections of the betacoronavirus BtCoV/Philippines/1525G2/08 by infecting *Rousettus leschenaulti* bats with intestinal specimens from *Cynopterus brachyotis* (one of the host bat species from which the BtCoV/Phil/1525G2/08 was detected). The virus was capable of infection and propagation (via detecting increased levels of CoV

mRNA) within the intestines of a new host species but showed no signs of clinical symptoms.

### 1.6.10 Bat coronaviruses and the origin of non-bat coronaviruses

The previous sections have discussed the diversity of bat coronaviruses. However, an observation can be made that the current knowledge of BtCoV diversity may in some part be attributed to significant sampling bias. Since the identification of SARS-related BtCoV present in *Rhinolophus* spp., bat species have been greatly sampled and analysed for the presence of coronaviruses. It may be that due to the increasing surveillance of a particular viral species within a specific wildlife species has allowed for skewed sampling bias. A large diversity of BtCoV has thus far been detected within bats because bats have been the subject to detailed coronavirus investigations. Likewise, a larger diversity of bird coronaviruses are currently being detected due to increased sampling within bird populations (Woo *et al.,* 2009). This particular observation however may only be supported with significant sampling being performed within other wild life populations such as rodents, felines, and canines.

Phylogenetic investigations of the newly identified BtCoV have shown similarities to the previously identified non-bat CoV. In 2006, Tang *et al.*, hypothesized that due to the phylogenetic grouping of the novel BtCoV to other animal host coronaviruses, it would seem to suggest that viral transmission may occur between bats and domestic (cats) and farm animals (pigs). These transmissions from bats to other animal species may create the opportunity for transmissions to humans as well. For example the human betacoronavirus HCoVOC43 and Bovine CoV generally cluster closely together within the same clade in phylogenetic trees (Figures 1.9 and 1.10). It is theorised that BCoV may have been established in bovine species due to the viral transmission from an unknown BtCoV, which in turn lead to the transmission of BCoV to humans and the establishment of HCoVOC43, a common cold virus, in humans (Perlman and Netland, 2009).

Vijaykrishna *et al.*, (2007) studied the ecology, evolutionary pathways and diversity of CoV, attempting to compare population dynamics and divergence dates of all known groups of coronaviruses. Their results conclude that BtCoV appear to be more ancient than the CoV found in other animals. Population growth models of the CoV revealed that the CoV population growth in hosts such as bats was at a constant growth rate and that the CoV in other animal hosts displayed an epidemic-like increase in population growth also associated with mild to severe disease symptoms not observed to date within bats. Typically when a virus population's growth changes from constant low level replication to sudden epidemic-like increases within the hosts, it indicates a change in host species. Vijaykrishna *et al.*, (2007) concluded that CoV are endemic to various bat species, and that

the CoV present in the other animal species are due to repeated introductions and subsequent establishment of the viruses.

The authors also used the ORF1 helicase gene in molecular clocking. The phylogenetic tree in Figure 1.17 shows and supports their conclusions that BtCoV are older than the CoV from any other animal species. The diversity of CoV is also greater than that seen in other animal species and it would appear as if bats harbouring CoV are healthy with no symptoms indicative of infection. From the evidence they deduced that it is likely that all CoV present in other animals are derived from the CoV present in bats. The phylogenetic tree in Figure 1.17 suggests that the SARSr-Rh-BtCoV and HSARS-CoV diverged approximately 17 years before the 2002 SARS outbreak. However, the helicase gene region used in Vijaykrishna *et al.,* 2007 may not the most optimum region to use in order to infer evolutionary history. Later studies that use the RdRp gene for example, are able to infer a much more precise phylogenetic history and a time of the most common recent ancestor for SARSr-Rh-BtCoV and HSARS-CoV was estimated to be 4.08 years before the 2002 SARS outbreak (Hon *et al.*, 2008).

The conclusions theorised by Vijaykrishna *et al.*, (2007) were perhaps devised prematurely, as the authors were lacking essential information reported in later coronavirus studies. The *Gammacoronavirus* genus consisted previously of only avian CoV such as IBV. New viruses identified that belong to this genus include a beluga whale coronavirus SW1 (Mihindukulasuriya *et al.*, 2008), novel bird CoV such as BuCoV-HKU11 in *Pycnonotus* birds, ThCoV-HKU12 in *Turdus* birds, and MuCoV-HKU13 in *Lonchura* birds, as well as the identification of related gammacoronaviruses in Asian leopard cats (*Prionailurus bengalensis*) and Chinese ferret badgers (*Melogale moschata)* (Dong *et al.*, 2007). There may yet be a much larger diversity of undiscovered coronaviruses to be found in birds and no BtCoV that has been identified to date have been from the *Gammacoronavirus* genus.

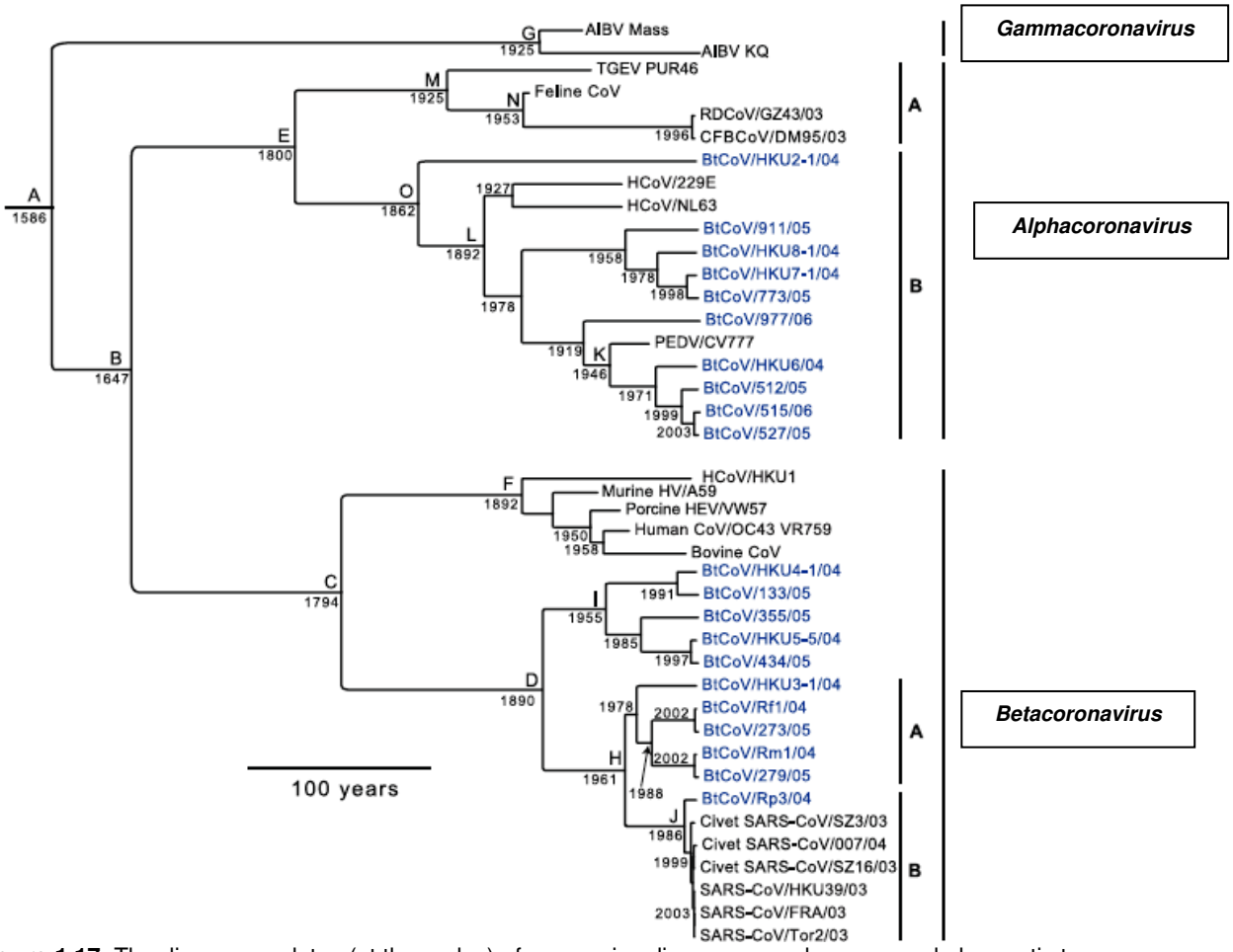


**Figure 1.17**: The divergence dates (at the nodes) of coronavirus lineages are shown on a phylogenetic tree based on 1,797 nt of the helicase domain. The divergence dates were calculated with an uncorrelated exponential relaxed-clock model in BEAST v1.4. (Modified from Vijaykrishna *et al.,* 2007).

Due to these new developments, a formal coronavirus evolutionary origin was proposed by Woo *et al.*, (2009), which suggested that the natural reservoirs for all *Alpha-* and *Betacoronavirus* lineages are bats, and the natural reservoirs for the *Gammacoronavirus* lineage are birds. Thus the coronaviruses that infected humans and other mammals were originally derived from either a bat or bird coronavirus ancestor. It may be that the ancient ancestor of coronaviruses may have infected a bat, which subsequently may have spread to a bird (or vice versa) leading to dichotomous evolution (Figure 1.18). The CoV still present in the bats may have spread to other bat species, mammals and humans resulting in the CoV distribution that is the *Alpha-* and *Betacoronaviruses*. A similar divergence can be seen with the bird CoV in the *Gammacoronavirus* genus.

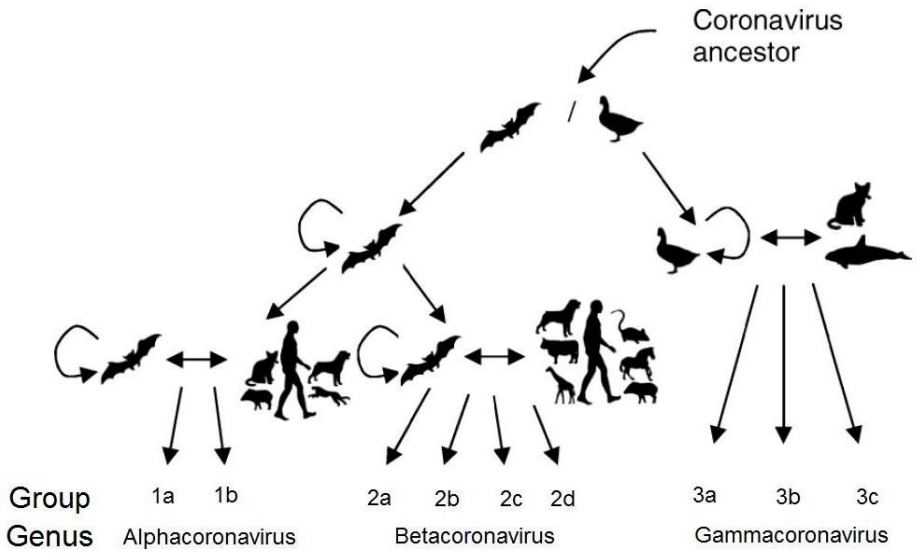


**Figure 1.18:** A model of coronavirus evolution hypothesised by Woo et al. 2009. The coronaviruses in the *Alpha-* and *Betacoronavirus* genera are derived from bat coronaviruses, and the coronaviruses in the *Gammacoronavirus* genus are derived from bird coronaviruses (Modified from Woo *et al.,* 2009).

It has been hypothesized that it may be features unique to these two groups of animals that may enable them to act as coronavirus reservoirs, such as the large species diversity of bats (20% of the 4800 mammalian species recorded) and birds (10,000 species) themselves, the ability to fly and migrate over large distances may enable virus exchange to many other species, and the fact that these groups of animals roost/flock together in large numbers, easily facilitating virus exchange between members of the same species.

## 1.7 Chiropteran classification, biogeographical origin of bat lineages and species associated with coronaviruses

### 1.7.1 Bat taxonomy and evolution

#### A. Bat taxonomy

Bats inhabit almost every continent on the globe, with the exception of Antarctica and perform essential ecological functions in many ecosystems as predators of insects and pollinators of flowers. Bats are also adapted to utilise a diverse range of food sources such as nectar, pollen, fruit, insects, small vertebrates as well as blood, and unlike other mammalian species many bat species may coexist in large numbers (up to 110 different species reported) within the same community (Simmons, 2005). They also constitute 20% of all extant

mammalian species recorded to date, and possess two features unique to all other mammals - true powered flight and echolocation.

There is a greatly lacking fossil record for chiropterans and due to the conflicting nature between molecular and morphological data for bats, the higher level phylogeny of bats (such as suborders, infraorders, superfamilies, families and subfamilies) has been a subject of debate for years (Simmons, 2005; Teeling *et al.*, 2005; Van den Bussche and Hoofer, 2004). The order of bats, C*hiroptera,* was traditionally divided into 2 suborders, the *Megachiroptera* (fruit bats with primitive echolocation adaptations; *Pteropodidae*) and *Microchiroptera* (mainly insect eating bats that have highly developed echolocation adaptations). This grouping necessitated review with the phylogenetic finding that the *Pteropodidae* megabat family and the putative *Rhinolophoidea* superfamily of previously classified microbats (*Rhinolopidae, Megadermatidae, Craseonycteridae and Rhinopomatidae*) were more closely related to each other than to other microbats. Thus the suborders Yinpterochiroptera (*Pteropodidae* and *Rhinolophoidea*) and Yangochiroptera (all other Microbats) were suggested (Teeling *et al.*, 2005). Other superfamily designations along with various sub- and infra- orders were also proposed (Teeling *et al.*, 2005). Due to various discrepancies, the higher level systematic phylogeny of chiropterans is poorly understood as is the understanding of chiropteran adaptive radiation.

Thus for the purposes of this review on bat taxonomy, we follow taxonomic classification set down by the 2011 African Chiropteran Report (ISSN 1990-6471), that follows the suggested taxonomic rearrangement suggested by Hutcheon and Kirsch (2006). The authors suggest two suborder groupings, the *Pteropodiformes* and *Verpertilioniformes,* which will be immune to subsequent changes regardless of the addition or removal of bat families within these suborders. The new *Pteropodiformes* subgroup currently consists of the *Pteropodiformacei* and *Rhinolophiformacei* infraorders:

**Suborder: *Pteropodiformes***

Infraorder: *Pteropodiformacei*

Superfamily: *Pteropodoidea*

Familiy: *Pteropodidae* (Fruit bats/ Mega bats)

Subfamily: *Pteropodinae, Macroglossinae,* and *Propottininae*

Infraorder: *Rhinolophiformacei*

Superfamily: *Rhinolophoidea*

Familiy: *Hipposideridae* (Leaf nose bats)

Subfamily: *Hipposiderinae*

Familiy: *Rhinolopidae* (Horseshoe bats)

Familiy: *Megadermatidae* (False vampire bats/Yellow-winged bats)

Superfamily: *Rhinopomatoidea*

Familiy: *Rhinopomatidae* (Mouse tailed bats)

The *Verpertilioniformes* subgroup currently consists of the *Noctilioniformacei, Nycteriformacei,* and *Verpertilioniformacei* infraorders:

**Suborder: *Verpertilioniformes***

Infraorder: *Noctilioniformacei*

Superfamily: *Noctilionoidea*

Familiy: *Noctilionidae* (Bulldog bats/fisherman bats)

Familiy: *Myzopodidae* (Sucker-footed bat)

Infraorder: *Nycteriformacei*

Superfamily: *Nycteroidea*

Familiy: *Emballonuridae* (Sac-winged bats, Sheath-tailed bats)

Familiy: *Nycteridae* (Slit-faced or Hollow-faced bats)

Infraorder: *Vespertilioniformacei*

Superfamily: *Molossoidea*

Familiy: *Molossidae* (Free-tailed bats)

Subfamily: *Molossinae*

Superfamily: *Verpertilionoidea*

Familiy: *Miniopteridae* (Bent-winged/Long fingered bats)

Familiy: *Verpertilionidae* (Evening/Common bats)

Subfamily: *Kerivoulinae, Myotinae, Scotophilinae, Vespertilioninae*

The taxonomic groupings given above are represented as they are given in the 2011 African Chiropteran report (ISSN 1990-6471), and as such families of Asian, European, North or South American bats may not be listed above since they do not occur in Africa. Table 1.9 includes non-African bat families (where relevant) within the most appropriate superfamily groupings as they are used by the African Chiropteran report (ISSN 1990-6471).

At present, there are 18 living chiropteran families grouped together through shared morphological/anatomical specializations and echolocation behaviour as well as 6 extinct families created from available fossil records (Teeling *et al.,* 2005). The phylogenetic tree in Figure 1.19 from Eick *et al.*, (2005) shows the recent phylogenetic separation of bat families and species.

## B. Biogeographical origins of bats

The earliest fossil records for bats are from early in the Eocene epoch in the Cenozoic era approximately 56 million years ago (mya) (Teeling *et al.*, 2005, Simmons, 2005) (Figure 1.20). However, these fossils identified in Europe, Australia and North America was already specialized for flight and echolocation, indicating an even earlier

origin of bats. Phylogenetic studies performed in 2005 using 13.7kb sequence data of 17 nuclear genes on extant bat families as well as available fossil records support a Northern hemisphere or Laurasian origin of bat species possibly in the early Paleocene epoch (Teeling *et al.*, 2005). The established groups may subsequently have diverged into different lineages and to different continents from there. Teeling *et al.,* (2005) estimates that the crown groups of bats last shared a common ancestor 64 mya (at the start of the Cenozoic era). However Eick *et al.,* (2005), using 4kb of sequence data from 4 novel nuclear intron markers and dispersal-vicariance (Diva) analysis concludes an African origin of extant bat families (with 39 dispersal and 2 vicariance events), and that chiropterans emerged 65 mya (at the Cretaceous-Tertiary boundary). Eick *et al.,* (2005) reported little phylogenetic resolution between fossil and extant bats when morphological characters that contradict microbat paraphyly were excluded. Thus only data of extant bat families were used for biogeographical reconstructions.

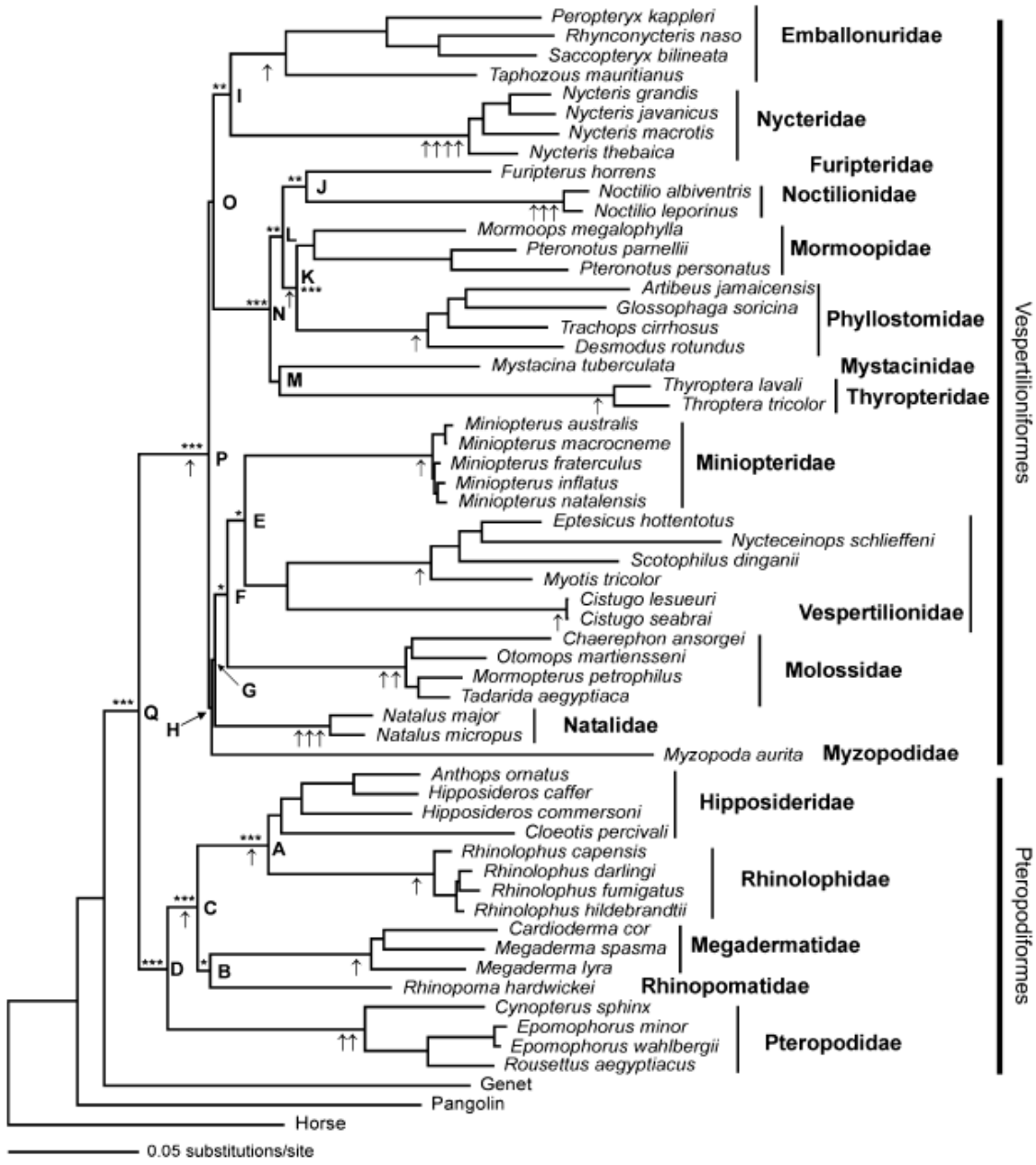


**Figure 1.19**: Maximum likelihood phylogenetic analysis showing the family designations of the Chiropteran order using analysis of the intron supermatrix using a model for nucleotide evolution. Vertical arrows indicate unique indel events supporting phylogenetic associations. The number of asterisks indicate whether labelled nodes were recovered with >70% bootstrap or >0.95 Bayesian posterior probability by all three (***), two (**), or only one (*) of the three methods of phylogenetic inference used by Eick *et al.* 2005. The branch lengths are proportional to the number of substitutions as indicated by the scale bar. (Eick *et al.*, 2005, Permission to use from Oxford University Press, Licence no. 2880640227752).

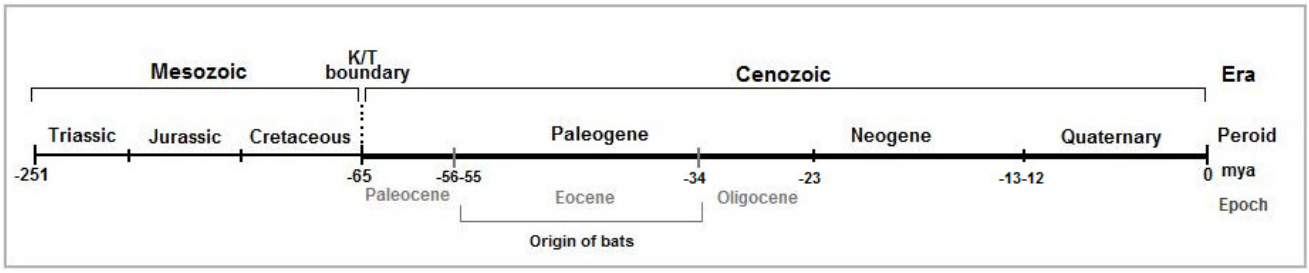


**Figure 1.20:** The geological time line from present to the beginning of the Mesozoic era, 250 million years ago. The timeline shows the origin of Chiropterans in the Eocene epoch reported in Teeling *et al.,* (2005) and Eick *et al.,* (2005) using the available fossil records.

The paraphyletic microbat bat lineages comprising of the *Rhinolophoidea, Emballonuroidea, Noctilionoidea* and *Vespertilionoidea* lineages all shared a common ancestor approximately 60-52 mya (Teeling *et al*., 2005; Miller-Butterworth *et al*., 2007). Chiropterans underwent rapid radiation in the Eocene epoch, with all extant bat families having emerged by the late Eocene. The majority of Africa during the early Eocene was covered in tropical rainforests, followed by a decrease in rainforests and an increase in woodland vegetation by the middle Eocene. Rapid diversification of bat echolocation and flight adaptations at the time may have been due to increasing plant and insect diversity as a result of global temperature increases.

Ancestral reconstructions by Teeling *et al*., (2005) of the *Pteropodiformes* support an Asian origin as compared to an African origin by Eick *et al*., (2005), with diversification in the late Paleocene epoch and all current distribution of these bats are exclusively in the Old world. *Hipposideridae* and *Rhinolophidae* divergence occurred within the middle Eocene to late Eocene with sister clades comprising of the *Rhinopomatidae* and *Megadermatidae* families. Discerning a biogeographical origin for the *Verpertilioniformes* is substantially more difficult to do due to their current global distribution. However, Teeling *et al*., (2005) suggests a Europe and Asia (Laurasian) origin for *Verpertilioniformes.*

Eick *et al*., (2005) reported 2 vicariance events from their biogeographical reconstruction with Chiropterans radiating from Africa to the Americas. The emergence of the *Noctilioidae* and *Natalidae* families show a termination of gene flow between African and American species. The African and North/South American continents spilt apart approximately 100-84 mya, with connecting land masses still in existence approximately 49 mya. Several situations are proposed to have allowed the radiation to bat species between hemispheres. Direct transatlantic migration may have occurred utilizing the land masses transversing the South Atlantic Ocean when the sea level was still low (‘Stepping stones’ proposal) (Figure 1.21). It may however also be possible for dispersal to have occurred from Africa to Eurasia across the Tethys sea, followed by entry into North America via the

'Beringa' land mass (connected Asia and North America) or other transatlantic bridges and subsequently down to South America by utilizing the Caribbean archipelago (Eick *et al.*, 2005) (Figure 1.21).

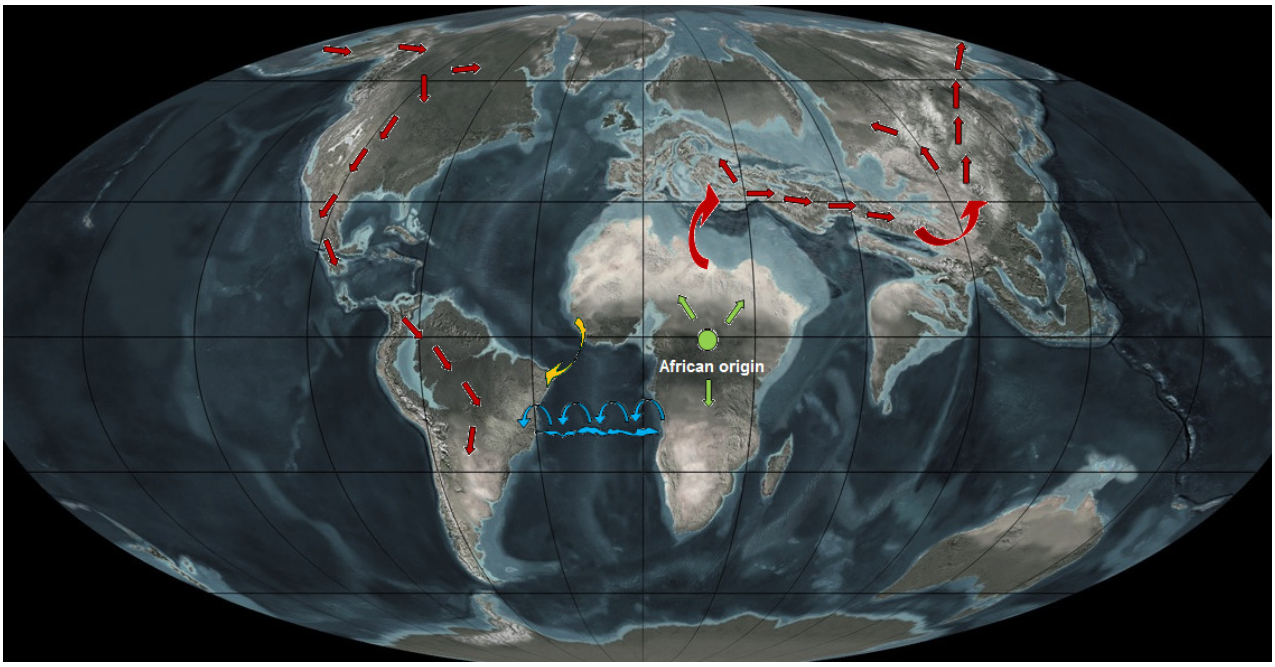


**Figure 1.21:** World Map of the Eocene epoch indicating the 3 major hypothesized methods of global bat migration. The **green** circle in the middle of the African land mass indicates the African origin of extant bat orders, the *Pteropodiformes* and *Vespertilioniformes,* as theorised by Eick et al., (2005). The hypothesis for transatlantic migration with the usage of shallow landmasses, known as 'stepping stones' is indicated with the **blue** arrows. The **orange** arrow displays possible transatlantic migration that may have occurred through vegetation rafts. The **red** arrows above indicate the possible global migration of bat species by using connecting land masses, allowing migration from Africa to Eurasia, North America and South America.

The *Molossidae* family was estimated to have diverged from the larger *Vespertilionidae* family (*Noctilionidae* and *Phyllostomatidae*) approximately 48 mya, with the *Miniopteridae* and *Verspertilionidae* families diverging approximately 43 mya (as a sister clade to the *Molossidae*) (Teeling *et al.*, 2005; Miller-Butterworth *et al.*, 2007). The *Noctilionidae* are mainly distributed within the neotropics with a possible origin in the Gondwana land mass, approximately 52 mya. Today, the distribution of *Emballonuridae* is restricted to the tropical regions of South America and Africa (opposite sides of the Atlantic ocean). Molecular dating and fossil records indicate that there was a split between the African and South American *Emballonurids* approximately 30 mya. The authors suggest possible theories as to how *Emballonurids* of Africa (Gabon) may have traversed the Atlantic to South America (Brazil), possibly utilizing 'vegetation rafts' as is hypothesized for *Rodentia* and *Carnivora*, or the 'stepping stones' proposal (small land masses that spanned the ocean approximately 31-25 mya) (Teeling *et al.*, 2005) (Figure 1.21).

The results reported by Teeling *et al.,* (2005) were concluded with the usage of available fossil records as well as 40 extant bat species, only 3% of the 1100 species of bat known to exist. The megabats were reported to be missing approximately 98% of the fossil history and the microbat lineages were reported to be missing between 56-86% of the fossil history (Teeling *et al*., 2005; Simmons, 2005). Therefore, conclusions drawn from Teeling *et al.,* (2005) as well as Eick *et al.,* (2005) are valuable in terms of preliminary data for the origin of bat families but requires more detailed further investigations on comparable genome regions and the inclusion of families not represented within these studies.

### 1.7.2 Bat species associated with bat coronaviruses

Table 1.9 lists all the bat species analysed to date in BtCoV surveillance studies throughout the world. The bat species are listed according to the current family designations as indicated in the 2011 African Chiropteran Report. The publications and countries in which the studies were performed are also included. The bat species that are negative for the presence of BtCoV are indicated in grey shading and the bold type shows the bat species from which BtCoV have been identified.

Table 1.9 shows interesting developments that may either be due to the co-evolutionary history between coronavirus species and bat hosts, or may simply be due to sampling bias. Bat coronaviruses have been detected in bat species from the *Pteropodidae, Hipposideridae*, *Megadermatidae*, *Rhinolophidae*, *Phyllostomidae, Vespertilionidae Miniopteridae* and *Molossidae* families*;* however no BtCoV have thus far been identified in the *Nycteroidea* bat superfamily (includes the *Nycteridae and Emballonuridae* families). This may simply due to sampling bias as this is the superfamily least sampled thus far, the majority of which have been sampled in the African countries of Kenya and Ghana as well as Thailand in Asia.

Interesting to observe is that all 8 of the *Miniopterus* spp. analysed in Asian, African and European countries have been shown to harbour bat coronaviruses. All of the *Miniopterus* BtCoVs are also related, more related to other *Miniopterus* BtCoV than any of the local BtCoV occurring in other genera, irrespective of location or country of the host bat species (*Miniopterus* BtCoV are discussed Section 1.5.7 A)

**Table 1.9: All bat species analysed to date for the presence of bat coronaviruses according to family grouping**

| *Taxonomic Level* | *Bat species* | CoV Positive/Total | Serology positive | Country | Reference |
|---|---|---|---|---|---|
| **PTEROPODIFORMI (SUBORDER)** | | | | | |
| **PTEROPODIFORMACEI (INFRAORDER)** | | | | | |
| **PTEROPODOIDEA (Super-family)** | | | | | |
| ***Pteropodidae* (Family)** | | | | | |
| *Pteropodinae* (Sub-family) | *Casinycteris argynnis* | - | 0/3 | Bandundu Province, DRC | Müller et al., 2007 |
| | *Cynopterus sphinx* | 0/15 | - | China, HKSAR | Poon et al. 2005 |
| | | 0/2 | - | China, HKSAR | Woo et al. 2006 |
| | | 0/27 | 0/17 | China, Guangdong | Li et al. 2005 |
| | | 0/6 | - | China | Tang et al. 2006 |
| | ***Cynopterus brachyotis*** | **2/4** | - | Philippines, Los Banos | Watanabe et al. 2010 |
| | | **7/19** | - | Philippines, Diliman | |
| | ***Eidolon helvum*** | **-** | 0/6 | Bandundu Province, DRC | Müller et al., 2007 |
| | | **6/10** | - | Kenya | Tong et al. 2009 |
| | | Negative, n=? | - | Nigeria | Quan et al. 2010 |
| | | 0/212 | - | Ghana | Pfefferle et al. 2009 |
| | ***Eonycteris spelaea*** | **2/3** | - | Philippines, Los Banos | Watanabe et al. 2010 |
| | | **2/2** | - | Philippines, Diliman | |
| | | 0/3 | - | Thailand | Gouilh et al., 2011 |
| | *Epomops franqueti* | - | 0/5 | Bandundu Province, DRC | Müller et al., 2007 |
| | *Epomophorus gambianus* | - | 0/10 | South Africa | Müller et al., 2007 |
| | *Epomophorus wahlbergi* | 0/3 | - | Kenya | Tong et al. 2009 |
| | | - | 0/2 | South Africa | Müller et al., 2007 |
| | *Hypsignathus monstrosus* | - | **1/11** | Bandundu Province, DRC | Müller et al., 2007 |
| | *Lissonycteris angolensis* | 0/10 | - | Kenya | Tong et al. 2009 |
| | | - | **1/18** | DRC | Müller et al., 2007 |
| | *Myonycteris torquata* | - | **1/7** | Bandundu Province, DRC | Müller et al., 2007 |
| | ***Ptenochirus jagori*** | **11/14** | - | Philippines, Los Banos | Watanabe et al. 2010 |
| | | 0/2 | - | Philippines, Diliman | |
| | ***Pteropus alecto*** | **4/29** | - | Australia | Smith *et al.*, 2010* |
| | ***Rousettus aegyptiacus*** | **12/39** | - | Kenya | Tong et al. 2009 |
| | | Negative, n=? | - | Nigeria | Quan et al. 2010 |
| | | **-** | **11/29** | South Africa | Müller et al., 2007 |
| | | | **17/142** | Oriental Province, DRC | Müller et al., 2007 |
| | ***Rousettus amplexicaudatus*** | **1/1** | - | Philippines, Diliman | Watanabe et al. 2010 |
| | ***Rousettus lechenaulti*** | 0/2 | - | China, HKSAR | Woo et al. 2006 |
| | | **43/350** | - | China, Guangdong | Woo et al. 2007 |
| | | 0/165 | **1/126** | China, Guangxi | Li et al. 2005 |
| | | 0/43 | - | China, Guangdong | |
| | | 0/31 | - | China | Tang et al. 2006 |
| | | 0/35 | - | Thailand | Gouilh et al., 2011 |
| **RHINOLOPHIFORMACEI (INFRAORDER)** | | | | | |
| **RHINOLOPHOIDEA (Super-family)** | | | | | |
| ***Craseonycteridae* (Family)** | | | | | |
| | *Craseonycteris thonlonyi* | 0/10 | - | Thailand | Gouilh et al., 2011 |
| ***Hipposideridae* (Family)** | | | | | |
| ***Hipposiderinae* (Sub-family)** | *Aselliscus stoliczkanus* | 0/7 | - | China | Tang et al. 2006 |
| | *Coelops frithi* | 0/6 | - | China | Tang et al. 2006 |
| | ***Hipposideros amiger*** | 0/4 | - | China, HKSAR | Poon et al. 2005 |
| | | 0/13 | - | China, HKSAR | Woo et al. 2006 |
| | | 0/26 | - | China, Guangdong | Woo et al. 2007 |
| | | 0/58 | - | China | Tang et al. 2006 |
| | | **4/55** | - | Thailand | Gouilh et al., 2011 |
| | *Hipposideros abae* | 0/16 | - | Ghana | Pfefferle et al. 2009 |
| | *Hipposideros cineraceus* | 0/2 | - | Thailand | Gouilh et al., 2011 |
| | *Hipposideros caffer* | - | 0/5 | South Africa | Müller et al., 2007 |
| | | | 0/9 | Oriental Province, DRC | Müller et al., 2007 |
| | ***Hipposideros caffer ruber*** | **12/59** | - | Ghana | Pfefferle et al. 2009 |
| | ***Hipposideros commersoni*** | 0/10 | - | Kenya | Tong et al. 2009 |
| | | **Positive, n=?** | - | Nigeria | Quan et al. 2010 |

| | | | | | |
|---|---|---|---|---|---|
| | | - | 0/16 | Oriental Province, DRC | Müller et al., 2007 |
| | *Hipposideros halophyllus* | 0/2 | - | Thailand | Gouilh et al., 2011 |
| | ***Hipposideros larvatus*** | 0/2 | - | China, Guangdong | Woo et al. 2007 |
| | | 0/3 | - | China | Tang et al. 2006 |
| | | 0/18 | - | China, HKSAR | Woo et al. 2006 |
| | | **24/59** | **-** | Thailand | Gouilh et al., 2011 |
| | *Hipposideros lekaguli* | 0/1 | - | Thailand | Gouilh et al., 2011 |
| | *Hipposideros lylei* | 0/4 | - | Thailand | Gouilh et al., 2011 |
| | *Hipposideros pomona* | 0/3 | - | China, HKSAR | Poon et al. 2005 |
| | | 0/1 | - | China, Guangdong | Woo et al. 2007 |
| | | 0/1 | - | China | Tang et al. 2006 |
| | | 0/6 | - | Thailand | Gouilh et al., 2011 |
| | *Hipposideros pratti* | 0/9 | - | China | Tang et al. 2006 |
| | *Hipposideros ruber* | 0/6 | - | Kenya | Tong et al. 2009 |
| | *Hipposideros stoliczkanus* | 0/3 | - | Thailand | Gouilh et al., 2011 |
| | ***Rhinonicteris aurantius*** | **1/125** | - | Australia | Smith *et al.*, 2010* |
| ***Megadermatidae* (Family)** | | | | | |
| | ***Cardioderma cor*** | **1/13** | - | Kenya | Tong et al. 2009 |
| | *Megaderma spasma* | 0/2 | - | Thailand | Gouilh et al., 2011 |
| ***Rhinolophidae* (Family)** | | | | | |
| | *Rhinolophus affinis* | 0/2 | - | China, HKSAR | Poon et al. 2005 |
| | | 0/7 | - | China, HKSAR | Woo et al. 2006 |
| | | 0/25 | - | China, Guangdong | Woo et al. 2007 |
| | | 0/60 | - | China | Tang et al. 2006 |
| | ***Rhinolophus blasii*** | **23/82** | - | Bulgaria | Drexler et al. 2010 |
| | *Rhinolophus coelophyllus* | 0/12 | - | Thailand | Gouilh et al., 2011 |
| | *Rhinolophus darling* | - | 0/1 | South Africa | Müller et al., 2007 |
| | ***Rhinolophus euryale*** | **111/243** | - | Bulgaria | Drexler et al. 2010 |
| | | 0/13 oral | - | Iberian Peninsula | Falcón et al.2011 |
| | ***Rhinolophus ferrumequinum*** | **1/8** | 0/4 | China, Hubei | Li et al. 2005 |
| | | **4/41** | - | China | Tang et al. 2006 |
| | | **14/45** | - | Bulgaria | Drexler et al. 2010 |
| | | 0/3 | - | Iberian Peninsula | Falcón et al.2011 |
| | *Rhinolophus fumigatus* | - | **1/204** | Oriental Province, DRC | Müller et al., 2007 |
| | *Rhinolophus hildebrandtii* | 0/4 | - | Kenya | Tong et al. 2009 |
| | ***Rhinolophus hipposideros*** | 0/6 | - | Bulgaria | Drexler et al. 2010 |
| | | **14/36** | - | Slovenia | Rihtarič et al. 2010 |
| | | 0/4 | - | Iberian Peninsula | Falcón et al.2011 |
| | *Rhinolophus landeri* | - | 0/2 | South Africa | Müller et al., 2007 |
| | *Rhinolophus luctus* | 0/4 | - | China | Tang et al. 2006 |
| | *Rhinolophus malayanus* | 0/15 | - | China | Tang et al. 2006 |
| | | 0/6 | - | Thailand | Gouilh et al., 2011 |
| | ***Rhinolophus marcotis*** | **1/8** | **5/7** | China, Hubei | Li et al. 2005 |
| | | **1/38** | - | China | Tang et al. 2006 |
| | ***Rhinolophus mehelyi*** | **7/13** | - | Bulgaria | Drexler et al. 2010 |
| | | 0/1 oral | - | Iberian Peninsula | Falcón et al.2011 |
| | ***Rhinolophus megaphyllus*** | **1/505** | - | Australia | Smith *et al.*, 2010* |
| | *Rhinolophus osgoodi* | 0/1 | - | China, Guangdong | Woo et al. 2007 |
| | | 0/1 | - | China | Tang et al. 2006 |
| | ***Rhinolophus pearsoni*** | **3/30** | **13/46** | China, Guangxi | Li et al. 2005 |
| | | **1/48** | - | China | Tang et al. 2006 |
| | | 0/6 | - | Thailand | Gouilh et al., 2011 |
| | *Rhinolophus pusillus* | 0/1 | - | China, HKSAR | Poon et al. 2005 |
| | | 0/12 | - | China, Guangdong | Woo et al. 2007 |
| | | 0/21 | **2/6** | China, Guangxi | Li et al. 2005 |
| | | 0/101 | - | China | Tang et al. 2006 |
| | *Rhinolophus rex* | 0/2 | - | China | Tang et al. 2006 |
| | *Rhinolophus rouxi* | 0/6 | - | China, HKSAR | Poon et al. 2005 |
| | ***Rhinolophus sinicus*** | **23/118** | - | China, HKSAR | Woo et al. 2006 |
| | | **7/64** | - | China, Guangdong | Woo et al. 2007 |
| | | **1/66** | - | China | Tang et al. 2006 |
| | | **171/1,337** | - | China, HKSAR | Lau et al. 2010 |
| | | **8/ 64** | - | China, Guangdong | Lau et al. 2010 |
| | *Rhinolophus stheno* | 0/1 | - | Thailand | Gouilh et al., 2011 |
| | *Rhinolophus thomasi* | 0/12 | - | China | Tang et al. 2006 |
| | | 0/1 | - | Thailand | Gouilh et al., 2011 |
| | *Rhinolophus sp.* | 0/7 | - | Kenya | Tong et al. 2009 |

| | | | | | |
|---|---|---|---|---|---|
| **VESPERTILIONIFORMI (SUBORDER)** | | | | | |
| **NOCTILIONIFORMACEI (INFRAORDER)** | | | | | |
| **NOCTILIONOIDEA (Super-family)** | | | | | |
| ***Noctilionidae*** **(Family)** | | | | | |
| | *Noctilio leporinus* | 0/6 | - | Trinidad, Couva | Carrington et al. 2008 |
| ***Mormoopidae*** **(Family)** | | | | | |
| | *Mormoops sp.* | 0/1 | - | Trinidad, Talmana | Carrington et al. 2008 |
| | *Pteronotus parnelli* | 0/31 | - | Trinidad | Carrington et al. 2008 |
| ***Phyllostomidae*** **(Family)** | | | | | |
| | ***Carollia perspicillata*** | **1/5** | - | Trinidad | Carrington et al. 2008 |
| | ***Desmodus rotundus*** | 0/14 | - | Trinidad | Carrington et al. 2008 |
| | | **1/3** | - | Brazil | Brandão et al. 2008 |
| | ***Glossophaga soricina*** | **1/21** | - | Trinidad | Carrington et al. 2008 |
| | *Phyllostomus hastatus* | 0/11 | - | Trinidad, Wallerfield | Carrington et al. 2008 |
| **NYCTERIFORMACEI (INFRAORDER)** | | | | | |
| **NYCTEROIDEA (Super-family)** | | | | | |
| ***Emballonuridae*** **(Family)** | | | | | |
| | *Coleura afra* | 0/2 | - | Kenya | Tong et al. 2009 |
| | | 0/33 | - | Ghana | Pfefferle et al. 2009 |
| | *Taphozous hildegardeae* | 0/3 | - | Kenya | Tong et al. 2009 |
| | *Taphozous longimanus* | 0/14 | - | Thailand | Gouilh et al., 2011 |
| | *Taphozous mauritianus* | - | 0/1 | South Africa | Müller et al., 2007 |
| | *Taphozous sp.* | 0/2 | - | Kenya | Tong et al. 2009 |
| ***Nycteridae*** **(Family)** | | | | | |
| | *Nycteris argae* | - | 0/1 | Oriental Province, DRC | Müller et al., 2007 |
| | *Nycteris hispida* | 0/1 | - | Ghana | Pfefferle et al. 2009 |
| | *Nycteris thebaica* | - | 0/6 | South Africa | Müller et al., 2007 |
| **VESPERTILIONIFORMACEI (INFRAORDER)** | | | | | |
| **MOLOSSOIDEA (Super-family)** | | | | | |
| ***Molossidae*** **(Family)** | | | | | |
| *Molossinae* (Sub-family) | ***Chaerophon pumilus*** | **2/7** | - | Kenya | Tong et al. 2009 |
| | *Chaerephon pumila* | **-** | 0/54 | South Africa | Müller et al., 2007 |
| | ***Chaerophon sp.*** | **7/38** | - | Kenya | Tong et al. 2009 |
| | | 0/6 | - | Ghana | Pfefferle et al. 2009 |
| | *Molossus major* | 0/25 | - | Trinidad, Talparo | Carrington et al. 2008 |
| | *Mops condylurus* | - | 14/115 | South Africa | Müller et al., 2007 |
| | *Mops midas* | - | 0/15 | South Africa | Müller et al., 2007 |
| | *Otomops martinsseni* | 0/4 | - | Kenya | Tong et al. 2009 |
| | *Tadarida brasiliensis* | 0/2 | - | U. S., Rocky Mountain | Dominguez et al. 2009 |
| | | 0/13 | - | U. S., Rocky Mountain | Osborne et al. 2011 |
| **VESPERTILIONOIDEA (Super-family)** | | | | | |
| ***Miniopteridae*** **(Family)** | | | | | |
| | ***Miniopterus africanus*** | **1/8** | - | Kenya | Tong et al. 2009 |
| | ***Miniopterus australis*** | **52/132** | - | Australia | Smith *et al.*, 2010* |
| | ***Miniopterus fuliginosus*** | **9/45** | - | Japan, Wakayama Prefecture | Shirato et al. 2011 |
| | ***Miniopterus inflatus*** | **7/12** | - | Kenya | Tong et al. 2009 |
| | | - | **1/34** | Oriental Province, DRC | Müller et al., 2007 |
| | ***Miniopterus magnater*** | **2/16** | | China, HKSAR | Poon et al. 2005 |
| | | **1/51** | - | China, HKSAR | Woo et al. 2006 |
| | | 0/14 | - | China, Guangdong | Woo et al. 2007 |
| | ***Miniopterus minor*** | **1/16** | - | Kenya | Tong et al. 2009 |
| | ***Miniopterus natalensis*** | **1/7** | - | Kenya | Tong et al. 2009 |
| | ***Miniopterus pusillus*** | **12/19** | - | China, HKSAR | Poon et al. 2005 |
| | | **4/25** | - | China, HKSAR | Woo et al. 2006 |
| | | **2/13** | - | China, Guangdong | Woo et al. 2007 |
| | ***Miniopterus schreibersii*** | **1/4** | - | China, HKSAR | Poon et al. 2005 |
| | | 0/1 | 0/1 | China, Hubei | Li et al. 2005 |
| | | **17/135** | - | China | Tang et al. 2006 |
| | | **18/38 (co-infec)** | - | Bulgaria | Drexler et al. 2010 |
| | | 0/2 | - | Thailand | Gouilh et al., 2011 |
| | | - | 0/1 | South Africa | Müller et al., 2007 |
| | | **1/71 oral** | - | Iberian Peninsula | Falcón et al.2011 |
| | | **69/228** | - | Australia | Smith *et al.*, 2010* |

| | | | | | |
|---|---|---|---|---|---|
| ***Vespertilionidae* (Family)** | | | | | |
| *Myotinae* (Sub-family) | *Corynorhinus townsendii* | 0/4 | - | U. S., Rocky Mountain | Osborne et al. 2011 |
| | *Euderma maculatum* | 0/2 | - | U. S., Rocky Mountain | Osborne et al. 2011 |
| | *Lasionycteris noctivagans* | 0/2 | - | U. S., Rocky Mountain | Dominguez et al. 2009 |
| | | 0/42 | - | U. S., Rocky Mountain | Osborne et al. 2011 |
| | *Myotis alcathoe* | 0/2 | - | Bulgaria | Drexler et al. 2010 |
| | | 0/1 | - | Iberian Peninsula | Falcón et al.2011 |
| | *Myotis altarium* | 0/1 | 0/1 | China, Hubei | Li et al. 2005 |
| | ***Myotis bechsteinii*** | 0/32 | - | Bulgaria | Drexler et al. 2010 |
| | | **1/9** | - | Germany, Bad Segeberg | Gloza-Raush et al. 2008 |
| | | 0/4 | - | Netherlands | Reusken et al. 2010 |
| | | 0/2 | - | Iberian Peninsula | Falcón et al.2011 |
| | ***Myotis blythii*** | **1/11 oral** | - | Iberian Peninsula | Falcón et al.2011 |
| | *Myotis bocagei* | - | 0/1 | South Africa | Müller et al., 2007 |
| | *Myotis brandtii* | 0/2 | - | Germany, Bad Segeberg | Gloza-Raush et al. 2008 |
| | | 0/2 | - | Netherlands | Reusken et al. 2010 |
| | *Myotis californicus* | 0/8 | - | U. S., Rocky Mountain | Osborne et al. 2011 |
| | *Myotis capaccini* | 0/1 | - | Bulgaria | Drexler et al. 2010 |
| | | 0/14 oral | - | Iberian Peninsula | Falcón et al.2011 |
| | *Myotis chinensis* | 0/8 | - | China, HKSAR | Woo et al. 2006 |
| | | 0/3 | - | China | Tang et al. 2006 |
| | *Myotis ciliolabrum* | 0/1 | - | U. S., Rocky Mountain | Dominguez et al. 2009 |
| | | 0/29 | - | U. S., Rocky Mountain | Osborne et al. 2011 |
| | ***Myotis dasycneme*** | **17/67** | - | Germany, Bad Segeberg | Gloza-Raush et al. 2008 |
| | | **20/105** | - | Netherlands | Reusken et al. 2010 |
| | ***Myotis daubentonii*** | 0/41 | - | China | Tang et al. 2006 |
| | | 0/7 | - | Bulgaria | Drexler et al. 2010 |
| | | 0/26 | - | Slovenia | Rihtarič et al. 2010 |
| | | **8/155** | - | Germany, Bad Segeberg | Gloza-Raush et al. 2008 |
| | | **8/50** | - | Netherlands | Reusken et al. 2010 |
| | | **1/39** | - | Iberian Peninsula | Falcón et al.2011 |
| | *Myotis emarginatus* | 0/5 | - | Bulgaria | Drexler et al. 2010 |
| | | 0/6 | - | Netherlands | Reusken et al. 2010 |
| | | 0/2 | - | Iberian Peninsula | Falcón et al.2011 |
| | *Myotis escalerai* | 0/15 oral | - | Iberian Peninsula | Falcón et al.2011 |
| | ***Myotis evotis*** | 0/4 | - | U. S., Rocky Mountain | Dominguez et al. 2009 |
| | | **1/55** | - | U. S., Rocky Mountain | Osborne et al. 2011 |
| | ***Myotis lucifugus*** | **1/31** | - | U. S., Rocky Mountain | Osborne et al. 2011 |
| | ***Myotis macropus*** | **13/51** | - | Australia | Smith *et al.*, 2010* |
| | ***Myotis myotis*** | 0/3 | - | China, HKSAR | Poon et al. 2005 |
| | | 0/3 | - | Bulgaria | Drexler et al. 2010 |
| | | **Colony: 20.2-100%** | - | Germany, Rhineland-Palatinate | Drexler et al. 2011 |
| | | 0/1 | - | Netherlands | Reusken et al. 2010 |
| | | 0/31 | - | Slovenia | Rihtarič et al. 2010 |
| | | **1/1** | - | Iberian Peninsula | Falcón et al.2011 |
| | *Myotis mystacinus* | 0/1 | - | China | Tang et al. 2006 |
| | | 0/3 | - | Netherlands | Reusken et al. 2010 |
| | | 0/4 | - | Slovenia | Rihtarič et al. 2010 |
| | | 0/1 | - | Bulgaria | Drexler et al. 2010 |
| | | 0/5 | - | Iberian Peninsula | Falcón et al.2011 |
| | *Myotis nattereri* | 0/1 | - | Bulgaria | Drexler et al. 2010 |
| | | 0/2 | - | Netherlands | Reusken et al. 2010 |
| | | 0/3 | - | Iberian Peninsula | Falcón et al.2011 |
| | ***Myotis occultus*** | **1/16** | - | U. S., Rocky Mountain | Dominguez et al. 2009 |
| | | 0/22 | - | U. S., Rocky Mountain | Osborne et al. 2011 |
| | *Myotis oxygnatus* | 0/1 | - | Bulgaria | Drexler et al. 2010 |
| | ***Myotis ricketti*** | 0/5 | - | China, HKSAR | Poon et al. 2005 |
| | | **1/21** | - | China, HKSAR | Woo et al. 2006 |
| | | 0/1 | - | China, Guangdong | Woo et al. 2007 |
| | | 0/21 | - | China, Guangxi | Li et al. 2005 |
| | | **13/53** | - | China | Tang et al. 2006 |
| | *Myotis siligorensis* | 0/5 | - | Thailand | Gouilh et al., 2011 |
| | *Myotis thysanodes* | 0/22 | - | U. S., Rocky Mountain | Osborne et al. 2011 |
| | ***Myotis volans*** | 0/7 | - | U. S., Rocky Mountain | Dominguez et al. 2009 |
| | | **12/147** | - | U. S., Rocky Mountain | Osborne et al. 2011 |
| | *Myotis yumanensis* | 0/18 | - | U. S., Rocky Mountain | Osborne et al. 2011 |

| | | | | | |
|---|---|---|---|---|---|
| | *Myotis sp.* | 0/80 | - | China | Tang et al. 2006 |
| *Scotophilinae* (Sub-family) | *Scotophilus borbonicus* | - | 0/1 | South Africa | Müller et al., 2007 |
| | *Scotophilus dinganii* | - | 0/5 | South Africa | Müller et al., 2007 |
| | ***Scotophilus kuhlii*** | **5/43** | - | China | Tang et al. 2006 |
| | | **4/4** | - | Philippines, Diliman | Watanabe et al. 2010 |
| | *Scotophilus leucogaster* | Negative, n=? | - | Nigeria | Quan et al. 2010 |
| | *Scotophilus nigrita* | Negative, n=? | - | Nigeria | Quan et al. 2010 |
| *Vespertilioninae* (Sub-family) | *Antrozous pallidus* | 0/13 | - | U. S., Rocky Mountain | Osborne et al. 2011 |
| | *Barbastella barbastellus* | 0/12 | - | Bulgaria | Drexler et al. 2010 |
| | | 0/4 | - | Spain | Falcon et al., 2011 |
| | *Barbastella leucomelas* | 0/1 | - | China | Tang et al. 2006 |
| | ***Eptesicus fuscus*** | **1/25** | - | U. S., Rocky Mountain | Dominguez et al. 2009 |
| | | **61/584** | - | U. S., Rocky Mountain | Osborne et al. 2011 |
| | ***Eptesicus isabellinus*** | **1/8** | - | Iberian Peninsula | Falcón et al.2011 |
| | *Eptesicus serotinus* | 0/1 | - | Netherlands | Reusken et al. 2010 |
| | | 0/4 | - | Slovenia | Rihtarič et al. 2010 |
| | | 0/7 | - | Iberian Peninsula | Falcón et al.2011 |
| | *Glauconycteris Beatrix* | 0/1 | - | Ghana | Pfefferle et al. 2009 |
| | ***Hypsugo savii*** | **2/26** | - | Iberian Peninsula | Falcón et al.2011 |
| | *Ia io* | 0/8 | - | China | Tang et al. 2006 |
| | *Lasiurus cinereus* | 0/39 | - | U. S., Rocky Mountain | Osborne et al. 2011 |
| | *Neoromicia tenuipinnis* | 0/4 | - | Kenya | Tong et al. 2009 |
| | *Murina leucogaster* | 0/5 | - | China | Tang et al. 2006 |
| | *Nyctalus aviator* | 0/6 | - | China | Tang et al. 2006 |
| | ***Nyctalus lasiopterus*** | **5/37** | - | Iberian Peninsula | Falcón et al.2011 |
| | ***Nyctalus leisleri*** | **1/3** | - | Bulgaria | Drexler et al. 2010 |
| | | 0/23 | - | Iberian Peninsula | Falcón et al.2011 |
| | ***Nyctalus noctula*** | 0/7 | - | China, HKSAR | Woo et al. 2006 |
| | | 0/17 | - | China | Tang et al. 2006 |
| | | 0/3 | - | Germany, Bad Segeberg | Gloza-Raush et al. 2008 |
| | | **5/14** | - | Netherlands | Reusken et al. 2010 |
| | *Nyctalus plancyi* | 0/1 | 0/1 | China, Hubei | Li et al. 2005 |
| | ***Pipistrellus abramus*** | 0/3 | - | China, HKSAR | Poon et al. 2005 |
| | | **4/14** | - | China, HKSAR | Woo et al. 2006 |
| | | **14/41** | - | China | Tang et al. 2006 |
| | *Pipistrellus capensis* | - | 0/1 | South Africa | Müller et al., 2007 |
| | *Pipistrellus deserti* | 0/1 | - | Ghana | Pfefferle et al. 2009 |
| | *Parastrellus hesperus* | 0/14 | - | U. S., Rocky Mountain | Osborne et al. 2011 |
| | *Pipistrellus javanicas* | 0/3 | - | Philippines, Diliman | Watanabe et al. 2010 |
| | ***Pipistrellus kuhlii*** | 0/3 | - | Slovenia | Rihtarič et al. 2010 |
| | | **1/4** | - | Iberian Peninsula | Falcón et al.2011 |
| | *Pipistrellus nanus* | 0/5 | - | Ghana | Pfefferle et al. 2009 |
| | *Pipistrellus nanulus* | 0/1 | - | Ghana | Pfefferle et al. 2009 |
| | ***Pipistrellus nathusii*** | **2/22** | - | Germany, Bad Segeberg | Gloza-Raush et al. 2008 |
| | | 0/8 | - | Netherlands | Reusken et al. 2010 |
| | | 0/2 | - | Slovenia | Rihtarič et al. 2010 |
| | ***Pipistrellus pipistrellus*** | **6/27** | - | China | Tang et al. 2006 |
| | | 2/8 | - | Netherlands | Reusken et al. 2010 |
| | | 0/3 | - | Iberian Peninsula | Falcón et al.2011 |
| | ***Pipistrellus pygmaeus*** | 0/2 | - | Bulgaria | Drexler et al. 2010 |
| | | **3/57** | - | Germany, Bad Segeberg | Gloza-Raush et al. 2008 |
| | | 0/1 oral | - | Iberian Peninsula | Falcón et al.2011 |
| | ***Pipistrellus sp.*** | 0/1 | - | Kenya | Tong et al. 2009 |
| | | Negative, n=? | - | Nigeria | Quan et al. 2010 |
| | | **1/29** | - | Iberian Peninsula | Falcón et al.2011 |
| | *Plecotus auritus* | 0/2 | - | Bulgaria | Drexler et al. 2010 |
| | | 0/7 | - | Netherlands | Reusken et al. 2010 |
| | | 0/7 | - | Iberian Peninsula | Falcón et al.2011 |
| | *Plecotus austriacus* | 0/7 | - | Iberian Peninsula | Falcón et al.2011 |
| | ***Tylonycteris pachypus*** | 0/21 | - | China, HKSAR | Woo et al. 2006 |
| | | **2/14** | - | China | Tang et al. 2006 |
| | *Scotomanes ornatus* | 0/1 | - | China | Tang et al. 2006 |

## 1.8 Coronaviruses detection methods

There are several different methods that can be applied to detect coronaviruses that include detecting the virus particle, detecting the exposure to the virus with serologic methods or detecting the viral nucleic acid with assays such as polymerase chain reactions (PCR).

### 1.8.1 Detection of the virus particle by electron microscopy

Coronaviruses may be detected with electron microscopy. The virus particle may be detected directly from a positive sample or to increase the amount of particles that may be viewed, after virus isolation in cell culture. In fact, the SARS coronavirus was initially identified as a coronavirus only after the typical 'corona' or crown-like morphology of the virus was observed under an electron microscope after isolating the virus from VeroE6 cells (Ksiazek *et al.*, 2003).

The concern with such methods is that not all coronaviruses can successfully be isolated in cell culture. The newly discovered bat coronaviruses in particular seem to be difficult to culture in standard cell lines and may require very specific cell lines to be constructed that possess the correct cellular receptors for virus replication.

### 1.8.2 Culturing coronaviruses

Previous attempts of culturing specifically bat coronaviruses have been unsuccessful (Dominguez *et al.*, 2007; Gloza-Rausch *et al.*, 2008; Lau *et al.*, 2007; Poon *et al.*, 2005; Tang *et al.*, 2006). Many standard cell lines have been tested in attempts to cultivate coronaviruses taken from positive bat samples. Cell lines such as Vero E6 (African green monkey kidney), FRhK4 (foetal rhesus kidney), MDCK (Mardin-Darby canine kidney), CaCo2 cells (human epithelial colorectal adenocarcinoma cells) as well as *Carollia* bat lung and kidney were used.

An explanation as to why bat coronaviruses are unable to be cultivated in these standard cell lines may be due to the strict species specificity of these bat coronaviruses. As is seen in nature some coronaviruses are only found in certain genera of bats, for example, some coronaviruses have only been detected in *Miniopterus* bats and not in *Myotis* bats even if the two bat species commonly roost together (Poon *et al.*, 2005). This may be why even when the *Carollia* bat lung and kidney cell lines were used by Gloza-Rausch *et al.*, (2008), no growth was observed- since no coronaviruses tested were specific to *Carollia* bats. Thus, by creating cell lines of bat species that have tested positive for coronaviruses previously, such as *Rousettus, Miniopterus* and *Myotis*; one may be able to create an environment suitable for these bat coronaviruses to grow.

It must also be noted however as seen in Lau *et al.*, (2007) that even when the correct host bat species is used that the coronaviruses may still be unculturable. The authors attempted to cultivate *Rh*-BatCoV-HKU2 in primary kidney epithelium and lung fibroblast cells that were derived from a Chinese horseshoe bat (*Rhinolophus sinicus*). *Rh*-BatCoV-HKU2 had previously been identified from Chinese horseshoe bat, though from alimentary tract specimens not lung or kidney samples.

It may be that not only the host specificity, but also the type of tissue that is taken from that host is an essential component in the construction of a bat cell line that will successfully be able to cultivate bat coronaviruses. Due to the high enteric tropism usually displayed by bat coronaviruses, it is possible that cells from the alimentary tract from specific bat species may be used to cultivate coronaviruses from bats. Also, since the viruses are asymptomatic in bats, one would not expect cytopathic effects to reveal infection of the cells. Instead, the cells should be tested regularly after the initial inoculation with RT-PCRs, electron microscopy, or using fluorescent antibodies against specific virus epitopes to determine whether the cells are infected with coronaviruses.

Attempts to isolate other bat viruses such as Nipah virus in mammalian cell lines have been as difficult as the isolation of the bat coronaviruses. There currently are some commercial bat cell lines such as Tbl-Lu (lung of *Tadarida brasiliensis*) and Mvi/lt (interscapular tumor of *Myotis velifer incautus*) available, though they have limited value and may not be susceptible to infection by the desired viruses (Crameri *et al.*, 2009).

Crameri *et al.* (2009) has recently created a successful Pteropid bat cell line with various tissue types taken from a black flying fox (*Pteropus alecto*) and essentially testing various methods that can be used to optimize the bat cell line growth. It was concluded that the primary cell line production methods which utilize enzymatic digestion to break up the tissues, such as overnight trypsin treatment at 4˚C, works better than physical methods such as pushing the tissue through a mesh strainer or simply cutting the tissue.

According to the authors, the main concern with the creation of a stable primary cell line is the issue of programmed cell death that occurs after a certain number of cell divisions. Therefore to be able to use the cell line one must immortalize the cells. There are essentially two methods by which cell immortalization can be achieved.

The first method involves the induction and expression of Simian virus 40 genes encoding the large T tumor antigen (SV40T). However, common problems that arise when using the SV40T method of immortalization are undesired genotypic and phenotypic changes in the cells. The second method of cell immortalization involves the stable expression of the catalytic subunit of human telomerase reverse transcriptase (hTERT). When hTERT is absent from cells, telomeres are known to be shorter and repeated cell divisions eventually result in the death of the cell.

The induced expression of hTERT has been successfully used in the production of primary cell lines for many mammalian species, these including swine kidney epithelial cells (Kwak *et al.*, 2006), goat mammary epithelial cells (He *et al.*, 2009), and human myometrial cells (Soloff, 2004) to name but a few. A benefit of using hTERT (unlike SV40T immortalization) is that the original characteristics of the cells are better preserved due to there being only small changes in the phenotype or physical appearance of the cell (Crameri *et al.*, 2009).

A notable concern for the creation of an intestinal culture for bat coronaviruses is the ease of contamination from fungi and bacteria that reside in these tissues (Crameri *et al.*, 2009). Brain cell cultures appeared to be the most successful cultures; although slow-growing, the brain cell culture was the best in actually sustaining immortalized cell growth. However, it is probable that coronaviruses would only grow in alimentary tract tissues (as could be seen from the failure of previous studies), making the creation of an intestinal bat cell line essential.

### 1.8.3 Serological methods

Coronaviruses can be detected with serological methods such as ELISA or virus neutralization assays and complement fixation tests. ELISA will detect the presence of antibodies against the virus or antigens of the virus (such as the nucleocapsid protein) in a sample. The spike protein in particular is an antigen usually targeted by antibodies for virus neutralizations. As such, it is being looked at for the construction of a SARS-CoV vaccine that will elicit protective immunity (He *et al.*, 2006). The coronavirus taxonomy used to be based on phylogroups because members of the phylogroups showed antigenic relatedness, as such the current genera will also possess antigenic relatedness.

However, serological methods used to detect coronaviruses may only indicate exposure to the virus. As such, serological methods may only be used as an initial screening but is rarely used in studying coronaviruses particularly when intending to examine the coronavirus diversity in an area.

### 1.8.4 Detection of the viral genome

Apart from detecting the actual virus particle, one can also target the viral RNA with various methods in an attempt to detect presence of the virus. The nucleocapsid gene is often used as target gene in phylogenetic and recombination studies due to its high degree of conservation (Woo *et al.*, 2010). However due to the high conservation in the RdRp, specifically ORF 1b, as well as its universal usage to indicate reliable coronavirus phylogeny it may be the best target for a consensus PCR (Stephensen *et al.*, 1999).

Reverse transcription PCR (RT-PCR) assays will reverse transcribe the viral RNA into DNA that can then undergo further PCR amplification.

Previously, random hexamer primers have been used to reverse transcribe viral RNA to cDNA which can then be used in PCRs that specifically target the RdRp gene with consensus primers (Poon *et al.*, 2005). Later on, other assays eliminated the usage of random hexamers and used consensus primers directly in the RT-PCR step (Stephensen *et al.*, 1999; Tang *et al.*, 2006; Woo *et al.*, 2005). More sensitive detection of the viral RNA came about with the formulation of nested PCR steps after the RT-PCR (de Souza Luna *et al.*, 2007; Tong *et al.*, 2009). This involves the amplification of a nested subset of the cDNA after reverse transcription. Table 1.10 summarizes the specific PCRs used in the various bat coronavirus studies in order to detect the low amounts of coronavirus present in samples.

**Table 1.10: The original protocols and subsequent modifications which are used primarily for the detection of bat coronaviruses by targeting the RNA dependent RNA polymerase gene**

| Publication/ name of original protocol: | Primer sequences (5-3) | Original protocol: Positive samples/total | Protocol | Studies in which it was used | Modifications | Modified protocol: Positive samples/total |
|---|---|---|---|---|---|---|
| **Poon *et al.*, 2005** | Forward Primer 1: GGTTGGGACTATCCTAAGTGTGA Reverse primer 2: CCATCATCAGATAGAATCATCATA | (n=162 bat samples) 12/19 (63%) *Mi. pusillus* samples. | **Random hexamer RT-step and CoV PCR:** Superscript II RT-step: incubated at 42℃ for 50 min, 72℃ for 15 min. **PCR conditions**: 95℃ (10min); 40 cycles: 95℃ (1min), 58℃ (1min), & 72℃ (1min). | Chu *et al.*, 2006 | Addition of a hemi-nested PCR: Nested Reverse primer 3: ATCAGATAGAATCATCATA GAGA | 17.6% (24/136) total bat samples |
| | | | | Dominguez *et al.*, 2007 | Addition of a hemi-nested PCR: Nested Forward primer: GTTGTACTGCTAGTGACA GG **RT-PCR:** 45 cycles Annealing temp: 48℃ **Nested PCR:** same conditions; 40 cycles. | 21.4% (6/28) fecal samples n= 6/79 bat samples |
| **Woo *et al.*, 2005** | P1: GGTTGGGACTATCCTAAGTGTGA P2: CCATCATCAGATAGAATCATCATA | Used for human CoV detection; | **RT-step and CoV PCR:** Superscript II RT-step: incubated at 42℃ for 50 min, 72℃ for 15 min. **PCR conditions**: 40 cycles: 94 ℃ (1min), 48 ℃ (1min), &72 ℃ (1min); 72℃ (10min) | *Lau et al., 2005a* | None | 39% (23/ 59) from *Rh. sinicus* |
| | | | | Woo *et al.*, 2006a | None | 12% (37/309) anal swabs |
| | | | | Lau *et al.*, 2007 | Enzyme change: RT-step with SuperScript **III** kit (Invitrogen). PCR using **60** cycles | 16.7% (58/348) bats in Hong Kong; 12.5% (8/64) bats in Guangdong. |
| | | | | Woo *et al.*, 2007 | Same as Lau *et al.*, 2007 | 10.2% (52/509) bat fecal specimens; 0.2% (1/509) bat respiratory specimens. |
| | | | | Lau *et al.*, 2010a | Same as Lau *et al.*, 2007 | SARS-Rh-CoV: [Hong Kong]126/ 1,337 (9.4%) alimentary and 2 respiratory [Guangdong] 4/64 (6.3%) BtCoV HKU2: [Hong Kong] 62/1,337 (4.6%) [Guangdong] 7/64 (10.9%) |
| **de Souza Luna *et al.*, (2007)** | PC2S2: equimolar mixture of 2 primers TTATGGGTTGGGATTATC and TGATGGGATGGGACTATC PC2As1: equimolar mixture 3 primers | Used for human CoV detection; | **One-step RT-PCR kit (Qiagen):** 200 nM of PC2S2, 900 nM of PC2As1. Conditions: | Gloza-Rausch *et al.*, 2008 | None | 9.8% (31/315) bat alimentary samples |

| | | | | | | |
|---|---|---|---|---|---|---|
| (multiple primer mixture nested RT-PCR) | TCATCACTCAGAATCATCA, TCATCAGAAAGAATCATCA, and TCGTCGGACAAGATCATCA<br>PCS: equimolar mixture of 2 primers CTTATGGGTTGGGATTATCCTAAGTGTGA, CTTATGGGTTGGGATTATCCCAAATGTGA<br>PCNAs: 1 primer CACACAACACCTTCATCAGATAGAATCATCA | | 50℃ (30min); 95℃ (15min); 10 cycles of 94℃ (20s), starting at 62℃ (30s) with a decrease of 1℃ per cycle, 72℃ (40s); and 30 cycles of 95℃(20s), 52℃ (30s), and 72℃(40s).<br>**The nested-PCR:** Platinum *Taq;* 80 nM PCS, 400 nM PCNAs.<br>**Conditions:** 94℃ (3min), 30 cycles of 94℃ (20s), 60℃ (30s), and 72℃ (30s). | Pfefferle *et al.*, 2009 | None | 9.76% (12/123) bat alimentary samples |
| **Stephensen *et al.*, 1999** | Primer 8p: TATGA(GA)GG(TC)GG(GC)TGTATACC<br>Primer 7m (antisense): ACTAGCATTGT(AG)TGTTG(AT)GAACA<br>Primer 1Ap: GATAAGAGTGC(TA)GGCTA(TC)CC | Used for human CoV detection; | **RT-PCR:** Superscript I; 992nt amplicon; Primers were used in primer pairs (8p/7m or 1Ap/7m)<br>**PCR conditions:** 98℃ (1min), 40 cycles of 45℃ -50℃ (1min), 72℃ (1min), 94℃ (1min). | Tang *et al.*, 2006 | None; References both Stephensen *et al.*, 1999 and Guan *et al.*, 2003 | 6.5% (64/985) positive bat alimentary specimens |
| | | | | Carrington *et al.*, 2008 | References Tang *et al.*, 2006 | 1.75% (2/114) positive bat alimentary specimens |
| **Guan *et al.*, 2003** *(Target the Nucleoprotein gene)* | Nucleoprotein Forward primer: TCAGCCCCAGATGGTACTTC<br>Nucleoprotein Reverse primer: CTCTGCTTCCCTCTGCGTAC | Detection of SARS-CoV in Himalayan palm civets and market traders | Condition of the PCR not available | | - | - |
| **Tong *et al.*, 2009** | **Pan-CoV Primer set**<br>1st and 2nd round forward: ATGGGITGGGAYTATCCWAARTGTG<br>1st round reverse: AATTATARCAIACAACISYRTCRTCA<br>2nd round reverse: CTAGTICCACCIGGYTTWANRTA<br>**Pan-bat primer set**<br>1st and 2nd round forward: ATGGGITGGGAYTATCCWAARTGTG<br>1st round reverse: TATTATARCAIACIACRCCATCRTC<br>2nd round reverse: CTGGTICCACCI GGYTTNACRTA | Total for PCRs: 19% (41/221) positive bat specimens | Two hemi-nested RT-PCR assays, PanCoV (general CoV primers) and PanBat (specific for bat CoV) targeting the highly conserved regions in the RdRp gene (1b).<br>**Hemi-nested RT-PCR:** Superscript III one step kit and platinum Taq kit (according to manufacturer's instructions) | None yet | - | - |

A new and increasingly commonly used nucleic acid amplification method that may be utilized for the detection of CoV is real-time PCR. Real-time PCR differs from conventional PCR in that it utilizes fluorogenically labelled primers, probes or even created amplicons to monitor the PCR product accumulation in a Light termocycler in real time. Real-time PCR is a closed, homogenous system that has eliminated the requirement for post-amplification processing of PCR products, such as the usage of agarose gel electrophoresis for the visualization of PCR amplicons (Mackay *et al.,* 2002). As such the potential contamination of samples is thus excluded and the PCR results are obtained much faster. The sensitivity of real-time PCR is also far greater than conventional PCR, capable of detecting copy numbers of template as low as <10, and as such is of great value in diagnostics and to monitor gene activity in expression studies. However, real-time PCR is limited in terms of amplicon length, approximately 200 bp, whereas conventional PCR may produce amplicons as large as 1000bp and has greater flexibility in differentiating between separate amplified sequences as fluorophores used to label primer/probes are not ideal to be utilised to do so (Mackay *et al.,* 2002).

Real-time PCR assays have been used to detect SARS-HCoV in patients in China (Lau *et al.,* 2003, Emery *et al.,* 2004), though Lau *et al.,* (2003) concluded that due to the low amounts of virus present in specimens taken from patients, a pre-amplification step (by conventional PCR) be incorporated prior to the real-time PCR which increased the sensitivity of the assay by $10^2$ fold than the standard real-time assay and $10^7$ fold more than the conventional PCR alone.

No publications have reported the usage of real-time assays for the detection of BtCoV. This may be due to the fact that for detection of SARS-CoV in human patients a rapid diagnosis to confirm or reject the presence of SARS is required (thus rapid diagnosis by real-time PCR), whereas for BtCoV the sequence diversity of the viruses are more desirable than simply the presence/absence of the virus. Therefore longer amplicons are required for phylogenetic studies and thus conventional nested PCR are more suited.

## 1.9 Aims of the study

With recent research collectively suggesting bats as the original reservoirs to all coronaviruses, it is warranted to study these mammals in greater detail with respect to the presence and diversity of coronaviruses and to evaluate the extent to which this presents a public health threat.

SARS-related coronaviruses have already been identified in bats from Kenya (Tong et al., 2009), Ghana (Pfefferle *et al.*, 2009), and Nigeria (Quan *et al.*, 2010) and antibodies against SARS-related coronaviruses have also been detected in bats from South Africa (Müller *et al.*, 2007). Thus, the focus point of this study was to shed light on the presence of coronaviruses in African bat species, targeting samples collected from South Africa and Rwanda.

**Main Objectives:**

**A. Development of nucleic acid detection methods to identify bat coronaviruses**

a. Establish a nested RT-PCR capable of targeting a conserved gene region of the RNA dependent RNA polymerase (RdRp) domain in ORF1ab.

**B. Specimen analysis for the presence of bat coronaviruses**

a. Use the established hemi-nested RT-PCR protocol to analyze RNA extracted from bat fecal samples collected in Rwanda and various locations within South Africa.

**C. Phylogenetic identification**

a. Sequence the RdRp gene amplicon generated from samples positive for coronavirus RNA from South Africa and Rwanda.

b. Evaluate the phylogenetic relationship and sequence diversity of the novel African coronaviruses as well as determine how they relate to the coronaviruses in bats from other parts of the globe.

c. Improve phylogenetic resolution of detected bat coronaviruses by designing coronavirus species-specific primers to sequence the RdRp gene and a small segment of the nucleoprotein gene.

# Chapter 2: Development of a bat coronavirus nucleic acid detection assay

## 2.1 Introduction

Bat coronaviruses have been found to be present in very low amounts within the alimentary tract of their bat hosts as compared to intestinal viruses found in humans ($10^4$ RNA copies and below in 2-4 bat fecal pellets to $10^{12}$ RNA copies/mg of human faeces) (Pfefferle *et al.*, 2009). Evidence has shown that these viruses may cause acute, self limiting infections within their hosts and may result in viral shedding through excrement for up to 2 weeks (Lau *et al.*, 2010a). As such, an assay is required that will be able to detect the low levels of BtCoV present in alimentary specimens. The most conserved gene in the CoV genome is the RNA dependent RNA polymerase gene (RdRp) in ORF1b, and is most often used as a target for PCR amplification. Other genes that have at times been used in conjunction with the RdRp gene include the nucleocapsid gene, spike gene as well as the helicase-exonuclease gene also in ORF1ab (Poon *et al.*, 2005). Though conserved, the nucleocapsid gene is not as conserved as the RdRp gene and as such some BtCoV may not be detected. The spike gene is however very variable among CoV and it may not be feasible to detect all the highly divergent BtCoV spike gene sequences. The helicase-exonuclease gene region is not often used as a target for PCR amplification and therefore comparing any resulting sequences to existing BtCoV may not be achievable.

The RdRp gene is thus the best gene region to target in PCR amplification for the detection of BtCoV RNA due to the fact that the majority of the data available on BtCoV are of the RdRp gene and since this gene is highly conserved. An analysis of the available CoV literature provides several examples of reverse transcription (RT) PCRs that have successfully been used to detect BtCoV (Table 1.9). There are five protocols described previously in the literature (Poon *et al.*, 2005; Woo *et al.*, 2005; de Souza Luna *et al.*, 2007; Stephensen *et al.*, 1999, Guan *et al.*, 2003) which have been used in later publications or have been the basis for newly developed protocols (Chu *et al.*, 2006; Dominguez *et al.*, 2007; Lau *et al.*, 2005b; Lau *et al.*, 2007; Tang *et al.*, 2006; Woo *et al.*, 2006b; Woo *et al.*, 2007).

The PCRs mainly differ in the usage of reagents, PCR cycling conditions and in some assays, the incorporation of a nested PCR step to an established RT-PCR. The primer target region utilised by the Poon *et al.,* 2005 and Woo *et al.,* 2005 protocols are in a conserved region of the RdRp domain and are excellent targets for the detection of BtCoV.

Initially two protocols were evaluated for their ability to detect BtCoV. The protocol used by Woo *et al.*, 2005 (and subsequently modified in other publications; Table 1.9) was evaluated originally at the start of the study. The assay was capable of amplifying the positive control; however it proved not to be sensitive enough to detect the very low amounts of BtCoV RNA that may be present in the specimens. Thus a nested PCR would have to be implemented. The Tong *et al.,* 2009 protocol was also evaluated for its possible use in the

detection of BtCoV, as it was used to great success in the Kenyan study in 2009. The protocol utilizes two hemi-nested RT-PCR primer sets; the PanCoV primer set was designed for general CoV amplification while the PanBat primer set was designed from known BtCoV to improve the specificity of BtCoV detection. However, the Tong *et al.* 2009 protocol was not optimal for the amplification of BtCoV in this study since it produced an amplicon of only 121bp and also due to the high number of degenerate nucleotides present in the primers, non-specific amplification from primer dimers was common.

Thus, it was decided that a new BtCoV detection protocol be developed that would incorporate all the features lacking in the previously published protocols such as a suitable nested PCR for the sensitive detection of the low quantities of viral nucleic acid present in the samples, and the usage of primers that may be able to detect the diverse range of possible African BtCoV present in specimens. Therefore, when primers were designed, the focus was put on using sequences from previously identified African bat coronaviruses.

## 2.2 Materials and Methods

### 2.2.1 Coronavirus PCR development

#### 2.2.1.1 SARS Coronavirus positive control to be used in the development of a coronavirus PCR assay

A coronavirus RNA positive control was required in order to develop and establish an RT-PCR that was capable of detecting coronavirus RNA. The human betacoronavirus, SARS-CoV, was used. The positive control was developed and constructed at the National Institute for Communicable Diseases, Sandringham, South Africa. A segment of the RdRp gene from a SARS coronavirus isolate CDC200301157 (Accession number: AY714217.1) was amplified with the two primer sets (the PanCoV and PanBat sets) designed in Tong *et al*., (2009) (Figure 2.1). The PCR product was cloned into PCR2.1 TOPO (Invitrogen, USA), a TA cloning vector, according to the manufacturer's instructions and subsequently transcribed as positive sense RNA in Megascript SP6 (Invitrogen, USA) according to the manufacturer's instructions.. The expressed RNA was thus only a segment of the coronavirus genome and therefore non-infectious (Refer to Figure 2.1 for a flow diagram of the positive control development). Since the Tong *et al*., (2009) and the Woo *et al*., (2005) primer sets amplify products from the same region of the RdRp gene in the coronavirus genome, it was decided that the positive control already constructed could still be used for new protocol development.

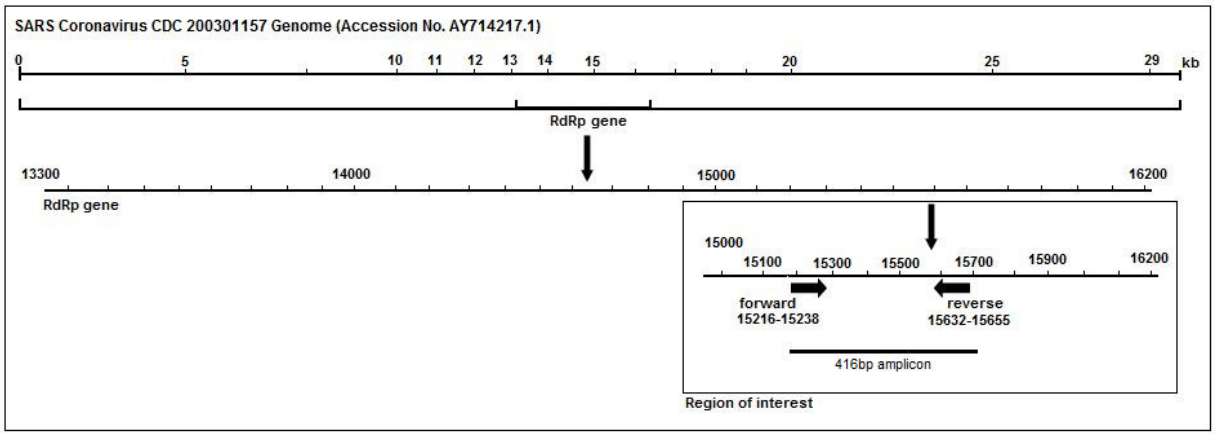


**Figure 2.1:** The conserved region of the RNA dependent RNA polymerase gene of the coronavirus genome that is used as the target region for amplification in the construction of the positive control RNA from SARS-CoV isolate CDC200301157 (AY714217.1). The SARS-CoV isolate is indicated as the reference strain in the figure to show the primer binding positions of the first round RT-PCR primers from Tong *et al.,* (2009) and Woo *et al.,* (2005) assays that were used for the construction of the positive control RNA transcripts.

The positive control was transcribed with the PanCoV primers and was available at a stock concentration of $5.05X10^{12}$ copies/µl, while the transcripts created with the PanBat primers was available at a stock concentration of $1.01X10^{12}$ copies/µl. The PanBat positive control was used in this study (with various dilutions) in the development of a bat coronavirus specific RT-PCR assay.

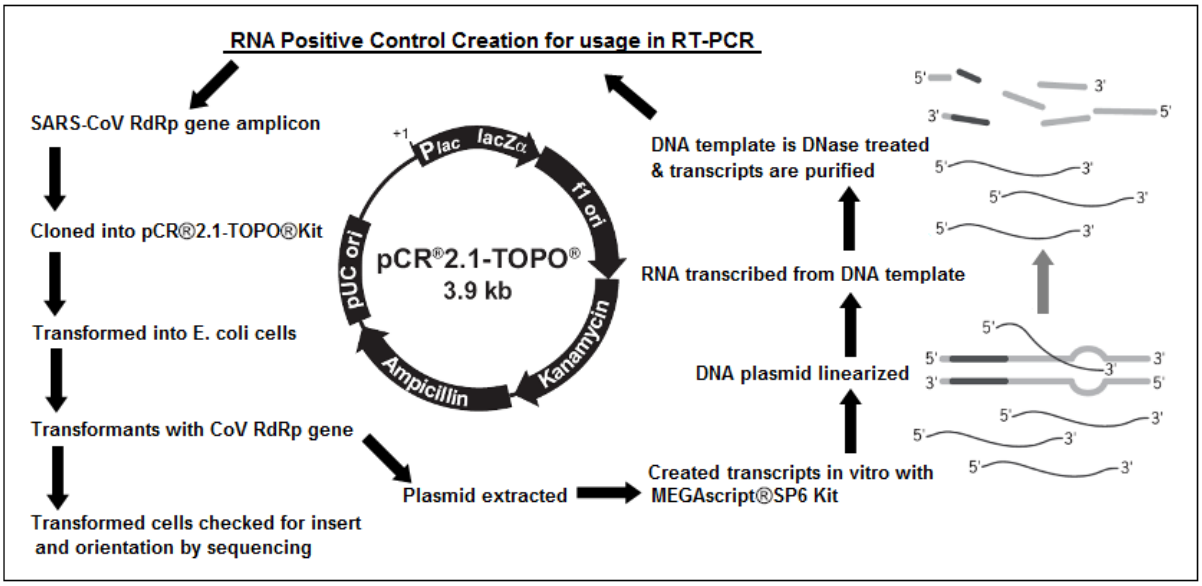


**Figure 2.2**: Overview of the positive control construction used in this study. The SARS-CoV isolate CDC200301157 (AY714217.1) was selected to be used as positive control template and was transcribed with the primers designed by Tong *et al.,* (2009). The products were cloned in the PCR2.1 TOPO kit (Invitrogen, USA) and expressed as RNA transcripts by the Megascript SP6 kit (Invitrogen, USA) (Modified from TOPO TA Cloning® user manual (Invitrogen, USA) and the MEGAScript® Kit user manual (Invitrogen, USA)).

### 2.2.2 Genus specific Nested RT-PCR with multiple primer set (PanBtCoV/9 primer).

New coronavirus primers were designed from alignment of BtCoV sequences to specifically amplify alpha- or betacoronaviruses that may be present in bat fecal RNA extracts. The new protocol was termed the PanBtCoV/9 primer assay.

#### 2.2.2.1 Designing coronavirus genus specific primer sets

Primers were designed after multiple alignments of several bat and non-bat coronavirus RdRp gene region sequences from both the *Alpha-* and *Betacoronavirus* genera (Table 2.1) using the CLCBio main workbench v6 (CLCBio, Denmark). All primers were produced by Integrated DNA Technologies (IDT, Germany) and used without further purification.

**Table 2.1: Bat coronavirus sequences of the RNA dependent RNA polymerase gene used in primer designing**

| Coronavirus Name | Genus | Host Species | Accession Number | Reference |
|---|---|---|---|---|
| Bat coronavirus HKU8 | *Alphacoronavirus* | *Miniopterus* spp. | NC_010438.1 | Chu *et al.,* 2008 |
| Bat coronavirus strain 61 | *Alphacoronavirus* | *Miniopterus* spp. | AY864196.1 | Poon *et al.,* 2005 |
| Bat coronavirus 1A | *Alphacoronavirus* | *Miniopterus* spp. | NC_010437.1 | Chu *et al.,* 2008 |
| Bat coronavirus 1B | *Alphacoronavirus* | *Miniopterus* spp. | NC_010436.1 | Chu *et al.,* 2008 |
| Bat coronavirus HKU2 | *Alphacoronavirus* | *Rhinolophus* spp. | NC_009988.1 | Lau *et al.,* 2007 |
| Bat coronavirus 512 | *Alphacoronavirus* | *Scotophilus* spp. | NC_009657.1 | Tang *et al.,* 2006 |
| Bat coronavirus HKU3 | *Betacoronavirus* | *Rhinolophus* spp. | NC_004718 | Lau *et al.,* 2005 |
| BtCoV/Phil/Dil/1525G2/08 | *Betacoronavirus* | *Rhinolophus* spp. | AB539081.1 | Watanabe *et al.,* 2010 |
| Bat coronavirus HKU4-1 | *Betacoronavirus* | *Tylonycteris* spp. | NC_009019.1 | Woo *et al.,* 2007 |
| Bat coronavirus HKU5-1 | *Betacoronavirus* | *Pipistrellus* spp, | NC_009020.1 | Woo *et al.,* 2007 |
| Bat coronavirus HKU9-1 | *Betacoronavirus* | *Rousettus* spp. | NC_009021.1 | Woo *et al.,* 2007 |

#### 2.2.2.2 cDNA synthesis

Synthesis of cDNA was performed with AMV Reverse transcriptase (Roche Molecular Diagnostics, Germany). Each synthesis step was performed with a standard concentration of the positive control, at $10^8$ copies/µl. A volume of 5 µl of the positive control RNA template was combined with 10pmol of the RT-PCR reverse primers. The template-primer mixture was added to the RT-step reaction mixture (14 µl) that consisted of 1.125X AMV incubation buffer (250 mM Tris-HCl; 40 mM $MgCl_2$; 150 mM KCl; 5 mM dithioerythritol; pH 8.5), 1.1 mM dNTPs, 8U AMV reverse transcriptase (Roche Molecular Diagnostics, Germany), 16U RNase inhibitor (Roche Molecular Diagnostics, Germany) and made up to 20 µl with Nucease free $H_2O$ (Promega, USA). The reaction was incubated at 42˚C for 90 minutes.

#### 2.2.2.3 RT-PCR

The RT-PCR reaction mixture (100 µl) consisted of 20 µl cDNA reaction with the addition of the PCR mixture consisting of 2.125X AMV Reverse transcriptase buffer (250 mM Tris-HCl; 40 mM $MgCl_2$; 150 mM KCl; 5 mM dithioerythritol; pH 8.5, (Roche Molecular Diagnostics, Germany), 0.38mM dNTPs, 1.25U Dream Taq (Fermentas, Inqaba biotechnologies, 20mM $MgCl_2$), with 10 pmol of each forward and reverse RT-PCR primers and made up to 80 µl with Nuclease free $H_2O$ (Promega, USA). The reaction was amplified with an initial denaturation of 94°C for 5 minutes, 35 cycles of 94˚C for 40 seconds, 48˚C for 50 seconds and 72˚C for 50 seconds and a final elongation for 7 minutes at 72˚C.

#### 2.2.2.4 Agarose gel electrophoresis

RT-PCR amplicons were analyzed on 1.5% (w/v) agarose gels, prepared in 1X TE buffer (10mM Tris at pH 7.4, 1mM EDTA at pH 8) with 0.5µg/ml ethidium bromide solution. Amplicons were compared to the O'Gene Ruler 100bp Marker (Fermentas, Life Sciences). Eight µl of the PCR sample with 2 µl loading dye (40% sucrose. 0.25% bromophenol blue) were loaded into the wells and then run at 100V in a horizontal gel tank system using a MAXICELL EC360M Electrophoretic Gel System (E.C Apparatus Corporation, USA). The results were visualized using a UV transilluminator.

#### 2.2.2.5 Nested PCR

The RT-PCR product was diluted 1:10 with RNase free $H_2O$ (Promega, USA) and 1 µl was used as the template for the hemi-nested PCR. The hemi-nested PCR mixture (50 µl) consisted of 2X Dream Taq buffer (Fermentas, Inqaba biotechnologies, 20mM $MgCl_2$), 0.4 mM dNTPs, 1mM $MgCl_2$, 0.2 % glycerol (Saarchem, Merck) with 1.25U Dream Taq (Fermentas, Inqaba biotechnologies), with 10 pmol of each forward and reverse nested primer and made up to 50 µl with RNase free $H_2O$ (Promega, USA). The nested PCR conditions consisted of an initial denaturation of 94°C for 5 minutes, 30 cycles of 94˚C for 50 seconds, 48˚C for 50 seconds, 72˚C for 50 seconds and a final elongation of 72˚C for 7 minutes. PCR products were analyzed by 1.5% agarose gel electrophoresis (Section 2.2.2.4).

#### 2.2.2.6 RT-PCR optimization

The RT-PCR was evaluated with both Superscript III (Invitrogen) and AMV (Roche Molecular Diagnostics, Germany) enzymes. The PanBat positive control available at $10^{12}$ copies/µl was serially diluted to $10^{-2}$. The positive control concentrations starting at $10^{10}$ to $10^{-2}$ were used to determine the sensitivity of the assay.

#### 2.2.2.7 Nested PCR optimization

The optimal RT-PCR template for the nested PCR was determined with template dilutions of 1:10, 1:50, 1:100, 1:500, and 1:1000, with the addition of 1µl to a nested reaction mixture. The annealing temperature for the nested PCR was optimized with a temperature

gradient of 46˚C-56˚C in an Eppendorf Mastercycler gradient thermocycler (USA Scientific) set at 50˚C at a gradient of 5.5˚C. Magnesium concentration was optimized by the addition of final magnesium concentrations of 0.5mM and 1mM or no additional magnesium added. Betaine at 0.03M (Sigma-Aldrich) and 0.2% glycerol were evaluated for effectiveness at increasing the specificity of the nested PCR.

#### 2.2.2.8 Purification of PCR amplicons and nucleotide sequence determination

The positive control products amplified in the PCR steps were gel-purified using the Wizard® SV Gel and PCR Clean-up system (Promega) according to the manufacturer's instructions. A total five µl of the purified DNA was quantified using the O'Gene Ruler 100bp Marker (Fermentas, Life Sciences) as reference on 1% agarose gel electrophoresis before sequencing.

Automated sequencing was performed using the BigDye Terminator 3.1 system (Applied Biosystems). A reaction mixture containing the BigDyeTerminator reaction solution (2 µl) and pre-made Sequencing buffer (1 µl) was combined with 3.2 pmol of the sequencing primer and 100ng of purified PCR product and was made up to 10µl with nuclease-free water. These reactions were cycled in a GeneAmp PCR system 2700 (Applied Biosystems, USA), using the following cycle conditions: initial denaturation at 94℃ for 1 minute, followed by 25 cycles of 94℃ for 10s, 50℃ for 5 s and 60℃ for 4 minutes.

The EDTA/NaOAc/EtOH method was used according to the BigDye Terminator v3.1 cycle sequencing protocol (Applied Biosystems, 2002). In brief, for each 10µl sequencing reaction, 1µl 25mM EDTA, 1µl 3M sodium acetate and 25µl of 100% ethanol were added to the previously amplified reaction solution. The reaction tubes were vortexed and incubated at room temperature for 15 minutes followed by centrifugation at 12 000g for 30 minutes, and subsequent removal of the supernatant. Hundred µl of 70% ethanol was added and centrifuged at maximum speed for 15 minutes, followed by supernatant removal. The 70% ethanol wash step was repeated again. The DNA pellets were air dried at room temperature for 20 minutes and stored at -20℃ until submission to the sequencing facility of the Faculty of Natural and Agricultural Sciences, University of Pretoria. These reactions were then analyzed on an ABI 3100 DNA sequencer (AE Applied Biosystems).

#### 2.2.2.9 Sequence editing and alignment

Positive control sequences were identified with the NCBI (National Center for Biotechnology Information) BLAST function. The control sequences were edited and consensus sequences assembled in CLCBio main workbench v6 (CLCBio, Denmark). The consensus sequences were aligned with the SARS-CoV reference isolate CDC200301157 (Accession number: AY714217.1) using ClustalX in BioEdit (Hall, 1999).

### 2.2.3 Improved Coronavirus genus-specific hemi-nested RT-PCR with multiple primer sets (PanBat/AB/6 primer assay)

The PanBtCoV/9 primer nested RT-PCR protocol was re-evaluated and adjusted for the usage of Improm-II Reverse Transcriptase (Promega, USA). At the same time the primers for the PCR were re-evaluated with particular attention to the AlphaCoV primer component of the assay.

#### 2.2.3.1 Primer design

The alphacoronavirus primers were re-examined and compared to the multiple alignments of bat and non-bat coronavirus RdRp gene region sequences from both the *Alpha-* and *Betacoronavirus* genera (Table 2.1). The primers were produced by Integrated DNA Technologies (IDT, Germany) and used without further purification.

#### 2.2.3.2 cDNA synthesis

Improm-II Reverse Transcriptase (Promega, USA) was used to synthesize cDNA. Each synthesis step was performed with a standard concentration of the positive control, at $10^8$ copies/µl. Briefly, 5 µl of the positive control RNA template was added to the 10 pmol RT-PCR reverse primers. The template-primer mix was incubated at 70˚C for 5 minutes and cooled on ice for 5 minutes to which 13 µl of the RT-step reaction mixture was added. The RT-step mixture contained 1X Improm-II reaction buffer (Promega, USA), 3 mM $MgCl_2$ (Promega, USA), 0.2 mM dNTPs, 20U RNase inhibitor (Roche Diagnostics), 1µl/reaction Improm-II Reverse Transcriptase (used according to manufacturer's instructions, Promega, USA) and made up to 20 µl with Nuclease free $H_2O$ (Promega, USA). The RT-step reaction was incubated at 25˚C for 5 minutes to anneal the primers, followed by 37˚C for 60 minutes of reverse transcription and 70˚C for 15 minutes to inactivate the enzyme.

#### 2.2.3.3 RT-PCR

The RT-PCR reaction mixture (100 µl) consisted of 20 µl cDNA reaction with the addition of the PCR mixture consisting of 1.25X Dream Taq buffer (Fermentas, Inqaba biotechnologies, 20mM $MgCl_2$), 10pmol RT-PCR forward and reverse primers, 1.25U Dream Taq (Fermentas, Inqaba biotechnologies, 20mM $MgCl_2$) and made up to 80 µl with Nuclease free $H_2O$ (Promega, USA). The reaction was amplified with an initial denaturation of 94°C for 5 minutes, 35 cycles of 94˚C for 30 seconds, 37˚C for 30 seconds and 72˚C for 45 seconds and a final elongation of 72˚C for 7 minutes. RT-PCR reactions were analyzed with 1.5% agarose gels electrophoresis (Section 2.2.2.4).

#### 2.2.3.4 Hemi-nested PCR

The RT-PCR product was diluted 1:10 with RNase free $H_2O$ (Promega, USA) and 1 µl was used as the template for the hemi-nested PCR. The hemi-nested PCR mixture (50

µl) consisted of 2X Dream Taq buffer (Fermentas, Inqaba biotechnologies, 20mM $MgCl_2$), 0.2 mM dNTPs, 0.5 mM $MgCl_2$ (Promega, USA), 0.2% glycerol (Saarchem, Merck) with 1.25U Dream Taq, 10pmol nested forward and reverse primers, and made up to 50 µl with RNase free $H_2O$ (Promega, USA). The nested PCR conditions consisted of an initial denaturation of 94℃ for 2 minutes, 25 cycles of 94˚C for 45 seconds, 37˚C for 50 seconds, 72˚C for 45 seconds and a final elongation of 72˚C for 7 minutes. PCR products were analyzed with 1.5% agarose gel electrophoresis (Section 2.2.2.4).

#### 2.2.3.5 RT-PCR optimization

The RT-step was performed with both AMV (Roche Molecular Diagnostics, Germany) and Improm-II (Promega, USA) enzymes, and the ice incubation step was either omitted/included. The RT-PCR was tested with the reaction buffers of both Improm-II and Dream Taq enzymes using different concentrations of the positive control at $10^8$ and $10^6$ copies/µl. A temperature gradient was performed of 35˚C-50˚C in an Eppendorf Mastercycler gradient thermocycler (USA Scientific) set at 44˚C at a gradient of 8˚C. The RT-step and RT-PCR were performed with the modified conditions.

#### 2.2.3.6 Hemi-nested PCR optimization

The PanBat/AB/6 primer nested step was optimized as described in Section 2.2.2.7. The genus specific primers were analysed separately (alpha- and betacoronavirus primers separately) and in mixes.

#### 2.2.3.7 Purification of PCR amplicons, sequence determination and editing

Amplified positive control sequences of the PanBat/AB/6 primer assay were purified and sequenced with the first round forward and reverse primer sequences as described in Section 2.2.2.8. Positive control sequences were edited and aligned to the SARS-CoV reference sequence (isolate CDC200301157, Accession number: AY714217.1) as described in Section 2.2.2.9.

## 2.3 Results

### 2.3.1 PanBtCoV/9 primer assay

#### 2.3.1.1 Primer design

A study of the alpha- and betacoronavirus alignments showed reoccurring differences between all the alpha- and betacoronavirus sequences that could be utilised in the creation of genus specific primer sets (Figure 2.3 and 2.4). Multiple primer sets were developed with the least possible amount of degeneracies. Nine primers (Table 2.2) in total were designed for the nested RT-PCR, with 6 alphacoronavirus (3 primers for the RT-PCR and 3 for the nested PCR) and 3 betacoronavirus primers (2 for the RT-PCR and an

additional nested PCR primer). The primer binding positions are shown in Figures 2.3 and 2.4.

**Table 2.2: Newly designed primers for cDNA synthesis, PCR and sequencing of the coronavirus RNA dependent RNA polymerase gene.**

| Primer Name | Sequence (5'-3') | Length (nt) | Sense | Tm ºC |
|---|---|---|---|---|
| P1AlphaWfor | GGCTGGGATTATCCTAAGTGTGA | 23 | + | 56.2 |
| P1BetaWfor | GGTTGGGACTACCCTAAGTGTGA | 23 | + | 58.1 |
| *P1AlphaWRev1* | CCATCATCAGACAGAATCATCAT**A** | 24 | - | 52.2 |
| *P1AlphaWRev2* | CCATCATCAGACAGAATCATCAT**G** | 24 | - | 53.5 |
| P1BetaWRev | CCATCATCAGAHAGDATCATCATA | 24 | - | 49-54 |
| *P2NAlphaFor25bp1* | TGATTTCTGC**T**ATGATT**C**T**G**GGTTC | 25 | + | 55.0 |
| *P2NAlphaFor25bp2* | TGATTTCTGC**C**ATGATT**T**T**T**GGTTC | 25 | + | 54.7 |
| P2NAlphaRev21bp | AGATCTATAACAATTGTCATA | 21 | - | 43.6 |
| P2NBetaFor25bp | ATTTTAGCNCGTAARCATASTACTT | 25 | + | 50-54.8 |

P1 indicates RT-PCR primers; P2 indicates nested primers. Bold type indicates nucleotide positions different within the same genus. Italics indicate two of the same primer with different nucleotide substitutions.

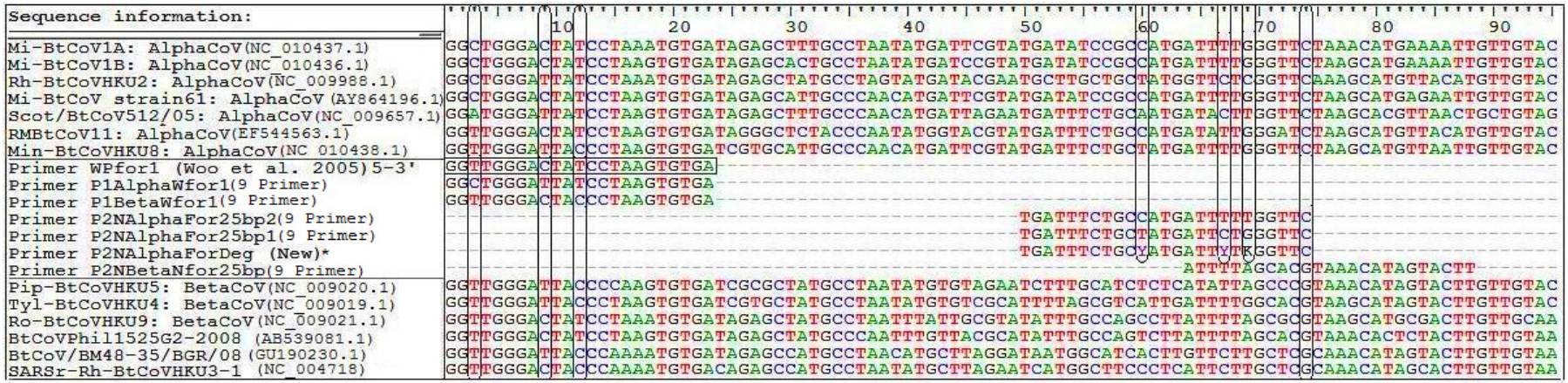


**Figure 2.3**: The alignment above shows the primer biding positions of the forward primers designed for the PanBtCoV/9 primer assay on the RNA dependent RNA polymerase gene (approximately position 15216 of the genome on the indicated reference sequences). The top sequences in the alignment are alphacoronavirus sequences, the bottom sequences are betacoronavirus sequences, and the middle block shows the forward primers designed. Primer WPFor1 is the template primer used in Woo *et al.* 2005.

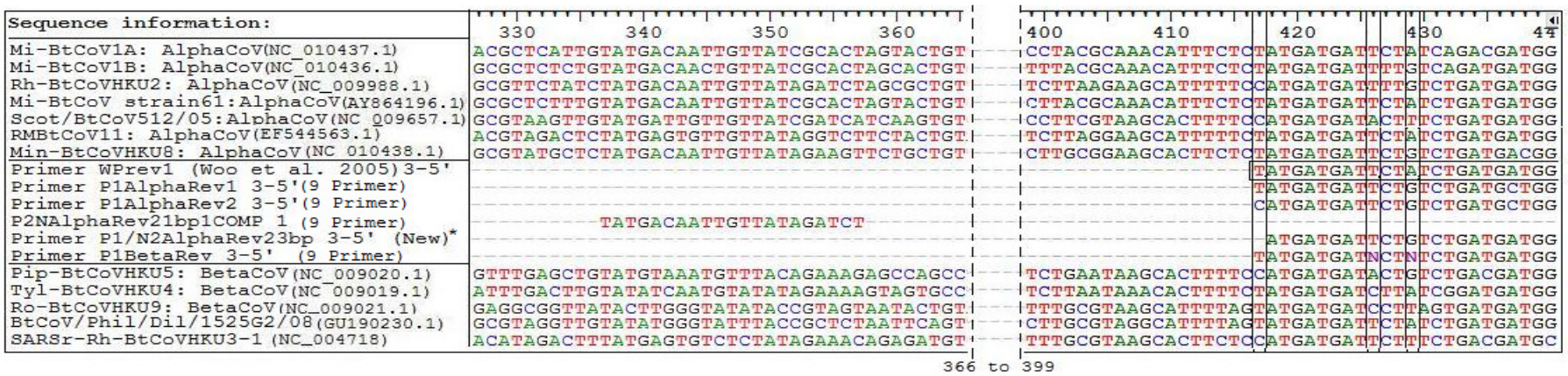


**Figure 2.4:** The alignment above shows the primer biding positions of the reverse primers designed for the PanBtCoV/9 primer assay on the RNA dependent RNA polymerase gene (approximately position 15632 of the genome on the indicated reference sequences). The top sequences in the alignment belong to the *Alphacoronavirus* genus, the bottom sequences belong to the *Betacoronavirus* genus, and the middle block shows the reverse primers designed. Primer WPFor1 is the template primer used in Woo *et al.* 2005. All primer sequences shown above are reverse complimented and in 3'-5' orientation so that the sequences match the reference sequences. Positions 366 to 399 on the alignment above were omitted.

### 2.3.1.2 RT-PCR

An amplicon of expected size, 420bp was amplified with the first round RT-PCR. The lowest concentration that could be visually detected with the PanBtCoV/9 primer RT-PCR assay was at a concentration of $10^4$ copies/µl (Figure 2.5).

### 2.3.1.3 Nested PCR

The serially diluted positive controls used for the sensitivity analysis of the RT-PCR were also used to analyse the increased sensitivity of the assay with the incorporation of a nested step. Clearly visible amplification of the positive control at the lowest concentration of $10^4$ can be seen in Figure 2.5. Lane 4 shows faint amplification of the $10^4$ copies/µl from the RT-PCR with improved amplification in the nested PCR (Lane 5).

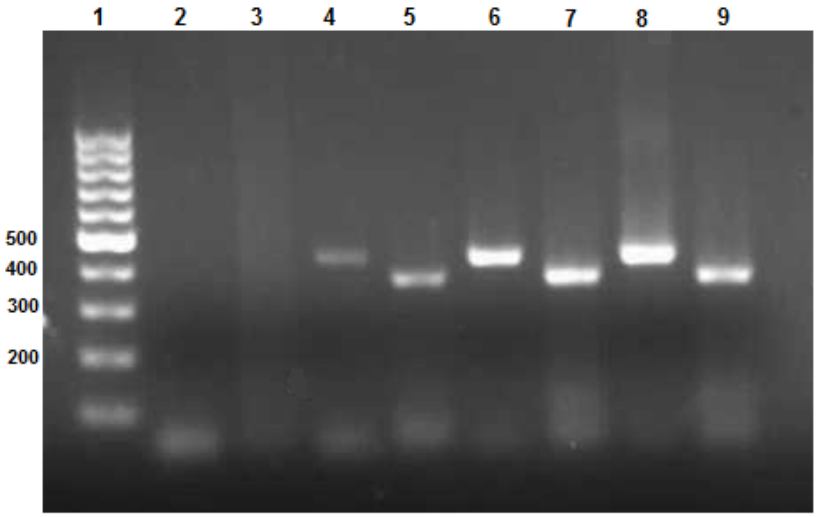


**Figure 2.5**: Agarose gel electrophoresis analysis of the PanBtCoV/9 primer nested RT-PCR protocol showing analysis with the SARS-CoV isolate CDC200301157 (AY714217.1) positive control, used at the concentrations $10^4$, $10^6$, $10^8$ copies/µl. **Lane 1**: O'Gene Ruler 100bp Marker (Fermentas, Life Sciences), **Lane 2**: (RT-PCR) Negative control from which template was excluded, **Lane 3**: Nested PCR negative control from which all template was excluded, **Lane 4:** RT-PCR $10^4$, **Lane 5**: Nested PCR $10^4$, **Lane 6**: RT-PCR $10^6$, **Lane 7**: Nested PCR $10^6$, **Lane8**: RT-PCR $10^8$, **Lane 9**: Nested PCR $10^8$.

### 2.3.1.4 Optimization

The RT-PCR was optimised as described in Section 2.2.2.6. The RT-PCR was evaluated with both Superscript III (Invitrogen) and AMV (Roche Molecular Diagnostics, Germany). Both enzymes were capable of amplifying the positive control and producing bright amplicon bands when viewed with 1.5% agarose gel electrophoresis.

The nested PCR was optimized as described in Section 2.2.2.7. The optimal RT-PCR template used for the nested PCR was determined with template dilutions to be 1:10. No improvement to nested amplification was observed after annealing temperature optimization with a temperature gradient of 46˚C-56˚C. Thus the most optimum conditions

for the nested PCR protocol was determined to be an annealing temperature at 48˚C with the addition of 1mM magnesium increasing the final concentration in the reaction to 2.5mM. Addition of betaine and glycerol to the nested PCR was evaluated to reduce smearing (Figure 2.6). The addition of 0.03M betaine (Sigma-Aldrich) had no significant difference to the amplicons created when compared to the addition of 0.2% glycerol, however, both together in one PCR created amplicon smearing. Subsequent reactions received 0.2% glycerol only.

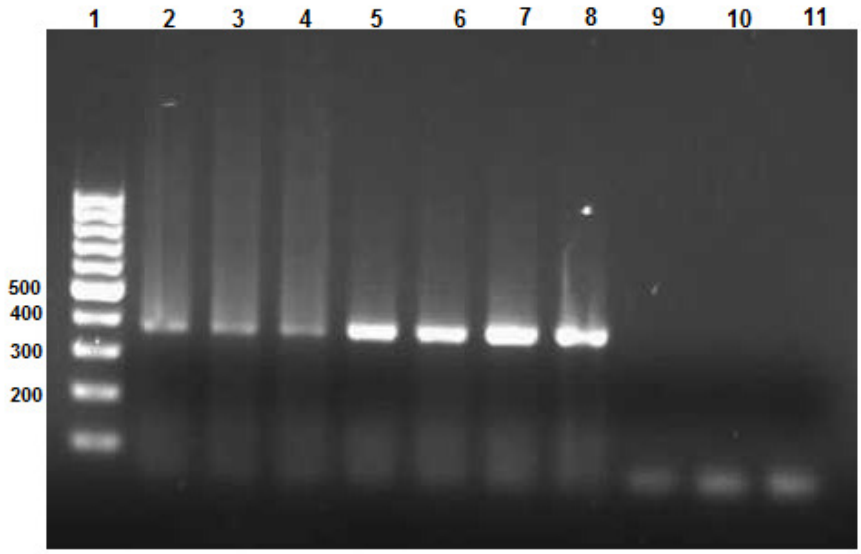


**Figure 2.6:** Agarose gel electrophoresis analysis of the optimization of the nested PCR of the PanBat/AB/9 primer nested RT-PCR protocol. The SARS-CoV (isolate CDC200301157 (AY714217.1)) positive control was used at $10^6$ copies/µl and $10^8$ copies/µl to evaluate the possible improved sensitivity of the nested PCR with the addition of 0.03M betaine, 0.2% glycerol or both. **Lane 1**: O'Gene Ruler 100bp Marker (Fermentas, Life Sciences), **Lane 2**: Nested PCR at $10^8$ copies/µl (No glycerol or betaine), **Lane 3**: Nested PCR at $10^8$ copies/µl with glycerol, **Lane 4**: Nested PCR at $10^8$ copies/µl with betaine, **Lane 5**: Nested PCR at $10^6$ copies/µl (No glycerol or betaine), **Lane 6**: Nested PCR at $10^6$ copies/µl with glycerol, **Lane7**: Nested PCR at $10^6$ copies/µl with betaine, **Lane 8**: Nested PCR at $10^8$ copies/µl with both glycerol and betaine, **Lane 9**: Negative control (exclusion of template, glycerol, and betaine), **Lane 10**: Negative control (template exclusion) with glycerol, **Lane 11**: Negative control (template exclusion) with betaine.

### 2.3.1.5 Nucleotide sequence determination

The sequence results by BLAST hit were that of several closely related SARS-CoV strains. Alignment of the amplified positive control to the SARS CoV CDC#200301157 reference sequence showed 100% nucleotide identity. An alignment of the consensus forward and reverse positive control sequence with the reference sequence and the RT-PCR BetaCoV forward primer is shown in Figure 2.7.

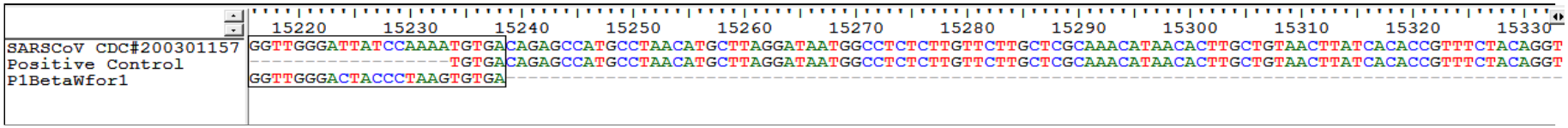


**Figure 2.7:** Alignment of the SARS-CoV isolate CDC200301157 reference strain (AY714217.1) with the consensus sequence of the positive control forward and reverse sequences, as well as the betacoronavirus RT-PCR forward primer for position reference. The primer sequence was trimmed from the positive control sequence during consensus sequence assembly.

### 2.3.2 PanBat/AB/6 primer hemi-nested RT-PCR

#### 2.3.2.1 Primer design

Six primers were designed in total, forward and reverse RT-PCR primers and one nested forward primer for both the *Alphacoronavirus* and *Betacoronavirus* genera (Table 2.3). The binding positions of the primers are shown in Figures 2.3 and 2.4 (The newly designed primers for the PanBat/AB/6 primer assay are indicated with an asterisk).

**Table 2.3: PanBat/AB/6 protocol primers for cDNA synthesis, PCR and sequencing of the coronavirus RNA dependent RNA polymerase gene.**

| Primer Name | Sequence (5'-3') | Length (bp) | Sense | Tm ºC |
|---|---|---|---|---|
| P1AlphaWfor | GGCTGGGATTATCCTAAGTGTGA | 23 | + | 56.2 |
| P1BetaWfor | GGTTGGGACTACCCTAAGTGTGA | 23 | + | 58.1 |
| P1AlphaRev23bp* | CCATCATCAGACAGAATCATCAT | 23 | - | 52.2 |
| P1BetaWRev | CCATCATCAGAHAGDATCATCATA | 24 | - | 49-54 |
| P2NAlphaForDeg* | TGATTTCTGCYATGATTYTKGGTTC | 25 | + | 52.5-57.4 |
| P2NBetaFor25bp | ATTTTAGCNCGTAARCATASTACTT | 25 | + | 50-54.8 |

* Indicates the newly designed primer sequences as compared to Table 2.3

#### 2.3.2.2 RT-PCR

The 3 concentrations, $10^8$, $10^6$ and $10^4$, were used in the analysis of the PanBat/AB/6 primer cDNA and RT-PCR steps. An amplicon of expected size, 420bp was amplified by the first round RT-PCR. Figure 2.8 shows the RT-PCR and nested PCR results with the betacoronavirus positive controls at $10^6$ and $10^4$ copies/µl and the alphacoronavirus positive control (UP1410).

#### 2.3.2.3 Hemi-nested PCR

The newly designed primers for the PanBat/AB/6 primer nested PCR increased the specificity of the primers so that they were able to discriminate between sequences of the *Alphacoronavirus* and *Betacoronavirus* genera. As such, the AlphaCoV primer set was unable to amplify the betacoronavirus positive control used in this study. Thus, the alphacoronavirus primers were evaluated by amplifying a positive alphacoronavirus sample detected (UP1410).

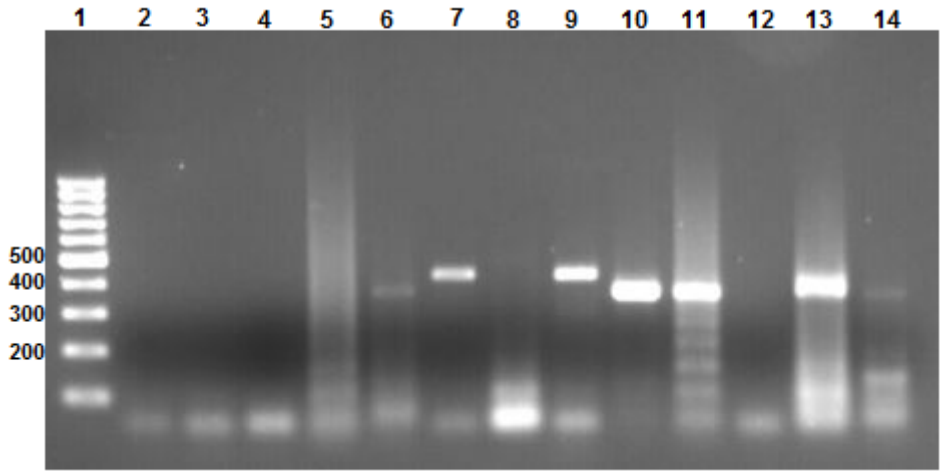


**Figure 2.8**: Agarose gel electrophoresis analysis of the PanBat/AB/6 primer protocol using the SARS-CoV isolate CDC200301157 (AY714217.1) positive control at $10^6$ copies/µl and $10^4$ copies/µl. **Lane 1:** O'Gene Ruler 100bp Marker (Fermentas, Life Sciences), **Lane 2:** RT-PCR negative control (template excluded) with both AlphaCoV and BetaCoV primer sets, **Lane 3**: Nested PCR negative control (template excluded) with both AlphaCoV and BetaCoV primer sets, **Lane 4:** RT-PCR at $10^4$ copies/µl with both AlphaCoV and BetaCoV primer sets. **Lane 5:** Nested PCR at $10^4$ copies/µl with both AlphaCoV and BetaCoV primer sets. **Lane 6:** Nested PCR at $10^4$ copies/µl with only the BetaCoV primer sets. **Lane 7:** RT-PCR at $10^6$ copies/µl with only the AlphaCoV primer sets. **Lane 8:** Nested PCR at $10^6$ copies/µl with only the AlphaCoV primer sets. **Lane 9:** RT-PCR at $10^6$ copies/µl with both AlphaCoV and BetaCoV primer sets. **Lane 10:** Nested PCR at $10^6$ copies/µl with only the BetaCoV primer sets. **Lane 11:** Nested PCR at $10^6$ copies/µl with both AlphaCoV and BetaCoV primer sets. **Lane 12:** RT-PCR of alphacoronavirus positive control (UP1410) with both AlphaCoV and BetaCoV primer sets. **Lane 13:** Nested PCR of alphacoronavirus positive control (UP1410) with only the AlphaCoV primer set. **Lane 14:** Nested PCR of alphacoronavirus positive control (UP1410) with only the BetaCoV primer set.

#### 2.3.2.4 Optimization

The optimization of the RT-step and RT-PCR assay showed that Improm-II reverse transcription enzyme requires the 5 minute ice incubation during the RT-step (Figure 2.9, lane 4) and that the Improm-II reverse transcriptase performed very well when used in conjunction with Dream Taq polymerase and buffer (Fermentas, Inqaba Biotechnologies) (Figure 2.9, lane 5&6).

The Improm-II protocol was used at first with the annealing temperature previously established, 48˚C, which is optimized for the primers. The temperature gradient performed for the RT-PCR showed an annealing temperature of 37˚C to be optimum (Section 2.2.2.6). The RT-PCR optimization showed an increase of PCR performance with the exclusion of dNTPs from the RT-PCR.

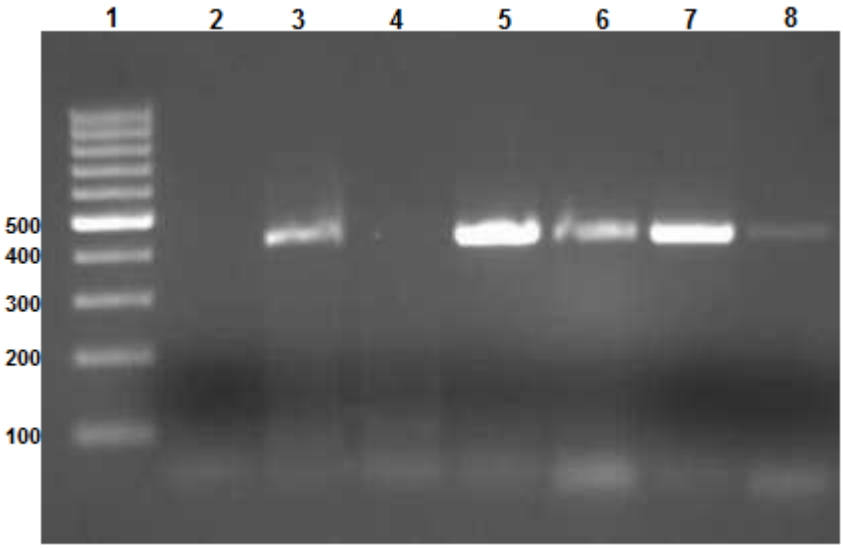


**Figure 2.9:** Agarose gel electrophoresis analysis of the PanBat/AB/6 primer protocol optimization using the SARS-CoV isolate CDC200301157 (AY714217.1) positive control at $10^6$ copies/µl and $10^8$ copies/µl. **Lane1:** O'Gene Ruler 100bp Marker (Fermentas, Life Sciences), **Lane2:** Negative control in which the template was excluded (with Dream Taq buffer), **Lane3:** Positive control $10^6$ copies/µl with AMV RT-PCR protocol (AMV buffer), **Lane4:** Positive control $10^6$ with Improm-II protocol but no ice incubation step, **Lane5:** Positive control $10^8$ with Improm-II protocol RT-step using Dream Taq Buffer in RT-PCR, **Lane6:** Positive control $10^6$ with Improm-II protocol RT-step using Dream Taq Buffer in RT-PCR, **Lane7**: Positive control $10^8$ with Improm-II protocol RT-step using Improm-II Buffer in RT-PCR, **Lane8:** Positive control $10^6$ with Improm-II protocol RT-step using Improm-II Buffer in RT-PCR.

Figure 2.10 shows the effects of varying the quantity of magnesium and glycerol added to the nested PCR (annealing at 37˚C). Increasing both the glycerol and magnesium by even 1µl will also increase non-specific amplification in the PCR (Lane 5 and 6). Lane 4 shows the amplification of the positive control when both the *Alpha*- and *Betacoronavirus* genera primers are added to the reaction in contrast to the bright band formation seen in Lane 3 where only the BetaCoV primers were added. Thus only 0.5mM magnesium and 0.2% glycerol was subsequently added to the nested PCR.

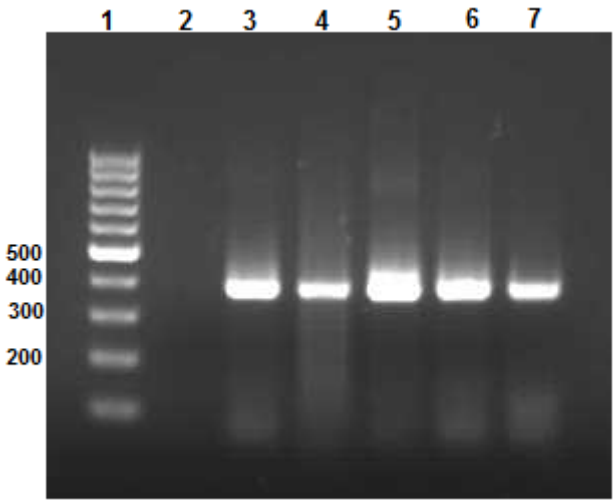


**Figure 2.10:** Agarose gel electrophoresis analysis of the PanBat/AB/6 primer nested PCR optimization using the SARS-CoV isolate CDC200301157 (AY714217.1) positive control at $10^6$ copies/µl. **Lane 1** O'Gene Ruler 100bp Marker (Fermentas, Life Sciences), **Lane 2:** Negative control in which template was excluded, **Lane3:** Positive control $10^6$ copies/µl with only BetaCoV primers, 0.5mM $MgCl_2$ and 0.2% glycerol, **Lane 4:** Positive control $10^6$ with both Alpha- and BetaCoV primers, 0.5mM $MgCl_2$ and 0.2% glycerol, **Lane 5:** Positive control $10^6$ with only BetaCoV primers, 0.5mM $MgCl_2$ and 0.4% glycerol (twice the volume glycerol), **Lane 6:** Positive control $10^6$ with only BetaCoV primers, 1mM $MgCl_2$ and 0.4% glycerol (twice the volume $Mg^{2+}$ and glycerol).

### 2.3.2.5 Nucleotide sequence determination

The sequence results by BLAST hit were several closely related human SARS-CoV strains. The positive control sequences and the SARS-CoV reference sequence show 100% sequence identity.

## 2.4 Discussion

The aim of the study was to develop and establish a sensitive nested RT-PCR protocol for the detection of bat coronavirus RNA from RNA extracts of samples collected from Rwanda and South Africa. Thus a suitable coronavirus RT-PCR would have to either be selected from the literature or developed. The RNA dependent RNA polymerase (RdRp) gene is the best gene region to target in PCR amplification for the detection of BtCoV RNA due to the fact that the majority of the data available on BtCoV are of the RdRp gene and since this gene is highly conserved. Through examination of available literature, coronaviruses primer sequences targeting the RdRp gene were selected from a previous publication to be used in the protocol. It quickly became apparent that a simple RT-PCR may not be sufficiently sensitive to detect the low amounts of bat coronaviruses present within bat alimentary specimens. We then developed two nested coronavirus RT-PCR assays that may be used for bat coronavirus detection, each protocol improving on the previously developed protocol. Real-time PCR for the detection of BtCoV was excluded for several reasons. First, real-time PCR requires the development of oligonucleotide probes or primers that can be labelled with fluorescent label. Moreover the size of a real-time amplicon is limited to approximately 200bp, thus a suitable region of the polymerase gene of approximately 200bp would be required from which probes and primers could be designed, a very difficult feat due to the divergence between non-BtCoV and BtCoV genomes and even between BtCoV genomes. Real-time PCR assays are excellent diagnostic assays for the determination of presence or absence of an etiological agent within a specimen. Ultimately however, the amplicon size of a real-time assay is too small for a proper phylogenetic analysis of any detected BtCoV and therefore will have to be re-analysed with a conventional PCR assay (hence the development of a conventional assay would still be necessary). The concern is also that a real-time assay may be able to detect very low amounts of the virus present in the sample but a follow up conventional PCR amplification may not be, and as such the viruses could not be studied in detail.

The initial RT-PCR assay (with no nested step) selected from the literature (Woo *et al.,* 2005) implemented the Superscript III one step kit and platinum Taq kit (Invitrogen) which is an excellent high fidelity, though expensive, reverse transcriptase enzyme with accompanying platinum Taq polymerase. From there we proceeded to a two-step RT-PCR with the implementation of AMV reverse transcriptase (Roche Molecular Diagnostics, Germany) and the usage of Dream Taq polymerase (Fermentas, Inqaba biotechnologies). The final reverse transcriptase enzyme implemented was the two-step reverse transcription enzyme, Improm-II Reverse Transcriptase (Promega, USA), an enzyme more cost effective

than AMV (Roche Molecular Diagnostics, Germany) and the reverse transcriptase used in our laboratory.

When comparing the RT-PCR and nested PCR amplicons of the positive controls produced by AMV (Roche) and Improm-II (Promega) though various assay it became apparent that the quality of the amplicons produced by AMV (Roche) was superior to that of Improm-II (Promega). This became especially apparent when RT-PCR products were used as templates for nested PCR assays. The RT-PCR products created with AMV (Roche) was even used as a nested PCR positive control to indicate the functionality of the nested PCR reaction mix.

The conserved primer set reported from Woo *et al.,* (2005) and Poon et al., (2005) was used as the guide for the subsequent PCR assay's primer development. At first only a single nested primer was selected, at the midpoint of the RT-PCR primers set amplicon. The primer was capable of positive control amplification; however we required a more sensitive assay. Therefore, to improve the detection limit of the assay multiple alignments of several bat and non-bat coronavirus RdRp gene regions from both alpha- and betacoronaviruses were made and reoccurring genus specific features were observed that could be used for primer designing (Figures 2.3 and 2.4). Genus-specific primer sets were constructed in the PanBtCoV/9 primer nested RT-PCR protocol with the aim of incorporating the least possible amount of degeneracy in the primers. Theoretically, the best primer for a specific segment of the RdRp gene would out-compete the less optimum primers and anneal to the template. Thus as certain positions there were more than 1 primer for specific annealing locations. In the genus specific PanBtCoV/9 primer nested RT-PCR protocol, 6 of the primers were alphacoronavirus primers (3 RT-PCR and 3 nested primers) and 3 were betacoronavirus primers (same reverse primer in both RT-PCR and nested PCR).

The development and implementation of genus specific PanBtCoV/9 primer RT-PCR and nested PCR assay successfully increased the sensitivity of the assay from being able to detect the positive control at a concentration of $10^6$ to the lower concentration of $10^4$ copies/µl. Both Superscript III (Invitrogen) and AMV (Roche Molecular Diagnostics, Germany) were used to evaluate the RT-PCR component of the assay, and were shown to work equally well. The RT-PCR and nested PCR were performed separately with Alpha and Beta primer sets as well as Alpha/Beta primer mixes, all of which were capable of amplifying the positive controls.

Later the genus specific nested PCR assay was simplified to a dual genus-level hemi-nested PCR assay. The alphacoronavirus component of the assay (previously two sets of non-degenerate) was re-evaluated and the double RT-PCR reverse primers and double nested forward primers were compressed into single primer sets. The AlphaCoV

reverse primer was subsequently used for both the RT-PCR and nested PCR (as with the BetaCoV component).

The sensitivity of the overall assay improved from detection of the positive control at a concentration of $10^8$ to $10^6$ with the nested PCR incorporation to the initial RT-PCR selected from literature, and later to $10^4$ with the incorporation of the genus specific primer sets (the PanBtCoV/9 primer assay). This sensitivity decreased slightly with the increase in genus-level specificity achieved with the dual genus-level hemi-nested PCR assay (PanBat/AB/6 primer assay). Each genus specific primer set optimally only amplified positive controls originating from its own genus. Mixing of the primer sets in an Alpha/Beta primer mixture would decrease the sensitivity of the assay so much so that the $10^4$ copies/µl BetaCoV positive control would barely amplify in a primer mix. However, according to literature, bat coronaviruses have been found to be present in 100mg of fecal material (2-4 pellets) up to $10^4$ copies of RNA (Pfefferle *et al.*, 2009). Likewise, an experimental study of oral infection of bat coronaviruses in their host showed that the viruses may be capable of amplification of up to $10^6$ copies/µl (Watanabe *et al.,* 2010). It is understood that some RNA may be lost during the RNA extraction process, however the PCRs designed in this study may still be sufficiently sensitive to detect the amount of RNA typically present in bat gastrointestinal samples.

The optimization and subsequent addition of 0.2% glycerol to the nested PCR resolved the 'smearing' seen on agarose electrophoresis gels. A review of PCR optimization literature suggested the addition of betaine (Sigma-Aldrich), Dimethyl Sulfoxide (DMSO), and glycerol. DMSO is generally used between concentrations of 1-10% and can increase the specificity of the PCR assay. However the chemical may inhibit the activity of Taq polymerase and is also toxic, requiring the usage of a chemical flow hood for reagent addition. Glycerol on the other hand improves efficiency and specificity of PCR assays, is non-toxic and is used at concentrations of between 5 and 20%, optimally at 10% (final concentration of 0.2%). Betaine or N,N,N-trimethylglycine is another PCR enhancer that can be used to improve specificity (Frackman *et al.*, 1998). Optimization of the nested showed that the glycerol performed slightly better than betaine in terms of reducing nested PCR smearing.

# Chapter 3: Surveillance and characterization of Coronaviruses in bat species from South Africa and Rwanda

## 3.1 Introduction

Bat coronavirus (BtCoV) detection studies have been performed worldwide in 16 different countries (Brandão *et al.*, 2008; Carrington *et al.*, 2008; Dominguez *et al.*, 2007; Drexler *et al.*, 2010; Drexler *et al.*, 2011; Falcón *et al.*, 2011; Gloza-Rausch *et al.*, 2008; Gouilh *et al.*, 2011; Lau *et al.*, 2005a; Pfefferle *et al.*, 2009; Poon *et al.*, 2005; Quan *et al.*, 2010; Rihtarič *et al.*, 2010; Reusken *et al.*, 2010; Smith *et al.*, 2008; Shirato *et al.*, 2011; Tang *et al.*, 2006; Tong *et al.*, 2009; Watanabe *et al.*, 2010; Woo *et al.*, 2006a; Woo *et al.*, 2007; Yuan *et al.*, 2010). BtCoV have been identified in families of both insectivorous and frugivorous bats that include the *Pteropodidae Hipposideridae, Megadermatidae, Rhinolophidae, Phyllostomidae, Molossidae, Miniopteridae and Vespertilionidae* families. As of yet no BtCoV have been identified within the *Nycteroidea* superfamily which includes the *Nycteridae* and *Emballonuridae* families.

Several studies have reported strict host specificity of the bat host and CoV species involved. For example, two different species of bats may roost together in the same cave; however each bat species will be infected with a CoV specific to that species of bat, and will be more closely related to CoV detected in the same bat species in a distant cave or even a different continent (Dominguez *et al.*, 2007) than the CoV present in a different bat species at the same geographic location. In contrast, exceptions to bat host species specificity have also been observed. Tong *et al.* (2009) detected 3 different BtCoV usually identified in different bat species within the same individual *Chaerephon* bat.

BtCoV are most often detected in alimentary specimens (specifically fecal and rectal specimens and rarely also in respiratory specimens) indicating that BtCoV are gastrointestinal in origin, and infected bats have not been observed to display any clinical symptoms of disease (Poon *et al.*, 2005; Falcón *et al.*, 2011).

Bats inhabit almost every continent on earth, constituting approximately 20% of the recorded mammalian species (>4000 species). Moreover, because bats are capable of flight they are able to migrate long distances and colonize a variety of habitats that not only include natural shelters for example caves and trees but also manmade constructions such as bridges and in buildings which provides opportunities for interaction with humans (Calisher *et al.*, 2006).

It has been reported that BtCoV such as SARSr-*Rh*-BtCoV appear to cause acute, self-limiting infections within their host species (Lau *et al.* 2010a). It has been postulated that bats infect other members of a colony with CoV (or become re-infected) during social interactions such as grooming, feeding and mating. This would be easily facilitated due to typical bat roosting behaviour; bats roost in large numbers, some colonies even range in the millions of members. Bats present in a colony are almost constantly in contact with each other and often groom each other. Thus bats previously infected with a

BtCoV may become re-infected from infected individuals within the same roost or from bats encountered during migration to alternative habitats.

In Africa, surveillance for bat coronavirus have been performed in only Kenya, Ghana and Nigeria (Tong *et al.*, 2009; Pfefferle *et al.*, 2009; Quan *et al.*, 2010). Both alpha- and betacoronaviruses have been detected in the 8 bat species analysed thus far. BtCoV related to known human CoV have been detected from both the coronavirus genera. In Ghana, a bat *alphacoronavirus* from a *Hipposideros ruber* was phylogenetically shown to share common ancestry with the Human CoV-229E (Pfefferle *et al.*, 2009). The same bat species also harboured a betacoronavirus that shared an ancestor with the SARSr-CoV cluster. Within the same bat genus in Nigeria, a novel betacoronavirus was detected in *Hipposideros commersoni*; Zaria bat coronavirus, though related to the SARSr-CoV cluster may indeed represent a new coronavirus species within the betacoronavirus genus (Quan *et al.*, 2010).

No bat coronavirus nucleic acid detection studies have thus far been performed in Rwanda or South Africa. A related study performed within South Africa suggests that there may be a high prevalence of BtCoV present in South African bat species. In 2007, Muller *et al.* performed serological surveillance of CoV on 248 serum samples collected since 1986 through to 1989 from bats in the Mpumalanga and Limpopo provinces of South Africa. Two of the 16 bat species collected were reported to possess antibodies against the SARS-CoV antigen detectable by the enzyme-linked immunosorbent assay (ELISA), which may also likely detect other antigentically similar members of the genus. Eleven of twenty nine (37.9%) *Rousettus aegyptiacus* serum specimens collected in Limpopo province (only) were seropositive for the SARS-CoV antigen as well as *Mops condylurus* collected in Limpopo and Mpumalanga provinces with seroprevalence of 15.8% (3/19) and 11.5% (11/96), respectively. In total, the seroprevalence detected in the two South African provinces was 10.08% (25/248). No CoV nucleic acids could be detected with an RT-PCR performed on RNA extracted from the bat serum, as is expected since BtCoV display enteric tissue tropism.

The aims of this study was to analyse bat gastrointestinal samples (fecal, rectal and intestinal specimens) collected from South Africa and Rwanda for the presence of bat coronavirus nucleic acid with the use of the genus specific nested RT-PCR assay (developed in Chapter 2), followed by sequence determination of the PCR amplicons and the evaluation of the phylogenetic relationships between the detected coronavirus RNA and coronaviruses detected previously from Africa and the rest of the world. RNA extracts that were found to be positive for bat coronavirus RNA were further analysed to attempt to amplify additional regions of the RdRp and nucleoprotein genes in order to improve the resolution of the phylogenetic trees.

## 3.2 Materials and methods

### 3.2.1 Biosafety considerations

Coronaviruses are positive sense RNA viruses, meaning that their genome is infectious and has the potential to cause disease. The existing human coronaviruses mainly cause respiratory illnesses and are thus transmitted through aerosols i.e. sputum droplets when coughing. Coronaviruses however are sensitive to heat as well as being susceptible to disinfectants such as a 1% sodium hypochlorite and 2% glutaraldehyde. The virus is also capable of surviving for up to 24 hours on metal surfaces at room temperature.

Special care is necessary to prevent infection due to careless handling since there is no treatment after infection or immunization available. When handling samples taken from bats the possibility of acquiring viral infections from several virus families (such as the *Paramyxoviridae, Filoviridae* or the *Rhabdoviridae* (the rabies related viruses)) which have been associated with bats should be considered. As a precaution a biosafety level 2 flow cabinet was used when working with RNA and extractions of RNA were performed in BSL-3 conditions (along with the appropriate protective clothing).

### 3.2.2 Sample collection

#### South Africa

Since 2006 faecal pellets, fecal swabs and rectal specimens were collected in several field trips to different provinces in South Africa that include Gauteng, Limpopo, the North West and KwaZulu Natal as part of an ongoing bat lyssavirus and other zoonotic disease surveillance program (Figure 3.1). Samples were collected from both frugivorous and insectivorous bats and frozen in liquid nitrogen and stored at -70˚C until RNA extraction (Section 3.2.4). In addition to the separate field trips individual bat samples of sick or dead bats were submitted that were also analyzed for bat coronaviruses. Appendix A shows the samples analysed from South Africa, including sample identity, bat host species, location, and PCR assays used in analysis.

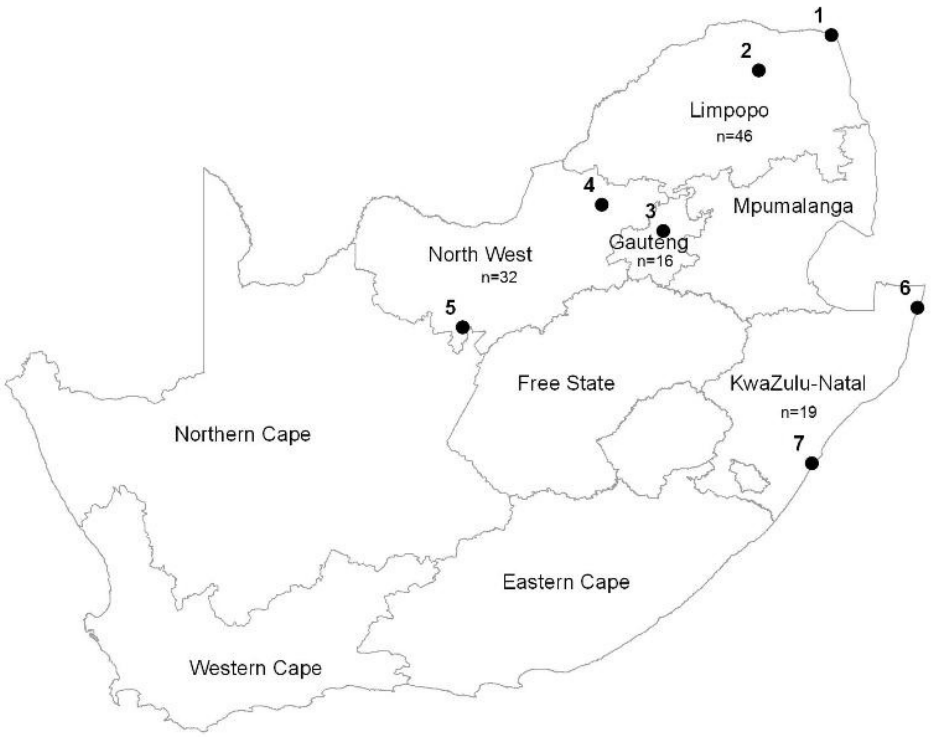


**Figure 3.1:** Map of South Africa showing the various sampling locations and sample number of bats collected at each location. **Limpopo: 1)** Pafuri, Kruger National Park, **2)** Makhado. **Gauteng: 3)** Irene Caves, Centurion. **North West: 4)** Kgaswane, **5)** Taung. **KwaZulu Natal: 6)** Rocktail bay, St. Lucia and **7)** Amanzimtoti, Durban.

### Rwanda

The Ruhengeri cave systems (GPS coordinates -1˚ 50’ 00.63”, 29˚ 63’ 32.17”) near Musanze in Rwanda’s Ruhengeri province was sampled as a single sampling event in 2008 focusing on possible zoonotic pathogens at the request of the Rwandan National Tourism Board. Samples were collected from both frugivorous and insectivorous bats and frozen in liquid nitrogen and stored at -70˚C until RNA extraction. Appendix B shows the all the samples analysed from Rwanda, including sample identity, bat host species, location, and PCR assays used in analysis.

### 3.2.3 Sample pre-extraction processing

Different sample types, fecal swabs, fecal matter or rectum specimens required separate initial extraction procedures. Fecal swabs were resuspended in 300-400µl of phosphate buffered saline or PBS (1.06 mM $KH_2PO_4$, 154 mM NaCl, and 5.6 mM $Na_2HPO_4$, Lonza). The fecal material collected on the swab was resuspended by vigorous vortexing. Fecal pellets were crushed with a pipette tip and 350µl PBS (Lonza) was added. The particles were allowed to settle in the PBS after vigorous vortexing. Rectum samples of approximately 7-10mm in length were added directly to 750µl TRIzol (Invitrogen) along with

two stainless steel beads (QIAGEN) and placed in the TissueLyser II (QIAGEN). The tissue was lysed at a frequency of 1300 at 1/second for 45 seconds.

### 3.2.4 RNA extraction

RNA was extracted by either one of two available methods. All samples collected before 2009 were processed with the QIAamp RNA mini kit (QIAGEN, USA) according to the manufacturer's instructions. Briefly, 140 µl of each sample (rectum/fecal/fecal swab) was placed in a 1.5 ml eppendorf tube containing 560µl lysis buffer AVL and 5.6 µl of the previously prepared Carrier RNA (prepared according to manufacturer's instructions). The contents of the tube was homogenised by vortexing for 15 seconds and incubated at room temperature for 10 minutes. Brief centrifugation was used to collect the droplets in the tube followed by the addition of 560µl ethanol (96-100%), the extract was subsequently vortexed for 15 seconds and again briefly centrifuged. A volume of 630 µl of the sample was transferred to the QIAGEN spin column and centrifuged at 6 000 x g for 1 minute after which the collection tube with filtrate was discarded and replaced with a new collection tube. This step was repeated until all the sample was processed through the spin column.

Five hundred µl buffer AWI was added and centrifuged at 6 000 x g for 1 minute. Again the collection tube was discarded and replaced and 500 µl buffer AW2 was added to the column, then centrifuged at 20 000 x g for 3 minutes. The collection tube was discarded and replaced with a new collection tube. The column was again centrifuged at 20 000 x g for 1 minute and the collection tube was replaced with a 1.5 ml eppendorf tube. The column was eluted by the addition of 40 µl buffer AVE, incubated for 1 minute and centrifuged at 6 000 x g for 1 minute. To increase the nucleic acid yield by 10% the elution step was repeated twice. The RNA pellet was resuspended in 50 µl nuclease-free water (Promega, USA) and used as the template for RT-PCR.

Samples collected since 2009 till present were processed for total RNA by extraction using TRIzol® reagent (Invitrogen). Briefly, a maximum of 500 µl of sample (rectum/fecal/fecal swab) was added to 750µl TRIzol reagent. The sample was homogenised by vigorous vortexing and left at room temperature to incubate for 5 minutes. Next, 200 µl of chloroform (Merck chemicals) was added, shaken for 15 seconds and incubated for a further 2-3 minutes. The solution was subsequently centrifuged at a maximum of 12 000 x g for 15 minutes to allow for phase separation.

The aqueous phase (upper phase containing the RNA) was transferred to another sterile 1.5ml eppendorf tube to which 500 µl of isopropyl alcohol (Rochelle Chemicals) was added. The RNA was precipitated by incubating the solution for 10 minutes at room temperature followed by centrifugation at a maximum of 12 000 x g for 10 minutes and

subsequent removal of the supernatant. The resultant RNA pellet was washed once with 750 µl of 75% molecular grade ethanol, (Merck chemicals) vortexed and centrifuged at a max of 7, 500 x g for 5 minutes.

The supernatant was removed again and the pellet air dried briefly after which it was re-dissolved in 50µl RNase free water (Promega) by pipetting up and down and incubate at 55-60˚C for 10 minutes if not completely dissolved. All extracted RNA was kept at -70˚C until analysed with RT-PCR.

### 3.2.5 Sample analysis: cDNA synthesis, RT-PCR and nested PCR analysis

The detection and amplification of BtCoV amplicons were performed as described in Chapter 2, Section 2.3 with the PanBtCoV/9 primer assay and 2.4 with the PanBat/AB/6 primer assay. Certain collected samples were available for analysis in more than one type of specimen collected such as rectum, fecal matter, fecal swab or all specimen types. Thus, certain samples were analysed for bat coronavirus RNA from RNA extracts obtained from more than one specimen type. Mostly, each sample was analysed with more than one of the developed coronavirus PCR assays. The majority of the samples from South Africa were processed with the PanBat/AB/6 protocol and are shown in Appendix A. The samples from Rwanda were analysed with either the protocol from the literature (Woo *et al.* 2005 protocol) followed by a nested PCR or the PanBtCoV/9 primer protocol and are shown in Appendix B.

### 3.2.6 Purification of PCR amplicons

All positive PCR amplicons were gel-purified using the Wizard® SV Gel and PCR Clean-up system (Promega) according to the manufacturer's instructions. Briefly, after loading 20 µl of the positive sample's PCR reaction onto a 1.2% agarose gel the gel was run at 120V until the resulting band had migrated half way down the gel. The amplicon band was excised from the gel and Membrane binding solution was added to the gel slice at a ratio of 10 µl binding solution per 10 mg gel slice and melted at 55℃.

The melted gel solution was moved to the mini column assembly tube and incubated for 1 minute at room temperature, followed by centrifugation at 12 000 x g for 1 minute. The column was washed with 700µl Membrane wash solution (to which 100% molecular grade ethanol has been added previously) and centrifuged for 1 minute at 12 000 x g. The column was washed again with 500µl of the Membrane wash solution and centrifuged at 12000 x g for 5 minutes and again for 1 minute to allow evaporation of any residual ethanol. The DNA was eluted from the column by adding 50µl nuclease-free water, incubating the column for 1 minute and centrifuging it for another minute at 12 000 x g.

Five µl of the eluted DNA was quantified using the O'Gene Ruler 100bp Marker (Fermentas, Life Sciences) as reference on a 1% agarose gel before sequencing.

### 3.2.7 Nucleotide DNA sequencing

Automated sequencing was performed as described in Chapter 2 Section 2.2.2.8.

### 3.2.8 Phylogenetic analysis

The resultant sequences were viewed, edited and consensus sequences assembled in CLCBio main workbench v6 (CLCBio, Denmark). Consensus sequences and relevant alpha- and betacoronavirus sequences were aligned using ClustalX in BioEdit (Hall, 1999). The neighbour-joining phylogenetic tree was constructed with 1000 bootstrap replicates in MEGA version 5 (Tamura *et al.*, 2011). The coronavirus nucleic acid sequences were translated in frame (-1) to amino acid residues in BioEdit (Hall, 1999) and amino acid phylogenetic trees were constructed again using neighbour-joining methods in MEGA version 5 (Tamura *et al.*, 2011). The nucleic acid and amino acid alignments were used in the construction of pairwise distance (p-distance) matrices in MEGA version 5 (Tamura *et al.*, 2011). The maximum composite likelihood method with 1000 bootstrap repetitions was used for the nucleic acid sequences and the Poisson method was used for the construction of the amino acid data set.

### 3.2.9 Amplifying additional regions of the RdRp gene

#### 3.2.9.1 Primer design

Primers were designed for the amplification of the RNA dependent RNA polymerase gene by multiple alignments of only bat coronavirus genomes closely related to the detected coronaviruses from South Africa using ClustalX in BioEdit (Hall, 1999). Only bat coronaviruses for which full length genomes were available were used in alignments (Table 3.1). Multiple regions of the RdRp gene were selected as primer binding sites to amplify overlapping sections of the 2000 bp gene. All primers were produced by Integrated DNA Technologies (IDT, Germany) and used without further purification.

**Table 3.1 Full length genomes of bat coronaviruses used in the design of primers for the amplification of 2000 bp of the RNA dependent RNA polymerase gene and 900 bp of the nucleoprotein gene.**

| Coronavirus name | Genus | Host species | Accession number | Reference |
|---|---|---|---|---|
| Mi-BtCoV 1A | *Alphacoronavirus* | *Miniopterus* spp. | NC_010437.1 | Chu *et al.,* 2008 |
| Mi-BtCoV BtKY27/Kenya/06 | *Alphacoronavirus* | *Miniopterus natalensis.* | HQ728484.1 | Tong *et al.,* 2009 |
| Chae-BtCoV BtKY22/Kenya/06 | *Alphacoronavirus* | *Chaerephon* spp. | HQ728486.1 | Tong *et al.,* 2009 |

### 3.2.9.2 cDNA synthesis

Synthesis of cDNA was performed with AMV Reverse transcriptase (Roche Molecular Diagnostics, Germany). Each synthesis step was performed in parallel with the standard PanBat/AB/6 primer PCR positive control at a concentration of $10^8$ copies/µl. A volume of five µl of the positive sample RNA template was combined with 10 pmol RdRp gene reverse primer. The template-primer mixture was added to the RT-step reaction mixture (15 µl) that consisted of 1.125X AMV incubation buffer (250 mM Tris-HCl; 40 mM $MgCl_2$; 150 mM KCl; 5 mM dithioerythritol; pH 8.5), 1.1 mM dNTPs, 8U AMV reverse transcriptase (Roche Molecular Diagnostics, Germany), 16U RNase inhibitor (Roche Molecular Diagnostics, Germany) and made up to 20 µl with Nuclease free $H_2O$ (Promega, USA). The reaction was incubated at 42˚C for 90 minutes.

### 3.2.9.3 RT-PCR

The RT-PCR reaction mixture (100 µl) consisted of 20 µl cDNA reaction with the addition of the PCR mixture consisting of 2.125X AMV Reverse transcriptase buffer (250 mM Tris-HCl; 40 mM $MgCl_2$; 150 mM KCl; 5 mM dithioerythritol; pH 8.5) (Roche Molecular Diagnostics, Germany), 0.38mM dNTPs, 1.25U Dream Taq (Fermentas, Inqaba biotechnologies), with 10 pmol of each specific forward and reverse RdRp gene primer pairs and made up to 80 µl with Nuclease free $H_2O$ (Promega, USA). The reaction was amplified with an initial denaturation of 94℃ for 5 minutes, 35 cycles of 94˚C for 40 seconds, 37˚C for 50 seconds and 72˚C for 50 seconds and a final elongation of 72˚C for 7 minutes.

## 3.2.10 Amplifying the nucleoprotein gene

### 3.2.10.1 Primer design

Primers were designed to amplify approximately 900bp of the coronavirus nucleoprotein gene. Only bat coronaviruses closely related to the detected South African coronaviruses for which complete genomes were available were used in alignments for the primer design (Table 3.1). All primers were produced by Integrated DNA Technologies (IDT, Germany) and used without further purification.

### 3.2.10.2 cDNA synthesis

Synthesis of the nucleoprotein cDNA was performed with AMV Reverse transcriptase (Roche Molecular Diagnostics, Germany). Each synthesis step was performed in parallel with the standard PanBat/AB/.6 primer PCR positive control at a concentration of $10^8$ copies/µl. Five µl of the positive sample RNA template was combined with 10 pmol of the nucleoprotein reverse primer. The template-primer mixture was added

to the RT-step reaction mixture (15 µl) that consisted of 1.125X AMV incubation buffer (250 mM Tris-HCl; 40 mM $MgCl_2$; 150 mM KCl; 5 mM dithioerythritol; pH 8.5), 1.1 mM dNTPs, 8U AMV reverse transcriptase (Roche Molecular Diagnostics, Germany), 16U RNase inhibitor (Roche Molecular Diagnostics, Germany).) and made up to 20 µl with Nucease free $H_2O$ (Promega, USA). The reaction was incubated at 42˚C for 90 minutes.

#### 3.2.10.3 RT-PCR

The RT-PCR reaction mixture (100 µl) consisted of 20 µl cDNA reaction with the addition of the PCR mixture consisting of 2.125X AMV Reverse transcriptase buffer (250 mM Tris-HCl; 40 mM $MgCl_2$; 150 mM KCl; 5 mM dithioerythritol; pH 8.5) (Roche Molecular Diagnostics, Germany), 0.38mM dNTPs, 1.25U Dream Taq (Fermentas, Inqaba biotechnologies), with 10 pmol of the nucleoprotein forward and reverse primers and made up to 80 µl with Nuclease free $H_2O$ (Promega, USA). The reaction was amplified with an initial denaturation of 94℃ for 5 minutes, 35 cycles of 94˚C for 40 seconds, 37˚C for 50 seconds and 72˚C for 50 seconds and a final elongation of 72˚C for 7 minutes.

## 3.3 Results

### Detection of coronavirus nucleic acid targeting partial RdRp gene

### 3.3.1 South Africa

A total of n=113 samples from South Africa were analysed. Several samples produced amplicons in an expected size range (between 260-440 bp) when analysed with agarose gel electrophoresis, with possible bat coronavirus RNA amplification (Appendix A). Table 3.2 shows the total analysed samples from South Africa by their bat host species. Samples from 21 bat species that include 14 bat genera were analysed (4 of the samples were obtained from unidentified insectivorous bat hosts, Table 3.2), with the detection of BtCoV RNA in 3 different bat species. The PanBtCoV/9-primer protocol was used to amplify products for the samples UP1410 (referred to as ‘Irene’; a 393bp band was only visible in the nested PCR) and UP167 (bands were produced in both the RT-PCR and the nested PCR (362bp)). The PanBat/AB/6 primer protocol was able to amplify a PCR product for the sample UP1364, (a 380bp band was only visible in the nested PCR). Sequencing results showed all three amplicons to be of the *Alphacoronavirus* genus.

Appendix A indicates that there were several amplicons created with various PCR assays (indicated in bold and by a *). The RNA extracts from several older samples such as UP75, UP160, UP161 and UP165 (extracted at the NICD with the QIAamp RNA mini kit (QIAGEN) in 2009) showed product amplification in a size range of 280-350 bp on an agarose electrophoresis gel. Preliminary sequence analysis with the BLAST function of

NCBI was performed for samples UP75, UP160 and UP165 which showed that the sequence, UP75, belonged to the *Betacoronavirus* genus and sequences from UP160 and UP165 belonged to the *Alphacoronavirus* genus. UP161 was of an insufficient quantity to sequence. Unfortunately no material of these samples is available for further analysis.

**Table 3.2: Bat-associated coronavirus RNA detected from bat populations in South Africa**

| Bat species analysed | Positive for CoV /total sampled | Sampling Location(s) | Phylogenetic Clustering (Genus level) |
|---|---|---|---|
| *Eptesicus* spp. (House bats) | 2 | | |
| *Eptesicus hottentotus* (Long-tailed house bat) | 0/2 | Taung, North West | - |
| *Epomophorus* spp. (Epauletted fruit bat) | 12 | | |
| • *Epomophorus wahlbergi* (Wahlberg's epauletted fruit bat) | 0/11 | Amanzimtoti and Durban.<br>Rocktail bay, St. Lucia.<br>Woodhurst, Chatsworth all in KwaZulu Natal. | - |
| • *Epomophorus gambianus* (Gambian epauletted fruit bat) | 0/1 | Pafuri. Kruger National Park, Limpopo. | - |
| *Glauconycteris* spp. (Butterfly bats) | 1 | | |
| • *Glauconycteris variegata* (Variegated butterfly bat) | 0/1 | Rocktail bay, St. Lucia, KZN. | - |
| *Hipposideros* spp. (Round-leaf bats) | 2 | | |
| • *Hipposideros caffer* | 0/2 | Pafuri. Kruger National Park, Limpopo. | - |
| ***Miniopterus* spp. (Long-fingered bat)** | 14 | | |
| • ***Miniopterus natalensis* (Natal long-fingered bat)** | **1/14** | **Irene Caves, Gauteng.**<br>Peppercorn cave in Modimole, Limpopo.<br>Venterskroon in Thabela thabeng, North West. | ***Alphacoronavirus*** |
| ***Molossinae* bats (Free tails)** | 15 | | |
| • *Mops condylurus* (Angolan free tail) | 0/2 | Palaborwa, Limpopo. | - |
| • ***Mops midas* (Midas Free-tailed bat)** | **1/2** | **Makhado, Limpopo.** | ***Alphacoronavirus*** |
| • *Chaerephon* spp. (Lesser mastiff bats) | 0/1 | Pafuri. Kruger National Park, Limpopo. | **-** |
| • *Chaerephon pumilus* | 0/3 | Rocktail bay, St. Lucia, KZN. | |
| • *Tadarida aegyptiaca* (Egyptian free-tailed bat) | 0/4 | Taung, North West. | - |
| • Molossid bat | 0/3 | Pafuri. Kruger National Park, Limpopo.<br>Kgaswane, North West. | - |
| ***Neuromicia* spp. (Serotine bats)** | 22 | | |
| • ***Neoromicia capensis* (Cape serotine)** | **1/10** | **Taung, North West**.<br>Pafuri. Kruger National Park, Limpopo.<br>Free Me rehabilitation centre, Gauteng. | ***Alphacoronavirus*** |

| | | | |
|---|---|---|---|
| • *Neuromicia nana* (Banana bat) | 0/7 | Pafuri. Kruger National Park, Limpopo. | - |
| • *Neuromicia helios* (Heller's pipistrelle) | 0/2 | Pafuri. Kruger National Park, Limpopo. | - |
| • *Neoromicia zuluensis* (Aloe serotine bat) | 0/1 | Pafuri. Kruger National Park, Limpopo. | - |
| • *Neoromicia spp.* | 0/2 | Hennopspruit, Gauteng | |
| *Nycticeinops* spp. (Twilight bat) | 7 | | |
| • *Nycticeinops schlieffenii* (Schlieffen's bat) | 0/7 | Pafuri. Kruger National Park, Limpopo. | - |
| *Nycteris* spp. (Slit-faced bats) | 2 | | |
| • *Nycteris thebaica* (Egyptian slit-Faced bat) | 0/2 | Rocktail bay, St. Lucia, KZN. | - |
| *Rhinolophus* spp. (Horsehoe bats) | 10 | | |
| • *Rhinolophus denti* (Dent's horseshoe bat) | 0/5 | Taung, North West. | - |
| • *Rhinolophus capensis* (Cape horseshoe bat) | 0/1 | Labuschagne farm, Louis Trichard, Limpopo. | - |
| • *Rhinolophus darlingi* damarensis (Darling's horseshoe bat) | 0/1 | Taung, North West. | - |
| • *Rhinolophus landeri* (Lander's horseshoe Bat) | 0/1 | Pafuri. Kruger National Park, Limpopo. | |
| • *Rhinolophus* spp. | 0/2 | Makhado, Limpopo. | - |
| *Rousettus* spp. (Dog-faced fruit bats) | 3 | | |
| • *Rousettus aegyptiacus* (Egyptian fruit bat) | 0/3 | Pafuri. Kruger National Park, Limpopo. | - |
| *Scotophilus* spp. (Yellow bats) | 19 | | |
| • *Scotophilus dinganii* (African yellow house bat) | 0/9 | Pafuri. Kruger National Park, Limpopo.<br>Kgaswane, North West. | - |
| • *Scotophilus leucogaster* (White-bellied yellow bat) | 0/2 | Pafuri. Kruger National Park, Limpopo. | - |
| • *Scotophilus viridis* (Greenish yellow bat) | 0/1 | Pafuri. Kruger National Park, Limpopo. | |
| • *Scotophilus* spp. | 0/7 | Pafuri. Kruger National Park, Limpopo.<br>Kgaswane, North West.<br>Rocktail bay, St. Lucia, KZN. | - |
| Insectivorous bat | 4 | | |
| • Insectivorous bat species | 0/4 | Taung and Kgaswane, North West.<br>Pafuri. Kruger National Park, Limpopo. | - |
| **Total genera analysed: 14** | | | |
| **Total coronavirus RNA detected in South Africa: 3/113 (2.66%) All alphacoronaviruses** | | | |

### 3.3.2 Rwanda

A total of n=88 samples from Ruhengeri, Rwanda were analysed. Several samples produced amplicons in an expected size range (between 260-440 bp) when analysed with agarose gel electrophoresis, with possible bat coronavirus RNA amplification (Appendix B). Table 3.3 shows the total analysed samples from Rwanda by their bat host species. Samples from 5 bat genera were analysed, with the detection of BtCoV RNA in 2 separate *Rhinolophus* bat specimens. Samples UP441 and UP445, both amplified with the PanBtCoV/9 primer protocol produced nested PCR amplicons of 350bp each. Sequencing results showed both amplicons to be of the *Betacoronavirus* genus.

In Appendix B it is shown that there were several amplicons created with the various PCR assays (indicated in bold and by an asterix [*]). Several of the samples produced bands that were faintly visible with initial agarose gel electrophoresis, and after PCR-clean up no amplicons could be recovered (UP409, UP419, UP478, UP487, UP488, UP500, UP530, UP583, UP585, UP593, UP595, UP597, UP626). Further analysis with different protocols yielded no amplicons. Thus, these samples could not be confirmed for the presence of bat coronavirus RNA.

| Table 3.3: Bat-associated coronavirus RNA detected from Ruhengeri caves in Rwanda | | | |
|---|---|---|---|
| **Bat species analyzed** | **Positive for CoV /total sampled** | **Ruhengeri Cave** | **Phylogenetic Clustering (Genus level)** |
| *Hipposideros* spp (Round-leaf bats) | **2** | | |
| • *Hipposideros* spp | 0/2 | **Cave 1** | - |
| *Otomops* spp (Mastiff bats) | **13** | | |
| • *Otomops* spp | 0/13 | **Cave 1** | |
| *Rousettus* spp. (Dog faced fruit bats) | **66** | | |
| • *Rousettus* spp. | 0/66 | **Cave 1** | - |
| ***Rhinolophus* spp. (Horsehoe bats)** | **6** | | |
| • ***Rhinolophus* spp.** | **2/6** | **Cave 2** | ***Betacoronavirus*** |
| *Epomophorus* spp. (Epauletted fruit bat) | **1** | | |
| • *Epomophorus* spp. | 0/1 | **Cave 1** | - |
| **Total genera analysed: 5** | | | |
| **Total coronavirus RNA detected in Rwanda: 2/88 (2.27%) All Betacoronaviruses** | | | |

### 3.3.3 Phylogenetic analysis

*Alphacoronavirus* and *Betacoronavirus* sequences detected in this study are indicated in Table 3.4 as well as the GenBank accession numbers received after submission to the National Center for Biotechnology Information (NCBI). The isolates shown in Table 3.4 were named by standard coronavirus convention designated by the ICTV.

**Table 3.4: Detected coronaviruses isolated from bats species- names and accession numbers**

| Isolate | Abbreviation | Genus | Accession Number |
|---|---|---|---|
| *Miniopterus*-Bat coronavirus/Irene/South Africa/2009 | Mi-BtCoV/Irene/SA/09 | AlphaCoV | JQ519817 |
| *Neoromicia*-Bat coronavirus/167/South Africa/2007 | Neo-BtCoV/167/SA/07 | AlphaCoV | JQ519818 |
| *Mops*-Bat coronavirus/1364/South Africa/2011 | Mo-BtCoV/1364/SA/11 | AlphaCoV | JQ519819 |
| *Rhinolophus*-Bat coronavirus/441/Rwanda/2008 | Rh-BtCoV/441/Rwanda/08 | BetaCoV | JQ649535 |
| *Rhinolophus*-Bat coronavirus/445/Rwanda/2008 | Rh-BtCoV/445/Rwanda/08 | BetaCoV | JQ649536 |

The detected BtCoV RNA sequences of approximately 350 base pairs (bp) were phylogenetically analysed with relevant BtCoV sequences as well as other known human and animal coronaviruses. All sequences were trimmed to be the same length, approximately 277 bp. Figure 3.2 shows the phylogenetic tree constructed of the *Alpha*- and *Betacoronavirus* genera with 277 base pair sequences of the RdRp gene (at position 15216 on the SARS-CoV CDC isolate 200301157 reference strain). Figure 3.3 shows the amino acid phylogenetic tree constructed of the same genera with 90 amino acid residues (275 nucleotide sequence) of the RdRp gene.

#### 3.3.3.1 South African bat coronaviruses

In Figure 3.2 and 3.3, it can be seen the detected BtCoV RNA sequences group in with existing BtCoV sequences. *Miniopterus*-BtCoV/Irene/SA/09 clusters together with several other AlphaCoV previously detected within the same host genus and shares 88.4%, 87.5%, 86.8%, 86.1%, and 77.4% nucleotide identity to Mi-BtCoVKY66 (Kenya), Mi-BtCoVKY65 (Kenya), BtCoVKY27 (Kenya), Mi-BtCoV1A (China) and Mi-BtCoVHKU8 (China), respectively (Figure 3.4). However, *Mi*-BtCoV/Irene/SA/09 shares 97.8% amino acid identity to all the compared African *Miniopterus* BtCoV (Mi-BtCoVKY66, Mi-BtCoVKY65, Mi-BtCoVKY27), and only 94.3% and 93.2% amino acid similarity to the Asian *Miniopterus* BtCoV (Mi-BtCoV1A and Mi-BtCoVHKU8) (Figure 3.5).

Figures 3.2 and 3.3 show that the South African BtCoV identified from *Mops midas* (*Mops*-BtCoV/1364/SA/11) is very closely related to *Chaerephon*-BtKY22 from Kenya and shares a 98.5% nucleotide and 100% amino acid identity (Figures 3.4 and 3.5).

The South African BtCoV identified from *Neoromicia capensis* (*Neo*-BtCoV167/SA/07) is most closely related to European alphacoronaviruses identified in the

*Nyctalus* genus from the Netherlands and Bulgaria (Figures 3.2 and 3.3). The alphacoronavirus from *Nyctalus noctula*, BtCoV/*N. noc*/NL-VM176/10, identified in the Netherlands shares 83.9% nucleotide and 93.2% amino acid identity to *Neo*-BtCoV167/SA/07. BtCoV/*N. lei*/BNM98-30/08 identified in *Nyctalus leisleri* from Bulgaria share 84.3% nucleotide and 93.2% amino acid identity to *Neo*-BtCoV167/SA/07 (Figures 3.4 and 3.5). The alphacoronavirus is also distantly related to the Human CoV NL63, sharing 70.7% nucleotide identity.

#### 3.3.3.2 Rwandan bat Coronaviruses

The Rwandan BtCoV identified from the *Rhinolophus* genus, cluster with the SARS-related BtCoV cluster in the *Betacoronavirus* clade (Figure 3.2 and 3.3). *Rh*-BtCoV/441/Rwanda/08 and *Rh*-BtCoV/445/Rwanda/08 share 100% nucleotide identity and 100% amino acid similarity (Figures 3.4 and 3.5). The closest phylogenetic relative available for comparison is the Kenyan BtCoV, *Rh*-BtCoVKY72 (unpublished), which shares 94.8% nucleotide identity and 100% amino acid similarity to the Rwandan *Rhinolophus* betacoronavirus. The Rwandan betacoronavirus also shares 85.3% nucleotide identity and 97.8% amino acid similarity to the Bulgarian *Rhinolophus* betacoronavirus *Rh*-BtCoV/BM48-31/BGR/08 (Figures 3.2 and 3.3). Comparing the Rwandan betacoronavirus sequences to the Asian *Rhinolophus* SARS-related BtCoV, SARSr-Rh-BtCoV/Rp3 and SARSr-Rh-BtCoV/Rm1, shows that they share 82.6% and 83.9% nucleic acid similarity and 87.8% and 98.9% amino acid similarity, respectively.

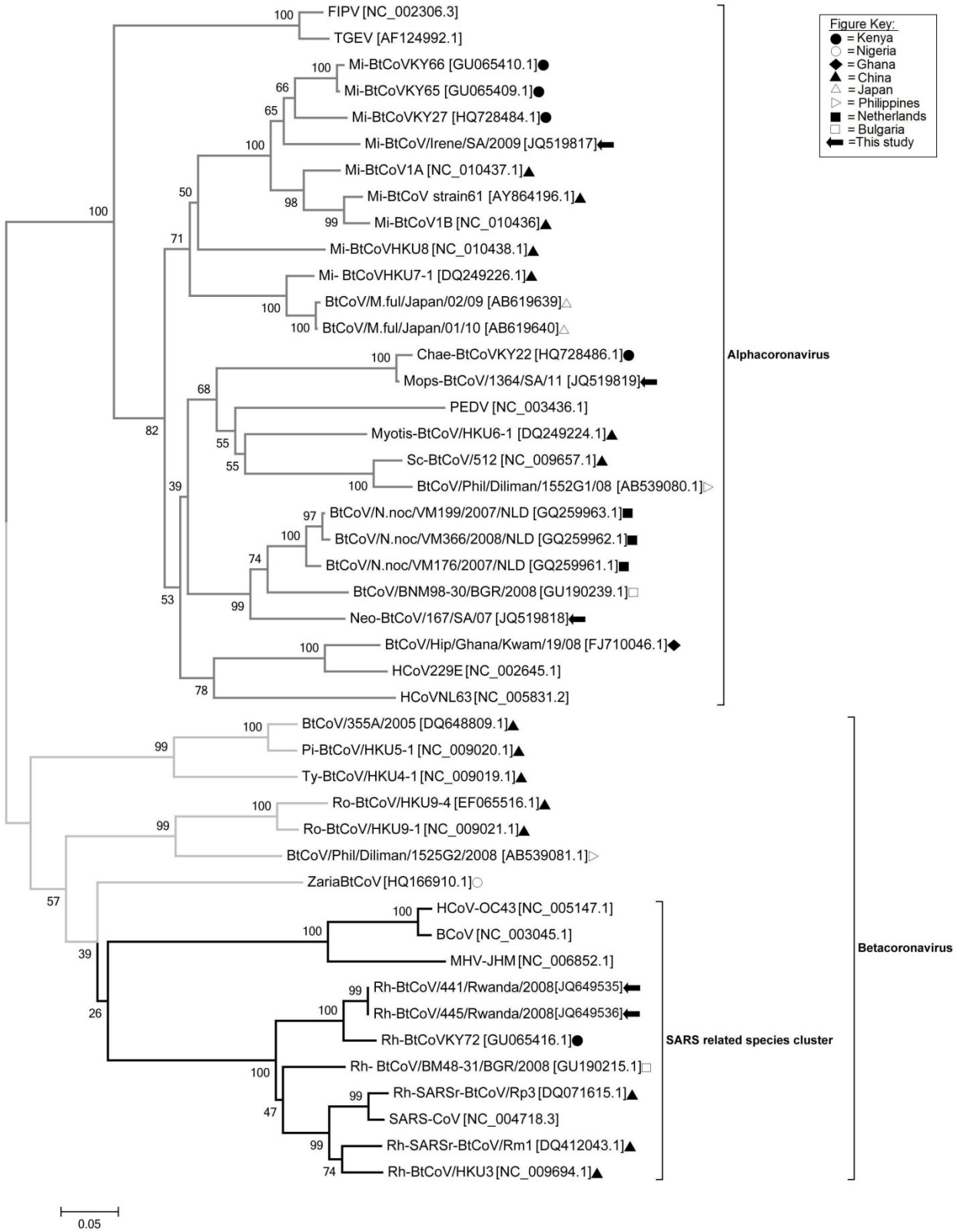


**Figure 3.2:** Phylogenetic analysis constructed in MEGA v5.05 using the neighbour-joining method with 45 sequences from the *Alpha-* and *Betacoronavirus* genera. The tree was constructed with a 277 base pair sequences of the 3' end of the conserved RNA dependent RNA polymerase gene using 1000 bootstrap repetitions. The symbols indicating the country of identification of relevant bat coronaviruses are shown in the phylogenetic tree next to the accession numbers and the symbol key is shown in the top right corner.

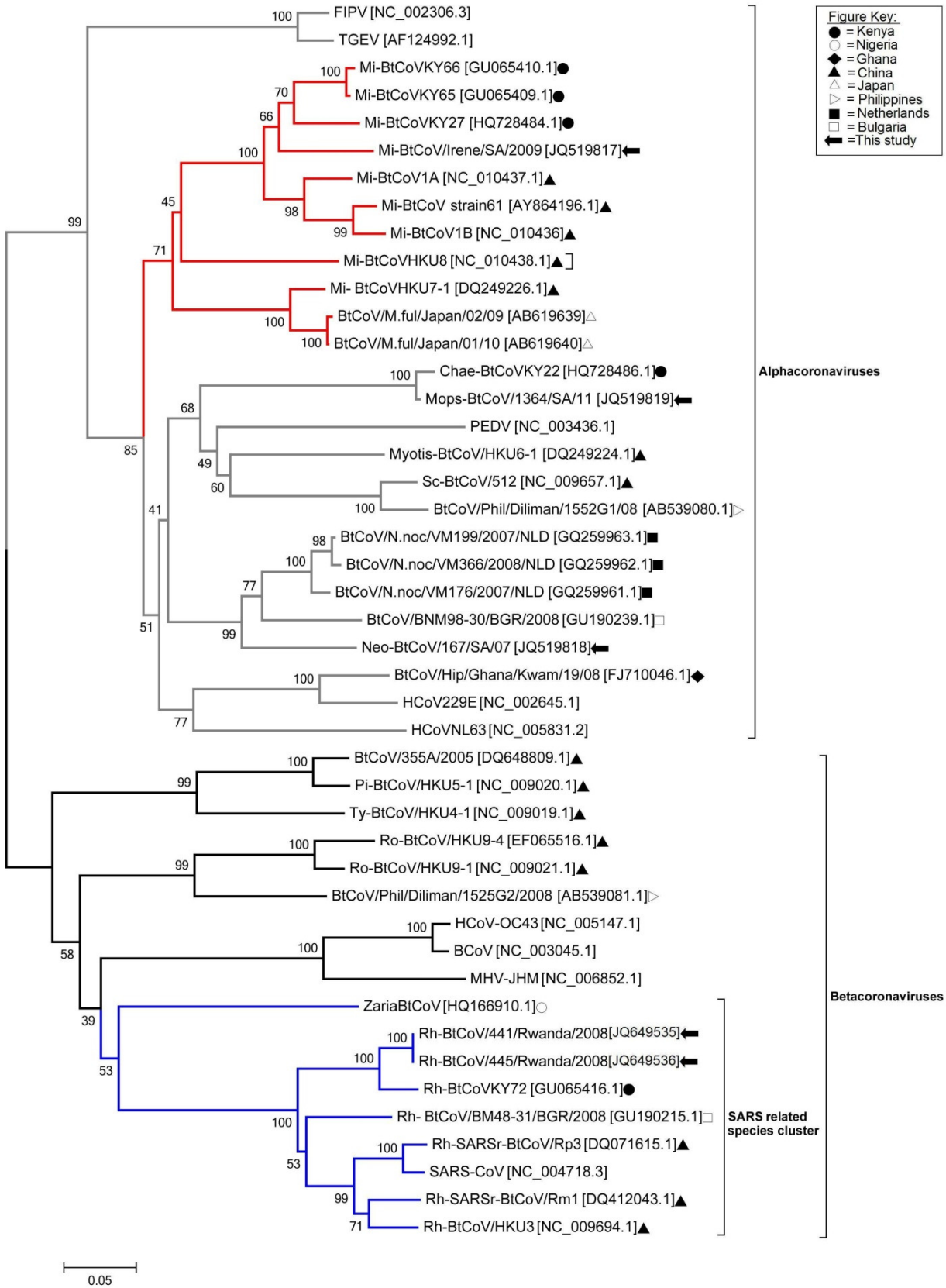


**Figure 3.3:** The amino acid phylogenetic tree was constructed with the neighbour-joining method from 90 amino acid residues of 45 sequences from both the *Alpha-* (Grey) and *Betacoronavirus* (Black) genera. The 90 amino acid residues correspond to a 275 nucleotide base pair region of the 3' end of the RNA dependent RNA polymerase gene. The symbols indicating the country of identification of relevant bat coronaviruses are shown in

the phylogenetic tree next to the accession numbers and the symbol key is shown in the top right corner. Red indicates the *Miniopterus* specific BtCoV clade, and blue indicates the SARS-related BtCoV species clade.

## Table 3.5: Pairwise distance matrix of relevant bat coronavirus nucleotide sequences

| | Bat Coronavirus Species | 1 | 2 | 3 | 4 | 5 | 6 | 7 | 8 | 9 | 10 | 11 | 12 | 13 | 14 | 15 | 16 | 17 | 18 | 19 | 20 | 21 | 22 | 23 |
|---|---|---|---|---|---|---|---|---|---|---|---|---|---|---|---|---|---|---|---|---|---|---|---|---|
| 1 | Mi-BtCoV1A | | 0.020 | 0.042 | 0.025 | 0.023 | 0.023 | 0.026 | 0.060 | 0.070 | 0.051 | 0.048 | 0.054 | 0.069 | 0.077 | 0.078 | 0.139 | 0.137 | 0.126 | 0.123 | 0.139 | 0.159 | 0.157 | 0.157 |
| 2 | Mi-BtCoV1B | 0.099 | | 0.048 | 0.026 | 0.025 | 0.027 | 0.031 | 0.068 | 0.070 | 0.063 | 0.053 | 0.057 | 0.075 | 0.076 | 0.077 | 0.139 | 0.140 | 0.135 | 0.133 | 0.142 | 0.164 | 0.162 | 0.162 |
| 3 | Mi-BtCoV/HKU8 | 0.256 | 0.297 | | 0.038 | 0.041 | 0.040 | 0.037 | 0.060 | 0.074 | 0.046 | 0.045 | 0.050 | 0.058 | 0.064 | 0.066 | 0.140 | 0.143 | 0.138 | 0.137 | 0.119 | 0.113 | 0.113 | 0.113 |
| 4 | Mi-BtCoV/BtKY27 | 0.138 | 0.149 | 0.221 | | 0.018 | 0.019 | 0.024 | 0.059 | 0.078 | 0.057 | 0.054 | 0.055 | 0.065 | 0.077 | 0.077 | 0.142 | 0.139 | 0.136 | 0.140 | 0.131 | 0.142 | 0.140 | 0.140 |
| 5 | Mi-BtCoV/BtKY65 | 0.116 | 0.137 | 0.242 | 0.087 | | 0.005 | 0.024 | 0.064 | 0.072 | 0.058 | 0.056 | 0.053 | 0.064 | 0.072 | 0.072 | 0.133 | 0.131 | 0.128 | 0.131 | 0.137 | 0.155 | 0.150 | 0.150 |
| 6 | Mi-BtCoV/BtKY66 | 0.117 | 0.146 | 0.232 | 0.087 | 0.007 | | 0.022 | 0.065 | 0.071 | 0.058 | 0.057 | 0.053 | 0.064 | 0.072 | 0.072 | 0.135 | 0.133 | 0.129 | 0.133 | 0.139 | 0.157 | 0.153 | 0.153 |
| 7 | Mi /Irene/SA/09 | 0.139 | 0.177 | 0.226 | 0.132 | 0.125 | 0.116 | | 0.060 | 0.076 | 0.057 | 0.059 | 0.058 | 0.068 | 0.079 | 0.079 | 0.137 | 0.139 | 0.134 | 0.127 | 0.134 | 0.137 | 0.135 | 0.135 |
| 8 | HCoVNL63 | 0.365 | 0.413 | 0.342 | 0.356 | 0.378 | 0.377 | 0.363 | | 0.077 | 0.049 | 0.049 | 0.059 | 0.060 | 0.073 | 0.075 | 0.158 | 0.163 | 0.164 | 0.168 | 0.156 | 0.162 | 0.152 | 0.152 |
| 9 | PEDV | 0.387 | 0.378 | 0.387 | 0.437 | 0.401 | 0.402 | 0.434 | 0.418 | | 0.076 | 0.072 | 0.077 | 0.048 | 0.058 | 0.060 | 0.118 | 0.122 | 0.118 | 0.118 | 0.109 | 0.122 | 0.119 | 0.119 |
| 10 | Neo-BtCoV/167 /07 | 0.297 | 0.375 | 0.284 | 0.361 | 0.348 | 0.349 | 0.347 | 0.293 | 0.382 | | 0.029 | 0.029 | 0.054 | 0.063 | 0.064 | 0.149 | 0.149 | 0.145 | 0.151 | 0.133 | 0.122 | 0.118 | 0.118 |
| 11 | Nyctalus-VM176 | 0.273 | 0.315 | 0.270 | 0.326 | 0.331 | 0.343 | 0.347 | 0.279 | 0.364 | 0.157 | | 0.024 | 0.058 | 0.050 | 0.052 | 0.146 | 0.147 | 0.145 | 0.146 | 0.139 | 0.141 | 0.134 | 0.134 |
| 12 | BNM98-30/BGR/08 | 0.316 | 0.348 | 0.320 | 0.347 | 0.322 | 0.323 | 0.357 | 0.353 | 0.392 | 0.161 | 0.120 | | 0.055 | 0.058 | 0.059 | 0.158 | 0.163 | 0.160 | 0.164 | 0.157 | 0.147 | 0.143 | 0.143 |
| 13 | Myotis-HKU6-1 | 0.371 | 0.406 | 0.310 | 0.360 | 0.354 | 0.355 | 0.379 | 0.321 | 0.298 | 0.294 | 0.306 | 0.305 | | 0.054 | 0.055 | 0.126 | 0.126 | 0.130 | 0.131 | 0.126 | 0.124 | 0.120 | 0.120 |
| 14 | Mops/1364/ SA /11 | 0.389 | 0.393 | 0.348 | 0.409 | 0.370 | 0.382 | 0.391 | 0.399 | 0.341 | 0.348 | 0.267 | 0.314 | 0.334 | | 0.007 | 0.122 | 0.120 | 0.126 | 0.123 | 0.125 | 0.142 | 0.134 | 0.134 |
| 15 | Chae-KY22/Kenya | 0.399 | 0.403 | 0.364 | 0.414 | 0.374 | 0.386 | 0.395 | 0.422 | 0.363 | 0.360 | 0.287 | 0.325 | 0.345 | 0.015 | | 0.122 | 0.119 | 0.126 | 0.123 | 0.123 | 0.142 | 0.133 | 0.133 |
| 16 | HSARS-CoV | 0.631 | 0.629 | 0.632 | 0.643 | 0.621 | 0.619 | 0.588 | 0.696 | 0.634 | 0.691 | 0.672 | 0.720 | 0.655 | 0.646 | 0.641 | | 0.010 | 0.020 | 0.021 | 0.025 | 0.031 | 0.031 | 0.031 |
| 17 | Rh-SARSr/Rp3 | 0.637 | 0.636 | 0.658 | 0.627 | 0.619 | 0.617 | 0.594 | 0.717 | 0.660 | 0.686 | 0.676 | 0.740 | 0.644 | 0.640 | 0.623 | 0.029 | | 0.020 | 0.021 | 0.024 | 0.031 | 0.029 | 0.029 |
| 18 | Rh-SARSr/Rm1 | 0.580 | 0.642 | 0.665 | 0.632 | 0.601 | 0.607 | 0.614 | 0.727 | 0.646 | 0.648 | 0.664 | 0.703 | 0.651 | 0.672 | 0.674 | 0.092 | 0.088 | | 0.017 | 0.028 | 0.029 | 0.030 | 0.030 |
| 19 | Rh-BtCoVHKU3 | 0.566 | 0.627 | 0.618 | 0.628 | 0.608 | 0.606 | 0.558 | 0.709 | 0.639 | 0.676 | 0.654 | 0.725 | 0.659 | 0.637 | 0.632 | 0.104 | 0.104 | 0.075 | | 0.026 | 0.031 | 0.031 | 0.031 |
| 20 | BM48-31/BGR/08 | 0.616 | 0.628 | 0.546 | 0.590 | 0.623 | 0.621 | 0.601 | 0.694 | 0.616 | 0.636 | 0.632 | 0.710 | 0.664 | 0.683 | 0.658 | 0.134 | 0.130 | 0.164 | 0.143 | | 0.029 | 0.027 | 0.027 |
| 21 | Rh-BtCoVKY72 | 0.641 | 0.696 | 0.564 | 0.633 | 0.689 | 0.687 | 0.601 | 0.680 | 0.668 | 0.585 | 0.628 | 0.662 | 0.658 | 0.757 | 0.752 | 0.170 | 0.171 | 0.153 | 0.175 | 0.161 | | 0.014 | 0.014 |
| 22 | Rh-441/Rwanda/08 | 0.636 | 0.682 | 0.559 | 0.633 | 0.667 | 0.664 | 0.595 | 0.649 | 0.657 | 0.603 | 0.621 | 0.677 | 0.635 | 0.733 | 0.728 | 0.169 | 0.161 | 0.174 | 0.179 | 0.147 | 0.052 | | 0.000 |
| 23 | Rh-445/Rwanda/08 | 0.636 | 0.682 | 0.559 | 0.633 | 0.667 | 0.664 | 0.595 | 0.649 | 0.657 | 0.603 | 0.621 | 0.677 | 0.635 | 0.733 | 0.728 | 0.169 | 0.161 | 0.174 | 0.179 | 0.147 | 0.052 | 0.000 | |

Table legend: Pairwise distance matrix of relevant bat coronavirus nucleotide sequences (277bp) showing the estimated evolutionary divergence between the sequences, using Maximum Composite Likelihood method with 1000 bootstrap repetitions. The number of base substitutions per site from between sequences is shown. **Standard error estimate(s) are shown above the diagonal.** Codon positions included were 1st+2nd+3rd+Noncoding. All positions containing gaps and missing data were eliminated. The p-distance matrix was constructed in MEGA v5.05 (Tamura *et al*., 2011). The grey shading highlights the samples from this study. The following sequences were included in the analysis: *Miniopterus*-BtCoV1A (NC_010437.1), *Miniopterus*-BtCoV 1B(NC_010436.1), *Miniopterus*-BtCoV/HKU8 (NC_010438.1), *Miniopterus*-BtCoV /BtKY27/Kenya (HQ728484.1), *Miniopterus*-BtCoV/BtKY65/Kenya (GU065409.1), *Miniopterus*-BtCoV/BtKY66/Kenya (GU065410.1), *Miniopterus*-BtCoV/Irene/SA/09 (JQ519817), HCoVNL63 (NC_005831.2), PEDV (NC_003436.1), Neo-BtCoV/167/SA/07 (JQ519818), BtCoV/N.noc/VM176/07/NLD (GQ259961.1), BtCoV/BNM98-30/BGR/08 (GU190239.1), Myotis-BtCoVHKU6-1 (DQ249224.1), Mops-BtCoV/1364/ SA /11 (JQ519819), Chae-BtCoV/BtKY22/Kenya (HQ728486.1), HSARS-CoV (NC_004718.3), Rh-SARSr-CoV/Rp3 (DQ071615.1), Rh-SARSr-CoV/Rm1 (DQ412043.1), Rh-BtCoV/HKU3 (NC_009694.1), BM48-31/BGR/08(GU190215.1), Rh-BtCoV/BtKY72/Kenya (GU065416.1), Rh-BtCoV/441/Rwanda/2008 (JQ649535),and Rh-BtCoV/445/Rwanda/2008 (JQ649536).

**Table 3.6: Pairwise distance matrix of relevant bat coronavirus amino acid sequences**

| | Bat coronavirus species | 1 | 2 | 3 | 4 | 5 | 6 | 7 | 8 | 9 | 10 | 11 | 12 | 13 | 14 | 15 | 16 | 17 | 18 | 19 | 20 | 21 | 22 | 23 |
|---|---|---|---|---|---|---|---|---|---|---|---|---|---|---|---|---|---|---|---|---|---|---|---|---|
| 1 | Mi-BtCoV1A | | | | | | | | | | | | | | | | | | | | | | | |
| 2 | Mi-BtCoV1B | 0.011 | | | | | | | | | | | | | | | | | | | | | | |
| 3 | Mi-BtCoV/HKU8 | 0.068 | 0.057 | | | | | | | | | | | | | | | | | | | | | |
| 4 | Mi-BtCoV/BtKY27 | 0.034 | 0.022 | 0.057 | | | | | | | | | | | | | | | | | | | | |
| 5 | Mi-BtCoV/BtKY65 | 0.034 | 0.022 | 0.057 | 0.000 | | | | | | | | | | | | | | | | | | | |
| 6 | Mi-BtCoV/BtKY66 | 0.034 | 0.022 | 0.057 | 0.000 | 0.000 | | | | | | | | | | | | | | | | | | |
| 7 | Mi /Irene/SA/09 | 0.057 | 0.045 | 0.068 | 0.022 | 0.022 | 0.022 | | | | | | | | | | | | | | | | | |
| 8 | HCoVNL63 | 0.248 | 0.248 | 0.262 | 0.248 | 0.248 | 0.248 | 0.248 | | | | | | | | | | | | | | | | |
| 9 | PEDV | 0.234 | 0.234 | 0.248 | 0.234 | 0.234 | 0.234 | 0.220 | 0.277 | | | | | | | | | | | | | | | |
| 10 | Neo-BtCoV/167 /07 | 0.141 | 0.141 | 0.129 | 0.167 | 0.167 | 0.167 | 0.167 | 0.220 | 0.220 | | | | | | | | | | | | | | |
| 11 | Nyctalus-VM176 | 0.116 | 0.116 | 0.104 | 0.129 | 0.129 | 0.129 | 0.116 | 0.193 | 0.220 | 0.068 | | | | | | | | | | | | | |
| 12 | BNM98-30/BGR/08 | 0.129 | 0.129 | 0.104 | 0.129 | 0.129 | 0.129 | 0.129 | 0.180 | 0.248 | 0.068 | 0.034 | | | | | | | | | | | | |
| 13 | Myotis-HKU6-1 | 0.129 | 0.129 | 0.141 | 0.141 | 0.141 | 0.141 | 0.141 | 0.248 | 0.129 | 0.141 | 0.129 | 0.129 | | | | | | | | | | | |
| 14 | Mops/1364/ SA /11 | 0.167 | 0.154 | 0.141 | 0.167 | 0.167 | 0.167 | 0.154 | 0.277 | 0.180 | 0.154 | 0.129 | 0.154 | 0.154 | | | | | | | | | | |
| 15 | Chae-KY22/Kenya | 0.167 | 0.154 | 0.141 | 0.167 | 0.167 | 0.167 | 0.154 | 0.277 | 0.180 | 0.154 | 0.129 | 0.154 | 0.154 | 0.000 | | | | | | | | | |
| 16 | HSARS-CoV | 0.560 | 0.560 | 0.560 | 0.560 | 0.560 | 0.560 | 0.560 | 0.560 | 0.468 | 0.522 | 0.504 | 0.522 | 0.486 | 0.504 | 0.504 | | | | | | | | |
| 17 | Rh-SARSr/Rp3 | 0.560 | 0.560 | 0.560 | 0.560 | 0.560 | 0.560 | 0.560 | 0.560 | 0.468 | 0.522 | 0.504 | 0.522 | 0.486 | 0.504 | 0.504 | 0.000 | | | | | | | |
| 18 | Rh-SARSr/Rm1 | 0.560 | 0.560 | 0.560 | 0.560 | 0.560 | 0.560 | 0.560 | 0.560 | 0.486 | 0.522 | 0.504 | 0.522 | 0.504 | 0.522 | 0.522 | 0.011 | 0.011 | | | | | | |
| 19 | Rh-BtCoVHKU3 | 0.560 | 0.560 | 0.560 | 0.560 | 0.560 | 0.560 | 0.560 | 0.560 | 0.468 | 0.522 | 0.504 | 0.522 | 0.486 | 0.504 | 0.504 | 0.000 | 0.000 | 0.011 | | | | | |
| 20 | BM48-31/BGR/08 | 0.579 | 0.579 | 0.579 | 0.579 | 0.579 | 0.579 | 0.579 | 0.579 | 0.486 | 0.541 | 0.522 | 0.541 | 0.504 | 0.522 | 0.522 | 0.011 | 0.011 | 0.022 | 0.011 | | | | |
| 21 | Rh-BtCoVKY72 | 0.541 | 0.541 | 0.541 | 0.541 | 0.541 | 0.541 | 0.541 | 0.541 | 0.468 | 0.504 | 0.486 | 0.504 | 0.468 | 0.504 | 0.504 | 0.011 | 0.011 | 0.022 | 0.011 | 0.022 | | | |
| 22 | Rh-441/Rwanda/08 | 0.541 | 0.541 | 0.541 | 0.541 | 0.541 | 0.541 | 0.541 | 0.541 | 0.468 | 0.504 | 0.486 | 0.504 | 0.468 | 0.504 | 0.504 | 0.011 | 0.011 | 0.022 | 0.011 | 0.022 | 0.000 | | |
| 23 | Rh-445/Rwanda/08 | 0.541 | 0.541 | 0.541 | 0.541 | 0.541 | 0.541 | 0.541 | 0.541 | 0.468 | 0.504 | 0.486 | 0.504 | 0.468 | 0.504 | 0.504 | 0.011 | 0.011 | 0.022 | 0.011 | 0.022 | 0.000 | 0.000 | |

**Table Legend:** Pairwise distance matrix of relevant bat coronavirus amino acid sequences (91 amino acids) showing the estimated evolutionary divergence between the sequences using the Poisson correction model. The number of amino acid substitutions per site from between sequences is shown above. All positions containing gaps and

missing data were eliminated. The p-distance matrix was constructed in MEGA v5.05 (Tamura *et al.*, 2011). The grey shading highlights the samples from this study. The following sequences were included in the analysis: *Miniopterus*-BtCoV1A (NC_010437.1), *Miniopterus*-BtCoV 1B(NC_010436.1), *Miniopterus*-BtCoV/HKU8 (NC_010438.1), *Miniopterus*-BtCoV /BtKY27/Kenya (HQ728484.1), *Miniopterus*-BtCoV/BtKY65/Kenya (GU065409.1), *Miniopterus*-BtCoV/BtKY66/Kenya (GU065410.1), *Miniopterus*-BtCoV/Irene/SA/09 (JQ519817), HCoVNL63 (NC_005831.2), PEDV (NC_003436.1), Neo-BtCoV/167/SA/07 (JQ519818), BtCoV/N.noc/VM176/07/NLD (GQ259961.1), BtCoV/BNM98-30/BGR/08 (GU190239.1), Myotis-BtCoVHKU6-1 (DQ249224.1), Mops-BtCoV/1364/ SA /11 (JQ519819), Chae-BtCoV/BtKY22/Kenya (HQ728486.1), HSARS-CoV (NC_004718.3), Rh-SARSr-CoV/Rp3 (DQ071615.1), Rh-SARSr-CoV/Rm1 (DQ412043.1), Rh-BtCoV/HKU3 (NC_009694.1), BM48-31/BGR/08(GU190215.1), Rh-BtCoV/BtKY72/Kenya (GU065416.1), Rh-BtCoV/441/Rwanda/2008 (JQ649535), and Rh-BtCoV/445/Rwanda/2008 (JQ649536).

### 3.3.4 Amplification of additional regions of the RdRp gene

#### 3.3.4.1 Primer design

Longer amplicon length amplification for the detected bat coronaviruses were attempted from available RNA. Using the preliminary phylogenetic analysis of the detected alphacoronaviruses from South Africa, only closely related BtCoV were selected as reference sequences for primer design (Table 3.1). Primer pairs (Table 3.5) were selected which were capable of producing amplicons between 700 to 1000 bp. BtFor22Pos**30** and Bt5-3Rev20Pos**750** produce an amplicon of +/-720 bp, and pair BtFor24Pos**710** and Bt5-3Rev20Pos**1470** produces an amplicon of +/-760 bp. Forward Primer, Bt**For**23Pos**1220,** amplifies approximately 1,140 bp amplicon in a pair with the PanBat/AB/6 primer protocol AlphaCoV reverse primer, P1AlphaRev23bp. Likewise, the PanBat/AB/6 primer protocol AlphaCoV forward primer, P1AlphaWfor, amplifies a 760 bp amplicon with Bt5-3**Rev**20Pos**2650.** The amplification strategy covers overlapping sections of the polymerase gene (Figure 3.6). Unfortunately, no full length reference sequences were available for comparison to *Neo*-BtCoV167/SA/07. However, since the RdRp gene of coronaviruses is one of the most conserved genes of the genome it is likely that the designed primers may also amplify the *Neoromicia* BtCoV.

**Table 3.7: Primers designed for the amplification and sequencing of the coronavirus RNA dependent RNA polymerase gene.**

| Primer Name | Sequence (5'-3') | Length (bp) | Genome Sense | Tm ºC | Binding Position* |
|---|---|---|---|---|---|
| BtFor22Pos**30** | GGCTCTAGTGCAGCTCGACTAG | 22 | + | 58.9 | 13058 |
| BtRev20Pos**750** | ATRTCACTYTTRATAAARCA | 20 | - | 44.3 | 13769 |
| BtFor24Pos**710** | TAYATGATGCCWGYYATGGGTATG | 24 | + | 55.5 | 13724 |
| BtRev20Pos**1470** | TTATTAAGGTTKGTAACAAC | 20 | - | 44.2 | 14489 |
| Bt**For**23Pos**1220** | AAGCCAGGYCAYTTTAATAARGA | 23 | + | 53.4 | 14240 |
| Bt**Rev**20Pos**2650** | TTDARGTGTTTWACCCAMTC | 20 | - | 48.6 | 15665 |

* indicates the primer binding positions on reference strain Miniopterus BtCoV 1A (NC_010437.1).

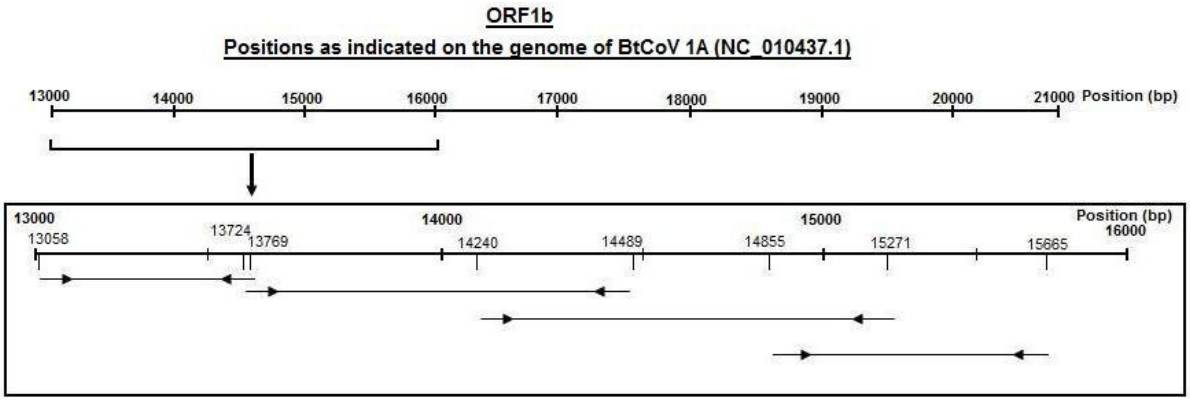


**Figure 3.6:** Genome map of *Miniopterus* bat coronavirus 1A (NC_010437.1) as a reference sequence indicating the RNA dependent RNA polymerase gene amplification strategy, with the amplification of 4 amplicons varying between 700-1000 base pairs. Primer pair binding sites are situated at positions 13058 (forward primer BtFor22Pos30) and 13769 (reverse primer BtRev20Pos750), 13724 (forward primer BtFor24Pos710) and 14489 (reverse primer BtRev20Pos1470), 14240 (forward primer BtFor23Pos1220) and 15271 (reverse primer P1AlphaRev23bp) and 14855 (forward primer P1AlphaWfor) and 15665 (reverse primer BtRev20Pos2650).

#### 3.3.4.2 cDNA synthesis and RT-PCR

The first two primer sets (P1AlphaWfor and BtRev20Pos2650, and BtFor23Pos1220 and P1AlphaRev23bp) were used in an attempt to amplify the RdRp gene. No amplicons were visible with 1% agarose electrophoresis. Due to the non-amplification, further attempts to amplify larger segments of the genomes were discontinued due to the limited quantities of RNA remaining.

### 3.3.5 Amplification of nucleoprotein gene

#### 3.3.5.1 Primer design

Positions 26900 and 27722, on the reference strain *Mi*-BtCoV 1A were selected for the production of an amplicon +/-1000 bp (Figure 3.7 and 3.8). Species specific alphacoronavirus primers were designed for the nucleoprotein (Table 3.6). The only available comparative sequence for the Mops BtCoV is *Chaerophon*-BtCoVKY22 and due to the high similarity in the previously amplified segment of the RdRp primers were designed specific to the reference sequence. The South African *Miniopterus* BtCoV nucleoprotein primers were designed based on similarities between *Mi*-BtCoV 1A and *Mi*-BtCoVKY27/06. Again, no comparative sequences are available for the *Neoromicia* BtCoV, and as such a cocktail of the *Mops* and *Miniopterus* BtCoV nucleoprotein primers were used in an attempt to amplify the *Neoromicia* nucleoprotein gene.

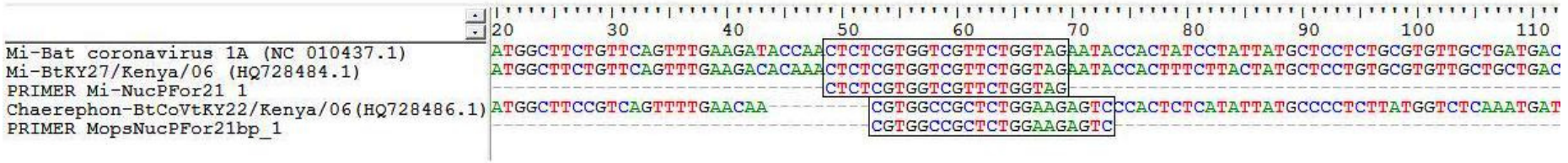


**Figure 3.7:** Alignment of the coronavirus nucleoprotein forward primers designed using alignments of bat coronavirus reference sequences that are closely related to the alphacoronaviruses detected from South Africa. Based on differences between the alphacoronavirus species, separate forward primers were designed for each of the *Mops* spp. and *Miniopterus* spp. bat coronaviruses. No nucleoprotein gene sequences were available of bat coronaviruses closely related to the South African *Neoromicia* spp. alphacoronavirus.

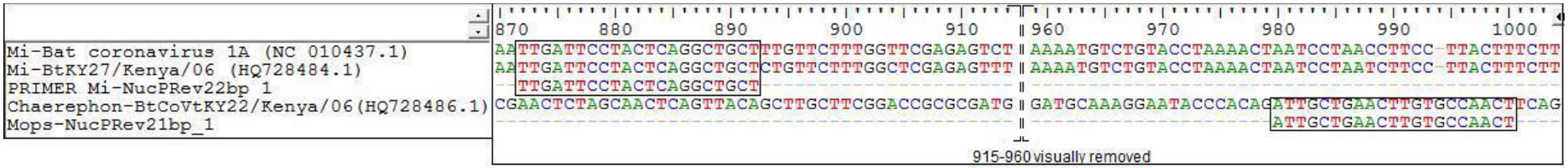


**Figure 3.8**: Alignment of bat coronavirus reference sequences which were closely related to the alphacoronaviruses detected from South Africa, from which nucleoprotein reverse primers were designed. Based on differences between the alphacoronavirus species, separate reverse primers were designed for each of the Mops spp. and Miniopterus spp. bat coronaviruses. The alignment was trimmed between 915 to 960 base pairs to fit the alignment to viewable size. No nucleoprotein gene sequences were available of bat coronaviruses closely related to the South African Neoromicia spp. alphacoronavirus.

**Table 3.8: Primers designed for the amplification and sequencing of the coronavirus Nucleoprotein gene.**

| Primer Name | Sequence (5'-3') | Length (bp) | Genome Sense | Tm ºC | Binding Position* |
|---|---|---|---|---|---|
| | ***Miniopterus* bat coronavirus specific** | | | | |
| Mi-NucPFor21 | CTCTCGTGGTCGTTCTGGTAG | 21 | + | 56.8 | +/-26900 |
| Mi-NucPRev21 | AGCAGCCTGAGTAGGAATCAA | 21 | - | 55.8 | +/-27722 |
| | ***Mops* bat coronavirus specific** | | | | |
| Mops-NucPFor21 | CGTGGCCGCTCTGGAAGAGTC | 21 | + | 62.5 | +/-26900 |
| Mops-NucPRev21bp | AGTTGGCACAAGTTCAGCAAT | 21 | - | 55.5 | +/-27722 |

* indicates the primer binding positions on reference strain Miniopterus BtCoV 1A (NC_010437.1).

#### 3.3.5.2 cDNA synthesis and RT-PCR

The nucleoprotein primers designed for the specific species of alphacoronaviruses were used in cDNA synthesis and RT-PCR assay. No amplicons was visible with 1% agarose electrophoresis and further attempts to amplify larger segments of the genomes were discontinued.

## 3.4 Discussion

The first aim of the study was accomplished in Chapter 2 with the development of a sensitive nested RT-PCR assay for the detection of bat coronavirus (BtCoV) RNA. This tool was used to accomplish the second aim of the study, which was the analysis of a cohort of collected bat samples, kept in the specimen bank of our laboratory at the University of Pretoria for the presence of BtCoV RNA. The RNA of 201 samples from our specimen bank (113 samples from South Africa and 88 from Rwanda) was analysed. Samples from 15 bat genera were included, 14 genera from South Africa and 5 from Rwanda (Tables 3.2 and 3.3). Three positive samples were detected from the 113 South African samples and two positive samples were detected from the 88 Rwandan samples. The sequences from South Africa were from 3 separate alphacoronaviruses identified in 3 different bat species from the *Miniopterus, Neoromicia* and *Mops* genera. The 2 positives detected from Rwanda were both from the *Rhinolophus* genus and nucleotide similarity between the two betacoronaviruses indicated that they were of the same virus.

The phylogenetic tree shown in Figure 3.2 was constructed with a 277 amplicon of the RdRp gene and the phylogenetic tree shown in Figure 3.3 was constructed with the corresponding 90 amino acid sequence. Comparison of the trees indicated that there were no significant differences between the phylogenetic conclusions the two trees. Due to the higher conservation of amino acid sequence residues in comparison to nucleotide base pairs, the bootstrap support of the internal nodes in the amino acid tree are slightly better

resolved than those in the phylogenetic tree constructed with the nucleotide sequence. Several of the internal nodes in Figure 3.2 are supported with low bootstrap values, particularly the nodes branching off into the different *Betacoronavirus* clades. The low bootstrap resolution may be attributed to the limited amplicon length used in the phylogenetic tree construction and may be improved by increasing the length of the compared amplicons. However, due to the large diversity between coronaviruses, the highly conserved sequences necessary for efficient amplification are somewhat limited in length, allowing only short amplicons to be initially amplified.

Unfortunately, no amplicons could be generated in the second set of RT-PCRs aimed at amplifying 700-1000bp of the RdRp gene. The primers used for the creation of longer amplicon sequences were designed by using closely related BtCoV genomes. It is possible that RNA degradation prevented successful amplification of further polymerase sequence.

***Miniopterus* Bat Coronavirus**

Of the total 9 *Miniopterus* species that have thus far been analysed globally for the presence of BtCoV (in Australia, Kenya, DRC, Iberian Peninsula, Bulgaria, Japan, China, and Thailand), all have been found to harbour alphacoronaviruses (Table 1.9). *Miniopterus* alphacoronaviruses have been identified in each study which has included samples taken from *Miniopterus* colonies, with the exception of only a few studies with low sampling numbers.

In this study, 14 samples, either fecal pools taken from the cave floor or fecal swabs taken from individual bats, were collected from the *Miniopterus* colony at the ARC Irene caves in Gauteng. Only one of the fecal pools (UP1410) was positive for alphacoronavirus nucleic acid with the PanBtCoV/9 primer nested RT-PCR assay (Appendix A). Phylogenetic analysis of the sequenced alphacoronavirus nucleic acid clusters *Miniopterus*-BtCoV/Irene/SA/09 most closely with the *Miniopterus* BtCoV identified in Kenya in 2009 (Tong *et al.*, 2009) (Figure 3.2). As discussed in Section 1.5.7, the *Miniopterus* alphacoronaviruses identified globally cluster together, irrespective of country of origin. Likewise, *Miniopterus*-BtCoV/Irene/SA/09 identified in this study also clusters with the existing *Miniopterus* BtCoV, being most closely related to previously identified *Miniopterus* BtCoV from Kenya (BtCoV27, BtCoVKY65, BtCoVKY66) and Asia (BtCoV 1A & BtCoVHKU8).

*Miniopterus*-BtCoV/Irene/SA/09 shares the greatest nucleotide identity with the 3 *Miniopterus* BtCoV from Kenya (88.4% with *Mi*-BtCoVKY66, 87.5% with *Mi*-BtCoVKY65, and 86.8% with *Mi*-BtCoVKY27) and 97.8% amino acid identity to all 3 BtCoV. Interestingly, *Mi*-BtCoV/Irene/SA/09 shares 86.1% and 77.4% nucleotide identity to the Asian *Miniopterus* BtCoV, *Mi*-BtCoV1A and *Mi*-BtCoVHKU8, respectively. However, while *Mi*-

BtCoV/Irene/SA/09 shares only 93.2-94.3% amino acid identity to the 2 Asian *Miniopterus* BtCoV (*Mi*-BtCoV1A and *Mi*-BtCoVHKU8) it possesses 97.8% amino acid identity to all 3 Kenyan *Miniopterus* BtCoV (*Mi*-BtCoVKY66, *Mi*-BtCoVKY65 and *Mi*-BtCoVKY27). The amino acid identities appear to be more conserved within the African *Miniopterus* BtCoV than to the Asian *Miniopterus* BtCoV.

The global phylogenetic clustering of the *Miniopterus* BtCoV may indicate the existence of an original *Miniopterus* BtCoV ancestor present in ancient *Miniopterus* spp. before that species migrated to other continents from where the BtCoV began to slowly diverge into separate species. Thus the phylogenetic relationships of the *Miniopterus* BtCoV clade may have been driven by host phylogeny rather than geographical isolation (Gouilh *et al.*, 2011).

***Mops* bat coronavirus**

The bat genus, *Mops* spp. belongs to the *Molossidae* bat family along with the *Chaerophon* genus (Table 1.9). Several different lineages of BtCoV have previously been identified within the *Chaerophon* genus in Kenya such as the BtHKU7-like, BtCoVKY18-like and SARS-related BtCoV (Table 1.8). In 2007, Muller *et al.,* screened several South African bat species for the presence of antibodies against the SARS-CoV including *Mops midas* (n=15) and *Mops condylurus* (n=115). The antibodies were detected in two bats, one being *Mops condylurus* (n=14/115). Prior to this study, the presence of CoV RNA in the *Mops* genus has not been demonstrated.

In the present study, we have detected alphacoronavirus RNA, *Mops*-BtCoV1364/SA/11, in the fecal swab collected from *Mops midas* in Limpopo Province. Samples were collected from 2 *Mops midas* bats inhabiting an urban colony in Makhado, Limpopo, one of which was found dead on the ground. A fecal swab was collected from both the dead and live bats, however the alphacoronavirus, *Mops*-BtCoV1364/SA/11, was detected in only the dead bat.

Phylogenetic analysis of *Mops*-BtCoV1364/SA/11 shows that it is closely related to *Chaerephon*-BtKY22 from Kenya and they share a 98.5% nucleotide and 100% amino acid identity. Due to the high bootstrap support seen in Figures 3.2 and 3.3 as well as the high nucleotide and amino acid identity values, it may be possible that these two alphacoronaviruses are different isolates of the same virus species that was first identified in another bat genus of the same family, viz. the *Chaerephon spp.* in Kenya (Tong *et al.*, 2009). Like other bat coronaviruses that do not display the strict species specificity typically seen with the *Miniopterus* BtCoVs, it may be that this alphacoronavirus may have spilled over into the *Mops* genus from the *Chaerephon* genus or another member of the *Molossidae* bat family, or vice versa.

### *Neoromicia* Bat Coronavirus

The only documented study to have analysed the *Neoromicia* genus for the presence of BtCoV was in Kenya (2009) which found 4 *Neoromicia tenuipinnis* fecal samples to be negative for BtCoV (Tong *et al.*, 2009). As such, the closest phylogenetic relatives of the alphacoronavirus *Neo*-BtCoV167/SA/07, based on the available RdRp sequences on GenBank (NCBI), are the alphacoronaviruses identified in the *Nyctalus* genus from the Netherlands and Bulgaria, another member of the *Vespertilioninae* subfamily in the *Vespertilionidae* bat family.

The alphacoronavirus from *Nyctalus noctula,* BtCoV/*N. noc*/NL-VM176/10, identified in the Netherlands (Reusken *et al.*, 2010) shares 83.9% nucleotide and 93.2% amino acid identity to *Neo*-BtCoV167/SA/07. The *Nyctalus leisleri* BtCoV/*N. lei*/BNM98-30/08 identified in Bulgaria share 84.3% nucleotide and 93.2% amino acid identity to *Neo*-BtCoV167/SA/07. The two alphacoronaviruses from the *Nyctalus* genus share 88% nucleotide and 96.6% amino acid identity thus based on only limited sequence data available for these alphacoronaviruses and due to the high amino acid identity value, it could be speculated that these two European alphacoronaviruses are different strains of the same *Nyctalus* BtCoV. More viruses belonging to this lineage will be required to determine the phylogenetic history of the *Neoromicia* alphacoronaviruses.

*Neo*-BtCoV167/SA/07 and the European *Nyctalus* alphacoronaviruses cluster in a sister clade to *Molossidae* alphacoronaviruses (*Mops* and *Chaerophon* spp.) and the *Myotis* and *Scotophilus* alphacoronaviruses. Both of these BtCoV clades are in a sister clade to the human alphacoronaviruses, HCoV229E (and related BtCoV from Ghana) and HCoVNL63, the latter sharing 70.7% nucleotide identity to *Neo*-BtCoV167/SA/07.

### *Rhinolophus* Bat Coronavirus

A total of 16 *Rhinolophus* alimentary specimens were analysed in this study, 10 from South Africa and 6 from Rwanda. Of these, two samples from the 6 Rwandan samples were found to contain BtCoV nucleic acid. The *Rhinolophus* spp. that inhabit the Ruhengeri caves in Rwanda were however not identified to species level and can thus only be reported to genus level.

The two Rwandan bat coronaviruses, *Rh*-BtCoV/441/Rwanda/08 and *Rh*-BtCoV/445/Rwanda/08, were sequenced and identified to belong to the SARS-related species cluster of the *Betacoronavirus* genus. Analysis of the two positive sequences showed 100% nucleotide and amino acid identity. Thus, it may be concluded that these two sequences belong to the same species of virus. Due to the detection of the same virus in two individuals inhabiting the same roost, it could be suggested that this betacoronavirus may be circulating throughout the *Rhinolophus* spp, residing in the Ruhengeri cave systems.

However, a deduction based on only a population sampling of 6 bats, is a very preliminary assessment.

Phylogenetic analysis of the Rwandan betacoronavirus with available betacoronaviruses from Genbank (NCBI) identifies its closest phylogenetic relative as the Kenyan BtCoV, *Rh*-BtCoVKY72, and shares 94.8% nucleotide identity and 100% amino acid similarity to the Rwandan *Rhinolophus* betacoronavirus. Thus, due to these close identity values, it is possible that the same betacoronavirus may be harboured by both Kenyan and Rwandan *Rhinolophus* spp. The Rwandan betacoronavirus also shares 85.3% nucleotide identity and 97.8% amino acid similarity to the Bulgarian *Rhinolophus* betacoronavirus *Rh*-BtCoV/BM48-31/BGR/08 (Figures 3.2 and 3.3) and 82.6% and 83.9% nucleic acid similarity and 87.8% and 98.9% amino acid similarity to the Asian *Rhinolophus* SARS-related BtCoV, SARSr-Rh-BtCoV/Rp3 and SARSr-Rh-BtCoV/Rm1, respectively The exact phylogenetic evolutionary history of the African, European and Asian SARSr-BtCoV is difficult to discern considering their geographical separation.

It has been hypothesised that the SARSr-CoV species cluster may have originated within the *Rhinolophoidea* superfamily since the SARSr-CoV species cluster have almost exclusively been identified from the *Rhinolophidae* family with closely related viruses being detected within the *Hipposideridae* family. Thus, much like the *Miniopterus* and *Myotis* bat coronavirus species that may have been present in their host bat species before the host migration to different continents, it is possible that the *Rhinolophoidea* ancestor bat that gave rise to the *Rhinolophidae* and *Hipposideridae* families may already have contained the ancestor of betacoronavirus which later diverged into the *Rhinolophus* SARSr-BtCoV species and the *Hipposideros* betacoronaviruses.

This study identified bat coronaviruses in South African bat species by analysis of the fecal and rectal samples of the specimen collection of our laboratory at the University of Pretoria. These specimens were collected from various species in the South African provinces at convenient opportunities and as such some species have been sampled more often than others due to convenience and ease of access. The results from this study therefore provide a first indication as to the particular bat coronavirus species that are present within the native South African bat populations. Thus, more detailed population studies focusing on specific bat species may be performed in future to determine the prevalence of particular bat coronaviruses within regularly sampled bat populations. Frequent sampling of the bat coronaviruses circulating in a particular population also improves the knowledge of the infection cycle of these viruses in their native host species including re-infections, clearance times and antibody levels of infected bats.

The majority of the samples from the Ruhengeri caves in Rwanda were from *Rousettus* spp., and none of which tested positive for bat coronavirus RNA. However, these

caves are considered as potential sites for tourist visits and as such the detection of a SARS-related bat coronavirus that may potentially be circulating within the Rhinolophus population in the Ruhengeri region may merit further investigation, especially due to the small population size sampled in this study.

One major aim regarding the detection of viral species within wildlife populations is to improve surveillance for potential zoonotic agents and to evaluate any threat to public and veterinarian public health. The alphacoronaviruses identified within the South African bat species sampled most likely pose very little threat to human and domesticated animal health. The SARS-related BtCoV detected within *Rhinolophus* spp. in Rwanda may pose a slightly higher threat to public health due to the association with SARS-CoV. The possibility of either these alpha- or betacoronaviruses viruses jumping to, and eventually adapting to and infecting other species cannot be completely excluded since such events are hypothesised to be the origin of coronaviruses in humans and domestic farm and pet animals. Even though such events are likely to be rare, caution is merited when interacting with bats in roosts and caves.

# Chapter 4: Concluding remarks

The aim of this study was to determine if there were any bat coronaviruses present within the bat species of South Africa and Rwanda and to determine how they were related to other bat coronaviruses, globally. Two assays, the PanBtCoV/9 primer and PanBat/AB/6 primer assay, were developed for coronavirus detection and were capable of detecting $10^4$ copies/µl of the developed betacoronavirus positive control. When comparing the developed protocols, results would seem to indicate that the PanBtCoV/9 primer nested PCR protocol was the most successful assay since it detected the most positive samples and the lowest concentration of the betacoronavirus positive control. The combined assays amplified 5 samples from the analysed 201 samples collected in South Africa and Rwanda.

Only alphacoronaviruses were detected in 3 South African bat species, *Mi*-BtCoV/Irene/SA/09 from *Miniopterus* spp., *Neo*-BtCoV/167/SA/07 from *Neoromicia* spp., and *Mops*-BtCoV/1364/SA/11 from *Mops midas*. From Rwanda, a single betacoronavirus, a SARSr-CoV was detected within 2 *Rhinolophus* individuals (*Rh*-BtCoV/441/Rwanda/08 and *Rh*-BtCoV/445/Rwanda/08). These viruses were the first bat coronaviruses identified from the native bat species of South Africa and Rwanda, providing the first confirmation of bat coronaviruses possibly circulating in these countries. The study also identified the first bat coronavirus detected within the *Neoromicia* genus as well as bat coronaviruses similar to previously detected viruses within the *Miniopterus* and *Rhinolophus* genera. From these first results further investigations into the prevalence and infection cycles of bat coronaviruses in specific bat populations may be performed. Selected bat populations may now be investigated in long term studies to determine the prevalences of the circulating BtCoV in these species as well as the persistence of these viruses within individual colonies. Investigations into experimental infections of laboratory bats may also provide opportunities to study pathogenesis of these viruses in their natural hosts.

Unfortunately, no amplicons of the RNA dependent RNA polymerase or nucleoprotein genes could be generated of sufficient length to improve the preliminary resolution of the phylogenetic relationships between the South African and Rwandan BtCoV, and their close relatives. A major limitation in the study of BtCoVs is the difficulty in culturing the viruses in standard cell lines in order to have enough material for further analyses. As such, future work will attempt to establish bat cell lines from selected tissue types from known BtCoV hosts such as *Miniopterus* spp. Attempts by other groups at cultivating BtCoVs in bat cell lines have been unsuccessful; however, those groups used cell lines derived from tissue types which possibly do not contain the correct receptor types as would be found in the gastrointestinal tract. Therefore creating intestinal bat cell lines of specific host species may provide BtCoV with suitable environments to infect and multiply in.

In conclusion, this study has confirmed the widespread presence of BtCoV with the detection of these viruses in selected bat populations from South Africa and Rwanda.

Further investigations into the circulation and persistence of BtCoV within specific bat populations are warranted to understand the potential for spill over infections into new species. The nested RT-PCR assays developed in this study may be implemented to aid further analysis of BtCoVs and to improve the epidemiological understanding of these viruses.

# Chapter 5: Appendices

**Appendix A: Total samples processed from South Africa**

***Key: +** = positive band amplified; **-** =no amplification; **NtD**= not definative; **NC**= Needs confimation; **NtC**=previous result not confirmed; **Nest+** =amplification in nested PCR*

| Sample | Type | Province | Location | *Host species* | Protocol (RT-PCR/nPCR) | Result | Date | RNA Location | RNA Extraction | Comment |
|---|---|---|---|---|---|---|---|---|---|---|
| UP72 | NA | KZN | Durban | *Epomophorus wahlbergi* | 2009; (Hons.)Tong Primers | NtD | 2009-07-07 | Rack1; Box5 | Qiagen kit at NICD | Abnormal behaviour |
| | | | | | 2011; PanBtCoV/9 nested PCR | - | 2011-05-09 | | | |
| UP73 | NA | KZN | Glenwood area, Durban | *Epomophorus wahlbergi* | 2009; (Hons.)Tong Primers | NtD | 2009-06-18 | Rack1; Box5 | Qiagen kit at NICD | Abnormal behaviour |
| UP74 | NA | KZN | Chelsen Durban | *Epomophorus wahlbergi* | 2009; (Hons.)Tong Primers | NtD | 2009-06-18 | Rack1; Box5 | Qiagen kit at NICD | Abnormal behaviour |
| | | | | | 2011; PanBtCoV/9 nested PCR | - | 2011-05-04 | | | |
| **UP75*** | **NA** | **KZN** | **Amanzimtoti** | ***Epomophorus wahlbergi*** | **2009; (Hons.)Tong Primers** | **+** | **2009-06-18** | **Rack1; Box5** | **Qiagen kit at NICD** | **Abnormal behaviour** |
| | | | | | 2011; PanBtCoV/9 nested PCR | NtD | 2011-04-20 | NO MORE RNA | | |
| UP77 | NA | KZN | Durban | *Epomophorus wahlbergi* | 2009; (Hons.)Tong Primers | NtD | 2009-06-18 | Rack1; Box5 | Qiagen kit at NICD | Abnormal behaviour |
| | | | | | 2011; PanBtCoV/9 nested PCR | - | 2011-05-04 | | | |
| UP142 | NA | KZN | | *Epomophorus wahlbergi* | 2009; (Hons.)Tong Primers | NtD | 2009-07-07 | Rack1; Box5 | Qiagen kit at NICD | |
| | | | | | 2010; 1 primer heminested | NtD | 2010-08-02 | | | |
| | | | | | 2011; PanBtCoV/9 nested PCR | - | 2011-05-09 | | | |
| UP143 | NA | KZN | | *Epomophorus wahlbergi* | 2009; (Hons.)Tong Primers | NtD | 2009-07-07 | Rack1; Box5 | Qiagen kit at NICD | Juvenile |
| | | | | | 2010; 1 primer heminested | NtD | 2010-08-02 | | | |
| | | | | | 2011; PanBtCoV/9 nested PCR | - | 2011-05-04 | | | |
| UP144 | NA | KZN | | *Epomophorus wahlbergi* | 2009; (Hons.)Tong Primers | NtD | 2009-07-07 | Rack1; Box5 | Qiagen kit at NICD | Juvenile |
| | | | | | 2010; 1 primer heminested | NtD | 2010-08-02 | | | |
| | | | | | 2011; PanBtCoV/9 nested PCR | NtD | 2011-05-04 | | | |
| UP156 | Rectum | North West | Taung | *Tadarida aegyptiaca* | 2011; PanBtCoV/9 nested PCR | - | 2011-05-09 | Rack1; Box5 | Qiagen kit at NICD | |
| UP157 | NA | North West | Taung | *Tadarida aegyptiaca* | 2009; (Hons.)Tong Primers | NtD | 2009-07-07 | Rack1; Box5 | Qiagen kit at NICD | |
| | | | | | 2011; PanBtCoV/9 nested PCR | - | 2011-05-09 | | | |
| UP158 | NA | North West | Taung | *Tadarida aegyptiaca* | 2009; (Hons.)Tong Primers | - | 2009-06-19 | Rack1; Box5 | Qiagen kit at NICD | |
| | | | | | 2011; PanBtCoV/9 nested PCR | - | 2011-04-15 | | | |
| UP159 | NA | North West | Taung | *Tadarida aegyptiaca* | 2009; (Hons.)Tong Primers | NtD | 2009-06-19 | Rack1; Box5 | Qiagen kit at NICD | |
| | | | | | 2011; PanBtCoV/9 nested PCR | - | 2011-05-09 | | | |
| **UP160*** | **Rectum** | **North West** | **Taung** | ***Rhinolophus denti*** | **2010; 1 primer heminested** | **Nest+** | **2010-08-02** | **NO MORE RNA** | **Qiagen kit at NICD** | |
| | | | | | **2010; 1 primer heminested** | **NtD, Nest+** | **2010-08-13** | | | |
| **UP161*** | **Rectum** | **North West** | **Taung** | ***Neoromicia capensis*** | **2010; 1 primer heminested** | **Nest+** | **2010-08-02** | **NO MORE RNA** | **Qiagen kit at NICD** | |
| | | | | | **2010; 1 primer heminested** | **NtD, Nest+** | **2010-08-13** | | | |
| | | | | | 2010; 1 primer heminested | Smear | 2010-08-26 | | | |
| UP162 | Rectum | North West | Taung | *Rhinolophus denti* | 2010; 1 primer heminested | NtD | 2010-08-02 | NO MORE RNA | Qiagen kit at NICD | |
| | | | | | 2011; PanBtCoV/9 nested PCR | - | 2011-05-04 | | | |
| UP163 | Rectum | North West | Taung | *Rhinolophus denti* | 2011; PanBtCoV/9 nested PCR | - | 2011-04-15 | Rack1; Box5 | | |
| **UP165*** | **Rectum** | **North West** | **Taung** | ***Neuromicia capensis*** | **2010; 1 primer heminested** | **Nest+** | **2010-08-02** | **NO MORE RNA** | **Qiagen kit at NICD** | |
| | | | | | **2010; 1 primer heminested** | **NtD, Nest+** | **2010-08-13** | | | |
| | | | | | 2010; 1 primer heminested | Smear | 2010-08-26 | | | |
| UP166 | Rectum | North West | Taung | *Neuromicia capensis* | 2010; 1 primer heminested | NtD | 2010-08-02 | Rack1; Box5 | Qiagen kit at NICD | |
| **UP167*** | **Rectum** | **North West** | **Taung** | ***Neuromicia capensis*** | **2011; PanBtCoV/9 nested PCR** | **+** | **2011-05-09** | **Rack1; Box5** | **Qiagen kit at NICD** | |
| UP168 | Rectum | North West | Taung | *Neuromicia capensis* | 2011; PanBtCoV/9 nested PCR | - | 2011-05-09 | Rack1; Box5 | Qiagen kit at NICD | |

| | | | | | | | | | | |
|---|---|---|---|---|---|---|---|---|---|---|
| UP169 | Rectum | North West | Taung | *Neuromicia capensis* | 2011; PanBtCoV/9 nested PCR | - | 2011-05-09 | Rack1; Box5 | Qiagen kit at NICD | |
| UP170 | NA | North West | Taung | *Eptesicus Hottentotus* | 2009; (Hons.)Tong Primers | - | 2009-06-19 | Rack1; Box5 | Qiagen kit at NICD | |
| | | | | | 2011; PanBtCoV/9 nested PCR | - | 2011-05-04 | | | |
| UP171 | Rectum | North West | Taung | *Rhinolophus denti* | 2011; PanBtCoV/9 nested PCR | - | 2011-05-26 | Rack1; Box5 | Qiagen kit at NICD | |
| | | | | | 2011; PanBat/AB/6 | - | 2011/09/26 | | | |
| UP172 | Rectum | North West | Taung | *Rhinolophus denti* | 2011; PanBtCoV/9 nested PCR | - | 2011-05-26 | Rack1; Box5 | Qiagen kit at NICD | |
| UP173 | NA | North West | Taung | *Eptesicus Hottentotus* | 2009; (Hons.)Tong Primers | - | 2009-06-19 | Rack1; Box5 | Qiagen kit at NICD | |
| | | | | | 2011; PanBtCoV/9 nested PCR | - | 2011-05-04 | | | |
| UP174 | Rectum | North West | Taung | *Rh. darlingi damarensis* | 2011; PanBtCoV/9 nested PCR | - | 2011-05-26 | Rack1; Box5 | Qiagen kit at NICD | |
| | | | | | 2011; PanBat/AB/6 | - | 2011/09/26 | | | |
| UP178 | NA | North West | Taung | *Insectivorous bat* | 2009; (Hons.)Tong Primers | - | 2009-06-19 | Rack1; Box5 | Qiagen kit at NICD | |
| | | | | | 2011; PanBtCoV/9 nested PCR | - | 2011-05-04 | | | |
| UP288 | NA | North West | Thabela thabeng | *Miniopterus* | 2011; PanBtCoV/9 nested PCR | - | 2011-05-24 | Rack1; Box5 | Qiagen kit at NICD | Dead bat picked up in cave |
| | | | | | 2011; PanBat/AB/6 | - | 2011-09-28 | | | |
| Up413 | Fecal Swab | Gauteng | Hennopspruit | *Neoromicia* | 2010; MSc with Woo 2005 | - | 2010-05-17 | Rack1; Box2 | Qiagen kit at NICD | |
| | | | | | *Followed up with nested pcr* | - | 2011-01-18 | | | |
| | Fecal swab | | | | 2011; PanBat/AB/6 | - | 2011-09-26 | Rack1; Box3 | Trizol/UP/16/03/11 | |
| Up473 | Fecal swab | Limpopo | Palaborwa mining company | *Mops condylurus* | 2011; PanBat/AB/6 | - | 2011-09-26 | Rack1; Box3 | Trizol/UP/16/03/11 | |
| Up474 | Fecal swab | Gauteng | Hennopspruit | *Neoromicia* | 2011; PanBat/AB/6 | - | 2011-09-26 | Rack1; Box3 | Trizol/UP/16/03/11 | |
| Up825 | Fecal swab | Limpopo | Pafuri. Kruger National Park | *Epomophorus wahlbergi* | 2011; PanBat/AB/6 | - | 2011/10/20 | Rack7; Box4 | Trizol/UP/11/10/11 | |
| Up826 | Rectum | KZN | Rocktail bay: St. Lucia | *Epomophorus wahlbergi* | 2011; PanBat/AB/6 | - | 2011/10/20 | Rack7; Box4 | Trizol/UP/11/10/11 | |
| Up827 | Rectum | KZN | Rocktail bay: St. Lucia | *Glauconycteris variegata* | 2011; PanBat/AB/6 | - | 2011/10/20 | Rack7; Box4 | Trizol/UP/11/10/11 | |
| Up828 | Rectum | KZN | Rocktail bay: St. Lucia | *Nycteris thebaica* | 2011; PanBat/AB/6 | - | 2011/10/20 | Rack7; Box4 | Trizol/UP/11/10/11 | |
| Up829 | Rectum | KZN | Rocktail bay: St. Lucia | *Nycteris thebaica* | 2011; PanBat/AB/6 | - | 2011/10/20 | Rack7; Box4 | Trizol/UP/11/10/11 | |
| Up831 | Rectum | KZN | Rocktail bay: St. Lucia | *Scotophilus dinganii* | 2011; PanBat/AB/6 | - | 2011/10/20 | Rack7; Box4 | Trizol/UP/11/10/11 | |
| Up833 | Rectum | KZN | Rocktail bay: St. Lucia | *Scotophilus dinganii* | 2011; PanBat/AB/6 | - | 2011/10/20 | Rack7; Box4 | Trizol/UP/11/10/11 | |
| Up834 | Rectum | KZN | Rocktail bay: St. Lucia | *Scotophilus dinganii* | 2011; PanBat/AB/6 | - | 2011/10/20 | Rack7; Box4 | Trizol/UP/11/10/11 | |
| Up835 | Rectum | KZN | Rocktail bay: St. Lucia | *Chaerephon pumilus* | 2011; PanBat/AB/6 | - | 2011/10/20 | Rack7; Box4 | Trizol/UP/11/10/11 | |
| Up836 | Rectum | KZN | Rocktail bay: St. Lucia | *Chaerephon pumilus* | 2011; PanBat/AB/6 | - | 2011/10/20 | Rack7; Box4 | Trizol/UP/11/10/11 | |
| Up837 | Rectum | KZN | Rocktail bay: St. Lucia | *Chaerephon pumilus* | 2011; PanBat/AB/6 | - | 2011/10/20 | Rack7; Box4 | Trizol/UP/11/10/11 | |
| Up901 | Fecal swab | Limpopo | Modimole | *Miniopterus* | 2011; PanBtCoV/9 nested PCR | - | 2011-04-15 | Rack1; Box3 | Trizol/UP/16/03/11 | Dead in cave |
| Up902 | Fecal swab | Gauteng | Irene cave | *Miniopterus natalensis* | 2011; PanBat/AB/6 | - | 2011/11/03 | Rack5; Box12 | Trizol/UP/29/09/11 | Dead in cave |
| Up903 | Fecal swab | Gauteng | Irene cave | *Miniopterus natalensis* | 2011; PanBat/AB/6 | - | 2011/11/03 | Rack5; Box12 | Trizol/UP/29/09/11 | |
| Up904 | Fecal swab | Gauteng | Irene cave | *Miniopterus natalensis* | 2011; PanBat/AB/6 | - | 2011/11/03 | Rack5; Box12 | Trizol/UP/29/09/11 | |
| Up905 | Fecal swab | KZN | Woodhurst, Chatsworth | *Epomophorus wahlbergi* | 2011; PanBat/AB/6 | - | 2011/11/03 | Rack5; Box12 | Trizol/UP/29/09/11 | Rehab bat; snake bite |
| Up909 | Fecal swab | Limpopo | Pafuri. Kruger National Park | *Rousettus Aegyptiacus* | 2011; PanBat/AB/6 | - | 2011/09/28 | Rack5; Box12 | Trizol/UP/16/03/11 | |
| Up910 | Fecal swab | Limpopo | Pafuri. Kruger National Park | *Rousettus Aegyptiacus* | 2011; PanBat/AB/6 | - | 2011/09/28 | Rack5; Box12 | Trizol/UP/16/03/11 | Baby |
| Up915 | Fecal swab | Limpopo | Pafuri. Kruger National Park | *Neuromicia capensis* | 2011; PanBat/AB/6 | - | 2011/09/28 | Rack5; Box12 | Trizol/UP/16/03/11 | Pregnant |
| Up917 | Rectum | Limpopo | Pafuri. Kruger National Park | *Neuromicia nana* | 2011; PanBat/AB/6 | - | 2011/09/28 | Rack5; Box12 | Trizol/UP/16/03/11 | Released |
| Up921 | Rectum | Limpopo | Pafuri. Kruger National Park | *Neuromicia helios* | 2011; PanBat/AB/6 | - | 2011-09-01 | Rack5; Box12 | Trizol/UP/30/08/11 | Pregnant |
| Up922 | Rectum | Limpopo | Pafuri. Kruger National Park | *Neuromicia nana* | 2011; PanBat/AB/6 | - | 2011-09-01 | Rack5; Box12 | Trizol/UP/30/08/11 | Pregnant |
| Up927 | Fecal | Limpopo | Pafuri. Kruger National Park | *Rousettus Aegyptiacus* | 2011; PanBat/AB/6 | - | 2011/09/28 | Rack5; Box12 | Trizol/UP/16/03/11 | |

| | | | | | | | | | | |
|---|---|---|---|---|---|---|---|---|---|---|
| Up932 | Fecal swab | Limpopo | Pafuri. Kruger National Park | *Neuromicia nana* | 2011; PanBat/AB/6 | - | 2011/09/28 | Rack5; Box12 | Trizol/UP/16/03/11 | Pregnant |
| UP934 | Rectum | Limpopo | Pafuri. Kruger National Park | *Chaerophon* | 2011; PanBat/AB/6 | - | 2011-09-01 | Rack5; Box12 | Trizol/UP/30/08/11 | Pregnant |
| Up936 | Fecal | Limpopo | Pafuri. Kruger National Park | *Molossid* | 2011; PanBat/AB/6 | - | 2011/09/28 | Rack5; Box12 | Trizol/UP/15/08/11 | Pregnant |
| Up940 | Fecal | Limpopo | Pafuri. Kruger National Park | *Molossid* | 2011; PanBat/AB/6 | - | 2011/09/28 | Rack5; Box12 | Trizol/UP/16/03/11 | Pregnant |
| Up942 | Fecal | Limpopo | Pafuri. Kruger National Park | *Neuromica nana* | 2011; PanBat/AB/6 | - | 2011-09-06 | Rack5; Box12 | Trizol/UP/15/08/11 | Pregnant |
| Up944 | Fecal | Limpopo | Pafuri. Kruger National Park | *Neuromica nana* | 2011; PanBat/AB/6 | - | 2011/09/28 | Rack5; Box12 | Trizol/UP/16/03/11 | Pregnant |
| Up946 | Fecal | Limpopo | Pafuri. Kruger National Park | *Neuromica nana* | 2011; PanBat/AB/6 | - | 2011/09/28 | Rack5; Box12 | Trizol/UP/16/03/11 | Pregnant |
| Up947 | Fecal swab | Limpopo | Pafuri. Kruger National Park | *Rhinolophus landeri* | 2011; PanBat/AB/6 | - | 2011-09-06 | Rack5; Box12 | Trizol/UP/15/08/11 | Pregnant |
| Up948 | Rectum | Limpopo | Pafuri. Kruger National Park | *Hipposideros caffer* | 2011; PanBat/AB/6 | - | 2011-09-01 | Rack5; Box12 | Trizol/UP/30/08/11 | Pregnant |
| Up951 | Rectum | Limpopo | Pafuri. Kruger National Park | *Hipposideros caffer* | 2011; PanBat/AB/6 | - | 2011-09-01 | Rack5; Box12 | Trizol/UP/30/08/11 | Pregnant |
| Up952 | Fecal | Limpopo | Pafuri. Kruger National Park | *Neoromicia helios* | 2011; PanBat/AB/6 | - | 2011/09/01 | Rack5; Box12 | Trizol/UP/16/03/11 | |
| UP955 | Rectum | Limpopo | Pafuri. Kruger National Park | *Scotophilus dinganii* | 2011; PanBat/AB/6 | - | 2011-09-01 | Rack5; Box12 | Trizol/UP/30/08/11 | |
| Up956 | Fecal | Limpopo | Pafuri. Kruger National Park | *Scotophilus dinganii* | 2011; PanBat/AB/6 | - | 2011/09/28 | Rack5; Box12 | Trizol/UP/16/03/11 | |
| Up957 | Fecal swab | Limpopo | Pafuri. Kruger National Park | *Scotophilus viridis* | 2011; PanBat/AB/6 | - | 2011/09/28 | Rack5; Box12 | Trizol/UP/16/03/11 | Pregnant |
| | X2 | | | | 2011; PanBat/AB/6 | - | 2011-09-06 | Rack5; Box12 | Trizol/UP/15/08/11 | |
| Up959 | Fecal | Limpopo | Pafuri. Kruger National Park | *Scotophilus dinganii* | 2011; PanBat/AB/6 | - | 2011-09-06 | Rack5; Box12 | Trizol/UP/15/08/11 | |
| | | | | | 2011; PanBat/AB/6 | - | 2011-09-01 | Rack5; Box12 | Trizol/UP/30/08/11 | |
| Up960 | | Limpopo | Pafuri. Kruger National Park | *Scotophilus leucogaster* | 2011; PanBat/AB/6 | - | 2011-09-06 | Rack5; Box12 | Trizol/UP/15/08/11 | Pregnant |
| | Rectum | | | | 2011; PanBat/AB/6 | - | 2011-09-01 | Rack5; Box12 | Trizol/UP/30/08/11 | |
| Up961 | | Limpopo | Pafuri. Kruger National Park | *Neoromicia zuluensis* | 2011; PanBat/AB/6 | - | 2011-09-06 | Rack5; Box12 | Trizol/UP/15/08/11 | |
| | Rectum | | | | 2011; PanBat/AB/6 | - | 2011-09-01 | Rack5; Box12 | Trizol/UP/30/08/11 | |
| **Up962*** | **Fecal** | **Limpopo** | **Pafuri. Kruger National Park** | ***Neoromicia nana*** | 2011; PanBat/AB/6 | NC | 2011-09-02 | Rack5; Box12 | Trizol/UP/02/08/11 | **Pregnant** |
| | | | | | 2011; PanBat/AB/6 | - | 2011-09-22 | | | |
| | | | | | 2011; PanBat/AB/6 | - | 2011-09-28 | | | |
| | **Rectum** | | | | **2011; PanBat/AB/6** | **+** | **2011-09-28** | **Rack7; Box4** | **Trizol/UP/30/08/11** | |
| Up963 | Rectum | Limpopo | Pafuri. Kruger National Park | *Neoromicia capensis* | 2011; PanBat/AB/6 | - | 2011-09-01 | Rack5; Box12 | Trizol/UP/30/08/11 | |
| Up967 | Fecal | Limpopo | Pafuri. Kruger National Park | *Mops condylurus* | 2011; PanBat/AB/6 | - | 2011-08-04 | Rack5; Box12 | Trizol/UP/02/08/11 | Pregnant |
| Up973 | Fecal | Limpopo | Pafuri. Kruger National Park | *Scotophilus dinganii* | 2011; PanBat/AB/6 | - | 2011-09-22 | Rack5; Box12 | Trizol/UP/02/08/11 | Released |
| Up976 | Fecal | Limpopo | Pafuri. Kruger National Park | *Scotophilus leucogaster* | 2011; PanBat/AB/6 | - | 2011-09-22 | Rack5; Box12 | Trizol/UP/02/08/11 | Released |
| Up977 | Fecal | Limpopo | Pafuri. Kruger National Park | *Nycticeinops schlieffenii* | 2011; PanBat/AB/6 | - | 2011-08-04 | Rack5; Box12 | Trizol/UP/02/08/11 | Released |
| Up978 | Fecal | Limpopo | Pafuri. Kruger National Park | *Insectivorous bat* | 2011; PanBat/AB/6 | - | 2011-08-04 | Rack5; Box12 | Trizol/UP/02/08/11 | Released |
| Up979 | Fecal | Limpopo | Pafuri. Kruger National Park | *Nycticeinops schlieffenii* | 2011; PanBat/AB/6 | - | 2011-09-22 | Rack5; Box12 | Trizol/UP/02/08/11 | Released |
| Up983 | Fecal | Limpopo | Pafuri. Kruger National Park | *Nycticeinops schlieffenii* | 2011; PanBat/AB/6 | - | 2011-08-04 | Rack5; Box12 | Trizol/UP/02/08/11 | Released |
| Up985 | Fecal | Limpopo | Pafuri. Kruger National Park | *Nycticeinops schlieffenii* | 2011; PanBat/AB/6 | - | 2011-09-22 | Rack5; Box12 | Trizol/UP/02/08/11 | Released |
| Up993 | Fecal | Limpopo | Pafuri. Kruger National Park | *Nycticeinops schlieffenii* | 2011; PanBat/AB/6 | - | 2011-08-04 | Rack5; Box12 | Trizol/UP/02/08/11 | Released |
| Up997 | Fecal | Limpopo | Pafuri. Kruger National Park | *Nycticeinops schlieffenii* | 2011; PanBat/AB/6 | - | 2011-08-04 | Rack5; Box12 | Trizol/UP/02/08/11 | Released |
| Up999 | Fecal | Limpopo | Pafuri. Kruger National Park | *Nycticeinops schlieffenii* | 2011; PanBat/AB/6 | - | 2011-09-22 | Rack5; Box12 | Trizol/UP/02/08/11 | Released |
| Up1005 | Rectum | Limpopo | Pafuri. Kruger National Park | *E. gambianus* | 2011; PanBat/AB/6 | - | 2011-09-01 | Rack5; Box12 | Trizol/UP/30/08/11 | Pregnant |
| Up1007 | Fecal | North West | Kgaswane | *Molossid* | 2011; PanBat/AB/6 | - | 2011/10/31 | Rack1; Box3 | Trizol/UP/19/05/11 | |
| Up1009 | Fecal | North West | Kgaswane | *Scotophilus* | 2011; PanBat/AB/6 | - | 2011/10/31 | Rack1; Box3 | Trizol/UP/19/05/11 | |
| Up1011 | Fecal | North West | Kgaswane | *Insectivorous bat* | 2011; PanBat/AB/6 | - | 2011/10/31 | Rack1; Box3 | Trizol/UP/19/05/11 | |
| Up1012 | Fecal | North West | Kgaswane | *Insectivorous bat* | 2011; PanBat/AB/6 | - | 2011/10/31 | Rack1; Box3 | Trizol/UP/19/05/11 | |

| | | | | | | | | | | |
|---|---|---|---|---|---|---|---|---|---|---|
| Up1014 | Fecal | North West | Kgaswane | *Scotophilus* | 2011; PanBat/AB/6 | - | 2011/10/31 | Rack1; Box3 | Trizol/UP/19/05/11 | |
| Up1018 | Fecal | North West | Kgaswane | *Scotophilus* | 2011; PanBat/AB/6 | - | 2011/10/31 | Rack1; Box3 | Trizol/UP/19/05/11 | |
| Up1020 | Fecal | North West | Kgaswane | *Scotophilus* | 2011; PanBat/AB/6 | - | 2011/10/31 | Rack1; Box3 | Trizol/UP/19/05/11 | |
| Up1024 | Fecal | North West | Kgaswane | *Scotophilus dinganii* | 2011; PanBat/AB/6 | - | 2011/10/31 | Rack1; Box3 | Trizol/UP/19/05/11 | Released |
| Up1034 | Fecal | North West | Kgaswane | *Scotophilus* | 2011; PanBat/AB/6 | - | 2011/10/31 | Rack1; Box3 | Trizol/UP/19/05/11 | Released |
| Up1035 | Fecal | North West | Kgaswane | *Scotophilus* | 2011; PanBat/AB/6 | - | 2011/10/31 | Rack1; Box3 | Trizol/UP/19/05/11 | Released |
| Up1043 | Fecal | North West | Kgaswane | *Scotophilus* | 2011; PanBat/AB/6 | - | 2011/10/31 | Rack1; Box3 | Trizol/UP/19/05/11 | Released |
| Up1048 | Fecal | North West | Kgaswane | *Scotophilus dinganii* | 2011; PanBat/AB/6 | - | 2011/10/31 | Rack1; Box3 | Trizol/UP/19/05/11 | Released |
| UP1349 | Fecal | Gauteng | Irene caves | *Miniopterus natalensis* | 2011; PanBat/AB/6 | - | 2011/11/03 | Rack7; Box4 | Trizol/UP/29/09/11 | dead bat in cave (1060) |
| Up1362 | Fecal swab | ? | bird park? | *Neoromicia capensis* | 2011; PanBat/AB/6 | - | 2011/11/03 | Rack7; Box4 | Trizol/UP/29/09/11 | Infectious lung disease |
| **Up1364*** | **Fecal swab** | **Limpopo** | **Kameel St. Makhado** | ***Mops midas*** | **2011; PanBat/AB/6** | **+** | **2011/11/03** | **Rack7; Box4** | **Trizol/UP/29/09/11** | **Found Dead** |
| UP1367 | Fecal | Limpopo | Labuschagne farm, Makhado | *Rhinolophus capensis* | 2011; PanBat/AB/6 | - | 2011/11/03 | Rack7; Box4 | Trizol/UP/29/09/11 | |
| Up1369 | Rectum | Gauteng | Free Me rehab | *Neoromicia capensis* | 2011; PanBat/AB/6 | - | 2011/10/18 | Rack7; Box4 | Trizol/UP/11/10/11 | suffering hair loss |
| UP1393 | Fecal | Gauteng | Irene caves | *Miniopterus natalensis* | 2011; PanBat/AB/6 | - | 2011/11/03 | Rack7; Box4 | Trizol/UP/29/09/11 | dead bat in cave (1059) |
| UP1399 | Fecal swab | Gauteng | Irene caves | *Miniopterus natalensis* | 2011; PanBat/AB/6 | - | 2011-09-06 | Rack5; Box12 | Trizol/UP/15/08/11 | |
| UP1400 | 31 Rectum | Gauteng | Irene caves | *Miniopterus natalensis* | 2011; PanBat/AB/6 | - | 2011/10/18 | Rack7; Box4 | Trizol/UP/11/10/11 | |
| | Fecal swab | | | | 2011; PanBat/AB/6 | - | 2011-09-06 | Rack5; Box12 | Trizol/UP/15/08/11 | |
| UP1401 | 32 Rectum | Gauteng | Irene caves | *Miniopterus natalensis* | 2011; PanBat/AB/6 | - | 2011/10/18 | Rack7; Box4 | Trizol/UP/11/10/11 | |
| | Fecal swab | | | | 2011; PanBat/AB/6 | - | 2011-09-06 | Rack5; Box12 | Trizol/UP/15/08/11 | |
| UP1402 | 33 Rectum | Gauteng | Irene caves | *Miniopterus natalensis* | 2011; PanBat/AB/6 | - | 2011/10/18 | Rack7; Box4 | Trizol/UP/11/10/11 | |
| | Fecal swab | | | | 2011; PanBat/AB/6 | - | 2011-09-06 | Rack5; Box12 | Trizol/UP/15/08/11 | |
| UP1403 | 34 Rectum | Gauteng | Irene caves | *Miniopterus natalensis* | 2011; PanBat/AB/6 | - | 2011/10/18 | Rack7; Box4 | Trizol/UP/11/10/11 | |
| UP1404 | 35 Rectum | Gauteng | Irene caves | *Miniopterus natalensis* | 2011; PanBat/AB/6 | - | 2011/10/18 | Rack7; Box4 | Trizol/UP/11/10/11 | |
| | Fecal swab | | | | 2011; PanBat/AB/6 | - | 2011-09-06 | Rack5; Box12 | Trizol/UP/15/08/11 | |
| **UP1410*** | **Fecal** | Gauteng | **Irene Caves** | ***Miniopterus natalensis*** | **2011; PanBtCoV/9 nested PCR** | **+** | 2011-04-17 | Rack1; Box3 | Trizol/UP/04/04/11 | Fecal pellets -cave floor |
| Up1420 | Fecal swab | Limpopo | Kameel St. Makhado | *Mops midas* | 2011; PanBat/AB/6 | - | 2011/11/03 | Rack7; Box4 | Trizol/UP/29/09/11 | released |
| *Cavewall* | Fecal mix | Limpopo | Labuschagne farm, Makhado | *Rhinolophus* | 2011; PanBat/AB/6 | - | 2011/11/03 | Rack7; Box4 | Trizol/UP/29/09/11 | |
| *CaveEnt.* | Fecal mix | Limpopo | Labuschagne farm, Makhado | *Rhinolophus* | 2011; PanBat/AB/6 | - | 2011/11/03 | Rack7; Box4 | Trizol/UP/29/09/11 | |

**Appendix B: Total samples processed from Ruhengeri, Rwanda**

***Key: +** = positive band amplified; **-** =no amplification; **NtD**= not definative; **NC**= Needs confimation; **NtC**=previous result not confirmed; **Nest+** =amplification in nested PCR*

| Sample | Type | Location | *Host species* | Protocol (RT-PCR/nPCR) | Result | Date | RNA Location | RNA Extraction | **Comments** |
|---|---|---|---|---|---|---|---|---|---|
| Up401 | Fecal Swab | Cave 1 | *H. Caffer* | 2010; MSc with Woo et al. 2005 | - | 2010-05-26 | Rack1; Box2 | Qiagen kit at NICD | Died while bleeding |
| | | | | *Followed up with nested PCR* | - | 2011-01-25 | | | |
| Up402 | Fecal | Cave 1 | *Epomohorus* | 2011; PanBtCoV/9 nested PCR | - | 2011-04-15 | Rack 1; Box3 | Qiagen/UP/22/10/10 | |
| Up403 | Fecal Swab | Cave 1 | *Rousettus* | 2010; MSc with Woo et al. 2005 | - | 2010-05-11 | Rack1; Box2 | Qiagen kit at NICD | |
| | | | | *Followed up with nested PCR* | - | 2011-01-21 | | | |
| Up404 | Fecal Swab | Cave 1 | *Rousettus* | 2010; MSc with Woo et al. 2005 | - | 2010-05-24 | Rack1; Box2 | Qiagen kit at NICD | |
| | | | | *Followed up with nested PCR* | - | 2011-01-20 | | | |
| Up405 | Fecal Swab | Cave 1 | *Rousettus* | 2010; MSc with Woo et al. 2005 | - | 2010-05-26 | Rack1; Box2 | Qiagen kit at NICD | |

| | | | | | | | | | |
|---|---|---|---|---|---|---|---|---|---|
| | | | | *Followed up with nested PCR* | - | 2011-01-25 | | | |
| Up406 | Fecal Swab | Cave 1 | *Rousettus* | 2010; MSc with Woo et al. 2005 | - | 2010-05-11 | Rack1; Box2 | Qiagen kit at NICD | |
| | | | | *Followed up with nested PCR* | - | 2011-01-21 | | | |
| Up407 | Fecal Swab | Cave 1 | *Rousettus* | 2010; MSc with Woo et al. 2005 | - | 2010-05-24 | Rack1; Box2 | Qiagen kit at NICD | |
| | | | | *Followed up with nested PCR* | - | 2011-01-20 | | | |
| Up408 | Fecal Swab | Cave 1 | *Rousettus* | 2010; MSc with Woo et al. 2005 | - | 2010-05-11 | Rack1; Box2 | Qiagen kit at NICD | |
| | | | | *Followed up with nested PCR* | - | 2011-01-21 | | | |
| **Up409*** | **Fecal Swab** | **Cave 1** | ***Rousettus*** | **2010; MSc with Woo et al. 2005** | **faint band; 440** | **2010-05-26** | **Rack1; Box2** | **Qiagen kit at NICD** | |
| | | | | **2010; MSc with Woo et al. 2005** | **faint band** | **2010-05-28** | | | |
| | | | | *Followed up with nested PCR* | - | 2011-01-25 | | | |
| | | | | 2011; PanBtCoV/9 nested PCR | - | 2011-04-19 | | | |
| Up410 | Fecal Swab | Cave 1 | *Rousettus* | 2010; MSc with Woo et al. 2005 Twice | - | 2010-05-12 | Rack1; Box2 | Qiagen kit at NICD | |
| | | | | *Followed up with nested PCR* | - | 2011-01-20 | | | |
| Up411 | Fecal Swab | Cave 1 | *Rousettus* | 2010; MSc with Woo et al. 2005 | - | 2010-05-17 | Rack1; Box2 | Qiagen kit at NICD | |
| | | | | *Followed up with nested PCR* | - | 2011-01-18 | | | |
| Up417 | Fecal | Cave 1 | *Rousettus* | 2009; (Hons.)Tong Protocol | - | 2009-09-03 | Rack1; Box2 | Qiagen kit at NICD | |
| | | | | 2011; PanBtCoV/9 nested PCR | - | 2011-05-24 | | | |
| Up418 | Fecal Swab | Cave 1 | *Rousettus* | 2010; MSc with Woo et al. 2005 | - | 2010-05-11 | Rack1; Box2 | Qiagen kit at NICD | |
| | | | | *Followed up with nested PCR* | - | 2011-01-21 | | | |
| **Up419*** | **Fecal Swab** | **Cave 1** | ***Rousettus*** | **2010; MSc with Woo et al. 2005** | **faint band** | **2010-05-24** | **Rack1; Box2** | **Qiagen kit at NICD** | |
| | | | | 2010; MSc with Woo et al. 2005 | - | 2010-05-28 | | | |
| | | | | 2010; 1 primer heminested | - | 2010-11-17 | | | |
| | | | | *Followed up with nested PCR* | - | 2011-01-20 | | | |
| | | | | 2011; PanBtCoV/9 nested PCR | - | 2011-04-17 | | | |
| Up421 | Fecal Swab | Cave 1 | *Rousettus* | 2010; MSc with Woo et al. 2005 | - | 2010-05-17 | Rack1; Box2 | Qiagen kit at NICD | Died durind Handling |
| | | | | *Followed up with nested PCR* | - | 2011-01-18 | | | |
| Up423 | Fecal Swab | Cave 1 | *Rousettus* | 2010; MSc with Woo et al. 2005 | - | 2010-05-18 | Rack1; Box2 | Qiagen kit at NICD | |
| | | | | *Followed up with nested PCR* | - | 2010-01-20 | | | |
| Up424 | Fecal Swab | Cave 1 | *Rousettus* | 2010; MSc with Woo et al. 2005 | - | 2010-05-18 | Rack1; Box2 | Qiagen kit at NICD | |
| | | | | *Followed up with nested PCR* | - | 2011-01-20 | | | |
| Up426 | Fecal | Cave 1 | *Rousettus* | 2010; 1 primer heminested | - | 2010-08-04 | Rack1; Box5 | | |
| Up433 | Fecal | | *Rousettus* | 2010; 1 primer heminested | NtD | 2010-08-04 | NO MORE RNA | Qiagen kit at NICD | |
| | | | | 2010; 1 primer heminested | - | 2010-11-11 | Rack1; Box3 | | |
| **Up441*** | **Fecal** | **Cave 2** | ***Rhinolopus*** | **2011; PanBtCoV/9 nested PCR** | **Nest+** | **2011-05-24** | **Rack1; Box5** | **Qiagen kit at NICD** | **Hair loss, red throat& skin leasions,red ears** |
| | | | | | | | | | **Sequencing: Betacoronavirus** |
| **Up442*** | **Fecal** | **Cave 2** | ***Rhinolopus*** | 2009; (Hons.)Tong Protocol | - | 2009-08-26 | Rack1; Box2 | Qiagen kit at NICD | Lactating |
| | | | | **2011; PanBtCoV/9 nested PCR** | **Nest+** | **2011-05-04** | | | **Sequencing confirms false positive: SARS-CoV Taiwan** |
| Up443 | Fecal | Cave 2 | *Rhinolopus* | 2011; PanBtCoV/9 nested PCR | - | 2011-05-13 | Rack1; Box5 | Qiagen kit at NICD | Lactating |
| | | | | 2011; PanBat/AB/6 | - | 2011-09-23 | | | |
| | Fecal | | | 2011; PanBtCoV/9 nested PCR | - | 2011-05-13 | Rack1; Box3 | Qiagen/UP/27/10/10 | |
| | | | | 2011; PanBat/AB/6 | - | 2011-09-23 | | | |

| | | | | | | | | | |
|---|---|---|---|---|---|---|---|---|---|
| Up444 | Fecal | Cave 2 | *Rhinolopus* | 2011; PanBtCoV/9 nested PCR | - | 2011-05-24 | Rack1; Box5 | Qiagen kit at NICD | euthanized,lots of parasites and under weight |
| **Up445*** | **Fecal** | **Cave 2** | ***Rhinolopus*** | **2011; PanBtCoV/9 nested PCR** | **Nest+** | **2011-04-15** | **Rack1; Box3** | **Qiagen/UP/22/10/10** | **Scrotal male; Sequencing: Betacoronavirus** |
| Up446 | Fecal | Cave 2 | *Rhinolopus* | 2009; (Hons.)Tong Protocol | - | 2009-08-26 | Rack1; Box2 | Qiagen kit at NICD | Pregnant |
| | | | | 2010; MSc with Woo et al. 2005 | - | 2010-05-26 | | | |
| | | | | *Followed up with nested PCR* | - | 2011-01-25 | | | |
| **Up450** | **Fecal** | **Cave 1** | ***Hipposideros*** | **2010; 1 primer heminested** | **Nest faint +** | **2010-08-05** | **Rack1; Box5** | **Qiagen kit at NICD** | **Died** |
| | | | | 2010; 1 primer heminested | Smear | 2010-08-13 | | | **faint amplification observed several times; no Seq.** |
| | | | | 2010; 1 primer heminested | NtD | 2010-08-26 | | | |
| | | | | 2011; PanBtCoV/9 nested PCR | - | 2011-05-04 | | | |
| | Fecal | | | 2011; PanBtCoV/9 nested PCR | + | 2011-04-20 | Rack1; Box3 | Qiagen/UP/15/09/10 | **faint amplification observed several times; no Seq.** |
| | | | | 2011; PanBtCoV/9 nested PCR | - | 2011-05-04 | | | |
| **Up452** | **Fecal** | **Cave 1** | ***Otomops*** | **2010; 1 primer heminested** | **Nest faint +** | **2010-08-04** | **Rack1; Box5** | **Qiagen kit at NICD** | |
| | | | | 2010; 1 primer heminested | Smear | 2010-08-13 | | | |
| | | | | 2010; 1 primer heminested | NtD | 2010-08-26 | | | |
| | | | | **2011; PanBtCoV/9 nested PCR** | **+** | **2011-04-20** | | | **faint amplification observed several times; no Seq.** |
| | | | | 2011; PanBtCoV/9 nested PCR | - | 2011-05-04 | | | |
| | **Fecal** | | | **2011; PanBtCoV/9 nested PCR** | **+** | **2011-04-20** | **Rack1; Box3** | **Qiagen/UP/15/09/10** | **faint amplification observed several times; no Seq.** |
| | | | | 2011; PanBtCoV/9 nested PCR | - | 2011-05-04 | | | |
| Up455 | Fecal | Cave 1 | *Otomops* | 2011; PanBtCoV/9 nested PCR | | | Rack1; Box5 | Qiagen kit at NICD | |
| Up463 | Fecal | Cave 1 | *Otomops* | 2009; (Hons.)Tong Protocol | - | 2009-09-03 | Rack1; Box2 | Qiagen kit at NICD | |
| | | | | 2011; PanBtCoV/9 nested PCR | - | 2011-05-05 | | | |
| | fecal | | | 2011; PanBtCoV/9 nested PCR | - | 2011-09-26 | Rack1; Box3 | Qiagen/UP/15/09/10 | |
| | | | | 2011; PanBtCoV/9 nested PCR | - | 2011-09-26 | | | |
| Up476 | Fecal | Cave 1 | *Rousettus* | 2010; 1 primer heminested | NtD | 2010-08-04 | Rack1; Box5 | | |
| Up477 | Fecal Swab | Cave 1 | *Rousettus* | 2010; MSc with Woo et al. 2005 | - | 2010-05-12 | Rack1; Box2 | Qiagen kit at NICD | Lactating |
| | | | | *Followed up with nested PCR* | - | 2011-01-20 | | | |
| **Up478*** | **Fecal Swab** | **Cave 1** | ***Rousettus*** | **2010; MSc with Woo et al. 2005** | **faint band** | **2010-05-24** | **Rack1; Box2** | **Qiagen kit at NICD** | **Urine swab** |
| | | | | **2010; MSc with Woo et al. 2005** | **faint band** | **2010-05-28** | | | **Faint band - positive control amplification** |
| | | | | 2010; 1 primer heminested | - | 2010-11-16 | | | |
| | | | | *Followed up with nested PCR* | - | 2011-01-20 | | | |
| | | | | 2011; PanBtCoV/9 nested PCR | - | 2011-04-17 | | | |
| Up479 | Fecal Swab | Cave 1 | *Rousettus* | 2010; MSc with Woo et al. 2005 | - | 2010-05-18 | Rack1; Box2 | Qiagen kit at NICD | |
| | | | | *Followed up with nested PCR* | - | 2011-01-20 | | | |
| Up480 | Fecal | Cave 1 | *Rousettus* | 2010; MSc with Woo et al. 2005 | - | 2010-05-12 | Rack1; Box2 | Qiagen kit at NICD | |
| | | | | *Followed up with nested PCR* | - | 2011-01-20 | | | |
| | Fecal Swab | | | 2011; PanBat/AB/6 | - | 2011-09-26 | Rack1; Box3 | Qiagen/UP/27/10/10 | |
| Up481 | Fecal Swab | Cave 1 | *Rousettus* | 2010; MSc with Woo et al. 2005 | 400bp band | 2011-05-10 | Rack1; Box2 | Qiagen kit at NICD | Sequencing confirms PCR contamination |
| | | | | 2010; MSc with Woo et al. 2005 | 400bp band | 2010-05-18 | | | |
| | | | | *Followed up with nested PCR* | - | 2010-11-16 | | | |
| | | | | 2011; PanBtCoV/9 nested PCR | - | 2011-04-19 | | | |
| Up482 | Fecal Swab | | *Rousettus* | 2010; MSc with Woo et al. 2005 | - | 2010-05-12 | Rack1; Box2 | Qiagen kit at NICD | |
| | | | | *Followed up with nested PCR* | - | 2011-01-20 | | | |

| | | | | | | | | | |
|---|---|---|---|---|---|---|---|---|---|
| Up483 | Fecal Swab | Cave 1 | *Rousettus* | 2010; MSc with Woo et al. 2005 | - | 2010-05-26 | Rack1; Box2 | Qiagen kit at NICD | |
| | | | | *Followed up with nested PCR* | - | 2011-01-25 | | | |
| Up484 | Fecal Swab | Cave 1 | *Rousettus* | 2010; MSc with Woo et al. 2005 | - | 2010-05-18 | Rack1; Box2 | Qiagen kit at NICD | |
| | | | | *Followed up with nested PCR* | - | 2011-01-20 | | | |
| Up486 | Fecal | Cave 1 | *Rousettus* | 2009; (Hons.)Tong Protocol | - | 2009-09-03 | NO MORE RNA | | |
| | | | | 2010; MSc with Woo et al. 2005 | - | 2010-05-26 | | | |
| | | | | *Followed up with nested PCR* | - | 2011-01-25 | | | |
| | | | | 2011; PanBtCoV/9 nested PCR | - | 2011-05-05 | | | |
| **Up487*** | **Fecal Swab** | **Cave 1** | ***Rousettus*** | **2010; MSc with Woo et al. 2005** | **faint band** | **2010-05-26** | **Rack1; Box2** | **Qiagen kit at NICD** | |
| | | | | **2010; MSc with Woo et al. 2005** | **faint band** | **2010-05-28** | | | |
| | | | | 2010; 1 primer heminested | - | 2010-11-16 | | | |
| | | | | *Followed up with nested PCR* | - | 2011-01-25 | | | |
| | | | | 2011; PanBtCoV/9 nested PCR | - | 2011-04-19 | | | |
| **Up488*** | **Fecal Swab** | **Cave 1** | ***Rousettus*** | **2010; MSc with Woo et al. 2005** | **faint band** | **2010-05-24** | **Rack1; Box2** | **Qiagen kit at NICD** | |
| | | | | *Followed up with nested PCR* | - | 2011-01-20 | | | |
| | | | | 2011; PanBtCoV/9 nested PCR | - | 2011-05-05 | | | |
| Up490 | Fecal Swab | Cave 1 | *Rousettus* | 2010; MSc with Woo et al. 2005 | - | 2010-05-24 | Rack1; Box2 | Qiagen kit at NICD | |
| | | | | *Followed up with nested PCR* | - | 2011-01-25 | | | |
| Up491 | Fecal | Cave 1 | *Rousettus* | 2009; (Hons.)Tong Protocol | - | 2009-08-26 | NO MORE RNA | Qiagen kit at NICD | |
| | | | | 2011; PanBtCoV/9 nested PCR | - | 2011-05-05 | | | |
| Up494 | Fecal | Cave 1 | *Rousettus* | 2009; (Hons.)Tong Protocol | NtD | 2009-08-26 | Rack1; Box2 | Qiagen kit at NICD | |
| | | | | 2011; PanBtCoV/9 nested PCR | - | 2011-05-05 | | | |
| Up497 | Fecal | Cave 1 | *Rousettus* | 2011; PanBtCoV/9 nested PCR | REDO | 2011-05-10 | | | |
| Up498 | Fecal | Cave 1 | *Rousettus* | 2009; (Hons.)Tong Protocol | - | 2009-09-03 | Rack1; Box5 | Qiagen kit at NICD | |
| | | | | 2011; PanBtCoV/9 nested PCR | - | 2011-05-05 | | | |
| Up499 | Fecal Swab | Cave 1 | *Rousettus* | 2010; MSc with Woo et al. 2005 | - | 2010-05-06 | Rack1; Box2 | Qiagen kit at NICD | Pregnant and died after processing |
| | | | | *Followed up with nested PCR* | - | 2011-01-20 | | | |
| **Up500*** | **Fecal** | **Cave 1** | ***Rousettus*** | 2009; (Hons.)Tong Protocol | - | 2009-08-26 | **NO MORE RNA** | **Qiagen kit at NICD** | |
| | | | | **2010; MSc with Woo et al. 2005** | **faint band** | **2010-05-26** | | | |
| | | | | 2010; 1 primer heminested | - | 2010-11-16 | | | |
| | | | | *Followed up with nested PCR* | - | 2011-01-25 | | | |
| | | | | 2011; PanBtCoV/9 nested PCR | - | 2011-04-19 | | | |
| Up501 | Fecal | Cave 1 | *Rousettus* | 2011; PanBtCoV/9 nested PCR | - | 2011-05-13 | Rack1; Box5 | Qiagen kit at NICD | |
| | Fecal | | | 2010; 1 primer heminested | - | 2010-11-16 | Rack1; Box3 | Qiagen/UP/16/09/10 | |
| | | | | 2011; PanBat/AB/6 | - | 2011-09-23 | | | |
| Up505 | Fecal Swab | Cave 1 | *Rousettus* | 2010; MSc with Woo et al. 2005 | - | 2010-05-26 | Rack1; Box2 | Qiagen kit at NICD | |
| | | | | *Followed up with nested PCR* | REDO | 2011-01-25 | | | |
| Up506 | Fecal Swab | Cave 1 | *Rousettus* | 2010; MSc with Woo et al. 2005 | - | 2010-05-12 | Rack1; Box2 | Qiagen kit at NICD | |
| | | | | *Followed up with nested PCR* | - | 2011-01-20 | | | |
| Up507 | Fecal Swab | Cave 1 | *Rousettus* | 2010; MSc with Woo et al. 2005 | - | 2010-05-12 | Rack1; Box2 | Qiagen kit at NICD | |
| | | | | *Followed up with nested PCR* | - | 2011-01-19 | | | |
| Up508 | Fecal Swab | Cave 1 | *Rousettus* | 2010; MSc with Woo et al. 2005 | - | 2017-05-10 | Rack1; Box 2 | Qiagen kit at NICD | |

| | | | | | | | | | |
|---|---|---|---|---|---|---|---|---|---|
| | | | | *Followed up with nested PCR* | - | 2011-01-18 | | | |
| Up509 | Fecal Swab | Cave 1 | *Rousettus* | 2010; MSc with Woo et al. 2005 | - | 2010-05-11 | Rack1; Box2 | Qiagen kit at NICD | |
| | | | | 2010; 1 primer heminested | - | 2010-11-16 | | | |
| | | | | *Followed up with nested PCR* | - | 2010-01-20 | | | |
| | | | | 2011; PanBtCoV/9 nested PCR | - | 2011-04-19 | | | |
| Up513 | Fecal Swab | Cave 1 | *Rousettus* | 2010; MSc with Woo et al. 2005 | - | 2010-05-11 | Rack1; Box2 | Qiagen kit at NICD | Pregnant |
| | | | | *Followed up with nested PCR* | - | 2011-01-20 | | | |
| Up514 | Fecal Swab | Cave 1 | *Rousettus* | 2010; MSc with Woo et al. 2005 | - | 2010-05-11 | Rack1; Box2 | Qiagen kit at NICD | |
| | | | | *Followed up with nested PCR* | - | 2011-01-20 | | | |
| Up519 | Fecal | Cave 1 | *Rousettus* | 2010; 1 primer heminested | - | 2010-11-11 | Rack1; Box3 | Qiagen/UP/15/09/10 | |
| | | | | 2011; AB nested - 9 primer mix | - | 2011-05-13 | | | |
| | | | | 2011; PanBat/AB/6 | - | 2011-09-23 | | | |
| Up520 | Fecal | Cave 1 | *Rousettus* | 2011; PanBtCoV/9 nested PCR | - | 2011-04-15 | Rack1; Box3 | Qiagen/UP/16/09/10 | |
| Up525 | Fecal | Cave 1 | *Rousettus* | 2009; (Hons.)Tong Protocol | - | 2009-08-31 | Rack1; Box2 | Qiagen kit at NICD | |
| | | | | 2011; AB primer mix; RTaNdt | - | 2011-04-15 | | | |
| **Up530*** | **Fecal** | **Cave 1** | ***Otomops*** | 2009; (Hons.)Tong Protocol | - | 2009-08-31 | **Rack1; Box2** | **Qiagen kit at NICD** | |
| | | | | **2010; MSc with Woo et al. 2005** | **faint band** | **2010-05-26** | | | |
| | | | | **2010; MSc with Woo et al. 2005** | **faint band** | **2010-05-28** | | | |
| | | | | *Followed up with nested PCR* | - | 2011-01-25 | | | |
| | Fecal | | | 2010; 1 primer heminested | - | 2010-11-11 | Rack1; Box3 | Qiagen/UP/15/09/10 | |
| | | | | 2011; PanBtCoV/9 nested PCR | - | 2011-05-05 | | | |
| Up531 | Fecal | Cave 1 | *Otomops* | 2009; (Hons.)Tong Protocol | - | 2009-09-03 | Rack1; Box2 | Qiagen kit at NICD | |
| | | | | 2011; AB nested - 9 primer mix | - | 2011-05-05 | | | |
| Up534 | Fecal | Cave 1 | *Otomops* | 2009; (Hons.)Tong Protocol | - | 2009-08-31 | Rack1; Box2 | Qiagen kit at NICD | |
| | | | | 2011; PanBtCoV/9 nested PCR | - | 2011-05-05 | | | |
| | Fecal | | | 2010; 1 primer heminested | - | 2010-11-11 | ? | Qiagen/UP/15/09/10 | |
| | | | | 2011; PanBtCoV/9 nested PCR | - | 2011-05-05 | | | |
| Up538 | Fecal | Cave 1 | *Otomops* | 2009; (Hons.)Tong Protocol | - | 2009-09-03 | Rack1; Box2 | Qiagen kit at NICD | |
| | | | | 2011; PanBtCoV/9 nested PCR | - | 2011-05-03 | | | |
| Up582 | Fecal | Cave 1 | *Rousettus* | 2009; (Hons.)Tong Protocol | - | 2009-09-03 | Rack1; Box2 | Qiagen kit at NICD | |
| | | | | 2011; PanBtCoV/9 nested PCR | - | 2011-05-03 | | | |
| **Up583*** | **Fecal Swab** | **Cave 1** | ***Rousettus*** | 2010; MSc with Woo et al. 2005 | - | 2010-05-26 | **Rack1; Box2** | **Qiagen kit at NICD** | |
| | | | | **2010; MSc with Woo et al. 2005** | **faint band** | **2010-05-28** | | | |
| | | | | *Followed up with nested PCR* | - | 2011-01-25 | | | |
| | | | | 2011; PanBtCoV/9 nested PCR | - | 2011-05-03 | | | |
| Up584 | Fecal | Cave 1 | *Rousettus* | 2009; (Hons.)Tong Protocol | - | 2009-08-31 | Rack1; Box2 | Qiagen kit at NICD | |
| | | | | 2011; PanBtCoV/9 nested PCR | - | 2011-05-03 | | | |
| **Up585*** | **Fecal** | **Cave 1** | ***Rousettus*** | 2009; (Hons.)Tong Protocol | - | 2009-08-31 | **Rack1; Box2** | **Qiagen kit at NICD** | |
| | | | | **2010; MSc with Woo et al. 2005** | **faint band** | **2010-05-26** | | | |
| | | | | **2010; MSc with Woo et al. 2005** | **faint band** | **2010-05-28** | | | |
| | | | | 2011; PanBtCoV/9 nested PCR | - | 2011-05-03 | | | |
| | | | | 2010; 1 primer heminested | - | 2010-11-16 | | | |

| | | | | | | | | | |
|---|---|---|---|---|---|---|---|---|---|
| | | | | *MSc; RTWsNp 585A 585B* | - | 2011-01-25 | | | |
| | Fecal | | | 2011; PanBtCoV/9 nested PCR | - | 2011-04-17 | Rack1; Box3 | Qiagen/UP/15/09/10 | |
| Up586 | Fecal Swab | Cave 1 | *Rousettus* | 2010; MSc with Woo et al. 2005 | - | 2010-05-17 | Rack1; Box2 | Qiagen kit at NICD | Died after bleeding |
| | | | | *Followed up with nested PCR* | - | 2011-01-20 | | | |
| Up587 | Fecal Swab | | | 2010; MSc with Woo et al. 2005 | - | 2010-05-17 | Rack1; Box2 | Qiagen kit at NICD | |
| | | | | *Followed up with nested PCR* | - | 2011-01-20 | | | |
| Up588 | Fecal | Cave 1 | *Rousettus* | 2009; (Hons.)Tong Protocol | - | 2009-09-03 | Rack 1; Box5 | Qiagen kit at NICD | |
| | | | | 2011; PanBtCoV/9 nested PCR | - | 2011-05-03 | | | |
| Up589 | Fecal Swab | Cave 1 | *Rousettus* | 2010; MSc with Woo et al. 2005 | - | 2010-05-17 | Rack1; Box2 | Qiagen kit at NICD | |
| | | | | *Followed up with nested PCR* | - | 2011-01-20 | | | |
| | | | | 2011; PanBtCoV/9 nested PCR | - | 2011-05-03 | | | |
| | | | | 2011; PanBtCoV/9 nested PCR | - | 2011-09-23 | | | |
| Up591 | Fecal | Cave 1 | *Rousettus* | 2009; (Hons.)Tong Protocol | - | 2009-08-26 | Rack1; Box2 | Qiagen kit at NICD | |
| | | | | 2011; PanBtCoV/9 nested PCR | - | 2011-05-03 | | | |
| Up592 | Fecal | Cave 1 | *Rousettus* | 2011; PanBtCoV/9 nested PCR | - | 2011-04-15 | Rack 1; Box3 | Qiagen/UP/16/09/10 | |
| **Up593*** | **Fecal Swab** | **Cave 1** | ***Rousettus*** | 2009; (Hons.)Tong Protocol | - | 2009-08-31 | **Rack1; Box2** | **Qiagen kit at NICD** | |
| | | | | **2010; MSc with Woo et al. 2005** | **faint band** | **2010-05-24** | | | |
| | | | | **2010; MSc with Woo et al. 2005** | **faint band** | **2010-05-28** | | | |
| | | | | 2010; 1 primer heminested | - | 2010-11-16 | | | |
| | | | | *Followed up with nested PCR* | - | 2011-01-20 | | | |
| | Fecal | | | 2011; PanBtCoV/9 nested PCR | - | 2011-04-17 | Rack1; Box3 | Qiagen/UP/15/09/10 | |
| **Up594*** | **Fecal Swab** | **Cave 1** | ***Rousettus*** | **2010; MSc with Woo et al. 2005** | **faint band** | **2010-05-24** | **Rack1; Box2** | **Qiagen kit at NICD** | |
| | | | | **2010; MSc with Woo et al. 2005** | **faint band** | **2010-05-28** | | | |
| | | | | 2010; 1 primer heminested | - | 2010-11-16 | | | |
| | | | | *Followed up with nested PCR* | - | 2011-01-20 | | | |
| | | | | 2011; PanBtCoV/9 nested PCR | + | 2011-04-17 | Rack1; Box2 | | Sequencing confirms false positive: SARS-CoV Taiwan |
| **Up595*** | **Fecal** | **Cave 1** | ***Rousettus*** | **2009; (Hons.)Tong Primers** | **faint band** | **2009-08-31** | **Rack1; Box2** | **Qiagen kit at NICD** | |
| | | | | 2010; MSc with Woo et al. 2005 | - | 2010-05-18 | | | |
| | | | | *Followed up with nested PCR* | - | 2011-01-20 | | | |
| | | | | 2011; PanBtCoV/9 nested PCR | - | 2011-05-09 | | | |
| **Up597*** | **Fecal Swab** | **Cave 1** | ***Rousettus*** | **2010; MSc with Woo et al. 2005** | **faint band** | **2010-05-26** | **Rack1; Box2** | **Qiagen kit at NICD** | |
| | | | | **2010; MSc with Woo et al. 2005** | **faint band** | **2010-05-28** | | | |
| | | | | *Followed up with nested PCR* | - | 2011-01-25 | | | |
| | | | | 2011; PanBtCoV/9 nested PCR | - | 2011-05-09 | | | |
| Up598 | Fecal | Cave 1 | *Rousettus* | 2010; 1 primer heminested | - | 2010-11-11 | Rack1; Box2 | Qiagen/UP/15/09/10 | |
| | | | | PanBtCoV/9 nested PCR | - | 2011-05-13 | | | |
| Up599 | Fecal Swab | Cave 1 | *Rousettus* | 2010; MSc with Woo et al. 2005 | - | 2010-05-12 | Rack1; Box2 | Qiagen kit at NICD | |
| | | | | *Followed up with nested PCR* | - | 2011-01-19 | | | |
| Up601 | Fecal Swab | Cave 1 | *Rousettus* | 2010; MSc with Woo et al. 2005 | - | 2010-05-26 | Rack1; Box2 | Qiagen kit at NICD | |
| | | | | *Followed up with nested PCR* | - | 2011-01-25 | | | |
| Up602 | Fecal Swab | Cave 1 | *Rousettus* | 2010; MSc with Woo et al. 2005 | - | 2010-05-12 | Rack1; Box2 | Qiagen kit at NICD | |
| | | | | *Followed up with nested PCR* | - | 2011-01-19 | | | |

| | | | | | | | | | |
|---|---|---|---|---|---|---|---|---|---|
| Up606 | Fecal Swab | Cave 1 | *Rousettus* | 2010; MSc with Woo et al. 2005 | - | 2010-05-17 | Rack1; Box2 | Qiagen kit at NICD | |
| | | | | *Followed up with nested PCR* | - | 2011-01-20 | | | |
| Up619 | Fecal | Cave 1 | *Otomops* | 2011; PanBtCoV/9 nested PCR | - | 2011-04-15 | Rack1; Box3 | Trizol/UP/16/03/11 | |
| Up624 | Fecal | Cave 1 | *Otomops* | 2010; 1 primer heminested | NtD | 2010-08-04 | Rack1; Box5 | Qiagen kit at NICD | |
| | | | | 2010; 1 primer heminested | Smear | 2010-08-13 | | | |
| | | | | 2011; PanBtCoV/9 nested PCR | - | 2011-05-13 | | | |
| | | | | 2011; PanBat/AB/6 | - | 2011-09-23 | | | |
| | Fecal | | | 2010; 1 primer heminested | - | 2010-11-11 | Rack1; Box3 | Qiagen/UP/16/09/10 | |
| | | | | 2011; PanBtCoV/9 nested PCR | - | 2011-05-13 | | | |
| | | | | 2011; PanBat/AB/6 | - | 2011-09-23 | | | |
| Up625 | Fecal | Cave 1 | *Otomops* | 2010; 1 primer heminested | - | 2010-11-11 | Rack1; Box3 | Qiagen/UP/15/09/10 | |
| | | | | 2011; PanBtCoV/9 nested PCR | - | 2011-05-13 | | | |
| **Up626*** | **Fecal** | **Cave 1** | ***Otomops*** | **2010; 1 primer heminested** | **Nest+220bp** | **2010-08-04** | **Rack1; Box5** | **Qiagen kit at NICD** | |
| | | | | 2010; 1 primer heminested | NtD | 2010-08-13 | | | |
| | | | | 2010; 1 primer heminested | NtD | 2010-08-26 | | | |
| | | | | 2011; PanBtCoV/9 nested PCR | - | 2011-05-03 | | | |
| | **Fecal** | | | **2010; 1 primer heminested** | **Nest+220bp** | **2010-11-11** | **Rack1; Box3** | **Qiagen/UP/15/09/10** | |
| | | | | 2011; PanBtCoV/9 nested PCR | - | 2011-05-03 | | | |
| Up627 | Fecal | Cave 1 | *Otomops* | 2010; 1 primer heminested | - | 2010-11-11 | Rack1; Box3 | Qiagen/UP/27/10/10 | |
| | | | | 2011; PanBtCoV/9 nested PCR | - | 2011-05-13 | | | |
| | | | | 2011; PanBat/AB/6 | - | 2011-09-23 | | | |
| Up634 | Fecal | Cave 1 | *Otomops* | 2010; 1 primer heminested | - | 2010-08-04 | Rack1; Box5 | Qiagen kit at NICD | |
| | | | | 2011; PanBat/AB/6 | - | 2011-09-23 | | | |

# Chapter 6: References

ICTV Virus Taxonomy: 2009 release. Available online: http://icvtvonline.org/virusTaxonomy.asp?version=2009

Beaudette, F. R., and Hudson, C. R. (1937). Cultivation of the virus of infectious bronchitis. *Journal of the American Veterinary Medical Association* **90,** 51-60.

Benbacer, L., Kut, E., Besnardeau, L., Laude, H., and Delmas, B. (1997). Interspecies Aminopeptidase-N Chimeras Reveal Species-Specific Receptor Recognition by Canine Coronavirus, Feline Infectious Peritonitis Virus, and Transmissible Gastroenteritis Virus. *Journal of Virology* **71**(1)**,** 734-737.

Brandão, P. E., Scheffer, K., Villarreal, L. Y., Achkar, S.*, et al.* (2008). A Coronavirus Detected in the Vampire Bat Desmodus rotundus. *The Brazilian Journal of Infectious Diseases* **12**(6).

Calisher, C. H., Childs, J. E., Field, H. E., Holmes, K. V., and Schountz, T. (2006). Bats: Important Reservoir Hosts of Emerging Viruses. *Clinical Microbiology Reviews* **19**(3)**,** 531-545.

Carrington, C. V. F., Foster, J. E., Zhu, H. C., Zhang, J. X.*, et al.* (2008). Detection and Phylogenetic Analysis of Group 1 Coronaviruses in South American Bats. *Emerging Infectious Diseases* **14**(12)**,** 1890-1893.

Chu, D. K. W., Poon, L. L. M., Chan, K. H., Chen, H., Guan, Y., Yuen, K. Y., and Peiris, J. S. M. (2006). Coronaviruses in bent-winged bats (Miniopterus spp.). *Journal of General Virology* **87**(9)**,** 2461-2466.

Crameri, G., Todd, S., Grimley, S., McEachern, J. A.*, et al.* (2009). Establishment, Immortalisation and Characterisation of Pteropid Bat Cell Lines. *PLoS One* **4**(12)**,** e8266.

de Souza Luna, L. K., Heiser, V., Regamey, N., Panning, M.*, et al.* (2007). Generic Detection of Coronaviruses and Differentiation at the Prototype Strain Level by Reverse Transcription-PCR and Nonfluorescent Low-Density Microarray. *Journal of Clinical Microbiology* **45**(3)**,** 1049-1052.

Delmas, B., Gelfi, J., L'Haridon, R., Vogel, L. K., Sjostrom, H., Noren, O., and Laude, H. (1992). Aminopeptidase N is a major receptor for the entero-pathogenic coronavirus TGEV. *Nature* **357,** 417-420.

Delmas, B., Gelfi, J., Sjostrom, H., Noren, O., and Laude, H. (1994). Further characterization of aminopeptidase-N as a receptor for coronaviruses. *Advances in Experimental Medicine and Biology* **342,** 293-298.

Dominguez, S. R., O'Shea, T. J., Oko, L. M., and Holmes, K. V. (2007). Detection of Group I Coronaviruses in Bats in North America. *Emerging and Infectious Diseases* **13**(9)**,** 1295-1300

Dong, B. Q., Liu, W., Fan, X. H., Vijaykrishna, D.*, et al.* (2007). Detection of a Novel and Highly Divergent Coronavirus from Asian Leopard Cats and Chinese Ferret Badgers in Southern China. *Journal of Virology* **81**(13)**,** 6920-6926.

Drexler, J. F., Corman, V. M., Wegner, T., Tateno, A. F.*, et al.* (2011). Amplification of Emerging Viruses in a Bat Colony. *Emerging Infectious Diseases* **17**(3)**,** 449-456.

Drexler, J. F., Gloza-Rausch, F., Glende, J., Corman, V. M.*, et al.* (2010). Genomic Characterization of Severe Acute Respiratory Syndrome-Related Coronavirus in European Bats and Classification of Coronaviruses Based on Partial RNA-Dependent RNA Polymerase Gene Sequences. *Journal of Virology* **84**(21)**,** 11336-11349.

Eick, G. N., Jacobs, D. S., and Matthee, C. A. (2005). A Nuclear DNA Phylogenetic Perspective on the Evolution of Echolocation and Historical Biogeography of Extant Bats (Chiroptera). *Molecular Biology and Evolution* **22**(9)**,** 1869-1886.

Falcón, A., Vázquez-Morón, S., Casas, I., Aznar, C., *et al.* (2011). Detection of alpha and betacoronaviruses in multiple Iberian bat species. *Archives of Virology* **156**(10)**,** 1883-1890.

Frackman, S., Kobs, G., Simpson, D., and Storts, D. (1998). Betaine and DMSO: Enhancing Agents for PCR. *Promega Notes*(65)**,** 27-30.

Gloza-Rausch, F., Ipsen, A., Seebens, A., Göttsche, M., *et al.* (2008). Detection and Prevalence Patterns of Group I Coronaviruses in Bats, Northern Germany. *Emerging and Infectious Diseases* **14**(4)**,** 626-632.

Gonzãlez, J. M., Gomez-Puertas, P., Cavanagh, D., Gorbalenya, A. E., and Enjuanes, L. (2003). A comparative sequence analysis to revise the current taxonomy of the family Coronaviridae. *Archives of Virology* **148**(11)**,** 2207-2235.

Gorbalenya, A., Enjuanes, L., Ziebuhr, J., and Snijder, E. (2006). Nidovirales: Evolving the largest RNA virus genome. *Virus Research* **117**(1)**,** 17-37.

Gorbalenya, A., Snijder, E. J., and Spaan, W. J. M. (2004). Severe Acute Respiratory Syndrome Coronavirus Phylogeny: toward Consensus. *Journal of Virology* **78**(15)**,** 7863-7866.

Gouilh, M. A., Puechmaille, S. J., Gonzalez, J.-P., Teeling, E., Kittayapong, P., and Manuguerra, J.-C. (2011). SARS-Coronavirus ancestor's foot-prints in South-East Asian bat colonies and the refuge theory. *Infection, Genetics and Evolution* **11**(7)**,** 1690-1702.

Guan, X. R., Zheng, B., He, Y. Q., Liu, X. L., *et al.* (2003). Isolation and Characterization of Viruses Related to the SARS Coronavirus from Animals in Southern China. *Science* **302**(5643)**,** 276-278.

Hall, T. A. (1999). BioEdit: a user-friendly biological sequence alignment editor and analysis program for Windows 95/98/NT. *Nucleic Acids Symposium Series* **41,** 95-98.

He, Y., Li, J., Li, W., Lustigman, S., Farzan, M., and Jiang, S. (2006). Cross-Neutralization of Human and Palm Civet Severe Acute Respiratory Syndrome Coronaviruses by Antibodies Targeting the Receptor-Binding Domain of Spike Protein. *The Journal of Immunology* **176,** 6085-6092.

He, Y. L., Wu, Y. H., He, X. N., Liu, F. J., He, X. Y., and Zhang, Y. (2009). An immortalized goat mammary epithelial cell line induced with human telomerase reverse transcriptase (hTERT) gene transfer. *Theriogenology* **71**(9)**,** 1417-1424.

Hofmann, H., Pyrc, K., van der Hoek, L., Geier, M., Berkhout, B., and Pohlmann, S. (2005). Human coronavirus NL63 employs the severe acute respiratory syndrome coronavirus receptor for cellular entry. *Proceedings of the National Academy of Sciences* **102**(22)**,** 7988-7993.

Holmes, E. C., and Rambaut, A. (2004). Viral evolution and the emergence of SARS coronavirus. *Philosophical Transactions of the Royal Society B: Biological Sciences* **359**(1447)**,** 1059-1065.

Hon, C. C., Lam, T. Y., Shi, Z. L., Drummond, A. J., *et al.* (2008). Evidence of the Recombinant Origin of a Bat Severe Acute Respiratory Syndrome (SARS)-Like Coronavirus and Its Implications on the Direct Ancestor of SARS Coronavirus. *Journal of Virology* **82**(4)**,** 1819-1826.

Hutcheon, J. M., and Kirsch, J. A. W. (2006). A moveable face deconstructing the Microchiroptera and a new classification of extant bats. *Acta Chiropterologica* **8**(1)**,** 1-10.

Kan, B., Wang, M., Jing, H., Xu, H., *et al.* (2005). Molecular Evolution Analysis and Geographic Investigation of Severe Acute Respiratory Syndrome Coronavirus-Like Virus in Palm Civets at an Animal Market and on Farms. *Journal of Virology* **79**(18)**,** 11892-11900.

Ksiazek, T. G., Erdman, D., Goldsmith, C. S., Zaki, S. R., *et al.* (2003). A Novel Coronavirus Associated with Severe Acute Respiratory Syndrome'. . Vol. , No. ; pp. . *The New England Journal of Medicine* **348**(20)**,** 1953-1966.

Kwak, S., Jung, J., Jin, X., Kim, S., *et al.* (2006). Establishment of Immortal Swine Kidney Epithelial Cells. *Animal Biotechnology* **17**(1)**,** 51-58.

Lau, S. K. P., Li, K. S. M., Huang, Y., Shek, C. T., *et al.* (2010a). Ecoepidemiology and Complete Genome Comparison of Different Strains of Severe Acute Respiratory Syndrome-Related Rhinolophus Bat Coronavirus in China Reveal Bats as a Reservoir for Acute, Self-Limiting Infection That Allows Recombination Events. *Journal of Virology* **84**(6)**,** 2808-2819.

Lau, S. K. P., Poon, R. W. S., Wong, B. H. L., Wang, M., *et al.* (2010b). Coexistence of Different Genotypes in the Same Bat and Serological Characterization of Rousettus Bat Coronavirus HKU9 Belonging to a Novel Betacoronavirus Subgroup. *Journal of Virology* **84**(21)**,** 11385-11394.

Lau, S. K. P., Woo, P. C. Y., Li, K. S. M., Huang, Y., *et al.* (2005a). Diversity of Coronaviruses in Bats: Insights Into Origin of SARS Coronavirus. *13th International Congress on Infectious Diseases Abstracts (Oral Presentations)* **14.005,** e52.

Lau, S. K. P., Woo, P. C. Y., Li, K. S. M., Huang, Y., *et al.* (2005b). Severe acute respiratory syndrome coronavirus-like virus in Chinese horseshoe bats. *Proceedings of the National Academy of Sciences* **102**(39)**,** 14040-14045.

Lau, S. K. P., Woo, P. C. Y., Li, K. S. M., Huang, Y., *et al.* (2007). Complete genome sequence of bat coronavirus HKU2 from Chinese horseshoe bats revealed a much smaller spike gene with a different evolutionary lineage from the rest of the genome. *Virology* **367**(2)**,** 428-439.

Li, W., Moore, M. J., Vasilieva, N., Sui, J., *et al.* (2003). Angiotensin-converting enzyme 2 is a functional receptor for the SARS coronavirus. *Nature* **426,** 450-454.

Li, W., Shi, Z., Yu, M., Ren, W., *et al.* (2005). Bats Are Natural Reservoirs of SARS-Like Coronaviruses. *Science* **310**(5748)**,** 676-679.

Marra, M. A., Jones, S. J. M., Astell, C. R., Holt, R. A., *et al.* (2003). The Genome Sequence of the SARS-Associated Coronavirus. *Science* **300**(5624)**,** 1399-1404.

Masters, P. (2006). The Molecular Biology of Coronaviruses. *Advances in Virus Research* **66,** 193-292.

Mihindukulasuriya, K. A., Wu, G., St. Leger, J., Nordhausen, R. W., and Wang, D. (2008). Identification of a Novel Coronavirus from a Beluga Whale by Using a Panviral Microarray. *Journal of Virology* **82**(10)**,** 5084-5088.

Miller-Butterworth, C. M., Murphy, W. J., O'Brien, S. J., Jacobs, D. S., Springer, M. S., and Teeling, E. C. (2007). A Family Matter: Conclusive Resolution of the Taxonomic Position of the Long-Fingered Bats, Miniopterus. *Molecular Biology and Evolution* **24**(7)**,** 1553-1561.

Müller, M. A., Paweska, J. T., Leman, P. A., Drosten, C., *et al.* (2007). Coronavirus Antibodies in African Bat species , Vol. , No. ; pp. . *Emerging Infectious Diseases* **13**(9)**,** 1367-1370.

Nedellec, P., Dveksler, G. S., Daniels, E., Turbine, C., *et al.* (1994). Bgp2, a New Member of the Carcinoembryonic Antigen-Related Gene Family, Encodes an Alternative Receptor for Mouse Hepatitis Viruses. *Journal of Virology* **68**(7)**,** 4525-4537.

Osborne, C., Cryan, P. M., O'Shea, T. J., Oko, L. M., *et al.* (2011). Alphacoronaviruses in New World Bats: Prevalence, Persistence, Phylogeny, and Potential for Interaction with Humans. *PLoS One* **6**(5)**,** e19156.

Perlman, S., and Netland, J. (2009). Coronaviruses post-SARS: update on replication and pathogenesis. *Nature Reviews Microbiology* **7**(6)**,** 439-450.

Pfefferle, S., Oppong, S., Drexler, J. F., Gloza-Rausch, F., *et al.* (2009). Distant Relatives of Severe Acute Respiratory Syndrome Coronavirus and Close Relatives of Human Coronavirus 229E in Bats, Ghana. *Emerging Infectious Diseases*, 1377-1384.

Poon, L. L. M., Chu, D. K. W., Chan, K. H., Wong, O. K., *et al.* (2005). Identification of a Novel Coronavirus in Bats. *Journal of Virology* **79**(4), 2001-2009.

Quan, P. L., Firth, C., Street, C., Henriquez, J. A., *et al.* (2010). Identification of a Severe Acute Respiratory Syndrome Coronavirus-Like Virus in a Leaf-Nosed Bat in Nigeria. *MBio* **1**(4), e00208-10-e00208-18.

Reusken, C. B. E. M., Lina, P. H. C., Pielaat, A., de Vries, A., *et al.* (2010). Circulation of Group 2 Coronaviruses in a Bat Species Common to Urban Areas in Western Europe. *Vector-borne and Zoonotic Disaeases* **10**(00), 1-8.

Rihtarič, D., Hostnik, P., Steyer, A., Grom, J., and Toplak, I. (2010). Identification of SARS-like coronaviruses in horseshoe bats (Rhinolophus hipposideros) in Slovenia. *Archives of Virology* **155**(4), 507-514.

Schultze, B., Gross, H., Brossmer, R., and Herrleri, G. (1991). The S Protein of Bovine Coronavirus Is a Hemagglutinin Recognizing 9-0-Acetylated Sialic Acid as a Receptor Determinant. *Journal of Virology* **65**(11), 6232-6237.

Shirato, K., Maeda, K., Tsuda, S., Suzuki, K., *et al.* (2011). Detection of bat coronaviruses from Miniopterus fuliginosus in Japan. *Virus Genes*.

Simmons, N. B. (2005). An Eocene Big Bang for Bats. *Science* **307**(5709), 527-528.

Smith, C. S., de Jong, C. E., Crameri, G., McEachern, J., *et al.* (2010). *Identification and inter-species transmission of Australian bat coronaviruses: the precursors for emergence and indications of host taxonomy tropism suggesting co-evolution. Unpublished data presented at Australian Biosecurity Cooperative Research Centre for Emerging Infectious Disease, Brisbane, 28 February - 3 March 2010.*

Smith, C. S., de Jong, C. E., Crameri, G., McEachern, J., *et al.* (2008). Molecular Identification of Group 1 and Group 2 Coronaviruses in Australian Bats. Manuscript submitted for publication.

Snijder, E. J., Bredenbeek, P. J., Dobbe, J. C., Thiel, V., *et al.* (2003). Unique and Conserved Features of Genome and Proteome of SARS-coronavirus, an Early Split-off From the Coronavirus Group 2 Lineage. *Journal of Molecular Biology* **331**(5), 991-1004.

Soloff, M. S. (2004). Immortalization and characterization of human myometrial cells from term-pregnant patients using a telomerase expression vector. *Molecular Human Reproduction* **10**(9), 685-695.

Song, H. D., Tub, C., Zhanga, G., Wang, S., *et al.* (2005). Cross-host evolution of severe acute respiratory syndrome coronavirus in palm civet and human. *Proceedings of the National Academy of Sciences* **102**(7), 2430-2435.

Stephensen, C. B., Casebolt, D. B., and Gangopadhyay, N. N. (1999). Phylogenetic analysis of a highly conserved region of the polymerase gene from 11 coronaviruses and development of a consensus polymerase chain reaction assay. *Virus Research* **60**, 181-189.

Tamura, K., Peterson, D., Peterson, N., Stecher, G., Nei, M., and Kumar, S. (2011). MEGA5: Molecular Evolutionary Genetics Analysis using Maximum Likelihood, Evolutionary Distance, and Maximum Parsimony Methods. *Molecular Biology and Evolution* **28**(10), 2731-2739.

Tang, X. C., Zhang, J. X., Zhang, S. Y., Wang, P., *et al.* (2006). Prevalence and Genetic Diversity of Coronaviruses in Bats from China. *Journal of Virology* **80**(15), 7481-7490.

Teeling, E. C., Springer, M. S., Madsen, O., Bates, P., O'Brien, S. J., and Murphy, W. J. (2005). A Molecular Phylogeny for Bats Illuminates Biogeography and the Fossil Record. *Science* **307**(5709)**,** 580-584.

Tong, S., Conrardy, C., Ruone, S., Kuzmin, I. V.*, et al.* (2009). Detection of Novel SARS-like and Other Coronaviruses in Bats from Kenya. *Emerging Infectious Diseases* **15**(3)**,** 482-485.

Tresnan, D. B., Levis, R., and Holmes, K. V. (1996). Feline Aminopeptidase N Serves as a Receptor for Feline, Canine, Porcine, and Human Coronaviruses in Serogroup I. *Journal of Virology* **70**(12)**,** 8669-8674.

Van den Bussche, R. A., and Hoofer, S. R. (2004). Phylogenetic Relationships among recent Chiropteran Families and the Importance of Choosing Appropriate Out-group Taxa. *Journal of Mammalogy* **85**(2)**,** 321-330.

Vijaykrishna, D., Smith, G. J. D., Zhang, J. X., Peiris, J. S. M., Chen, H., and Guan, Y. (2007). Evolutionary Insights into the Ecology of Coronaviruses. *Journal of Virology* **81**(8)**,** 4012-4020.

Wang, L., Shi, Z., Zhang, S., Field, H. E., Daszak, P., and Eaton, B. T. (2006). Review of Bats and SARS. *Emerging Infectious Diseases* **12**(12).

Watanabe, S., Masangkay, J. S., Nagata, N., Morikawa, S.*, et al.* (2010). Bat Coronaviruses and Experimental Infection of Bats, the Philippines. *Emerging Infectious Diseases* **16**(8).

Weiss, S. R., and Navas-Martin, S. (2005). Coronavirus Pathogenesis and the Emerging Pathogen Severe Acute Respiratory Syndrome Coronavirus. *Microbiology and Molecular Biology Reviews* **69**(4)**,** 635-664.

Woo, P. C. Y., Huang, Y., Lau, S. K. P., and Yuen, K.-Y. (2010). Coronavirus Genomics and Bioinformatics Analysis. *Viruses* **2**(8)**,** 1804-1820.

Woo, P. C. Y., Lau, S. K. P., Chu, C. m., Chan, K. h.*, et al.* (2005). Characterization and Complete Genome Sequence of a Novel Coronavirus, Coronavirus HKU1, from Patients with Pneumonia. *Journal of Virology* **79**(2)**,** 884-895.

Woo, P. C. Y., Lau, S. K. P., Huang, Y., and Yuen, K. Y. (2009). Coronavirus Diversity, Phylogeny and Interspecies Jumping. *Experimental Biology and Medicine* **234**(10)**,** 1117-1127.

Woo, P. C. Y., Lau, S. K. P., Li, K. S. M., Poon, R. W. S.*, et al.* (2006a). Molecular diversity of coronaviruses in bats. *Virology* **351**(1)**,** 180-187.

Woo, P. C. Y., Lau, S. K. P., Yip, C. C. Y., Huang, Y., Tsoi, H. W., Chan, K. H., and Yuen, K. Y. (2006b). Comparative Analysis of 22 Coronavirus HKU1 Genomes Reveals a Novel Genotype and Evidence of Natural Recombination in Coronavirus HKU1. *Journal of Virology* **80**(14)**,** 7136-7145.

Woo, P. C. Y., Wang, M., Lau, S. K. P., Xu, H.*, et al.* (2007). Comparative Analysis of Twelve Genomes of Three Novel Group 2c and Group 2d Coronaviruses Reveals Unique Group and Subgroup Features. *Journal of Virology* **81**(4)**,** 1574-1585.

Yeager, C. L., Ashmun, R. A., Williams, R. K., Cardellichio, C. B., Shapiro, L. H., Look, A. T., and Holmes, K. V. (1992). Human aminopeptidase N is a receptor for human coronavirus 229E. *Nature* **357,** 420-422.

Yuan, J., Hon, C. C., Li, Y., Wang, D.*, et al.* (2010). Intraspecies diversity of SARS-like coronaviruses in Rhinolophus sinicus and its implications for the origin of SARS coronaviruses in humans. *Journal of General Virology* **91**(4)**,** 1058-1062.